~~GEODETIC~~ GEODETIC MEASUREMENTS AND THE TECTONICS OF ICELAND

A THESIS

SUBMITTED BY

JAMES LAURENCE BRANDER, B.Sc.,

FOR THE DEGREE OF

DOCTOR OF PHILOSOPHY

OF

THE UNIVERSITY OF LONDON

THE DEPARTMENT OF GEOPHYSICS,

IMPERIAL COLLEGE OF SCIENCE AND TECHNOLOGY,

LONDON.

NOVEMBER, 1973.

ABSTRACT

The feasibility of measuring earth strains is discussed, with particular reference to the primary triangulation work of the United States Coast and Geodetic Survey (U.S.C.G.S.), whose results are compared with the predicted patterns of shear on active faults.

The application of trilateration measurements, particularly those made with the N.P.L. Mekometer III, to the measurement of earth strain is then discussed. This discussion considers all aspects of field equipment and procedure, accuracy of measurements, and interpretation of changes. With suitable reservations the discussion is valid for other distance measuring instruments.

The effect of the atmosphere on the precision of the results and the ways of circumventing the problems it introduces are discussed in some detail.

Results of both vertical angle and trilateration surveys from several parts of Iceland are presented and interpreted according to the techniques previously described in the light of other measurements from the same and other areas.

Finally,all the results and as much additional structural and crustal dynamic information as is available are combined into a tectonic model of Iceland, whose principal feature is a pole of rotation situated at 65^{o}N 21^{o}E. It is emphasised that this pole neither does nor is expected to describe the historical opening of the Atlantic, but should be considered only as very much a current, possibly transient, arrangement.

Apart from this main thread of the thesis, several observations bearing directly on a geothermal field in south-west Iceland are considered, especially in the light of similar observations from an exploited field in New Zealand and in terms of the accepted models of geothermal regions.

These latter results are thought to have considerable importance for geothermal engineering.

The proposed pole of rotation must remain unproven until sufficient information is available from one key area of Iceland. Work of the nature described in the thesis has been begun there, but the results have not yet proved definite.

CONTENTS

CONTENTS			1
ACKNOWLEDGEMENTS			3
AN EARLY DESCRIPTION OF ICELAND			4
SYNOPSIS			5
CHAPTER I	SECTION I.1	INTRODUCTION	6
	SECTION I.2	GENERAL DISCUSSION OF THE MEASUREMENT OF EARTH STRAIN	9
	SECTION I.3	A RESUMÉ OF THE EXPECTED PATTERN OF ACCUMULATING STRAINS AND A COMPARISON WITH SOME RESULTS	13
CHAPTER II	SECTION II.1	THE N.P.L. MEKOMETER III	17
	SECTION II.2	DESIGN AND CONSTRUCTION OF BENCHMARKS	19
	SECTION II.3	DESIGN OF NETWORKS	19
	SECTION II.4	FIELD EQUIPMENT AND EXPERIMENTAL PROCEDURE	26
CHAPTER III.	SECTION III.1	THE INSTRUMENTAL CORRECTIONS	28
	SECTION III.2	THE INSTRUMENTAL SOURCES OF UNCERTAINTY	32
	SECTION III.3	ATMOSPHERIC CORRECTIONS	37
	SECTION III.4	ANALYSIS OF THE INFLUENCE OF THE ATMOSPHERE ON THE UNCERTAINTY	37
	SECTION III.5	SUMMARY OF THE VARIOUS CONTRIBUTIONS TO UNCERTAINTY AND COMPARISON WITH OBSERVATION	45
CHAPTER IV.	SECTION IV.1	A REVIEW OF THE VARIOUS TECHNIQUES USED IN PREVIOUS EARTH STRAIN STUDIES	48
	SECTION IV.2	THE DISPLACEMENT VECTOR ANALYSIS OF TRILATERATION RESULTS	50
	SECTION IV.3	THE HOMOGENEOUS STRAIN SOLUTION IN TRILATERATION	53
	SECTION IV.4	COMPARISON OF THE TWO ANALYSIS TECHNIQUES USED FOR THE TRILATERATION DATA, AND DISCUSSION OF THE LIMITATIONS OF EACH	54
CHAPTER V.	SECTION V.1	TILTMETER RESULTS	57
	SECTION V.2	VERTICAL ANGLE MEASUREMENTS	61
	SECTION V.3	TECTONIC INTERPRETATION OF THE VERTICAL CHANGES OBSERVED AT REYKJANES	66
CHAPTER VI	SECTION VI.1	THE MÝVATN MEASUREMENTS	72
	SECTION VI.2	DISCUSSION OF THE MÝVATN RESULTS IN	

		THE CONTEXT OF OTHER OBSERVATIONS FROM ICELAND	78
	SECTION VI.3	THE TECTONIC SITUATION OF THE THINGVELLIR NETWORK, AND THE RESULTS FROM IT	82
	SECTION VI.4	COMPARISON OF THE RESULTS FROM THE TRILATERAT--ION SURVEY WITH OTHER OBSERVATIONS FROM THE AREA	91
	SECTION VI.5	THE TECTONIC SETTING OF THE REYKJANES NETWORK	93
	SECTION VI.6	THE INTERPRETATION OF THE TRILATERATION RESULTS FROM THE REYKJANES NETWORK	99
	SECTION VI.7	CONSIDERATION OF THE ACCURACY OF THE STRAIN PARAMETER ANALYSIS	125
	SECTION VI.8	CONSIDERATION OF THE CHANGES OBSERVED AT THE NORTHERN END OF THE ORIGINAL REYKJANES NETWORK	127
	SECTION VI.9	DISCUSSION OF THE N85^{o}E PEAK IN THE HISTOGRAM OF MAXIMUM EXTENSION DIRECTIONS FROM THE REYKJANES NETWORK	129
CHAPTER VII	SECTION VII.1	THE TECTONICS OF SOUTHERN ICELAND	133
	SECTION VII.2	THE TECTONICS OF NORTHERN ICELAND	139
	SECTION VII.3	STRUCTURAL SYNTHESIS OF ICELAND	141
CONCLUSIONS			144
APPENDIX A		ILLUSTRATION OF THE DISPLACEMENT VECTOR SOLUTION TECHNIQUE	147
APPENDIX B		ILLUSTRATING THE STRAIN PARAMETER SOLUTION FOR A SQUARE UNDERGOING STRIKE-SLIP DEFORMATION	149
APPENDIX C		ILLUSTRATING THE STRAIN PARAMETER SOLUTION FOR A SQUARE UNDERGOING PURE EXTENSION	150
APPENDIX D		THE DISTANCE-TIME GRAPHS FOR THINGVELLIR	151
APPENDIX E		THE DISTANCE-TIME GRAPHS FOR THE REYKJANES MEASUREMENTS	177
REFERENCES CITED			223

ACKNOWLEDGEMENTS

The author wishes to thank all those people who have contributed in some way to making the work described in this thesis possible.

First among these must come Dr. K. Froome and Mr. R.H. Bradsell without whose generous support and technical assistance the distance measurements would never have been made.

Secondly come the Icelanders, Águst Böthvarsson of the Survey Department, Thorbjörn Sigurgeirsson of the Science Institute of the University of Iceland, and Steingrimur Hermannsson of The National Research Council of Iceland.

Professor Mason provided some encouragement and a lot of financial support for the work.

The Director of the N.P.L. generously allowed the prototypes of the Mekometer III to be used in some of the worst meteorological and geological conditions in the world.

Dr. R.W. Calvert began this work in Iceland, and his thesis, to which reference is periodically made, describes the early progress.

Dr. R.C. Lilwall of the International Seismological Service, Edinburgh, most obligingly provided computer listings of all recorded earthquakes in the Icelandic region.

Messrs. G. Worthington, C. Andrews, C. Sanders, F. Plénier, F. Daussun, D. Waggett, D. Wilson, G. Ásmundsson, C. Hewlett, G. Wadge, H. St. John, K. Will--iamson, T. Meredith, M. Lasserre, and Misses M. Thomas, E. Noyes, C. Chapman, A. Thórarinsdóttir, C. Trinder, J. Ásmunds, P. Cockcroft, all provided field assistance at some stage.

The author wishes to acknowledge the support of an N.E.R.C. studentship and the financial backing provided by the N.E.R.C. in the early stages of the project.

Mr. and Mrs. H. Swann have provided the author with much encouragement during the latter stages of the work.

AN EARLY DESCRIPTION OF ICELAND.

On the west of Norway comes the island called Ice-Land, with the mighty Ocean washing round it: a land very squalid to dwell in, but noteworthy for marvels, both strange occurrences and objects that pass belief. A spring there is which, by the malignant reek of its water, destroys the original nature of anything whatsoever. Indeed,all that is sprinkled with the breath of its vapour is changed into the hardness of stone. It remains a doubt whether it be more marvellous or more perilous, that soft and flowing water should be invested with such a stiffness, as by a sudden change to transmute into the nature of stone whatsoever is put to it and drenched with its reeking fume, nought but the shape surviving. Here also are said to be other springs, which now are fed with floods of rising water, and, overflowing in full channels, cast a mass of spray upwards; and now again their bubbling flags, and they can scarce be seen below at the bottom, and are swallowed into deep hiding far under ground. Hence, when they are gushing over, they bespatter everything about them with the white spume, but when they are spent the sharpest eye cannot discern them. In this island there is likewise a mountain, whose floods of incessant fire make it look like a glowing rock, and which,by belching out flames, keeps its crest in an everlasting blaze. This thing awakens our wonder as much as those aforesaid; namely, when a land lying close to the extreme of cold can have such abundance of matter to keep up the heat, as to furnish eternal fires with unseen fuel, and supply an endless provocative to feed the burning.

Here also is reported to bubble up the water of a pestilent flood, which if a man taste, he falls struck as though by poison. Also there are other springs, whose gushing waters are said to resemble the bowl of Ceres. There are also fires which, though they cannot consume linen, yet devour so fluent a thing as water. Also there is a rock, which flies over mountain-steeps, not from any outward impulse, but of its innate and proper motion.

From Saxo Grammaticus (tr. Oliver Elton) describing IXth century reports in the latter XIIth century.

SYNOPSIS

The ultimate aim of this thesis is to try to arrive at a coherent, unifying tectonic picture of Iceland.

It will accomplish this principally through the analysis of new geodetic results which are available for the first time from several sites in Iceland.

The development and interpretation of the geodetic techniques used and the results obtained from them constitute the major part of the thesis, while the assembly of relevant information from the other earth sciences, and the final synthesis of all available conclusions, is left to the last chapter.

The first chapter is an introduction, both to the particular situation of Iceland and its role in tectonic evolution, and to the application of geodetic techniques to the measurement of strains and movements on the earth's surface.

Chapter II deals with the experimental techniques employed in this particular investigation (already considered in more detail by R.W.Calvert in his thesis in 1969).

Chapter III covers the problems which have been encountered in obtaining the best possible accuracy from the techniques, and considers fully all the sources of uncertainty entering the results, making realistic quantitative assessments of all the contributing effects.

Chapter IV describes and compares the analysis techniques which have been developed to interpret the geodetic results obtained.

Chapters V and VI conduct the interpretation of all the results obtained, and fit them into local and regional structural patterns.

Chapter VII attempts to synthesise all the inferences from chapter VI with all other available information to produce a coherent model of the tectonics of Iceland.

There are five appendices in which various points of interpretation are considered and in which all the relevant results are presented.

CHAPTER I. INTRODUCTION AND GENERAL DISCUSSION OF THE MEASUREMENT OF EARTH STRAIN.

SECTION I.1 INTRODUCTION.

In recent years Wegener's (1924) original hypothesis of continental drift has become widely accepted.

The mechanism of the movements; which at the time of the advancement of the hypothesis was a primary reason for its non-acceptance, has now been found from magnetic evidence to involve production and extension of the sea floor perpendicular to the various mid-ocean ridges of the world rift system. Elsewhere on the earth's surface, usually at the margins of the great oceans, ancient sea floor is re-absorbed into the body of the earth through the deep trenches. Presumably, if the earth's surface area remains constant, the rates of production and reabsorption must be equal. Both production and absorption processes are accompanied by volcanic and seismic activity, though of very, and characteristically,different types; at ridges earthquakes are shallow and small, volcanoes small and basaltic; at trenches earthquakes are deep and often very large (e.g. Chile, 1960), volcanoes large and andesitic.

The areas between ridge and trench, which will generally include portions of both oceanic and continental crust, and arecalled the lithosphere, are found to behave rigidly, like solid plates moving around the surface of the earth under the forces of their production and absorption processes. Figure I.1 shows the world divided into plates, with the directions of the relative movement at each boundary.

The boundaries, defined by the widths of the zones of seismic and volcanic activity, are found to be extremely narrow. The seismicity on the mid-Atlantic ridge,for example, occupies a zone running the entire length of the ocean and only a few kilometres wide (epicentral locations are accurate to about $\pm$ 10 km.).

There are three possible plate interactions: examples of each are shown on figure I.1. Besides the production and absorption boundaries, there are strike-slip regions where plates slide past one another and sea floor is

THE WORLD - SHOWING THE PRINCIPAL PLATES AND THE BOUNDARIES BETWEEN THEM

□ Indicates area studied in this thesis.

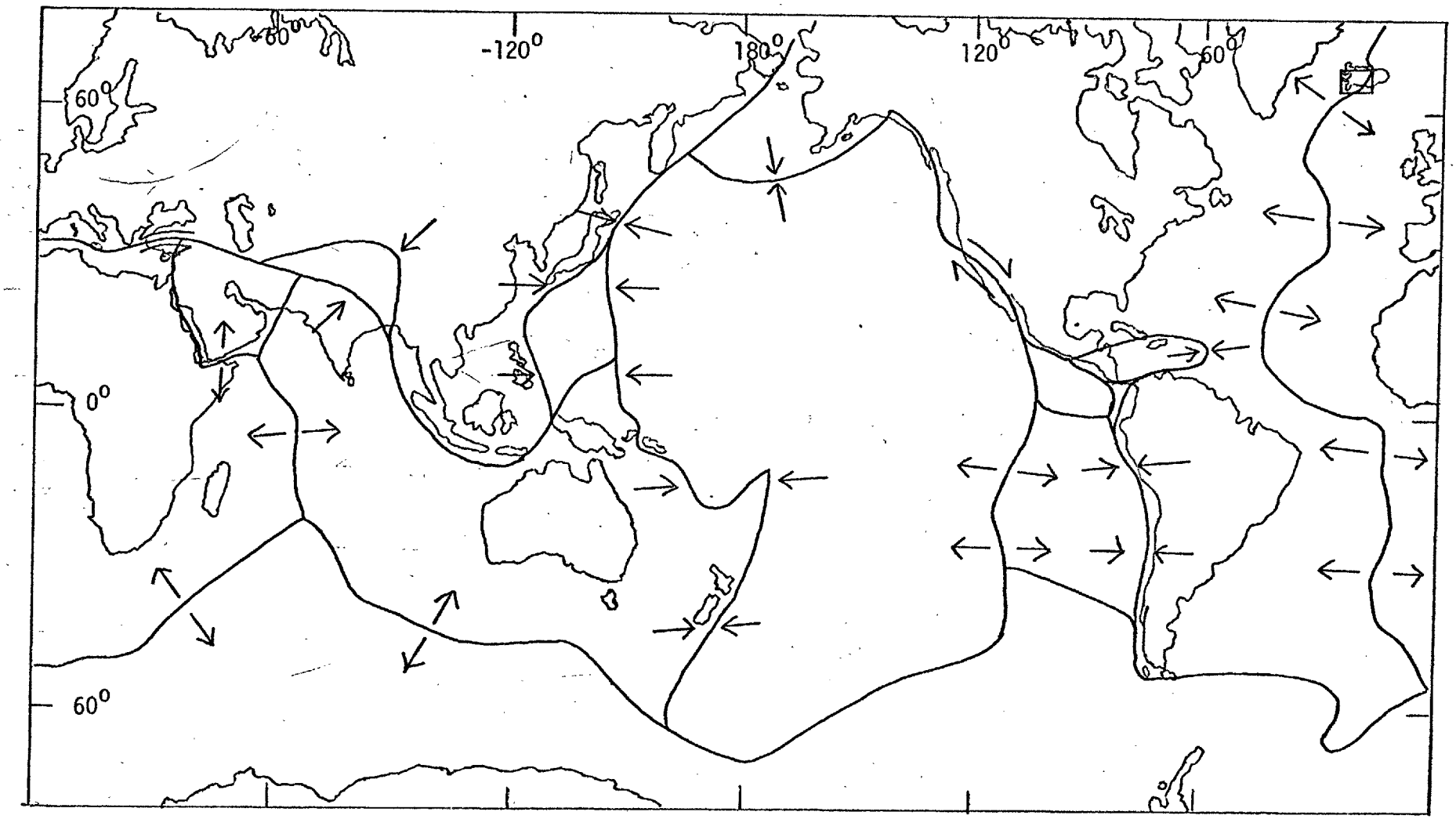


FIGURE I.1

neither created nor destroyed. The two most important examples of this latter type of plate boundary are the Anatolian fault zone of Turkey, and the San Andreas fault zone of California. In common with the other categories of boundary, these too show considerable seismic activity, also of a characteristic nature. Earthquakes on these boundaries tend to be large and shallow, such as was the great California earthquake of 1906, and are also often responsible for much loss of life.

Direct measurement of the relative movement between plates has come from geodetic work in California, where resurveys to discover premonitory earth movements before large earthquakes have been made since 1908. The estimates of the differential movement between the American and Pacific plates made from these measurements suggest that western North America is moving at 30 mm. per year south-east relative to the north-east Pacific floor (Savage and Burford, 1973).

This thesis describes measurements made on a diverging plate boundary, where new crust is being continually created by volcanic processes, and the sea floor on either side of the zone of creation is being moved slowly away.

Iceland is the largest land area to occupy a position directly on a diverging plate boundary, and as such offers the only possibility of easy study of the processes which operate on these boundaries, the mid-ocean ridge system.

By the very fact of its existence it may be very atypical of true mid-ocean ridges, but nevertheless it should be possible to learn something of general application by careful observation and consideration of the obvious differences.

Böthvarsson and Walker (1964) first proposed that the crust of Iceland had grown laterally about a narrow volcanic zone, much after the fashion envisaged by Dietz (1961) for the growth of the ocean floor. Böthvarsson and Walker considered that the force behind the growth came from the injection of dykes into the base of the Icelandic crust.

This view attracted immediate enthusiasm and is now generally accepted by everyone but a few of the most stalwart anti-continental drifters.

But its shortcomings are also recognised, such that there are many of the subtleties of Icelandic tectonics which are not immediately explicable by the

straightforward application of this model.

It is hoped that it will be found that the results presented in this thesis have some bearing on the outstanding tectonic problems, and that the interpretat-ions given them will help to rationalise many of the observations.

SECTION I.2 GENERAL DISCUSSION OF THE MEASUREMENT OF EARTH STRAIN.

Earthquakes have been known in many parts of the world since very early times, and in China at least are known to have provoked observation and elementary instrumentation some centuries before the beginning of the present era.

It was only after the great 1906 earthquake that the first theory with factual evidence was produced.

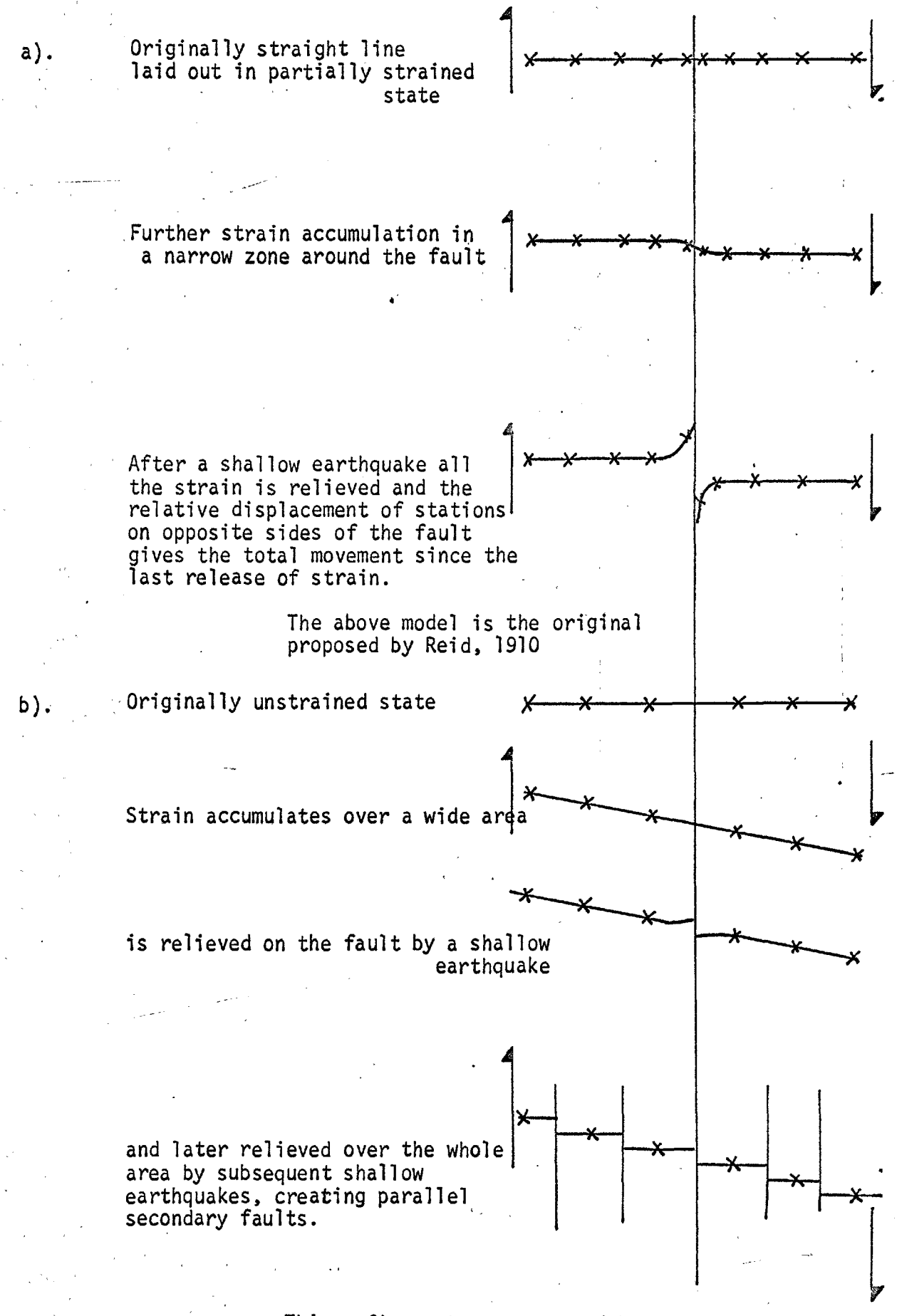
Reid (1910), from geodetic results obtained by Hayford and Baldwin (1908) proposed the elastic rebound theory, which remains the accepted model for the earth movements during earthquake cycles.

Reid proposed that strain accumulates at a constant rate across a narrow zone (probably a pre-existing fault), until after a time which is governed by the static friction on the pre-existing fault faces (or the shear strength of the rock if there is no previous faulting), the fault moves suddenly, releasing all or most of the accumulated strain, and radiating a large fraction of the stored energy as seismic waves. Figure I.2 illustrates his original theory, and an embellishment of it due to Richter.

Since the first formulation of these ideas a very large number of angle measurements on primary and secondary geodetic triangulation networks has been made in order to try to detect the strain accumulation which ought to precede an earthquake, and which might therefore be an indication of its approach. Almost all this work has been undertaken in California, most of it along the San Andreas fault (which was responsible for the 1906 earthquake), and much of it since the nineteen thirties. There have been numerous attempts at

Figure I.2

TWO POSSIBLE INTERPRETATIONS OF THE ELASTIC REBOUND THEORY.



interpretation of these results (e.g. Whitten, 1955; Whitten, 1960; Whitten and Claire, 1960; Scholtz, Wyss, and Smith, 1969; Scholtz and Fitch, 1969; Miller et al., 1970; Savage and Burford, 1970; Savage and Burford, 1973; Savage et al., 1973).

The outcome of all this work seems to be that in California the plates have a relative annual rate of movement of about 30 mm. (as mentioned before) and that strain does accumulate in the fashion required by the elastic rebound theory. However the relationship between strain accumulation and earthquake occurrence has not been determined, and indeed other mechanisms of strain release have been observed and must be deemed equally important (e.g. shaking induced stable sliding (Allen et al., 1972)).

In recent years the practice has grown of using electro-magnetic distance measurements in the study of strain accumulation and fault displacement.

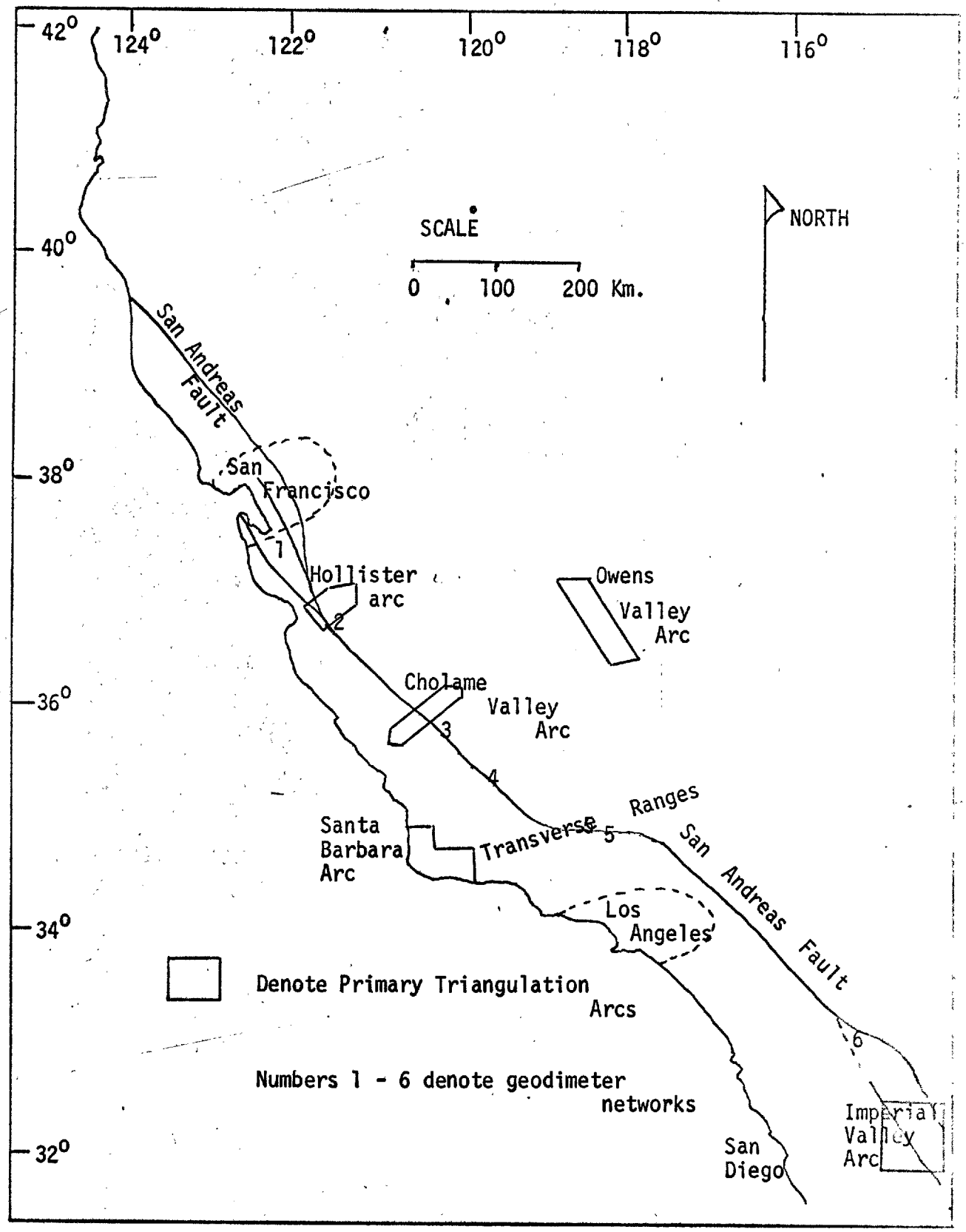
Hoffman (1968) describes the results of several years'geodimeter surveys from a series of small networks along the entire length of the San Andreas fault. These networks (figure I.3) were established in the late nineteen fifties by the Department of Water Resources of the State of California to monitor fault movements that might disrupt the canal system feeding the urban areas of the state.

Since (as is shown in detail in a later chapter) the use of distance measurements automatically provides more information on the state of strain than does triangulation data , the application of these techniques will presumably increase in years to come, especially as the accuracy of the commercially available instruments is now of the same order as that of theodolite measurements.

As was mentioned above, almost all the world effort in earth strain (in seismological applications) has been made in California, presumably as a result of a combination of circumstances, reflecting the material capacity of the State, its high and near-surface seismicity, and the vulnerability of modern structures to extensive damage.

In Japan, Russia, and some European countries, perfunctory efforts at

FIGURE I.3 MAP OF CALIFORNIA SHOWING U.S.C.G.S. PRIMARY TRIANGULATION ARCS AND DEPARTMENT OF WATER RESOURCES GEODIMETER NETWORKS.



measuring ground movements in earthquake cycles have been made, but in all these places the seismicity is much deeper so that the effects cannot be expected to be as great, and in Europe and Russia it is much less frequent, so of less social importance. Until recently in Japan earthquakes were so much a part of life that building styles and construction techniques were perfectly adapted to them, and it is only with the advent of modern high-rise concrete structures that the problem of earthquake prediction has been taken seriously in Japan.

The only other area of the world in which seismicity is at a high level, both frequency-wise and in terms of the depth of occurrence, is in the countries affected by the Anatolian Fault zone (almost the entire Middle East). Here work on earthquake prediction is just beginning, and may be expected to develop at a very high rate.

SECTION I.3 A RESUMÉ OF THE EXPECTED PATTERN OF ACCUMULATING STRAINS AND A COMPARISON WITH SOME RESULTS.

Figure I.4 shows two models of a supposed fault, as proposed by Savage and Burford (1970).

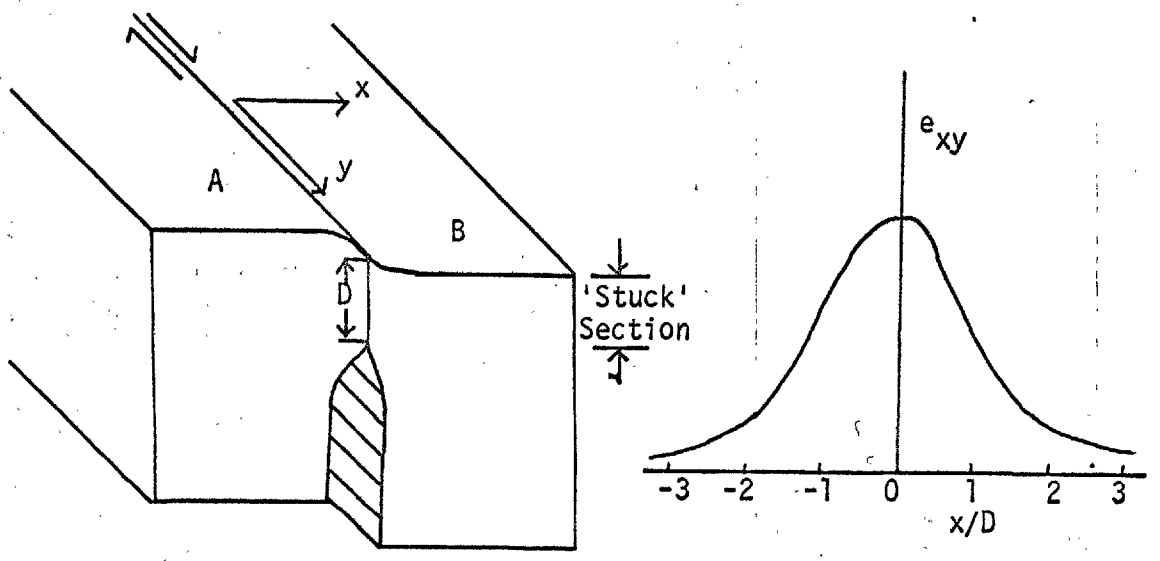
The upper one is of a deep fault whose lower part down from some depth D slides frictionlessly, aseismically. This model is assumed to apply to most of California from a depth of about 10 km. downwards, where crustal rocks are assumed to be hot enough for conditions of plasticity to prevail.

In the upper zone, from the surface to D, elastic rebound conditions are assumed to prevail, and strain accumulates, particularly in the transition zone around depth D, until earthquake occurrence. The shear strain pattern which would be expected to be observable at the surface would be as is shown on the inset diagram, with the maximum occurring across the surface trace of the fault. The maximum shear strain observed at the surface does not (as is shown by Chinnery, 1961) reflect the maximum shear occurring at depth, which is perhaps

Figure I.4

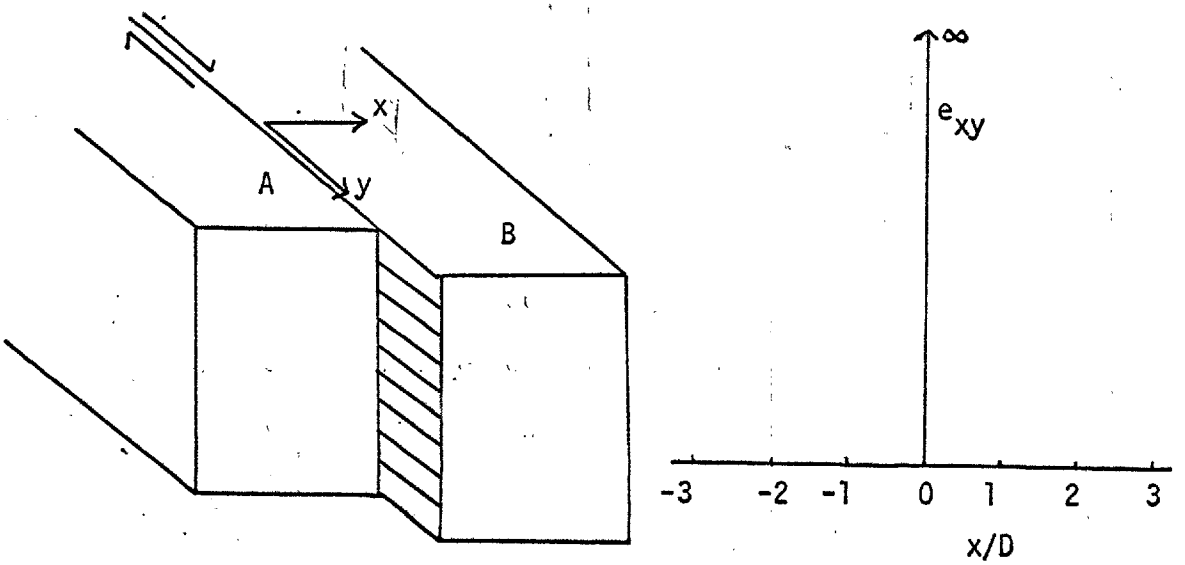
TWO MODELS OF AN ACTIVE FAULT, AND THE SHEAR PATTERN TO BE EXPECTED FROM EACH.

After Savage and Burford, 1970



The upper model is of a fault slipping smoothly over most of its vertical section, except for the uppermost part D, which is frictionally 'stuck'. The shear strain pattern developed at the surface is shown on the right.

Below, the blocks are moving freely along their entire surface of contact. In this case the shear strain is zero everywhere except on the fault, where it is infinite.



why measurements of strain accumulation have not yet been of any use in predict-ion.

The lower model of figure I.4 represents the case for when frictionless, stable movement occurs throughout the earth's crust, and strain accumulation does not occur.

Savage and Burford (1970) found examples of both situations in an extremely comprehensive analysis of geodetic results from several parts of California.

Figure I.5 illustrates their results from the Cholame valley primary triangulation arc, which lies just south of Parkfield where earthquakes have occurred in 1934 and 1966, and which is a good example of the strain pattern implied by their first model.

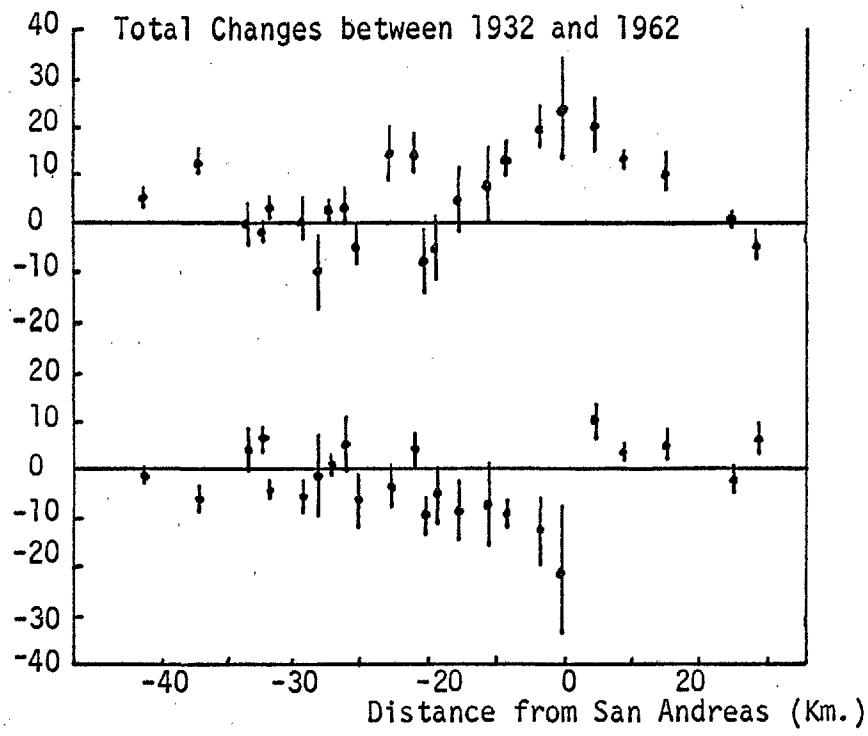
They also found an excellent example of their second model on the Hollister triangulation arc, where there was no observable strain accumulation away from the fault, and the results of Tocher (1960) show that there is a continuous displacement at an almost constant rate of about 20 mm. per year across a very well defined fault trace.

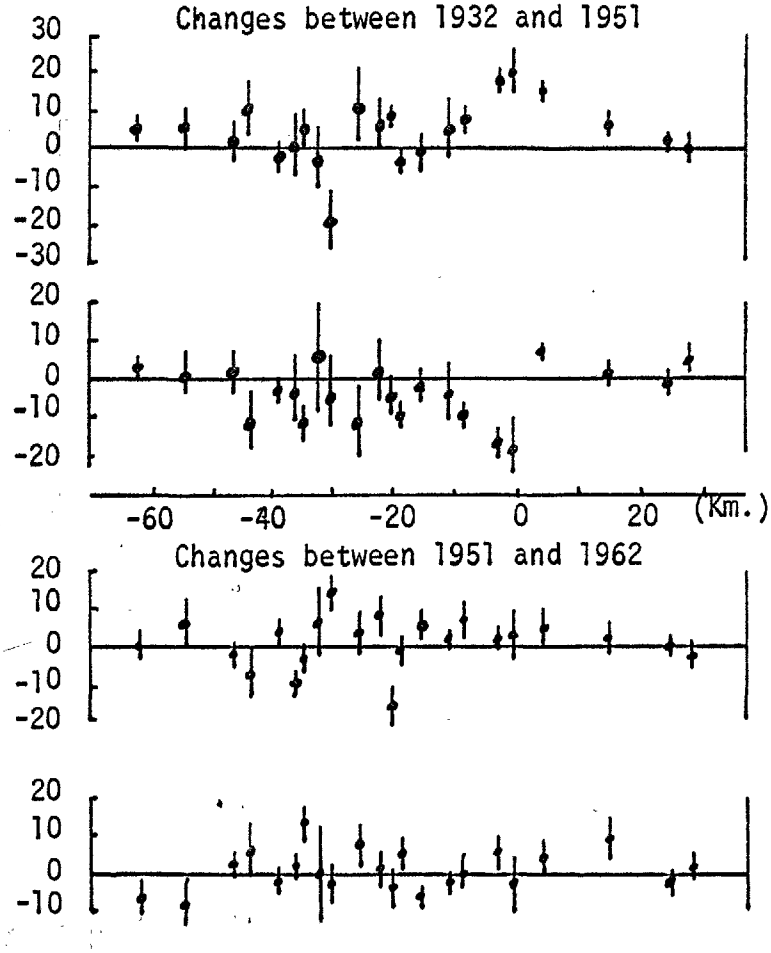
One interesting feature of the Cholame Valley result is the comparison of the strain accumulation pattern between 1932 and 1962 with that between 1932 and 1951. They are almost identical, suggesting that there was no strain built-up on that network between 1951 and 1962. This led the authors to suggest that the observed strain is purely a result of the 1934 earthquake, whose surface break ended immediately north of the network.

But whatever the detailed implications for earthquake mechanisms and recurrence the geodetic work which has been done shows quite definitely that earth strains can be detected by these methods, and that the results can be interpreted in ways which are compatible with respect to acceptable models.

Figure I.5

RESULTS FROM THE CHOLAME VALLEY TRIANGULATION ARC





After Savage and Burford, 1970

CHAPTER II DESCRIPTION OF THE EQUIPMENT AND EXPERIMENTAL PROCEDURES USED IN THIS WORK.

SECTION II.1 THE N.P.L. MEKOMETER III.

The basis of all the earth strain work undertaken by Imperial College has been the prototype of Mekometer III, designed and built by Dr. K. Froome and Mr. R.H. Bradsell (1961, 1966, 1971). This is an electromagnetic distance measuring device of considerable sophistication, whose sensitivity is of the order of 0.1 ppm. over path lengths up to 3 kilometres. Its operation is based upon the electro-optic effect, by which the polarisation vector of a short pulse of 486 nm. wavelength light is elliptically polarised at a frequency of about 491 MHz. The light, collimated to a beam whose spread is about 1 micro-radian, is transmitted from the front of the instrument to a distant cube-corner retro-reflector mounted at the far end of the line. Such reflectors return light exactly along its incident direction, so that the beam returns to the instrument, where it passes first round an internal, calibrated, variable light path, thence to be demodulated by the same signal as originally modulated it. The demodulated light, whose amplitude depends upon the phase relation between the modulating signal and the transit time (i.e. path length) of the light, is converted by a photomultiplier to an electrical signal which is amplified and displayed on a meter.

The modulating frequency of 491 MHz. corresponds to a wavelength of 2 feet, which gives a fundamental repeating unit of 1 foot. The calibrated light path has a total variability of 1 foot (304.8 mm.), so that it is always possible for any length of line to find one position of the light path which gives a maximum meter reading (when the incoming light is exactly in phase with the modulating signal), and also one which gives a minimum meter reading (when the returning light is exactly out of phase with the modulating signal).

The variable light path is attached to a graduated invar tape which can be read to $\pm$ 0.002 foot, and the system is calibrated so that when the meter reading is a minimum the tape-read distance gives the excess in the total

instrument-to-target distance over an integral number of fundamental repeating units.

This is an excellent system as it avoids the necessity for electronic phase comparison, which introduces cyclic errors and temperature dependence.

However, with a fundamental repeating unit of only one foot, it is obviously not possible to determine the entire distance without changing the modulating frequency, which is done.

The use of elliptical polarisation in the modulation is a great improvement over the amplitude modulation usually used in these electro-magnetic distance measuring devices (e.g. the Geodimeter), because phase distortion by random atmospheric fluctuations is very much less than the corresponding amplitude distortion, so that the Mekometer is inherently less susceptible to atmospheric influences than are other, similar instruments.

Frequency control in the Mekometer is by means of a very precisely made microwave cavity whose resonant frequency is about nine times the modulating frequency.

This cavity's resonant frequency changes with atmospheric temperature and pressure in a way which is designed to compensate exactly for the effects of these parameters on the refractive index of the light path, thus neatly avoiding the necessity for complex corrections.

The Mekometer is a pulsed instrument, operating at fifty Hertz.

In order to facilitate the meter settings (which it will be recalled from above, require that the photomultiplier output be set to a minimum) the modulating frequency on alternate pulses is arranged to be, by suitable mixing of sidebands, a few parts per million above , or an equal amount below, the nominal frequency defined by the reference cavity. This means that when the variable light path is accurately set so that the returning light is exactly out of phase with the modulating signal for the average (reference defined) modulating frequency, alternate pulses will show a certain residual signal. If the sign of the residual signal is changed by suitable switching, then the average output over a number of pulses will be zero, which is a very much easier setting (particularly on a centre null meter) than is a minimum.

This description of the Mekometer is not intended to be complete (for which the relevant papers by Froome and Bradsell, and the Ph.D. thesis of R.W.Calvert should be consulted) but is intended to show that there are three features of its design which make it capable of greater accuracy and less prone to external influences than other instruments of its type.

The operation of the instrument is summarised in the block diagram shown in figure II.1.

SECTION II. 2 DESIGN AND CONSTRUCTION OF BENCHMARKS.

The benchmarks which have been used in the Icelandic field-work which forms the basis of this thesis, are all of one type.

All are constructed of six inch internal diameter concrete pipes, founded on solid rock to which they are attached by steel stressing rods, filled with concrete and hard core, and capped with extremely well machined bronze mush--rooms, into whose one inch diameter sockets the instrument and reflector mounts fit exactly. The bronze is protected from the effects of weather and the corrosive atmosphere of a geothermal field by screw caps.

Measurements are described in chapter V which are designed to measure changes in inclination of the pillars, apparently not a significant effect (as will be discussed then).

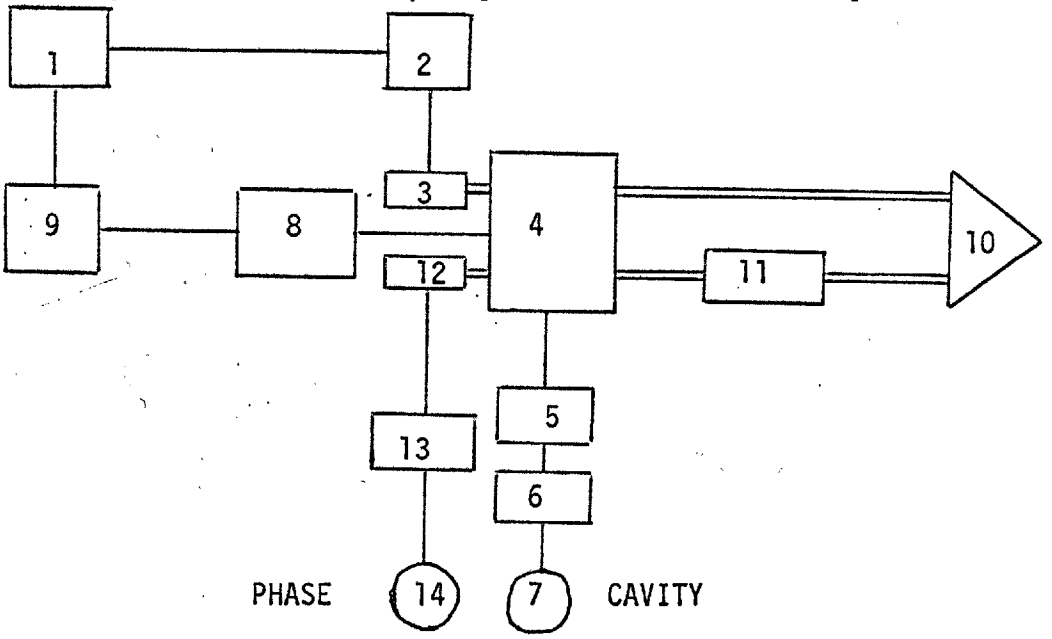
Figure II.2 shows the cross-section of a concrete pillar (after R.W. Calvert, 1969).

SECTION II.3 DESIGN OF NETWORKS.

Webster's international dictionary defines a network as any system of lines or channels interlacing and crossing like the threads of a net. Surveying networks for theodolite work, including the primary geodetic triangulation which has formed hitherto (as described in chapter I) the major part of

FIGURE II.1 BLOCK DIAGRAM OF MEKOMETER III.

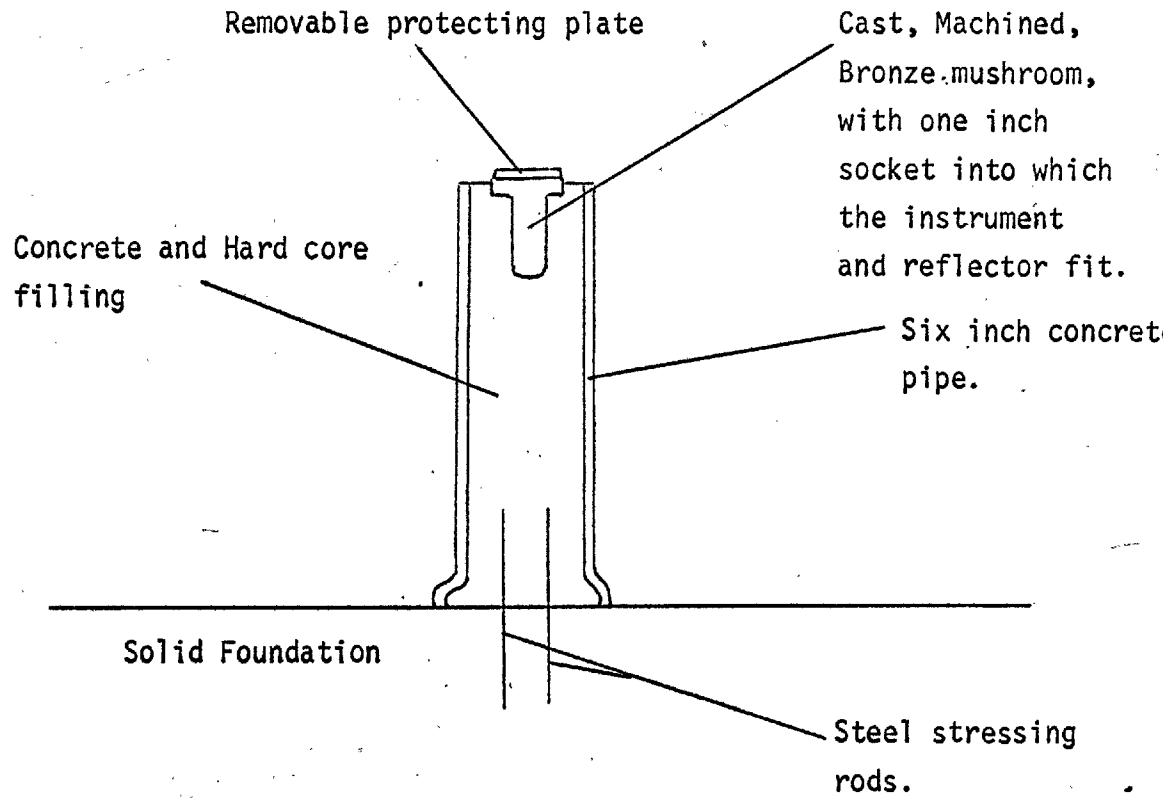
50 Hz. pulses from the pulse generator, 1 , trigger the flash-tube driver, 2, such that light from the Xenon flash-tube, 3, passes through the modulating and demodulating cavity, 4. The nominal frequency of this cavity, which is tunable, is set by the resonant frequency of the standard cavity, 5.



When the tuning on the modulating cavity is suitably set, a small signal taken from it induces resonance in 5, which produces after amplification and detection in 6, a reading on the CAVITY meter, 7. The nominal frequency in 4 is the average of each pair of pulses. 4 is driven by 8, the U.H.F. power amplifier and driver, and the U.H.F. frequency is displaced slightly above and below the mean on alternate pulses by the frequency modulator, 9, itself driven by the original pulse generator.

The light, after modulation, is transmitted to the distant target cube-corner reflector, 10, straight back to the instrument, where it first travels round the variable light path,11, before being demodulated in 4. After demodulation the light falls on the photomultiplier, 12, whence, after amplification and detection, 13, the resultant signal is displayed on the PHASE meter, 14.

FIGURE II.2 CROSS SECTION OF AN ICELANDIC CONCRETE PILLAR. (after R.W. Calvert)



earth strain studies, are usually large areal extents of intervisible stations, forming as nearly as possible close-packed hexagonal structures. The interstation spacing depends upon the application of the network and upon the accuracy of the instrument to be used.

For the primary geodetic earth strain studies in California, the station separation is usually about fifteen kilometres. This, assuming the accuracy of the theodolite measurements to be about ± 0.45 seconds of arc (Miller et al., 1970) entails a position accuracy of the target stations of about $\pm$ 30 mm.

Figure II.3 is a map of the Imperial Valley primary triangulation network (after Miller et al., 1970), which illustrates how the close-packed hexagonal structure turns out in practice; quite well in this case with a fairly even station coverage over a large area.

The reasons governing the surveyor's liking for large areal extents of evenly spaced networks stem from the statistical treatments that these make possible. Using the condition that the angles of a quadrilateral must sum to 180° and employing best fit techniques to the entire system, errors in measured angles may be distributed among adjacent angles. Such procedures work most satisfactorily if a network is not constrained in one direction, and if the elementary units, in this case equilateral triangles, are uniformly distributed.

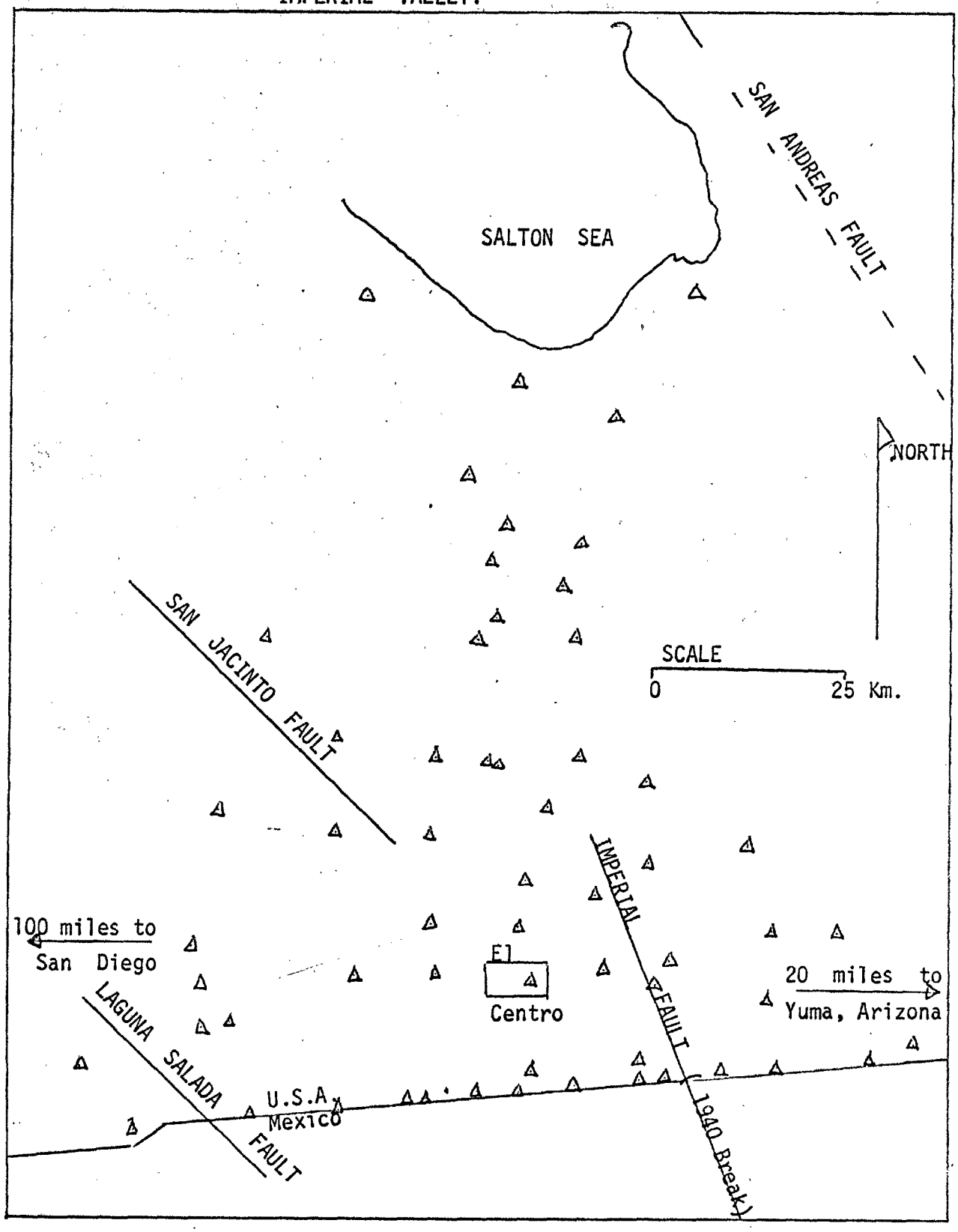
For networks on which it is intended to make distance measurements, the triangle is not a very useful basic unit, as it provides no check on the consistency of the measurements. The simplest figure to give a redundant line whose measured length can be compared with a value calculated from the lengths of the other lines is the double-braced quadrilateral (i.e. the quadrilateral with both diagonals measured).

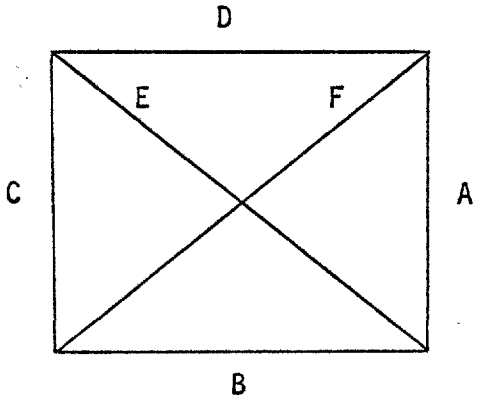
The formula for calculating the length of the second diagonal from the other five distances is.

$$F^2 = \sqrt{((P+Q)^2 + (E-(R+S))^2)}$$

FIGURE II. 3

THE U.S.C.G.S. PRIMARY TRIANGULATION ARC IN THE IMPERIAL VALLEY.





A DOUBLE - BRACED QUADRILATERAL.

where $R = (A^2 + E^2 - D^2)/2E$
$S = (C^2 + E^2 - B^2)/2E$
$P = (A^2 - R^2)^{1/2}$
$Q = (C^2 - S^2)^{1/2}$

Thus, in order to apply to distance measurements the same sort of adjust-ments as are made to triangulation results, it is necessary to use networks where the elementary unit is not the equilateral triangle, but the double-diagonal quadrilateral.

Unfortunately, this was not recognised in the early stages of the work in Iceland, and the first network built there, at Thingvellir (see chapter V), is composed of very fine equilateral triangles. Likewise, the other early Icelandic network, at Reykjanes, was also built around the elementary equilateral triangle, although there the interstation spacing is sufficiently small to allow the measurement of some ' filling-in ' lines.

The three more recent networks in Iceland are all built on the double-braced quadrilateral basis.

By analogy with standard surveying practice, it might be expected that these networks should be laid out areally. This has not been done, and in all cases the quadrilaterals are arranged end-to-end. The reason for this is simply one of coverage. Each network is designed to be perpendicular to the process it is supposed to detect. As the lateral extent of the area governed by the process is not known, it was thought advisable to make the total perpendicular coverage as great as possible for a given size of network.

Deciding on the optimum length of line to be measured is another aspect of

network design which should be considered.

All depends upon the sort of movement expected.

A fault which is slipping at a constant rate over a very narrow zone, as is found in parts of the San Andreas system, is best measured by a line whose strike is as nearly as possible parallel to the fault. This line should be short enough that the expected error, which will be shown later (chapter III) to be proportional to the measured distance, remains less than the expected movement: it should also be long enough that the sensitivity of the instrument is not reduced. The optimum length for a line for this purpose is about 300 m.

In order to measure strain it is useful to have as long a line as possible, so as to increase the displacement signal (which is of course proportional to the distance). However, this also increases the expected error, and the susceptibility of the line to atmospheric interference, so that in practice it is always preferable to keep the line length less than 1.5 Km. in Mekometer applications.

When laying out a network in difficult terrain (which is usually the case in Iceland), it is very important to appreciate the possible effects of vertical movements upon the line lengths.

The change in length of a line , dl, caused by vertical movement of one of the stations, is given by

$$dl = dh.\sin\theta$$

where dh is the relative vertical movement, and θ is the inclination of the line from horizontal.

According to this formula, it can be seen that a fairly modest 100 mm. of elevation change gives rise to almost 2 mm. distance change along a line whose slope is 1^{o}. On an 800 m. long line 1^{o} corresponds to an elevation difference between the ends of 14 m. Elevation differences between stations of ten times this amount have been encountered, and twenty to thirty metres is often found; unless it is intended to monitor vertical changes (by theodolite or precise levelling), it is necessary to keep lines as nearly as possible horizontal.

In summary then, networks used for trilateration (distance measurements) with the Mekometer should be composed of double-braced quadrilaterals (the more

regularly sided the better), in which the lines should be not longer than 1.5 Km. and not shorter (in a strain measuring application) than 800 m., and in which slope angles should not be more than 0.5^{o}. Regrettably few of these criteria for good Mekometer networks are achieved in Iceland.

SECTION II.4 FIELD EQUIPMENT AND EXPERIMENTAL PROCEDURE.

Apart from the Mekometer, its power supply, spare battery, and target reflector, the only field equipment required to conduct trilateration measurements are three mercury-in-glass thermometers and a barometer. These latter four items are required in order to monitor, and subsequently correct for (chapter III), atmospheric refractive index and modulating frequency.

The minimum number of people required for the work is two, one to set up and move the target reflector, the other to use the Mekometer. A third person is very useful at the instrument end, keeping records and measuring atmospheric temperatures, but not entirely essential. Sometimes there have been five or six people available on field trips, when it has been found that the work can be greatly speeded by using several target reflectors.

The total weight to be carried by the instrument man is about thirty kilogrammes, so that where access is difficult, as in parts of Iceland, one man can quite conveniently transport all the necessary equipment.

During the course of a measurement about ten distance readings will be made with the Mekometer. For each of these the instrumental and air temperatures are read. Atmospheric pressure is measured once for each line. At the reflector end, air temperature will be read once every half minute from the time of arrival to the station to the time of the ' move on ' signal.

It has been found that mercury-in-glass thermometers require about three minutes to reach equilibrium with the atmosphere, so that provided the reflector man begins measuring temperatures as soon as he arrives at a station, then the thermometers should be recording accurate air temperatures by the time the instrument is aligned and measuring has begun.

Signalling between the instrument and reflector is normally conducted by

rudimentary semaphore by day, or by systems of coloured lights by night; the private use of citizen band walkie-talkie sets is forbidden in Iceland.

Arrangements for full correction of the observations while still in the field have been tried, but without much success. Both sending back data for processing in London, attempting processing on a local computer, and complicated lists of field correction tables have been tried; none of these methods has a short enough time constant yet to enable mistakes to be immediately rectified.

CHAPTER III. THE CORRECTIONS APPLIED TO THE RESULTS, AND AN ANALYSIS OF THE SOURCES OF UNCERTAINTY.

SECTION III.1 THE INSTRUMENTAL CORRECTIONS.

There are two separate instrumental corrections which are applied to the Mekometer results in order to improve the accuracy, albeit slightly,over their raw, uncorrected level.of uncertainty.

The first of these is concerned with the modulating frequency of the instrument; the second is connected with the reflector used.

In the brief description of the Mekometer in chapter II, the compensating effect of the frequency standard is mentioned. Through the reference microwave cavity's temperature and pressure characteristics, the modulating frequency is varied so as to compensate for the changes in atmospheric refractive index caused by temperature and pressure changes.

This system is not perfect, so that the short-term precision of results relying on it is about $\pm$ 3 ppm. More seriously though, the reference cavity has drifted over the years of measurements so that comparing one year's results with the next is not possible to better than about (at worst) 12 ppm.

Thus it is found necessary to over-ride the compensation system, and to correct individually for modulating frequency (defined by measured pressure and instrumental temperature) and for atmospheric refractive index. It is to conduct these corrections that the temperature and pressure measurements described in the last chapter are performed.

Table III.1 compares some uncorrected results with the same ones after correction.

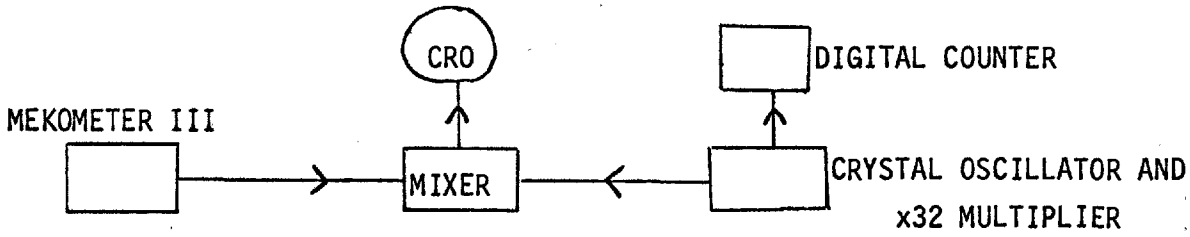
DATE	UNCORRECTED DISTANCE (m)	CORRECTED DISTANCE (m)
24.6.72	794.3313	794.3215
23.7.72	794.3200	794.3216
23.7.72	794.3198	794.3212
3.8.72	794.3224	794.3215
7.8.72	794.3206	794.3207
	Total Spread = 11.5 mm.	Total Spread = 0.9 mm.

It should be mentioned that these measurements were not all made with the same Mekometer. That on 24.6 was made with the earlier prototype, the remainder with the later version.

Even though there are only five measurements,which cannot possibly represent a statistical sample, and even if the June result is neglected (on the assump--tion that all measurements are made with the same instrument), there is still a genuine improvement in the grouping of the corrected results: and measurements are not always made with the same instrument.

As has been stated before, the modulating frequency is defined by the effects of atmospheric temperature and pressure on the reference cavity. The character--istics of this cavity's variations with these parameters have been determined empirically, by measuring frequency at constant temperature, and at constant pressure.

The experimental arrangement for these measurements is shown schematically below.



Direct measurement of the modulating frequency has not hitherto been possible because of the instrument's pulsed operation, so that the method used (as illustrated above) is somewhat circuitous, but simple enough, and employs cheap, portable equipment.

A crystal derived tunable frequency of about 15.3 MHz. is multiplied thirty two times (to about 491 MHz., the Mekometer modulating frequency) and mixed with a signal taken from the Mekometer's modulating cavity.

As was described in chapter II, the modulation frequency is changed from pulse to pulse, so that it is alternately above and below (by equal amounts) its nominal (reference cavity defined) value. Thus alternate pulses produce different sets of sum and difference signals when mixed with the multiplied crystal frequency. By using a low frequency oscilloscope only the two difference

signals are displayed, and if (by tuning the crystal oscillator when the Mekometer is correctly tuned) these two difference beats can be made entirely co-incident (identical in amplitude, frequency, and phase) then it is certain that the mean modulating frequency is exactly the same as the multiplied crystal frequency. The crystal oscillator frequency (which is continuous) is easily measured on a conventional digital counter, and the mutiplication factor is fixed, so that the mean modulating frequency is known. Temperature and pressure are easily measured, so that a calibration point has been determined.

The graphs of frequency against temperature, of which one is made on each measuring expedition, are known as frequency check curves; a typical one is shown in figure III.2.

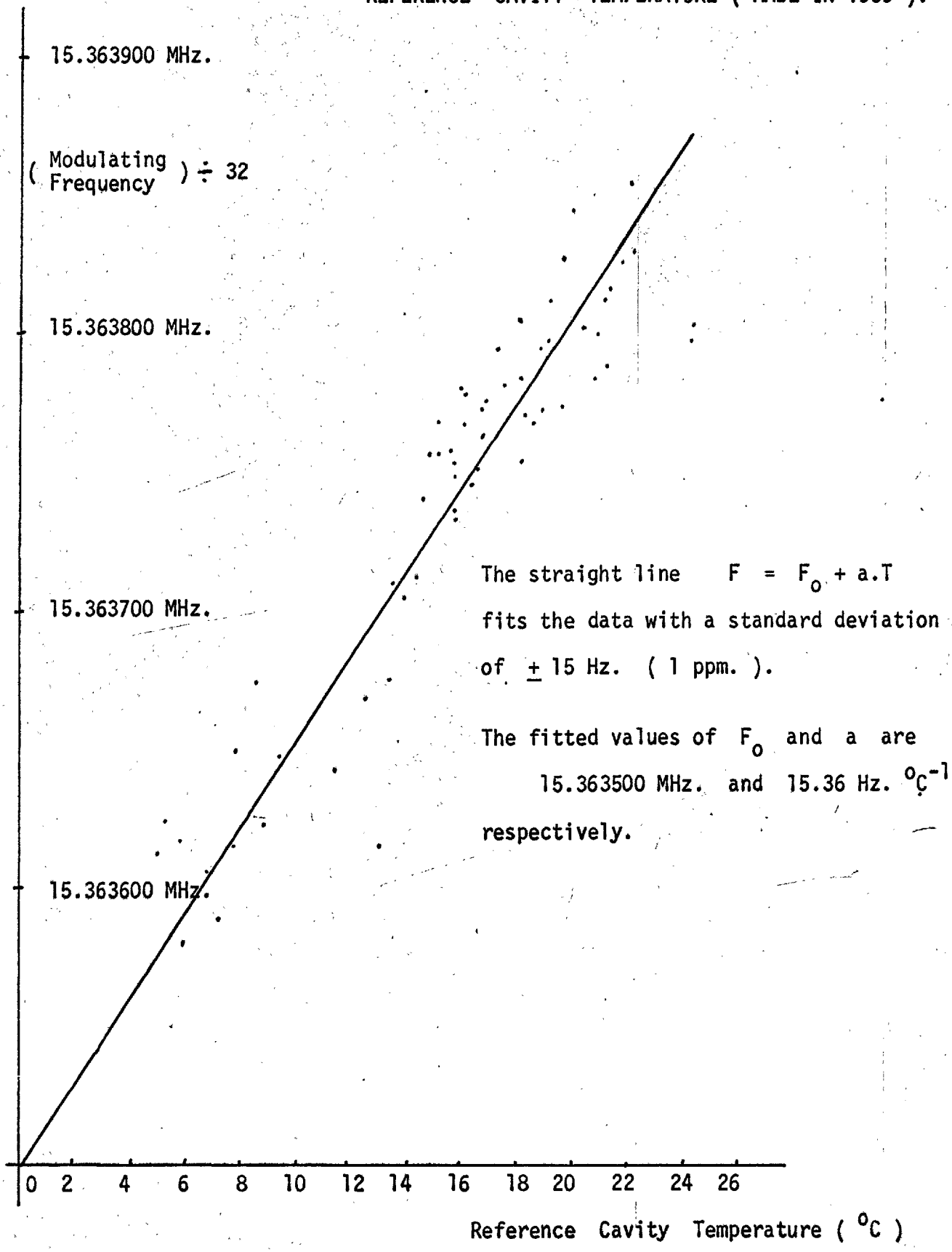
The relationship between temperature and frequency is linear, at least over the range $-5^{o}C$ to $+30^{o}C$, and the rate of change of frequency with temperature has been constant over the years at 10^{-6} $^{o}C^{-1}$, although the frequency at $0^{o}C$ (F_{o} on figure III.2) has varied considerably over the same time period. The change of F_{o} for the second of the Mekometer prototypes is illustrated on figure III.3.

The pressure characteristic is measured in exactly the way described above, but inside a decompression chamber so that pressure may be varied over a wide range. The pressure gradient is linear at sea-level, with a value of -2.84×10^{-7} mb^{-1}., but decreases in magnitude with elevation. At the heights encountered in Iceland though this non-linearity is not important.

Thus the correction for modulating frequency which is applied to the Mekometer measurements is a linear function of the temperature and pressure pertaining to the time of the measurements.

The second instrumental correction is a constant, simply subtracted from the (corrected) measured distance. It relates both to the target reflector and to the Mekometer used, and is usually about half a metre.

FIGURE III.2 THE GRAPH OF MODULATING FREQUENCY AGAINST REFERENCE CAVITY TEMPERATURE (MADE IN 1969).



SECTION III.2 THE INSTRUMENTAL SOURCES OF UNCERTAINTY.

The last section described the various instrumental corrections that are applied to the Mekometer measurements in order to obtain the most precise possible results. Here will be analysed the instrumentally-derived sources of limitation to that precision.

The Mekometer's compensation system has been described already, and the short-comings in it have already been invoked as the reason for making independent corrections for modulation frequency and refractive index.

However, the application of these independent corrections (as might be expected) brings about various possible sources of error.

In the first part of this section the sources of error arising from the application of the modulating frequency correction will be considered: in the second part the sources of error arising from the other instrumental correction, that for the retro-reflector, will be discussed.

The precision of the modulating frequency correction is determined by the accuracy of the frequency check curves, which is in turn governed by the precision with which the beat curves may be matched on the oscilloscope, the accuracy of the digital counter and of the standard cavity, and the precision of the temperature and pressure measurements.

The thermometers used in this application are accurate to $\pm$ 0.2^{o}C, and the barometer used is an aneroid electronic readout type with an accuracy of better than $\pm$ 0.1 mb. Thus from the values given above for the variation of modulating frequency with temperature and pressure, it may be seen that the uncertainty contribution from these two sources does not exceed $\pm$0.2 ppm.

The digital counter used to measure the crystal oscillator frequency is externally referenced to another crystal oscillator (a fast warm-up device manufactured by Messrs. Racal), whose frequency stability is claimed to be $\pm$ 0.01 ppm.

The short-term stability of the reference cavity is claimed to be better than 1 part in 10^{7} (though in the long-term it has been found to drift more).

None of the individual contributions considered above comes in any way close to explaining the observed uncertainty in the frequency checks of about 1 ppm. (c.f. figure III.2).

Thus the principal source of uncertainty in defining the curve of frequency against temperature,on which the modulating frequency correction is based, seems to come from the process of curve matching which is employed during the calibrat -ion. The magnitude of the uncertainty introduced in this way is found from the scatter of the calibration points to be $\pm$ 1 ppm.

As a further illustration of the problem of the modulating frequency uncertainty, figure III.4 shows a graph of a field measurement, in which the uncorrected distance reading is plotted against the temperature of the reference cavity. This graph corresponds (since atmospheric conditions remained constant during the course of the readings) to a frequency check curve, except that frequency is determined by its effect upon the measured distance, rather than by direct measurement.

This graph shows that the expected gradient of frequency with temperature is approximately followed, but also suggests that the assigned uncertainty of $\pm$ 1 ppm. in the modulating frequency correction is necessary.

The other instrumental correction which was considered in the last section and which is therefore likely to contribute some uncertainty to the final , corrected distance is the reflector correction.

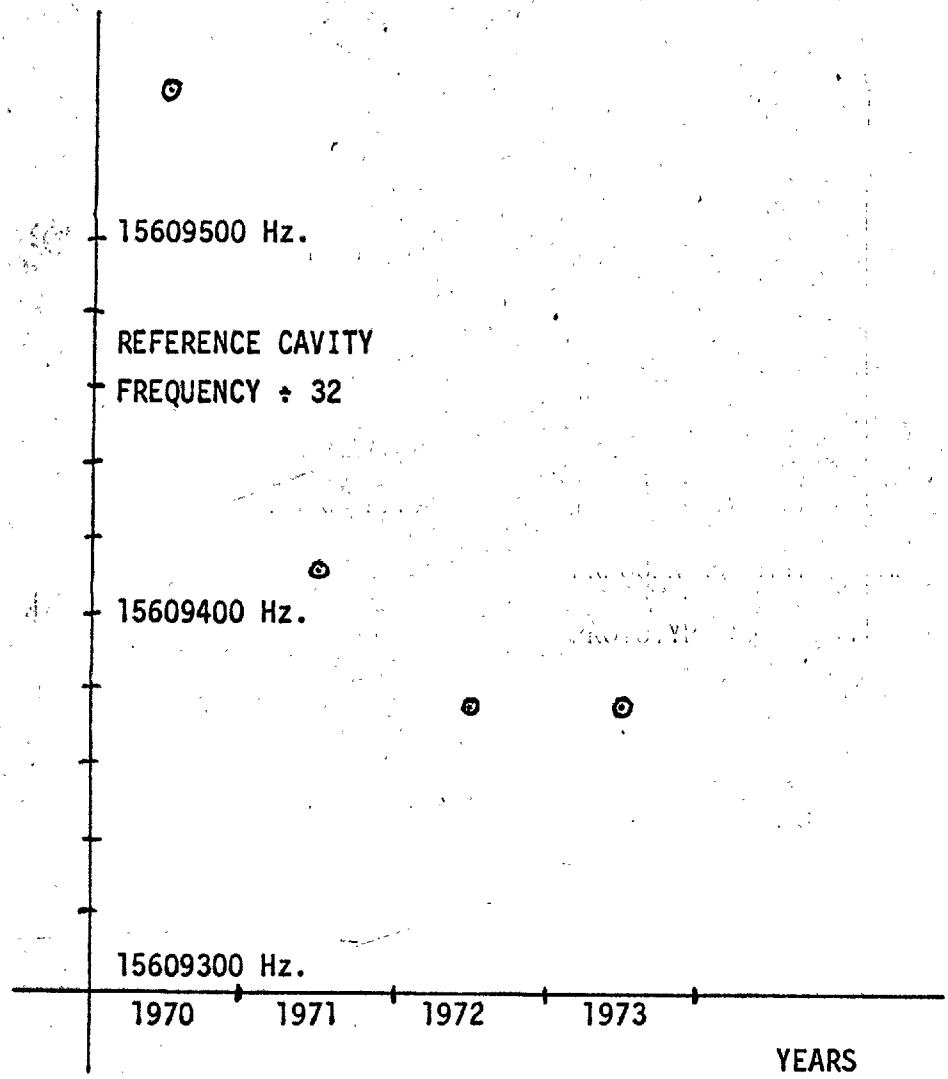
As was described before, this is simply a constant (independent of temperat -ure, pressure, or any of the usual variables) whose value depends both upon the target reflector used, and the version of the Mekometer.

The variation in its value from one reflector to another is about 30 mm.; and from one Mekometer to another about 150 mm. It is thus an important consideration.

The values of the corrections were originally determined to 1/100th mm. on an optical bench.

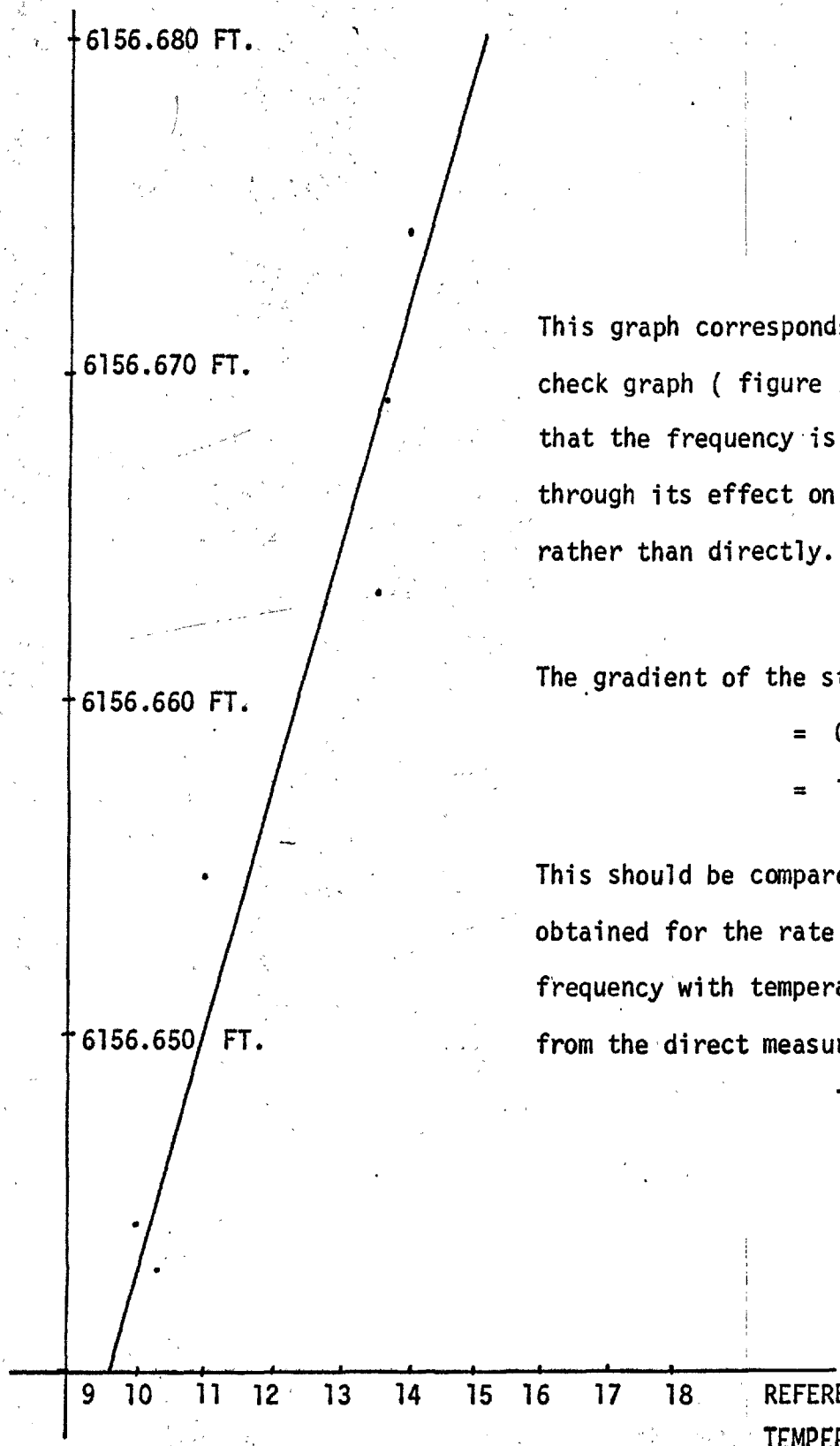
Since then they have been checked periodically by comparison with the N.P.L. standard cube corner, and no noticeable change in value has occurred throughout

FIGURE III.3 THE VARIATION OF REFERENCE CAVITY FREQUENCY WITH TIME, FOR THE SECOND PROTOTYPE MEKOMETER.



This curve suggests that, having been initially somewhat unstable, the reference cavity of the second prototype has now settled down such that its frequency at $0^{o}C$ is $(15609376 \pm 16) \times 32$ Hz.

FIGURE III.4 THE UNCORRECTED DISTANCE (AT CONSTANT REFRACTIVE INDEX) OF LINE 2 - 2/5 AT THINGVELLIR, MEASURED ON SEPTEMBER 26th, 1969.



This graph corresponds to a frequency check graph (figure III.2), except that the frequency is being determined through its effect on the distance rather than directly.

The gradient of the straight line

= 0.0073 FT. $^{o}C^{-1}$

= 1.2 ppm. $^{o}C^{-1}$

This should be compared with the value obtained for the rate of change of frequency with temperature determined from the direct measurements of

1.0 ppm. $^{o}C^{-1}$

the period of the measurements.

During this period too other target reflectors have been brought into use, notably triple cube-corner types, each of which has been calibrated by comparison with the N.P.L. standard.

To make this comparison the N.P.L. base-line is used. This line is about 300 m. long and has been measured and taped such that its length is known to ± 0.3 mm. However, its exact length is not important in the comparison of different reflectors. In the comparison the Mekometer is allowed to run for several tens of minutes on a cool, overcast day (the best weather conditions for making measurements, see a later section) so that it can come into equili--brium with the atmospheric temperature. The base-line length is then measured using the N.P.L. standard cube-corner. It is then remeasured with the unknown reflector, and then again measured with the N.P.L. standard. This process is continued for three or more stages and the resulting scatter in the various different estimates of the difference between the unknown reflector and the standard is found to be of the order of ± 0.2 mm. This is taken to be the accuracy of the method, and also of the various target reflector corrections.

Two other possible sources of uncertainty in the final distance results should be considered.

The first of these relates to the mounting brackets used for both the Mekom--eter and its retro-reflector; the second to the benchmarks.

No uncertainty which could be ascribed to the former source has ever been detected, despite efforts specifically designed to do so. This must be consider--ed a tribute to the skill of the machinists who built the mounting brackets.

The most likely source of error arising from the benchmarks is thought to be tilting of the concrete pillars. This has been monitored throughout the course of the measurements by means of a small inclinometer. The results show that there has been no observable effect. This is discussed further in chapter V.

Thus to summarise this section, all that need be said is that there are good grounds for believing that the modulating frequency correction is accurate to about ± 1 ppm., that the reflector correction is accurate to about ± 0.2 mm., and that other possible sources of instrumental uncertainty are unimportant.

SECTION III.3 ATMOSPHERIC CORRECTIONS.

The only correction involving atmospheric parameters is that for refractive index. This is a function of temperature, pressure, and, to a small extent, water vapour pressure (less than 1 part in 10^8 for the Mekometer wavelength). The empirical formula of Barrell and Sears (1939) describes the effects of temperature and pressure on the refractive index at S.T.P., derived for the relevant wavelength from the Cauchy expression, and including in this case an expression for group propagation.

The Barrell and Sears formula is

$$(n - 1) = (n_{st} - 1) . \frac{p . (1 + b_T . p) . (1 + 15.a)}{760 . (1 + b_{15} . 760) . (1 + a.T)}$$

with p the atmospheric pressure in mm. Hg.
T the effective atmospheric temperature in ^{o}C.
a = 0.003661
b = (1.049 - 0.015.T) x 10^{-6}
n_{st} the refractive index at S.T.P. (as above).

Thus, in order to correct for atmospheric refractive index all that need be measured are the temperature and the pressure.

SECTION III.4 ANALYSIS OF THE INFLUENCE OF THE ATMOSPHERE ON THE UNCERTAINTY.

Of the apparently simple measurements mentioned in the closing sentence of the last section, the second requires very little discussion. As was discussed in connection with the accuracy of the modulating frequency correction, pressure is measured with a commercial electronic readout aneroid barometer accurate to $\pm$ 0.1 mb., which means that the pressure contribution to the atmospheric refractive index is known to $\pm$ 0.1 ppm.

Air temperature measurements are, however, extremely difficult, and their accuracy depends very much upon the prevailing atmospheric conditions; these are divided into four classes by meteorologists, according to wind speed and

temperature fluctuations.

CLASS A THERMALLY INDUCED TURBULENCE: in which winds are very light and almost random in direction (records show direction changes of up to 180^{o} in a few minutes), and temperatures vary up to $10^{o}C$ in a minute. The temperature shows no well-defined mean such as might be used to calculate an effective refractive index.

CLASS B WIND INDUCED TURBULENCE: in which wind direction changes are normally less than 90^{o}, and temperatures fluctuate about a well-defined mean (which can be used to calculate aneffective refractive index.

CLASS C A mixture of classes A and B.

CLASS D STABLE: which is characterised by uni-directional, very light winds, with temperatures stable to $\pm 1^{o}C$ over long periods of time.

Measuring temperatures, or indeed distances, under conditions A or C is well-nigh impossible, and extremely inaccurate. These conditions are encountered almost always when the sun is shining, even in high latitudes through thin cloud. Measurements can only be made in sunshine when the air temperature is below $4^{o}C$.

Class B conditions are usable for Mekometer measurements provided that the wind speed does not exceed thirty kilometres per hour (Beaufort force four), and there is extremely thick cloud cover (as during the approach of a frontal system).

Class D represents perfect measuring weather. These conditions are met on fine days in late afternoon, and for the first few hours after nightfall. In high latitudes they can occur too on days of very heavy cloud cover and light winds. Late afternoon in Iceland begins at about 4 pm., even though there may be no darkness.

The possible influences that the atmosphere can exert on the accuracy of the measurements derive from three effects.

These are

a). Random perturbation of the refractive index causing both scattering of the propagating light beam with consequent loss of signal, and random phase fluctuations in the returning light (c.f. description of Mekom--eter, chapter II) which incur large scatter in the readings.

b). Misrepresentation of the true air path temperature due to inadequacies in the thermometric measurements.

c). Under extremely stable conditions, stratification of the air can cause great discontinuities in the temperature profile along the length of a line (extreme case of b). above), and even perhaps curvature of the light beam. This condition usually becomes noticeable after about 1 am.

Problems a). and b). are possible in atmospheric class B: problems b). and c). in class D.

The approach to overcoming these problems is different for each.

a). Random perturbations are dealt with statistically (Chernov, 1967), and the only way of treating their effects on distance measurements is to take a large number of readings. Hodara (1968) gives an approximate formula

$$\langle \Delta f_r^2 \rangle \simeq \frac{L L_c}{\lambda_0^2} \frac{\langle \Delta n^2 \rangle}{\tau_c^2}$$

where $\langle \Delta f_r^2 \rangle$ is the mean variance of the frequency fluctuations

L is the path length (c. 1000 m.)

L_c is the coherence length of the inhomogeneities (c. 0.1m

λ_0 is the wavelenght of the light beam (486 nm.)

T_c is the correlation time for the inhomogeneities ($=L_c/v_w$)

v_w is the wind speed

$\langle \Delta n^2 \rangle$ is the mean variance of the refractive index fluctuations

Thus frequency fluctuations of the order of 2 KHz. are to be expected in a wind of c. 10 $m.s^{-1}$ in conditions of moderate turbulence ($\langle \Delta n \rangle$ approximately 10^{-6}, corresponding to class B conditions).

Frequency fluctuations of this order will produce phase distortions of about 4 ppm., and distance measurement fluctuations of 4 mm. in a 1 Km. path length. The maximum which is ever encountered under class B is $\pm$ 3 mm., so that any form of analysis of these conditions is likely to be worthless.

b). Misrepresentation of the true air path temperature is considered to be the most likely source of serious error in both classes B and D. The problem really breaks down into three; finding air whose temperature is representative of the total path (difficult if the ground falls away steeply between the two end stations, or crosses water); estimating the effect of vertical gradients: and in class B measuring the station--ary mean temperature rather than the random fluctuations.

The first of these can only really be overcome by inspection. Temperature measurements should not be made too near the ground, near people or bushes, and they should be, whenever possible, in the free wind. If there is a water-crossing constituting a large proportion of the line then the air temperature must be measured above it specially. R.W.Calvert described the use of remote temperature sensors to overcome both this problem and that of vertical temperature gradients, but these have their own problems (notably calibration and deployment).

Only in very exceptional circumstances do vertical temperature gradients constitute much of a problem. Vertical lapse rates of more than $1.5^{o}C$ (either positive or negative) per 100 m. are not frequently encountered, and elevation differences between stations are very rarely more than 15 m., so that the effect is not likely to be partic--ularly great.($\pm$ $0.5^{o}C$).The practice (mentioned in chapter II) of measuring air temperatures at both ends of a line helps keep this effect down to minor importance.

The use of long time-constant mercury-in-glass thermometers is an effective way of removing the high frequency random fluctuations of temperature encountered in class B conditions, and leaving only the stationary mean to be used in the refractive index calculations. The obvious disadvantages of these thermometers are their fragility and the time required to come into equilibrium (section II.4).

Figure III.5 shows the results of an experiment designed to investig -ate the effectiveness of temperature measurements made at the ends of

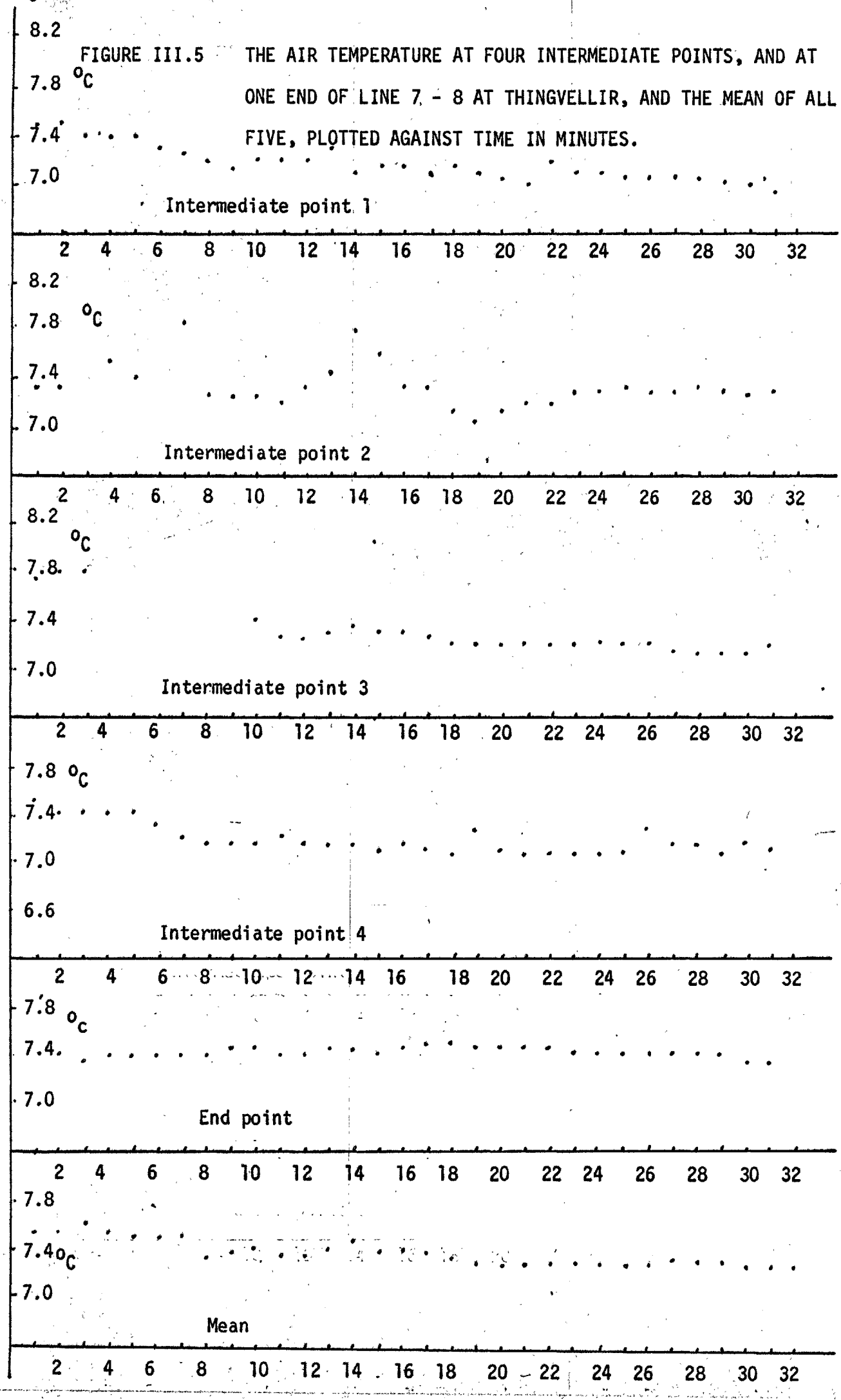


FIGURE III.5 THE AIR TEMPERATURE AT FOUR INTERMEDIATE POINTS, AND AT ONE END OF LINE 7 - 8 AT THINGVELLIR, AND THE MEAN OF ALL FIVE, PLOTTED AGAINST TIME IN MINUTES.

the line as indicators of the mean temperature along it.

In this experiment temperatures were measured every minute at four points along , and at one end of, a 1700m. long line in S.W. Iceland. The weather at the time was typical class D with heavy cloud cover, light southerly winds, and air temperatures around 7°C. The results for thirty minutes temperature measurements are shown, together with the average for all the stations each minute. The records are all essentially the same, although some are a little more erratic than others, and illustrate well the stability of class D conditions.

The mean air temperature is never more than 0.3°C from that observed at one end, and the two usually agree to within 0.1°C (which is the reading accuracy of the thermometers).

From this it is concluded that under atmospheric conditions of this sort, the uncertainty introduced by measuring air temperatures in this way is at most 0.5°C.

c). Normally the problem of path curvature due to refraction is completely unimportant (R.W.Calvert, 1969), but there are two particular situations which merit some particular attention.

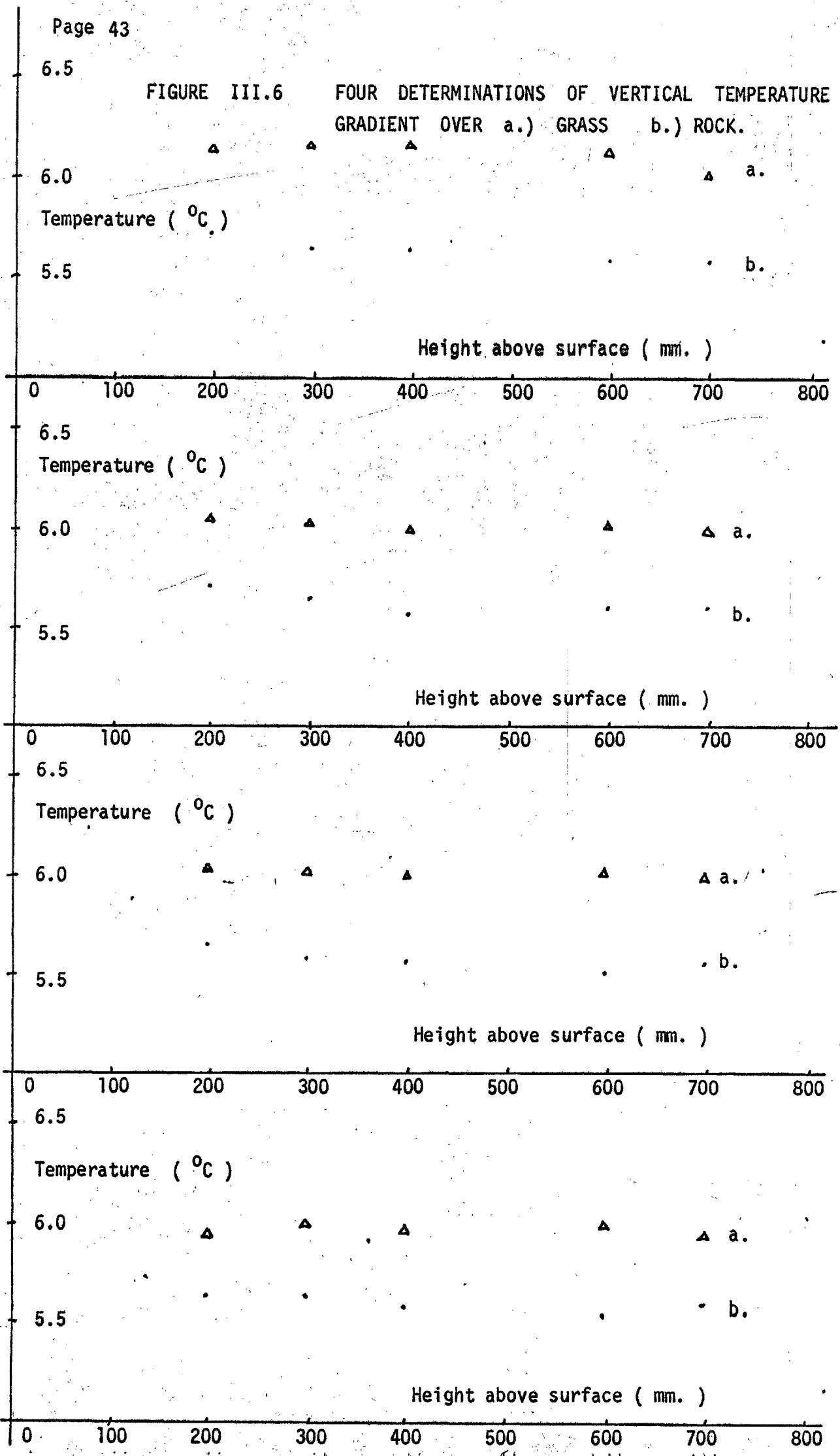
The first of thse concerns post- 2 am. conditions, which,as observed before,tend to be highly stratified; the second concerns lines which pass close to the earth's surface over long distances.

The first situation is easily dismissed by observing that it is not worth trying to make measurements at that time of day, as the degree of stratification is always serious, and will introduce some error even if it is not due to ray curvature.

To investigate the effect of the second situation, another experiment was conducted.

Five thermometers were mounted at fixed heights above ground level (200 mm., 300 mm., 400 mm., 600 mm., and 700 mm.).All were screened from sun and sky radiation, although well open to free air circulation (white polystyrene tiles lined with aluminium foil were used for the

FIGURE III.6 FOUR DETERMINATIONS OF VERTICAL TEMPERATURE GRADIENT OVER a.) GRASS b.) ROCK.



screens). Using this thermometer array the temperatures at these heights above rock and grass surfaces on a bright, sunny day (to accentuate any possible effect) were measured four times for each surface. The results of these measurements are shown in figure III.6.

It can be seen that there is some slight suggestion of a gradual temperature elevation at the lower heights above rock, which could amount to a gradient of a few degrees per metre at zero height. However, R.W. Calvert showed that gradients of at least $10^{o}C$ per metre operating over a large proportion of the air path if significant ray curvature was to be produced, so that it is justifiable to neglect this as a possible source of uncertainty.

The conclusion then from this section is that provided measuring is restrict--ed to times of the most suitable atmospheric conditions (at night if needs must), then the temperature measurements described in section II.4 are accurate to $\pm$ $0.5^{o}C$. If however measurements are made under other than ideal conditions (i.e. atmospheric classes A or C), then temperature uncertainties of perhaps as much as $\pm$ $5^{o}C$ are likely.

The effect of this uncertainty on the refractive index (and thus the corrected distance) determination may be ascertained by considering the partial derivative with temperature at constant pressure of the Barrell and Sears expression.

$$\frac{\partial n}{\partial T} = \frac{(n_{st}-1).(1 + 15a).p^{2}.\frac{\partial b_T}{\partial T}}{760.(1 + b_{15}.760).(1 + aT)} - \frac{(n_{st}- 1).(1 + 15a).(1 + b_T.p).p.a}{(1 + b_{15}.760).(1 + aT)^{2}.760}$$

At $15^{o}C$ and 760 mm. Hg. pressure, this expression reduces to

$$\frac{\partial n}{\partial T} = \frac{(n_{st}- 1).p.\frac{\partial b_T}{\partial T}}{(1 + b_{15}.760)} - \frac{(n_{st} - 1).a}{(1 + aT)}$$

With $a = 0.003661$
$n_{st} = 1.0003$

$\frac{\partial n}{\partial T} = -1.098 \times 10^{-6}$, so that $\pm$ 0.5 ^{o}C temperature uncert-ainty introduces $\pm$ 0.5 ppm. uncertainty into the refractive index.

SECTION III.5 SUMMARY OF THE VARIOUS CONTRIBUTIONS TO UNCERTAINTY AND COMPARISON WITH OBSERVATION.

This last section summarises the foregoing discussion of the various contributions to the uncertainty in the corrected distance measurements, and presents some experimental results in support of the conclusions.

The instrumental uncertainty has been shown to be almost wholly derived from the modulation frequency correction and amounts to $\pm$ 1 ppm. of the distance (the term arising from the reflector correction, $\pm$ 0.2 mm., is negligible in comparison on all the lines considered).

The atmospheric effect has been shown to be $\pm$ 0.5 ppm. of the measured distance (provided that suitable atmospheric conditions are used).

Thus the combined effect of the two is $\pm$ 1.5 ppm.

In figure III.7 (a) and (b) are shown the extreme scatter in the results from the lines at Thingvellir and at Reykjanes respectively. The scatter is determined either from the assumption of a linear change of distance with time (if there have been changes on a line) or from the apparent mean length throughout the measuring time if the distance has not changed.

Figure III.7 shows these scatters plotted against length of line.

Least squares fits have been made to both of the plots of scatter against length, with the following results.

At Thingvellir, the expression governing total scatter is

$$e = 0.5 + 2.3 \times D \times 10^{-3} \quad (\text{mm.})$$

and at Reykjanes, the corresponding expression is

$$e = 1.6 + 3.3 \times D \times 10^{-3} \quad (\text{mm.})$$

where, in both cases, D is the measured distance in metres.

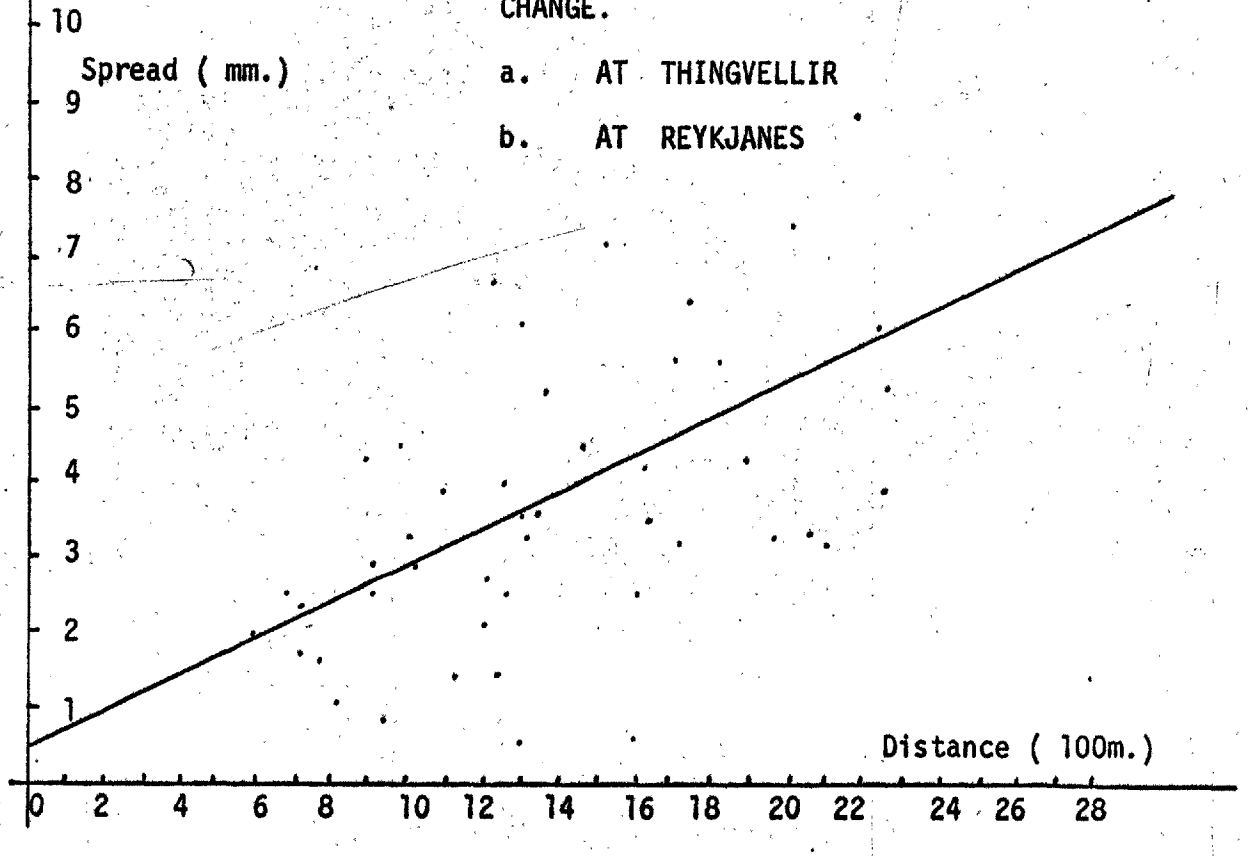
The scatters at Reykjanes are slightly larger than expected by a constant whose significance is not understood; but at Thingvellir the observed scatters are in excellent agreement with the quantitative analysis which has been conducted in the last few sections.

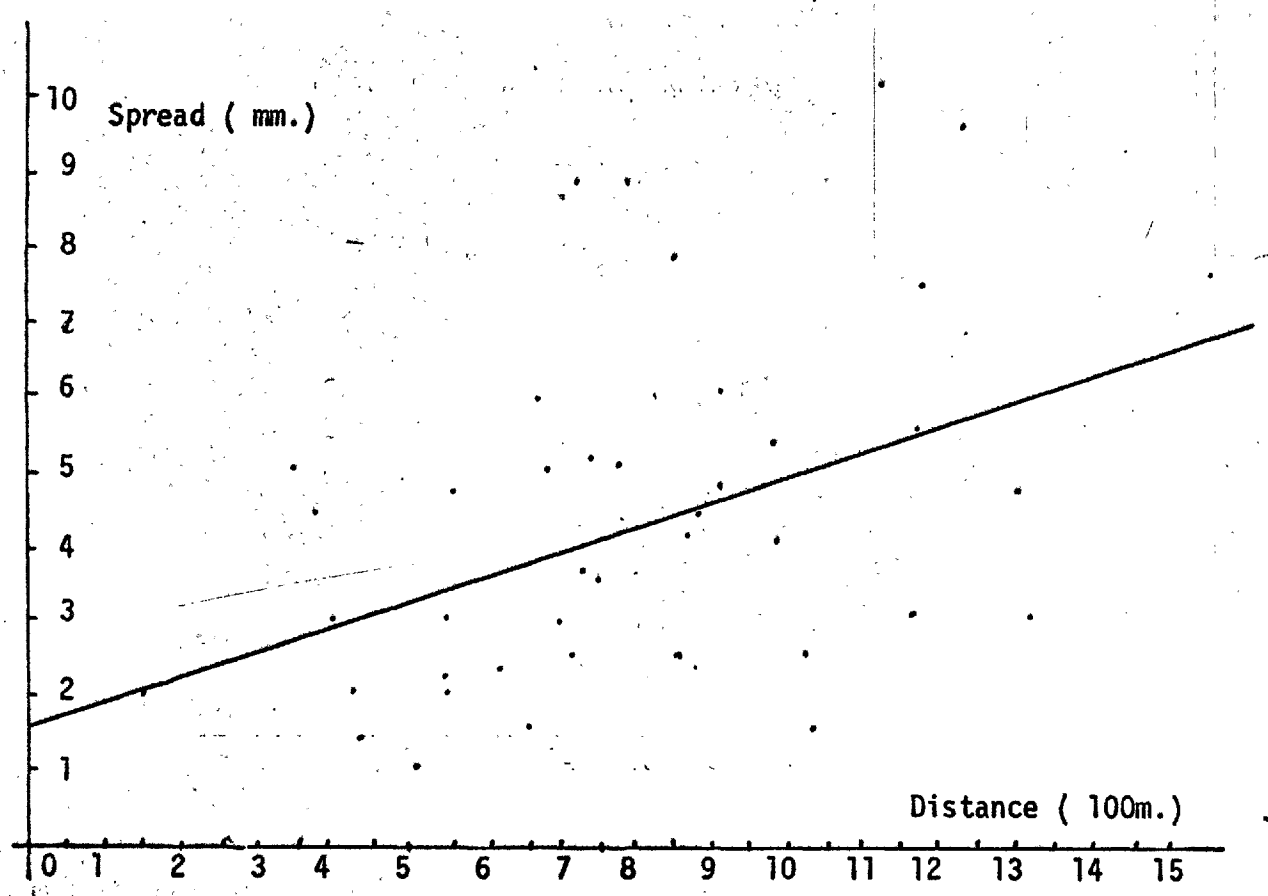
Whenever subsequently in this thesis an estimate is required of the likely

FIGURE III.7 THE GRAPH OF TOTAL SPREAD OF THE DISTANCE MEASUREMENTS ABOUT A CONSTANT RATE OF CHANGE.

a. AT THINGVELLIR

b. AT REYKJANES





The data from curve a. fit the straight line

$$\text{spread} = 0.511 + 2.3 \times D \times 10^{-6} \text{ mm.}$$

b. $$\text{spread} = 1.6 + 3.3 \times D \times 10^{-6} \text{ mm.}$$

uncertainty in a measured distance, the formula which will be used to evaluate it will be the analytically derived expression

$$e \text{ (mm.)} = \pm 1.5 \times D \times 10^{-3},$$ where D is the distance in metres.

Reference will be made to this expression later when the significance of observed changes is being considered, and when estimates of the uncertainty in calculated strain parameters and rates of movement are made.

CHAPTER IV. INTERPRETATIONAL TECHNIQUES.

SECTION IV.1 A REVIEW OF THE TECHNIQUES USED IN PREVIOUS EARTH STRAIN STUDIES.

This section, which discuses interpretational techniques applied to primary triangulation results, is included because it has been found that the problems which arise in triangulation have also great relevance to trilateration.

The standard surveying approach to the problem of determining displacements from repeat survey data is embodied in the method of Revised Geographical Co-ordinates.

This, briefly, involves the establishment of two- or sometimes three-dimens--ional Cartesian co-ordinate systems for all the stations in a network for each survey, and the comparison of the co-ordinates from each survey to give information on station displacements and thence on earth strains.

These co-ordinate systems are established from the adjusted survey angles and an assumed stable distance. (Adjustment in this context means least squares adjusting the observations from the entire network so that the discrepancy between the sum of the observed angles in each triangle and 180^{o} is minimised.)

In order that the co-ordinates for a station may be compared from one survey to another, it is necessary that each co-ordinate system be established relative to the same, unchanging origin. In usual triangulation surveys where inter-station spacing is about 15 Km. (chapter II), it is impracticable to tape the base station separation, so that until the very recent advent of long-range distance measuring instruments of high accuracy, the only control over the length of the base-line used to define the origin was the assumption that it had not changed between surveys. To make this physically justifiable the base-line had to be a long way from any areas of activity. Although exactly how far is not really completely known yet, it does seem from model studies (Chinnery, 1961) that the ground deformation associated with a fault on which strain is accumulat--ing extends to about five fault depths on either side of the surface trace (Savage and Burford, 1973). In California, where most of these studies have been undertaken, earthquake foci are normally about 7 to 10 km. deep. Assum-

-ing that this depth represents the region of maximum strain in Savage and Burford's (1970) first model (chapter I), then the effect of the 'sticking' section in their model may be expected to extend to as much as fifty kilometres on either side of the fault trace. That is to say that a base-line, in order to warrant the classification as stable, must be fifty kilometres, four standard primary geodetic stages (15 km. each) away from the fault.

Unfortunately, in establishing the co-ordinates of a station (perhaps one in an interesting area) it is necessary to make use of all the angles between that station and the base-line (origin). Thus all the observational errors (which will remain even after adjustment) between the area of interest and the origin will be included in the co-ordinates for each station, and after a few network stages these accumulated observational errors may easily become large enough to mask the possible ground movements.

These problems are exemplified by the results presented by Miller et al. (1970), which showed that the Imperial Valley underwent considerable right-lateral shear accumulation between 1951 and 1962. However, Nason (pers. comm. to C.R.Allen) has shown that the shear strain accumulated effectively disappears if a small length change of the (assumed fixed) base-line is allowed.

In order to circumvent these problems Frank (1966) proposed a method of interpreting survey results in which no assumptions of stability are made.

This method uses only the changes in a given triangle to evaluate the average shear strain operating over the area of the triangle, and thus neatly avoids the effects of survey error accumulation.

The principal shortcoming of the method is that it provides information only on the magnitude and direction of the shear strain, from which it is not possible to calculate the dilatation.

Another point of, as it turns out, minor importance concerning the method is its inherent assumption (by averaging the shear over the area of a triangle) that the strain is homogeneous. This is certainly not true in the case of displacements on a moving fault, although, as will be shown later, the error involved by this assumption is not very large.

As yet this method of Frank's has been used extensively by only one pair of authors to analyse the results from California (Savage and Burford, 1970), but the results obtained by them are generally more satisfactory than those from the same data by earlier workers. Indeed, using this technique they alone are able to find a consistent rate of movement along the entire length of the San Andreas fault.

The lack of information on dilatations and rotations (the fourth component of two-dimensional strain) is not considered in any way serious in California, where the movement is predominantly right-lateral shear.

It is hoped that the arguments presented in this section have effectively disposed the reader to the state of mind that grand co-ordinate analyses are wasteful and inaccurate, and that the subtler, local solution techniques are to be preferred, despite the decrease in the number of parameters which can be obtained (which is a much less serious problem in trilateration).

SECTION IV.2 THE DISPLACEMENT VECTOR ANALYSIS OF TRILATERATION RESULTS.

From the discussion presented in the last section it should be seen that 'local' solutions which use only the measurements from a given area to determine the parameters in that area are to be preferred to solutions requiring continuous carrying forward of results from one part of a network to the next.

Two different analysis techniques have been developed to deal with the trilateration results obtained during the course of this study; the first, which will be described in this section, produces displacement vectors from the changes of measured distance; the second, which will be considered later, is analogous to Frank's method (see above) in that it produces values of the (assumed homogeneous) strain parameters operating in an area.

The first technique is not entirely ' local ', in that in order to define a displacement vector there must be reference, whose motion is either known from some other information, assumed, or ignored.

The assumption of base-station stability was the root cause of both of the

problems associated with the Method of Revised Geographical Co-ordinates which was discussed in the last section.

Stability requires that the position vector between the two stations of the base-line does not change either in magnitude or direction; it has been shown that this requirement imposes considerable restraints on the suitability of lines to act as bases; violation of the requirement means that artificial displacements and rotations will be introduced into the station co-ordinates.

In trilateration unknown changes in station separation cannot occur, so that one part of the stability condition is no longer applicable. The other part of the condition, that involving the direction of the position vector, can in certain cases be ignored.

In an area (such as California, although it will not be considered in detail in this thesis) where a general tectonic direction is very well-defined and where there are no indications of activity in any other direction, it is very reasonable to assume that movements which are found on a base-line are in that direction, so that the second condition of stability is satisfied.

The consequences of this are that a 'pseudo-stable ' base-line can be used to calculate co-ordinates, and that this line can be very close to a fault.

It is as a result of this that it has been considered worthwhile to develop a displacement vector solution technique for the trilateration results, despite the conclusions of the last section.

Distance measurements lend themselves just as readily (or more so) as do angles to establishing Cartesian co-ordinate systems, except that the distances used must be horizontal. This entails measuring the elevation differences between stations (either by theodolite or by precise levelling profiles), and multiplying the measured distance by the cosine of the vertical angle, before proceeding to the Cartesian analysis.

This of course immediately introduces another source of error into the calculated co-ordinates, one which is, at least in the case of theodolite angles over more than three hundred metres, of somewhat larger magnitude than anything likely to be encountered in the distance measurements. Thus the

Cartesian analysis of trilateration results is likely to be as error-fraught as that of triangulation.

Despite this, displacement vectors have been analysed in this thesis, but using a form of analysis different from that of co-ordinates.

It is based upon the assumption that the displacements which occur are of very much smaller amplitude than the distances between stations, so that displacement of a station perpendicular to the line between it and its neighbour will have no effect upon the length of that line. In earth strain work, movements of more than a few millimetres are seldom encountered, and as the line lengths used in Mekometer surveys are generally of the order of 1 km. (chapter II) this assumption is valid. Indeed it only breaks down when the ratio of movement to station separation becomes as large as 10^{-3}, so that in Mekometer applications the technique should still be approximately valid even for the displacements occurring after large earthquakes (c. 5 m.).

The algebraic statement of this technique is

$$dL, \text{ the change in length of a line} = \frac{\underline{r}}{|\underline{r}|} d\underline{u}_1 + \frac{\underline{r}}{|\underline{r}|} d\underline{u}_2$$

where $\underline{r}$ is the position vector of the line

$|\underline{r}|$ its modulus

$d\underline{u}_1$ and $d\underline{u}_2$ are the displacement vectors of the end stations

and the dot vector product has its usual meaning.

The validity of the assumptions involved in this technique are illustrated in Appendix A, where an elementary solution is shown.

The great advantage in using this technique (apart from its extreme simplicity) lies in the fact that using slant distances instead of horizontal ones makes no appreciable difference to the result.

The example given in Appendix A can be described verbally as follows.

There are three stations forming the apices of a triangle, one of whose stations has moved . Thus there will be observable length changes on two of the three sides. The third side, which has not changed length, is chosen as the base line, and both stations are taken to be fixed. The components of the displacement vector of the moving station are the changes of length on the two lines, in the

directions of the two lines. Knowing two components of a vector makes it possible to calculate its magnitude and direction, so that the displacement may be determined.

In more complicated figures it is possible to propagate a solution based upon this across several stages of movements.

In the double-braced quadrilateral, which has been shown (chapter II) to be the most suitable figure for trilateration, displacement vector solutions can be made for two of the stations (in terms of a pseudo-stable base, see above) which involves only five of the available six lines, leaving a redundant one which can be used as a check on the consistency of the solution. Using this redundancy it is possible to least squares adjust the solution in an elementary quadrilateral in order to give the best fit to the observed and calculated length changes.

Using this technique it has been found possible to obtain displacement vectors across several stages of a network, and thereby gain some extremely interesting information, although the total distance that these solutions can be continued is limited by the effects of error accumulation.

SECTION IV.3 THE HOMOGENEOUS STRAIN SOLUTION IN TRILATERATION.

In much the same way as Frank's method derives local shear strain information from the angle changes within a triangle, it is possible to obtain values for both shear strain (magnitude and direction) and dilatation from length changes within a triangle.

By solving the expressions of the form

$$e_i = \tfrac{1}{2}.\Delta + \tfrac{1}{2}.\Gamma.\cos 2\phi_i$$

where Δ is the dilatation,

Γ is the shear,

and e_i is the strain in a given direction ϕ_i to the principal extension axis, simultaneously in three directions (i.e. the lines of a triangle) it is possible to determine the values of average shear, average dilatation, and

the direction of maximum extensional strain operating within the triangle.

As is the case with Frank's method applied to angles, this does not completely define the strain, as there is an unknown rotation component (which may only be defined with reference to an external fixed point e.g. astronomical observation).

The elementary quadrilaterals used in the trilateration networks each contain four triangles, so that from each quadrilateral four values of each parameter are available. These are not independent, but consistency among them gives some indication of the validity of the strain solution.

SECTION IV.4 COMPARISON OF THE TWO ANALYSIS METHODS USED FOR THE TRILATERATION DATA, AND DISCUSSION OF THE LIMITATIONS OF EACH.

From a theoretical viewpoint the analysis for displacement vectors is very much to be preferred to that for homogeneous strain.

There are three possible reasons for a station's position to change, only one of which involves true homogeneous strain, so that the displacement vector analysis is very much more general.

These three possible reasons are

1. Local disturbance of one station.
2. Fault slip.
3. Homogeneous strain.

The first of these should be apparent from the pattern of line changes, at least in a complicated network, so that if the only changes observed in a network are all associated with one station, it is fair to assume that the station has moved, probably in a non-tectonic way, although the latter conclusion does not necessarily follow.

In not-too-complicated networks, it should be possible to identify pure fault displacements, especially if a displacement vector solution is conducted.

However, as a network becomes more complex, the second and third cases will become more and more confusable, especially when a large number of faults is involved; indeed it is probably true to say that the movements on a large number of faults will approximate to a homogeneous strain state.

In a very confused situation where there is no well-defined tectonic direction, and almost every line has undergone some change of length, the choice of a suitable baseline from which to make a displacement vector analysis becomes impossible, and the only approach to analysing the results is through the homogeneous strain assumption.

Appendices B and C illustrate two of the situations that can arise when displacements arising from movement on faults are assumed to be due to homogene--ous strain.

Appendix B illustrates the position for a pure strike-slip fault: appendix C for pure extension.

The example of Appendix B is a 100m. square, two of whose stations are displaced right-laterally by a +X trending fault which bisects the quadrilateral. The homogeneous strain analysis of the subsequent distance changes shows the correct axis of maximum extension (45^{o} counterclockwise of +X, which according to elementary cosiderations of maximum shear directions indicates axes of maximum shear orientated at +X and +Y, the former right-lateral, the latter left-lateral). But it shows an overlarge value of the shear (1.4 instead of 1), and is of course unable to distinguish which is the true shear direction (although in this case inspection of the arrangement of the original changes would have revealed that).

The pure extension example (appendix C) gives very much more misleading results. Here the strain analysis indicates that there has been considerable shear in addition to the positive dilatation (which indicates the extension). In this simple example it is easy to see that the shear in each of the four triangles of the quadrilateral alternates between right- and left-lateral, and that these should be given alternate signs when considering the whole figure so that the net shear is zero. However, if this were not appreciated then an

entirely spurious shear would be attributed to this quadrilateral.

The behaviour of the direction of maximum extension is also noteworthy.

It can be seen in appendix C that there are two distinct directions indicated by the four triangles, neither of them correct, but equally spaced about the true axis of extension. Thus the average of these two groups will give the true direction of extension, and the alternation suggests the purely extensional nature of the real movement.

Thus it may be seen that considerable care should be exercised when inter--preting the results obtained by homogeneous shear analysis, particularly if the extension directions in a quadrilateral show the alternation noted above.

It will also be observed that applying the displacement vector solution would have given the correct result immediately.

Unfortunately though, the displacement vector solution does suffer from the problem of error accumulation, in much the same way as the Cartesian analysis of triangulation results does. It is not normally possible to continue a displacement solution across more than three network stages without a massive possible uncertainty building up. This, coupled with the difficulty of base-line choice in a tectonically confused area, effectively limits the application of displacement vector solutions to comparatively simple situations, leaving all more complex ones to the homogeneous strain analysis.

CHAPTER V. ANCILLARY MEASUREMENTS

SECTION V.1 TILTMETER RESULTS.

The tiltmeter is a small inclinometer used to monitor the stability of the Icelandic concrete pillars.

It consists of a four inch long spirit bubble, with five-second divisions on it. It is attached by phospher-bronze springs to a base plate at one end, whilst its other end may be moved up and down by means of a $1/1000^{th}$ inch micrometer.

The base plate, which is six and a half inches long, is supported clear of the surface whose tilt is being measured by three small feet, which are only three and three quarter inches inches apart. These ensure that the plate, which is wider than the bronze mushrooms used in the Icelandic bencharks, is not fouled by pieces of extraneous cement which often protrude above the level of the top of the mushroom.

In order to measure the tilt in any direction, this instrument is aligned in the direction required, and the micrometer is adjusted until the bubble is exactly level. The process does take a little time, but the observed repeatab--ility of tilt measurements made with this instrument is $\pm$ .0015 inches of the micrometer scale, which corresponds to 400 microradians. This, in turn, corresponds at the height of the top of a concrete pillar (they are all the same height) to an uncertainty of $\pm$ 0.5 mm.

Complete tilt surveys have been made on the two main Icelandic networks, Thingvellir and Reykjanes (figure V.1), twice, in 1969 and 1971, and partially in 1972 also. Of the one h undred or so pillars in these two networks none has tilted significantly over the measuring period (1968 - 1972). Figure V.2 shows the typical tilt rosette which is drawn for each pillar. Only the one (for pillar 6 at Reykjanes)is reproduced in this thesis.

This absence of observable tilt of the benchmarks is of interest in a tectonic context, as it presumably sets an upper limit on the rate of tilt deformation of the ground surface.

Figure V.3 is a map (reproduced from Piper (1971)) of the dips of the

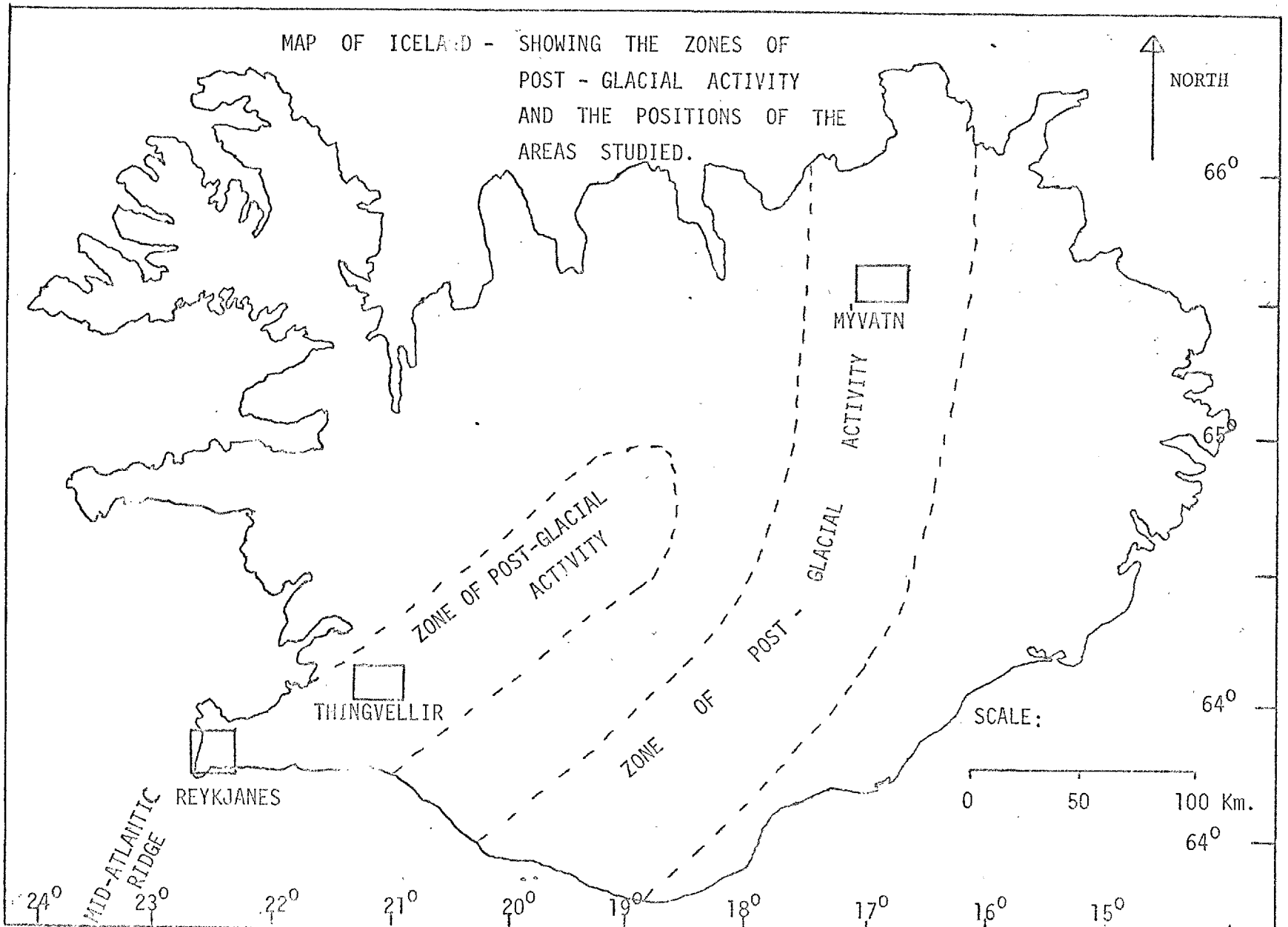

MAP OF ICELAND - SHOWING THE ZONES OF POST - GLACIAL ACTIVITY AND THE POSITIONS OF THE AREAS STUDIED.
NORTH
MYVATN
ZONE OF POST-GLACIAL ACTIVITY
ZONE OF POST - GLACIAL ACTIVITY
THINGVELLIR
REYKJANES
MID-ATLANTIC RIDGE
SCALE:
0
50
100 Km.
66°
65°
64°
64°
24°
23°
22°
21°
20°
19°
18°
17°
16°
15°

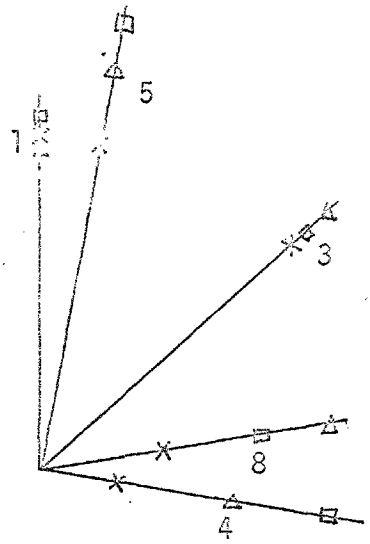
FIGURE V.1

FIGURE V.2 DIAGRAM SHOWING THE MAGNITUDES OF THE TILTS, IN VARIOUS DIRECTIONS, OF STATION 6 AT REYKJANES IN 1969, 1971, AND 1972.

△ 1969

□ 1971

× 1972



THE DIRECTIONS ARE GIVEN BY THE SMALL NUMBERS ALONGSIDE EACH LINE, WHICH REFER TO THE STATION CONCERNED.

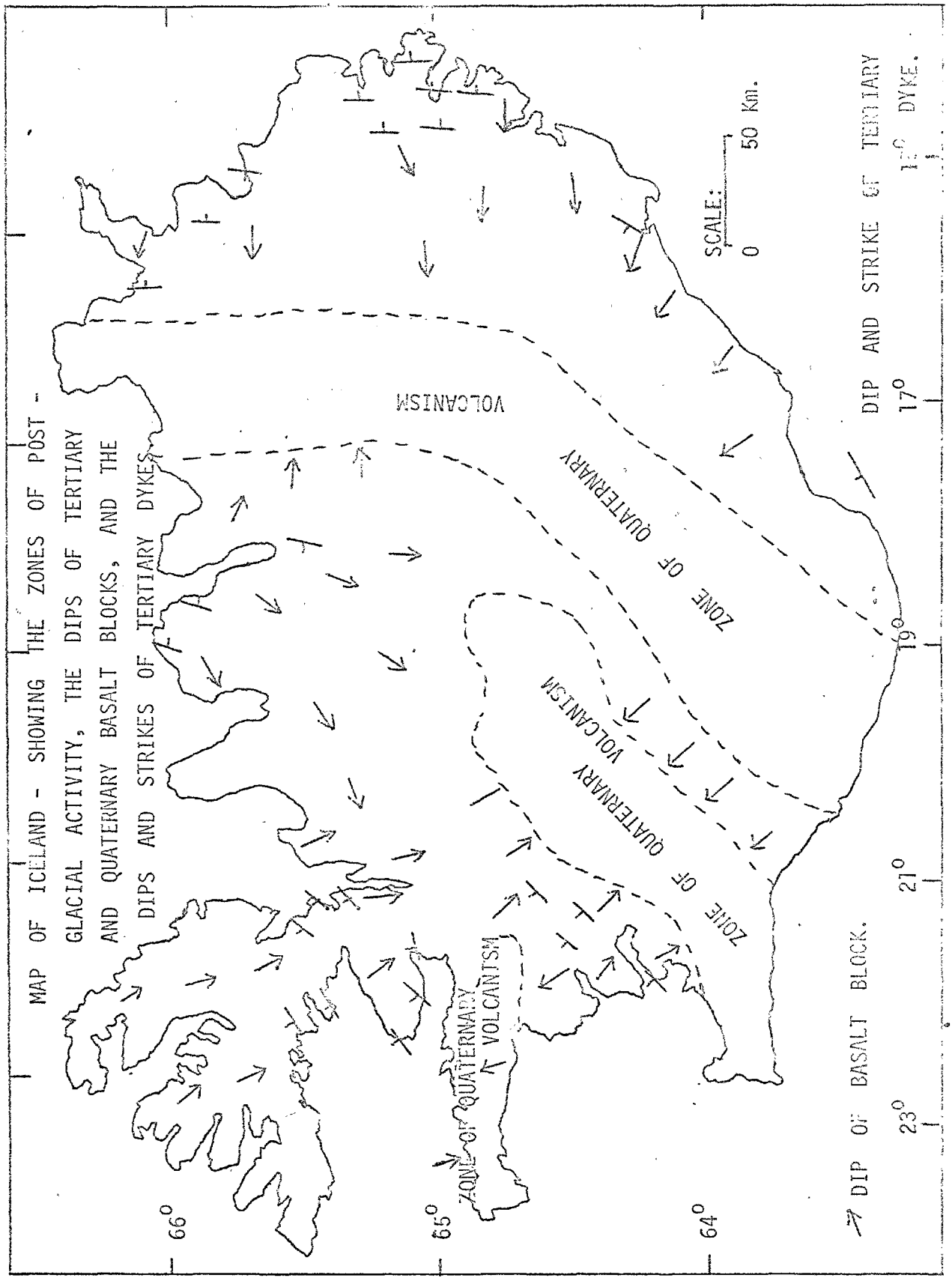
EACH VECTOR SHOWS THE MAGNITUDE OF THE DEVIATION FROM HORIZONTAL IN THAT DIRECTION.

THE VECTOR SCALE IS

1 cm. : 1.5 milliradians.

THE ESTIMATED UNCERTAINTY ON EACH TILT MEASUREMENT IS ± 0.4 milliradians.

FIGURE V.3


MAP OF ICELAND - SHOWING THE ZONES OF POST - GLACIAL ACTIVITY, THE DIPS OF TERTIARY AND QUATERNARY BASALT BLOCKS, AND THE DIPS AND STRIKES OF TERTIARY DYKES
VOLCANISM
ZONE OF QUATERNARY
ZONE OF QUATERNARY VOLCANISM
ZONE OF QUATERNARY VOLCANISM
SCALE: 0 50 Km.
DIP AND STRIKE OF TERTIARY DYKE.
DIP OF BASALT BLOCK.
66°
65°
64°
23°
21°
19°
17°

Tertiary basalt blocks. Many of the dips can be seen to be towards the currently active zones of south-west and central Iceland, and it is possible that there is some connection between the faulting and spreading processes in the active zones and the tilts of the older basalt blocks, although Walker (1965) and Gibson and Piper (1972) consider the dip to be of non-tectonic origin, and simply a consequence of the process of growth of the lava pile.

The lava blocks are usually of the order of 10 km. long, and the observed dips are about 10^{o} (between 6^{o} and 15^{o}).

If crustal extension is occurring at the rate of 20 mm. per year, then each block must spend about 10000 years immediately under the influence of the extensional processes. The annual rate of tilt indicated is thus 10^{-5} radians per annum, so that with the sensitivity of this instrument 100 years would be needed before any change of tilt was observed.

The null result indicated by the measurements is therefore not especially significant, tectonically, although it does show that the concrete pillars have been stable .

SECTION V.2 VERTICAL ANGLE MEASUREMENTS.

Tables V.1 and V.2 show the results of vertical angle measurements made with a Hilger and Watts Microptic No. 2 (1 second) instrument on the two principal Icelandic networks in 1968 and 1973.

At the time of the original survey these measurements were thought to be required only to make slope corrections to the measured distances (for analysis by Cartesian co-ordinates), but then it was noticed that many of the slope angles are greater than 1^{o} so that, as is shown in section II.3, vertical movements can easily contaminate the distance measurements.

Indeed it was further found more recently that extremely interesting solutions to the observed changes would be possible if very large vertical deformations had occurred ; thus a repeat angle survey was made in 1973, covering those lines which would have had to have shown large vertical changes

TABLE V.1 VERTICAL ANGLE MEASUREMENTS AT THINGVELLIR

LINE	1968	1973	DIFFERENCE	UNCERTAINTY
3/4 - 3	1 24 50	1 25 27	37	±35
3/4- 4	1 48 53	1 48 55	2	±35
3/6 - 3	1 13 29	1 12 29	60	±35
3/6 - 6	0 09 08	0 09 23	15	±35
4/5 - 4	0 31 02	0 30 48	14	±40
4/5 - 5	1 32 03	1 32 07	4	±40
4/6 - 4	0 33 36	0 33 39	3	±40
4/6- 6	-0 37 14	-0 36 30	44	±30
4/7 - 4	0 41 59	0 41 56	-3	±35
4/7 - 7	0 45 40	0 45 48	8	±30
4/8 - 4	0 29 08	0 29 23	15	±40
4/8 - 8	1 57 37	1 58 41	64	±40
6 - 7	0 40 36	0 39 47	-49	±40
6/11 - 6	0 14 44	0 14 01	-43	±40
6/11 - 11	2 48 37	2 48 26	-11	±40
7/11 - 7	-0 16 05	-0 15 52	13	±45
7/11 - 11	2 28 58	2 28 59	9	±35
7/12 - 7	-0 54 02	-0 53 39	-2	±40
7/12 - 12	5 34 59	5 35 12	11	±40
8/12 - 8	-0 41 09	-0 41 11	-2	±45
8/12 - 12	4 37 42	4 37 23	-19	±40
9/12 - 9	-0 11 38	-0 11 49	-11	±40
9/12 - 12	3 39 04	3 38 13	-51	±45
11/12 - 11	-2 08 36	-2 09 14	-38	±40

TABLE V.1 (Continued)

11/12 - 12	5 31 17	5 32 42	85	±40
12/13 - 12	1 03 37	1 03 39	2	±40
12/13 - 13	-2 32 00	-2 32 29	-29	±35
11/15 - 11	-3 47 19	-3 47 27	- 8	±35
11/15 - 15	3 49 21	3 49 39	18	±30
12/15 - 12	-0 43 16	-0 42 43	33	±35
12/15 - 15	1 54 04	1 53 40	-24	±35

TABLE V.2 VERTICAL ANGLE MEASUREMENTS AT REYKJANES

LINE	1968	1973	DIFFERENCE	UNCERTAINTY
1 - 2	-2 43 03	-2 42 46	17	±10
1 - 3	-3 59 11	-3 58 53	18	±10
3 - 1	3 58 24	3 58 30	6	±10
4 - 1	3 29 51	3 29 26	-25	±20
1 - 5	-2 08 59	-2 08 49	10	±20
5 - 1	2 08 05	2 07 47	-18	±20
1 - 6	-3 07 53	-3 08 08	-15	±20
6 - 1	3 07 37	3 07 43	6	±20
1 - 8	-0 37 30	-0 36 52	38	±35
1 - 27	4 29 05	4 29 35	30	±20
2 - 3	-2 10 26	-2 11 06	-40	±20
3 - 2	2 10 05	2 09 44	-21	±20
3 - 6	0 36 46	0 37 15	29	±25
2 - 7	-0 47 12	-0 47 29	-17	±30
2 - 27	5 18 02	5 17 42	-20	±20
3 - 7	0 06 07	0 06 11	4	±25
3 - 27	4 53 10	4 53 14	4	±20
4 - 6	2 01 56	2 01 56	0	±20
6 - 4	-2 02 34	-2 02 12	22	±20
5 - 4	-1 10 44	-1 11 01	-17	±20
5 - 6	0 18 34	0 18 22	-12	±10
6 - 5	-0 19 03	-0 18 53	10	±10
[illegible] - 8	0 51 10	0 51 16	6	±30
6 - 8	0 40 14	0 39 55	-19	±30

TABLE V.2 (Continued)

5 - 9	0 47 56	0 48 04	8	±20
10 - 8	0 40 56	0 41 26	30	±30
10 - 9	0 21 33	0 21 17	-16	±30
10 - 11	-0 30 16	-0 30 00	-16	±20
10 - 12	-0 29 04	-0 29 22	-18	±25
10 - 13	0 01 05	0 00 48	-17	±40
11 - 8	0 45 11	0 44 57	-14	±30
11 - 13	0 24 22	0 24 27	5	±25
11 - 14	1 03 10	1 02 52	-18	±30
12 - 9	0 30 02	0 29 48	-14	±40
12 - 13	0 41 44	0 41 13	-31	±30
12 - 15	1 06 14	1 05 57	-17	±35
11 - 10	0 29 39	0 29 42	3	±20
28 - 8	-1 05 11	-1 04 36	35	±35
28 - 27	0 05 49	0 05 41	- 8	±20

if the suggested solution was indeed correct.

The two tables show all the observed changes, and the uncertainty in the change (derived from the scatter in repeat observations).

In no instance does the observed change approach the requirement of the suggested solution, and the effects of the changes on the distance measurements are all very small, at most three millimetres on one of the Reykjanes lines which shows a total length change of 16 mm.

On short lines, which at Reykjanes are also the ones which show considerable slope, the precision of these vertical angle measurements is sufficient to impose maximum limits on the vertical movements which are quite small, such that the corresponding uncertainty effect on the distance measurements is $\pm$ 1 mm. All these short lines at Reykjanes show total length changes in excess of 10 mm., so that the effect of vertical movements is not after all very large on this network, although the odd millimetre which is involved has been taken into account in the final analysis.

At Thingvellir however, there are some very long lines which slope very steeply, and here the uncertainties in the vertical angle measurements are so large that there is no way of distinguishing how much, if any, of the observed distance changes are the result of vertical movements. In the analysis of the Thingvellir results, vertical movements have been considered unimportantly small, in keeping with the results of Tryggvason (1968).

SECTION V.3 TECTONIC INTERPRETATION OF THE VERTICAL CHANGES OBSERVED AT REYKJANES.

Table V.3 lists all the vertical movements found at Reykjanes between 1968 and 1973. It shows not only the vertical displacements derived directly from the observed angle changes, but also the displacements after adjustment for consistency.

The consistency criterion used was that the vertical movements should constitute a conservative field; adjustments were made within the bounds

TABLE V. 3 REYKJANES VERTICAL MOVEMENTS.

LINE	OBSERVED V.A. CHANGE	HEIGHT CHANGE (mm.)	ADJUSTED HEIGHT CHANGE (mm.)	EFFECT OF ADJ. HEIGHT CHANGE ON MEASURED DISTANCE
1 - 2	17 ± 10	33 ± 41	63	-3 mm.
1 - 3	18 ± 10	15 ± 50	15	-1 mm.
2 - 3	-40 ± 20	-19 ± 40	-49	2 mm.
1 - 4	25 ± 20	97 ± 64	44	-3 mm.
1 - 5	14 ± 20	52 ± 80	41	-2 mm.
1 - 6	- 4 ± 20	-25 ± 50	25	-1 mm.
5 - 6	-11 ± 10	-16 ± 29	-16	0
4 - 6	-11 ± 20	-19 ± 34	-19	0
1 - 8	38 ± 35	244 ± 128	161	-2 mm.
5 - 8	6 ± 30	30 ± 99	120	2 mm.
6 - 8	-19 ± 30	64 ± 112	136	2 mm.
1 - 27	30 ± 20	22 ± 15	7	0
2 - 27	-20 ± 20	-101± 50	-56	-5 mm.
3 - 27	4 ± 20	11 ± 54	- 8	-1 mm.
28 - 27	-8 ± 20	9 ± 30	7	0
28 - 8	35 ± 35	231 ± 132	161	-3 mm.
3 - 6	29 ± 25	99 ± 85	10	0
4 - 5	17 ± 20	44 ± 51	-3	0
2 - 7	-17 ± 30	-85 ± 90	-35	0
3 - 7	4 ± 25	14 ± 72	14	0
5 - 9	8 ± 25	25 ± 80	25	0

in one instance) of the observed uncertainty, with weighting to individual changes given in inverse proportion to that uncertainty.

A map, figure V.4, shows the distribution of vertical changes observed at Reykjanes.

The 1973 survey included only those lines that the initial solution showed to have involved large vertical changes. These were all on the southern end of the network, so that there is no information on the vertical movements at the northern end of the network.

On figure V.4, station 8 has been chosen as reference, and all the changes are shown relative to it.

All stations seem to have subsided to some degree, with particularly large downward movements associated with the geothermal field (stations 3, 4, 5,and 6) and with the small post-glacial shield volcano, Skálafell (stations 1, 27, and 28).

The geothermal field associated movements will be considered later, after the presentation of the distance measurements (chapter VI.).

Otherwise (disregarding the movements on Skálafell, which are probably related to the geothermal field as steam vents occur all up its sides), from the movement pattern shown by stations 2, 9, and 7 there is a suggestion of regional subsidence of the area to the north-west relative to the south-east, at a rate (highly uncertainly determined) of 25 mm. per year. The uncertainty limit on this estimate is easily as large as the estimate itself, so that in real terms the significance is very low. Despite this however, it is thought to be valuable to compare this result with the only other information on vertical movements which is available from the Reykjanes peninsula.

This comes from the precise levelling work of Tryggvason (1968), who established a short profile across Búrfellshraun (some thirty kilometres north-east of the trilateration network) in 1966.

Between 1966 and 1967 he observed subsidence of 10 mm. in a narrow graben, and 5 mm. regional subsidence towards the south-east.

His results are considerably more accurate than those obtained with the

theodolite, and it could be that the movements found on the triangulation network are so imprecisely determined that even the sign is wrong.

This is thought to be unlikely though, and another possibility of comparing the two results is considered worth investigating.

This is that the two groups of movements represent the situation on opposite sides of a broad zone of subsidence, such as might be associated with the axial zone of a mid-ocean rise. This would suggest that the centre of the axial zone lies to the north-west of the geothermal area, and to the south-east of the levelling profile at Bürfellshraun.

Figure V.5 is a tectonic map of the area of the trilateration network at Reykjanes , from which it may be seen that there is an area of considerable faulting to the north of the geothermal field. Many of the faults there are normal defining quite large grabens, and there is a continuous larger scale depression running inland from the bay which lies just north of 63^{o} 50'.

The microearthquake work of Klein et al. (1973) suggests very much that the axial zone of the mid-Atlantic ridge does indeed run along this larger scale depression, which would mean that the observed vertical movements represent continuing activity of the ridge.

The Bürfellshraun levelling profile can be seen on Kjartansson's (1960) geological map of south-west Iceland to be on the north-western flank of one of the en echelon eruption lines of which the Reykjanes peninsula is made up. Thus Tryggvason's results too might very well be construed as representing continued down-faulting of the axial zone of the mid-Atlantic ridge.

The trilateration network is a great deal nearer its section of the ridge axis than is the precise levelling profile, which difference may be responsible for the difference in average rates of subsidence. Indeed the observed rate of subsidence of station 7 relative to station 8 (25 mm. per year) is the sort of value which has been expressed as likely for the axial zone of a mid-ocean ridge (Tryggvason, 1970).

Thus it seems very much as though, despite their very much ancillary role in the research programme, the vertical angles have provided some most interesting results.

FIGURE V.4 THE VERTICAL MOVEMENTS OBSERVED AT REYKJANES BETWEEN 1968 AND 1973, IN MILLIMETRES.

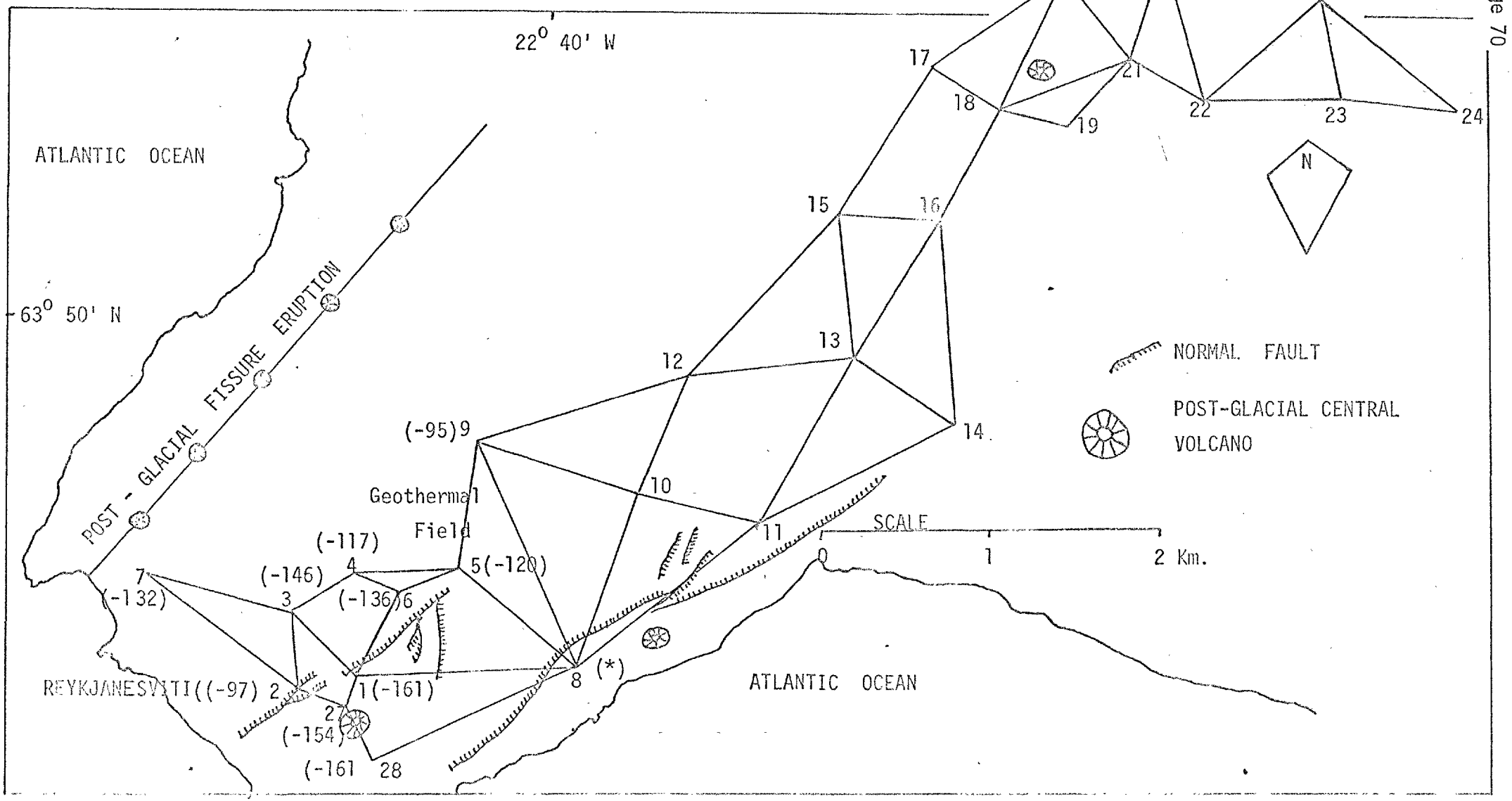
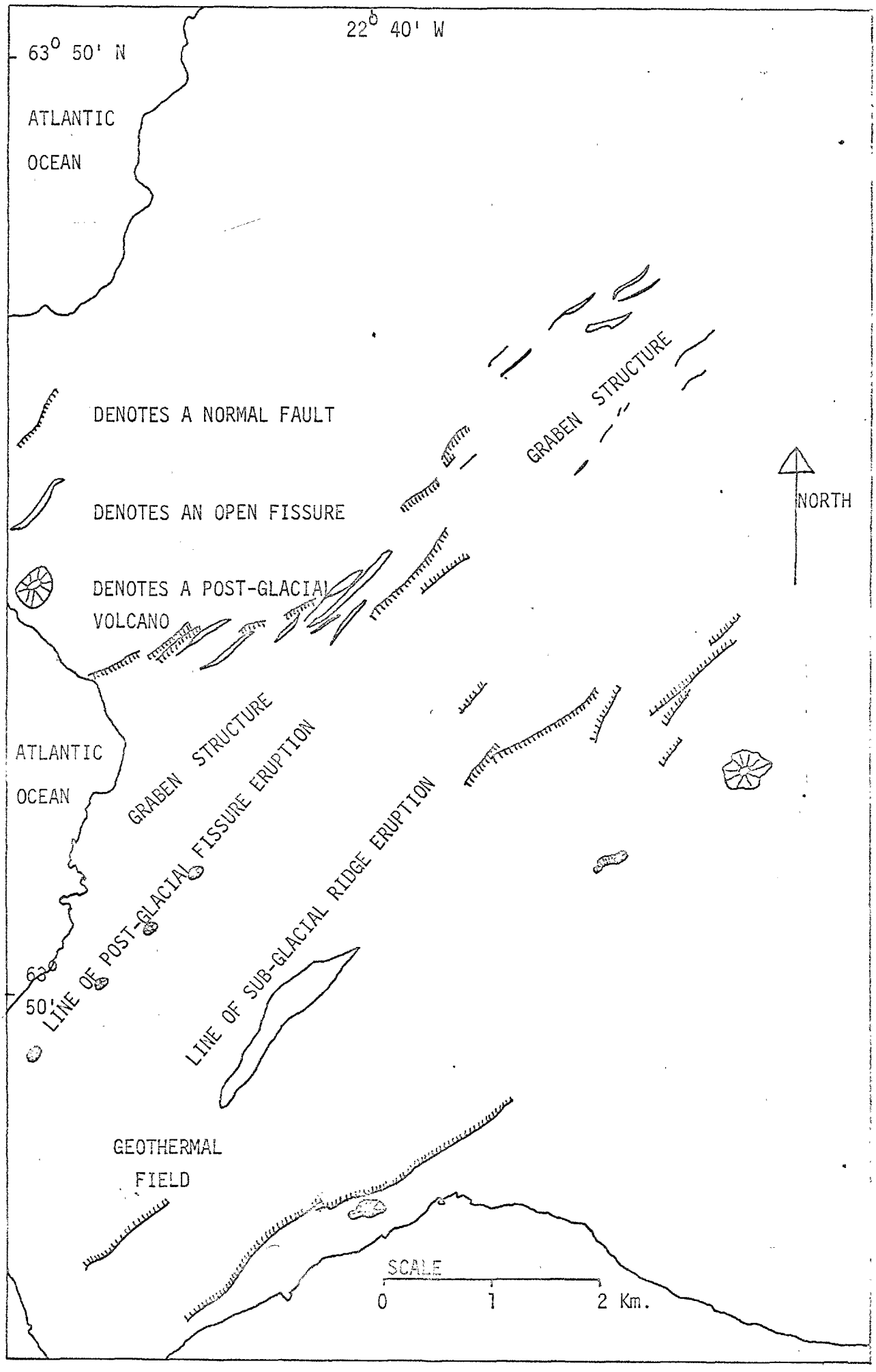


FIGURE V.5 TECTONIC MAP OF THE SOUTH-WESTERN END OF THE REYKJANES PENINSULA.



CHAPTER VI. THE RESULTS OF THE DISTANCE MEASUREMENTS IN ICELAND.

SECTION VI.1 THE MÝVATN MEASUREMENTS.

Figure VI.1 shows the positions of all the Icelandic trilateration networks whose results will be considered in this thesis. As has been observed before (Chapter II) all the benchmarks used in Iceland are of the concrete pillar type, for which the expression governing the accuracy of the distance measurements is given in Chapter III.

The tectonic setting of the Mývatn network is fairly simple. It lies, as is seen from figure VI.1, in an area of post-glacial activity (the north-central active zone), about 130 kilometres due north of Askja, one of Icelands most active volcanoes. There have been three recorded eruptions within fifteen kilometres of the network (Berninghausen, 1964) during the last two and a half centuries. Krafla, a volcano responsible for some of that activity, lies seven and a half kilometres due north of the trilateration network. This volcano was found by Ward et al. (1969) to be the focus of microearthquake activity in northern Iceland. All around the network, which is of eight stations arranged in three quadrilaterals, are numerous signs of extensional tectonics; open fissures, normal faults and grabens, fissure eruptions and central volcanoes abound (figure VI.2), and all of them suggest a regional extension axis directed almost exactly due east-west.

Distance measurements have been made on the network, which was built in 1969, on three occasions. In 1970 the measurement was not completed because of instrumental failure, but the two complete measurements in 1971 and 1972 were successful. The results of these latter two measurements are given in table VI.1, along with the observed distance changes, and a comment on the significance of these changes. A change is considered significant if it exceeds the sum of the expected errors of the two measurements (see Chapter III for a discussion of expected errors).

It will be seen immediately that the observed changes are not large, and

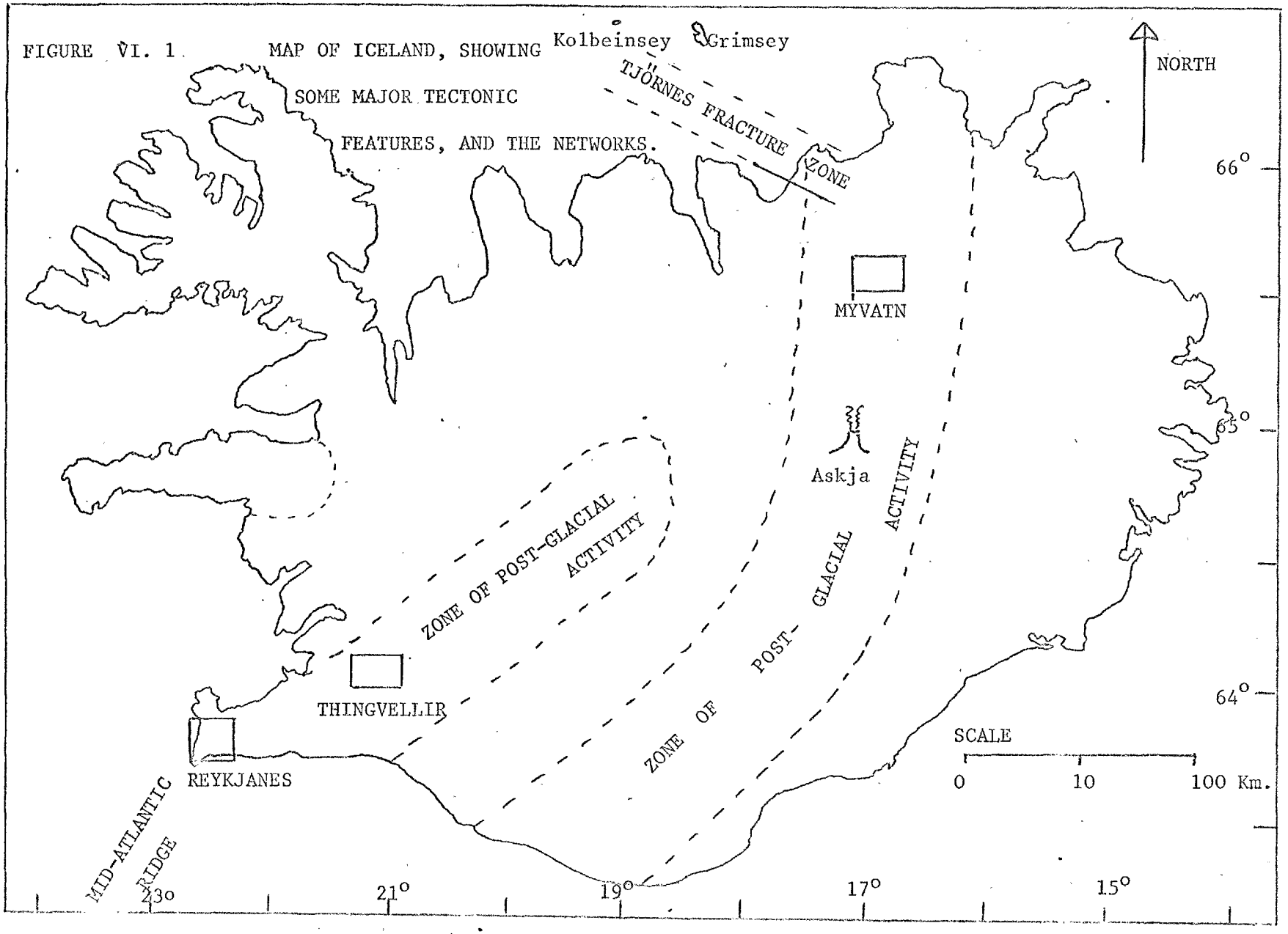


FIGURE VI. 1 MAP OF ICELAND, SHOWING SOME MAJOR TECTONIC FEATURES, AND THE NETWORKS.

TABLE VI.1 THE DISTANCE MEASUREMENTS AT MÝVATN.

LINE	1971	1972	CHANGE	SIGNIFICANT
MS1-N1	1161.9268	1161.9332	0.0064	YES
MN1-N2	875.4599	875.4579	-0.002	NO
MN2-S2	789.1302	789.1306	0.0004	NO
MS2-S1	702.8895	702.8906	0.0011	NO
MS2-N1	1096.1511	1096.1536	0.0025	NO
MN2-S1	1349.0856	1349.0851	-0.0005	NO
MN2-N3	558.7525	558.7519	-0.0006	NO
MN3-S3	838.3442	838.3457	0.0015	NO
MS3-S2	665.8639	665.8643	0.0004	NO
MN2-S3	1058.1382	1058.1370	-0.0012	NO
MS2-N3	973. 8262	973.8280	0.0018	NO
MN4-N3	763.4677	763.4722	0.0045	YES
MS4-N4	934.7476	934.7494	0.0018	NO
MS4-S3	597.2232	597.2232	0	NO
MS4-N3	1219.0084	1219.0069	-0.0015	NO
MN4-S3	991.9363	991.9406	0.0043	YES

that only three exceed the significance criterion. The fact that two of these are associated with one station, N4, suggests that there has been a displacement of this station relative to the rest of the network. Indeed, applying the displ--acement vector analysis described in chapter IV to the significant changes associated with this station shows that it has moved due east relative to its three neighbours (and therefore presumably also relative to the rest of the network) by 5 mm. Such a displacement would cause line S4 - N4 to extend by 2.5 mm.; the observed change on this line is + 1.8 mm., so that the eastwardly movement of this one station agrees very well with the measurements. (Unfortuna--tely, none of the lines associated with this movement was measured in 1970.)

The other change, that of line N1 - S1, is less immediately comprehensible, and it does seem possible that it should not be regarded too highly because that particular line is badly situated, passing very close to dusty ground over its entire length.

The question arises as to what interpretation should be put on the displacem--ent of station N4. As was observed in chapter IV., stations can move as a result of at least two distinct effects. Tectonic forces are assumed to be the prime movers, but there is always the possibility that the foundation has shifted. In this case, as will be shown later, the movement is so much in agreement with what might be expected from other information that it is assumed to be tectonic in origin.

All the observed changes, whether classed as significant or not, have been included in a homogeneous strain analysis (see chapter IV.), whose results are shown in table VI.2. The average values of the parameters shear, dilatation, and direction of maximum extension, are shown on the inset table of figure VI.2.

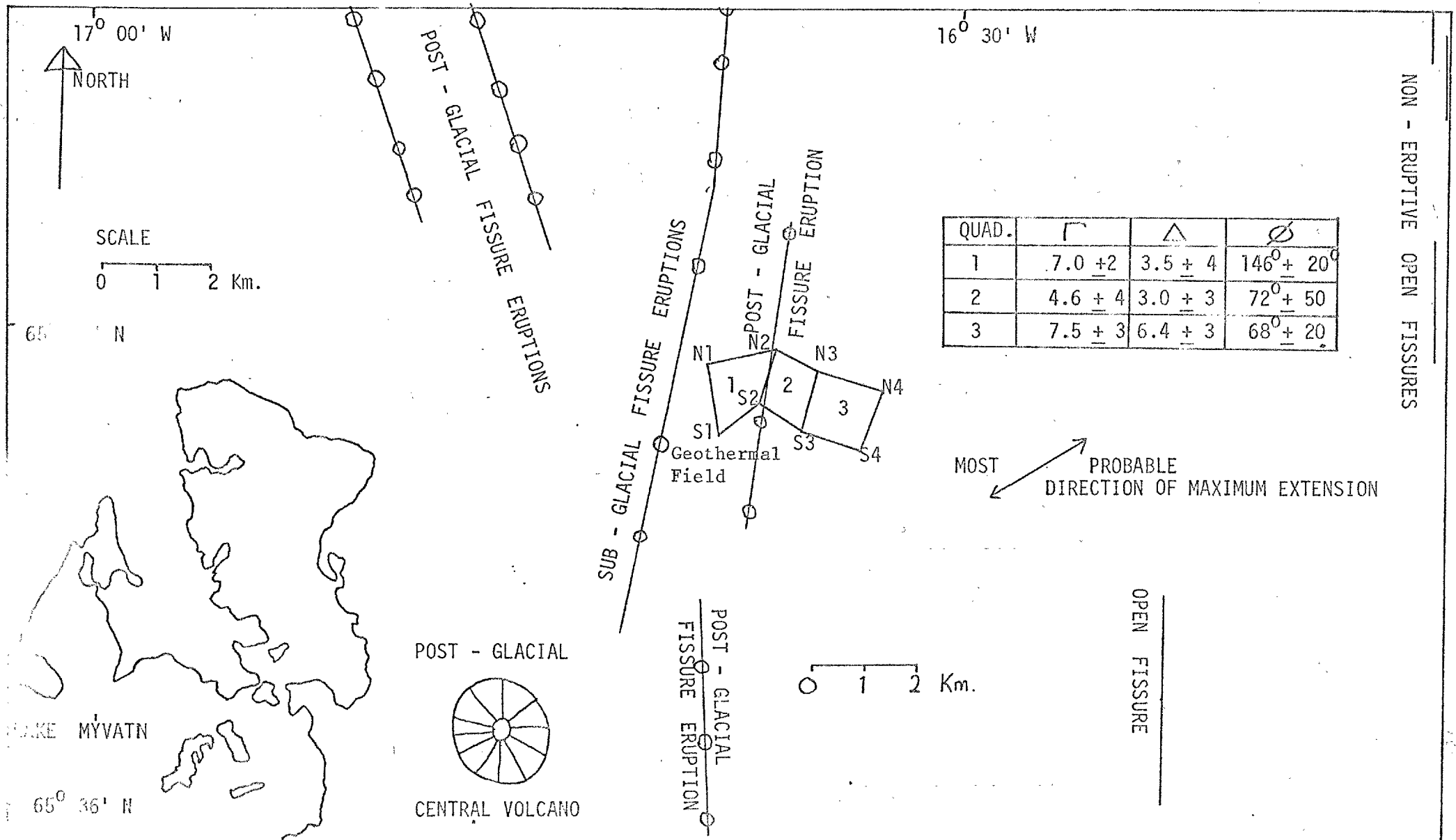
The direction of maximum extension in quadrilateral 3, which includes the changes associated with the movement off station N4, is seen to be quite well-defined, at about N68^{o}E. $\pm$ 20^{o}. The direction in quadrilateral 2 is very similar, but as there are no significant changes in this quadrilateral, it will not be considered further.

The direction of extension in quadrilateral 1 is also very well-defined, at

TABLE VI.2 THE RESULTS OF THE HOMOGENEOUS STRAIN ANALYSIS OF THE MÝVATN CHANGES.

TRIANGLE	SHEAR	DILATATION	BEARING OF MAX. EXT.
S 1 - N 1 - N2	9.5	2.4	N158^{o}E
S 1 - N 1 - S 2	6.3	5.3	N182^{o}E
S 1 - N 2 - S 2	4.3	-4.0	N110^{o}E
N 1 - N 2 - S 2	6.8	7.6	N134^{o}E
S 2 - N 2 - N 3	4.9	4.3	N172^{o}E
S 2- N 2 - S 3	8.8	4.7	N 48^{o}E
S 2 - N 3 - S 3	2.1	2.0	N 30^{o}E
N 2 - N 3 - S 3	2.7	1.1	N37 ^{o}E
S 3 - N 3 - N 4	4.3	7.9	N 90^{o}E
S 3- N 3 - S 4	10.0	6.8	N 54^{o}E
S 3 - N 4 - S 4	5.6	3.3	N58^{o}E
N 3 - N 4 - S 4	10.0	7.5	N 71^{o}E

FIGURE ILLUSTRATING THE RESULTS OF THE HOMOGENEOUS STRAIN ANALYSIS OF THE MÝVATN CHANGES.



QUAD.	⌜	△	∅
1	7.0 ±2	3.5 ± 4	146° ± 20°
2	4.6 ± 4	3.0 ± 3	72° ± 50
3	7.5 ± 3	6.4 ± 3	68° ± 20

N146°E. It does not however, seem to be possible to relate this direction to observable feature in the area, so that its significance is not at all understood.

The reason for the difference between the displacement direction of station N4 and the direction of maximum extension lies in the inclusion in the strain analysis of all the observed changes, rather than just the strictly-speaking significant ones. The justification for doing this will be seen later when these results are compared with other observations from this part of Iceland.

SECTION VI.2 DISCUSSION OF THE MÝVATN RESULTS IN THE FRAMEWORK OF OTHER OBSERVATIONS FROM ICELAND.

Böthvarsson and Walker, who first proposed the hypothesis of crustal growth in Iceland by dyke injection in a narrow zone of volcanic activity (1964), estimated that the rate of extension across the active zone had averaged about 20 mm. per year since the Tertiary.

Piper (1971) found about the same rate of extension in south-west Iceland by matching known polarity events determined by ground magnetic studies.

Heirtzler et al. (1966) and Talwani et al. (1971) found from magnetic studies on the Reykjanes ridge that the average half-rate of sea-floor spreading over the last four million years has been 10 mm. per year: a similar result was obtained by Vogt et al. (1970) from similar studies on the Iceland-Jan Mayen ridge to the north of Iceland.

Thus all these sources agree that the rate of crustal extension in and around Iceland has averaged 20 mm. per year since the late Tertiary.

Piper, Heirtzler et al., and Talwani et al. all find the extension direction to be N45°E in southern Iceland and on the Reykjanes ridge; Böthvarsson and Walker and Vogt et al. find the direction to be east-west in and immediately north of northern Iceland. Further north still the direction reverts to N45°E.

Thus there seems to be an anomalous spreading direction associated with

the northern active zone in Iceland (on which the Mývatn network is situated) and the mid-Atlantic ridge immediately to the north.

The 5 mm. eastward displacement of station N4 noted in the last section agrees exactly in direction with Böthvarsson and Walker's result, although the magnitude is somewhat low. This discrepancy may indicate that the measurements do not cover the entire zone, that the movement found in one year should not be compared with the average over four million years, or that there has been a genuine decrease in the spreading rate in recent years.

Some bearing on the first of these possibilities is given by the micro-earthquake surveys of Ward et al. (1969). As mentioned in the last section, these showed that the only detectable microearthquake activity in Northern Iceland comes from Krafla, which is seven kilometres due north of quadrilateral 3 of the trilateration network. This suggests that activity in this region is confined to a very narrow zone, whose southward extrapolation passes through the trilateration network, and therefore that the observed displacement does in fact represent the total extension across northern Iceland.

It is quite impossible to state with certainty on the basis of one year's measurements that the spreading rate has decreased, so that it is more sensible to assume that the rate varies from year to year, and that comparison with a geologically derived average is meaningless.

The homogeneous strain analysis of the changes observed in quadrilateral 3 of the trilateration network showed an extensional principal strain directed at N68^{o}E, which is somewhat different from the expected direction found by Böthvarsson and Walker and also from the extension direction indicated by the surface features in the area (which all strike almost due North) if these are assumed to result from pure extension.

However, there are several other sources of information bearing upon this question which suggest that the direction N60^{o} - 70^{o}E is well defined as an extensional axis in northern Iceland.

Saemundsson (1973) discussed the structure of the Tjörnes Fracture Zone (figure VI.1) which both he and Ward (1971) consider to be a dextral transform shear zone connecting the north central active zone of mainland

Iceland to northward continuation of the mid-Atlantic ridge (the Kolbeinsey ridge). He shows that the fracture zone strikes at N65°W and that it is bounded on its southern margin by the Húsavik faults(figure VI.1) which are recognisable on the mainland, and which he shows to represent considerable vertical and dextral shear movements.

Stefánsson (1966) and Sykes (1967) both obtained fault plane solutions for a magnitude 5.8 event which occurred on the western end of the fracture zone. Both solutions showed dextral motion on a N106°E striking plane.

The axis of extension indicated by the strike of the fracture zone, by the strike of the Húsavik faults, and by the fault plane solution(s) is, assuming a 30° angle of friction (Moody and Hill, 1956), N58°E.

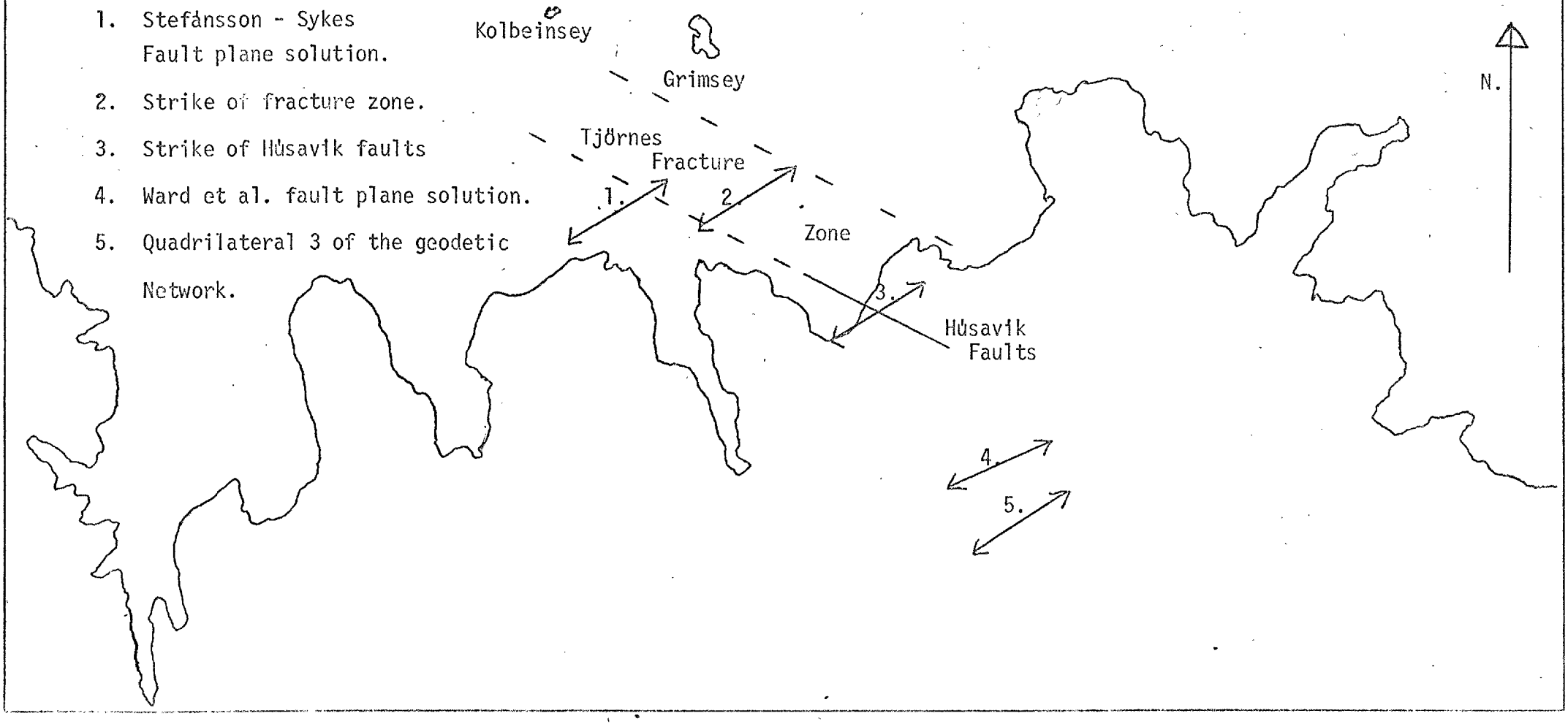
Ward et al. (1969) reporting on the microearthquake studies previously mentioned, give the results of a composite fault plane solution from the Krafla active zone which indicates thrusting with a component of left-lateral shear on a N5°E striking plane (choosing as the fault plane the nodal plane more nearly agreeing with observable structures; the auxiliary plane is perpendicular to this). Despite the somewhat peculiar mechanism indicated by this, the direction of the (assumed) fault plane is in excellent agreement with local surface tectonic directions, which does suggest that there is some meaning in the result. The extensional principal stress direction indicated by this solut-ion is N65°E, allowing,as before,a 30° angle of friction.

Allowing the same angle of friction for the results of the trilateration measurements indicates an extensional principal stress direction of N55°E.

Figure VI.3 summarises the three directions of extensional principal stress determined from the various different observations, whose close grouping suggests that the north central active zone, the Tjörnes fracture zone, and (presumably) the Kolbeinsey ridge are all governed by the same stress pattern, whose extensional principal component strikes at N60°E.

This in turn suggests that the surface fractures in the north central active zone are not, as their appearance would suggest, tensional, but left-lateral shear fractures in a medium whose angle of friction is 30° (in which case their

FIGURE VI.3 THE DIRECTIONS OF THE EXTENSIONAL PRINCIPAL STRESS INFERRED FROM VARIOUS OBSERVATIONS IN NORTHERN ICELAND.



strikes would be expected to be due north, as is indeed the case).

Thus, to summarise, the distance measurements from the north of Iceland show not only crustal extension of 5 mm. in a year in an east-west direction but also suggest that the extensional principal stress governing the area covered by the trilateration network is directed at N60^{o}E.

The former result is in quite good agreement with the geologically derived extension rate and direction for the area; the latter result agrees well with other observations from that region, and indicates that the north central active zone in Iceland, while predominantly an extensional axis, also includes a modicum of left-lateral shear in its movement. The further consequences of this observation will be considered later.

SECTION VI.3 THE TECTONIC SITUATION OF THE THINGVELLIR NETWORK, AND THE RESULTS FROM IT.

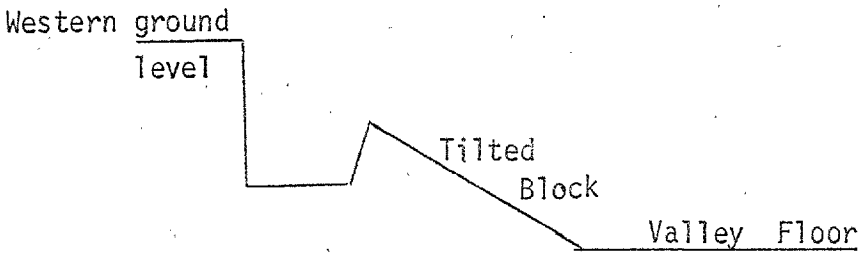
The Thingvellir network was the first built in the course of this study of Icelandic tectonics.

Thingvellir itself is an oustanding graben structure, about 4 km. wide, situated on the south-western active zone in Iceland (figure VI.1). The graben is bounded by very large normal faults whose strikes are fairly constant at N30^{o}E, and its floor is broken by numerous smaller normal faults and open fissures (some of them water-filled) all of which strike at N30^{o}E.

The western boundary of the graben is a single normal fault called Almannagjá, whose vertical throw is some twenty metres, and which can be followed on the ground for about twenty kilometres as a continuous structure. For much of its length this fault acts as the western margin of lake Thingvall--avatn, Iceland's largest lake (figure VI.4).

In addition to its twenty metres of vertical throw, this fault also shows about the same amount of horizontal opening.

It is not a clean, single break, but for much of its length is associated with a tilted block which forms the eastern side of the fault. The resulting cross-section is illustrated below.



The rift formed by the horizontal opening between the western wall and the eastern tilted block was held in great awe by the early pagan settlers of Iceland, who considered it to be one of the acts of Thor, and held their mid-summer games in his honour there.

Almannagjá becomes less impressive north-east along its strike, and between stations 4 and 5 of the trilateration network (figure VI.4) degenerates into a series of parallel normal faults and fissures, which together take up the horizontal and vertical displacements.

By this stage too the valley floor has risen considerably so that the total vertical displacement between stations 4 and 5 is much less than that further south.

On the eastern side of the graben the vertical throw is very much greater as the ground to the east of the graben is higher than that to the west.

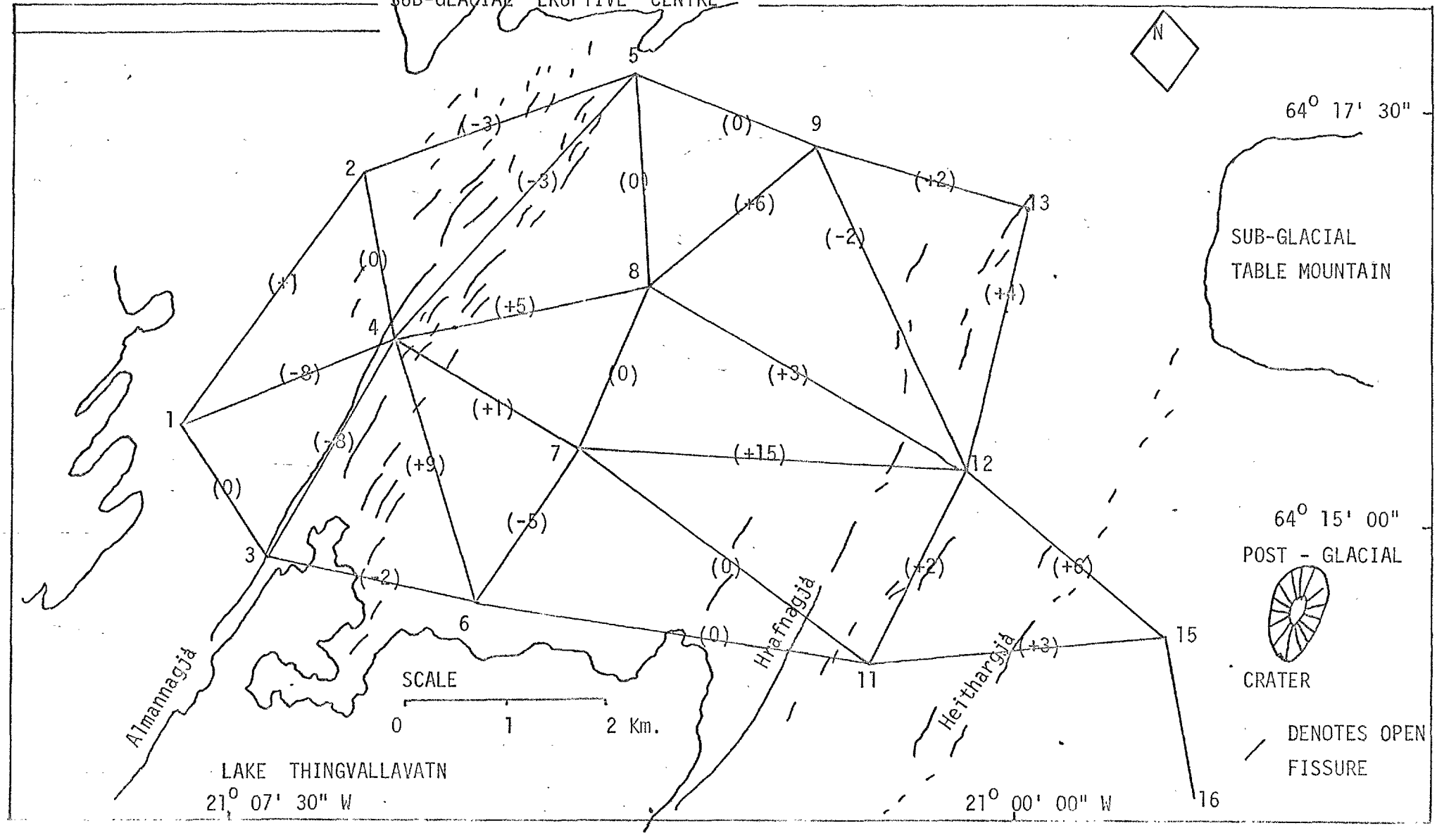
Here the horizontal and vertical displacements are taken up by movement on two faults, each similar in structure to Almannagjá, called Heitharagjá and Hrafnagjá.

The view was widely expressed at the Symposium on The World Rift System (Ottawa, 1965) that Thingvellir was the expression of the mid-Atlantic ridge median valley in Iceland, which is why the trilateration network was built there.

The network consisted originally of sixteen stations, all concrete pillars, arranged in seventeen almost perfectly equilateral triangles. Unlike later networks, which are all long and thin, the one at Thingvellir is only slightly extended perpendicular to the graben.

Unfortunately the original network was laid out on the assumption that the Mekometer was able to measure distances up to three miles, rather than, as is in fact the case, up to three kilometres. Thus in order to make the network

FIGURE VI.4 THE HORIZONTAL DISTANCE CHANGES OBSERVED AT THINGVELLIR BETWEEN 1968 AND 1973, IN MILLIMETRES.



usable, almost all the lines had to be filled in with supplementary stations visible from both the original ends. The main stations are numbered 1 - 16, the supplementary ones are denoted by the fraction given by the two end numbers, i.e. station 3/4 fills in the line between original stations 3 and 4.

Partly because of this unfortunate accident of the line lengths (even after filling-in most of the lines are over 1300 m. long, and many are over 1700 m.), and partly because of the use of equilateral triangles as elementary units (see chapter II), this network is extremely weak, providing no method of checking the self-consistency of the measurements, and being composed entirely of lines on which the expected errors are extremely large (chapter III).

Two of the original stations, 10 and 14, and all their filling-in stations have never been used, indeed this author doesn't know where they are.

Distance measurements have been made on all the remaining lines at least three, and in some cases as many as eight, times, between August, 1968, and July, 1972; the corrected (chapter III) results are shown in appendix D, as graphs of corected distance against time (in years).

The changes derived from fitting straight lines to all the distance-time graphs are summarised in table VI.3 and illustrated in figure VI.4. The fitting has been done by eye in all cases, and where there are violently inconsistent changes (two or three of the most difficult lines), these are ignored.

In almost all cases the fitted straight lines come within one ' expected error ' of each plotted point on the graphs, though there are exceptions.

The changes observed are rarely more than the uncertainties suggested in them by changing the gradient of the fitted line within the plotted error limits. Indeed if only the changes which exceed their possible uncertainty are considered significant, then the lengths of only seven lines have changed.

In this case the distribution of changes is shown on figure VI.5, and suggests that there has been north-west south-east extension across the network with some north-east south-west contraction on its western side. It is also significant that the extensions are confined to lines 4 - 4/6, 12 - 8/12, 12 - 7/12, and 15 - 12/15, each of which can be seen from figure VI.4 to cross one

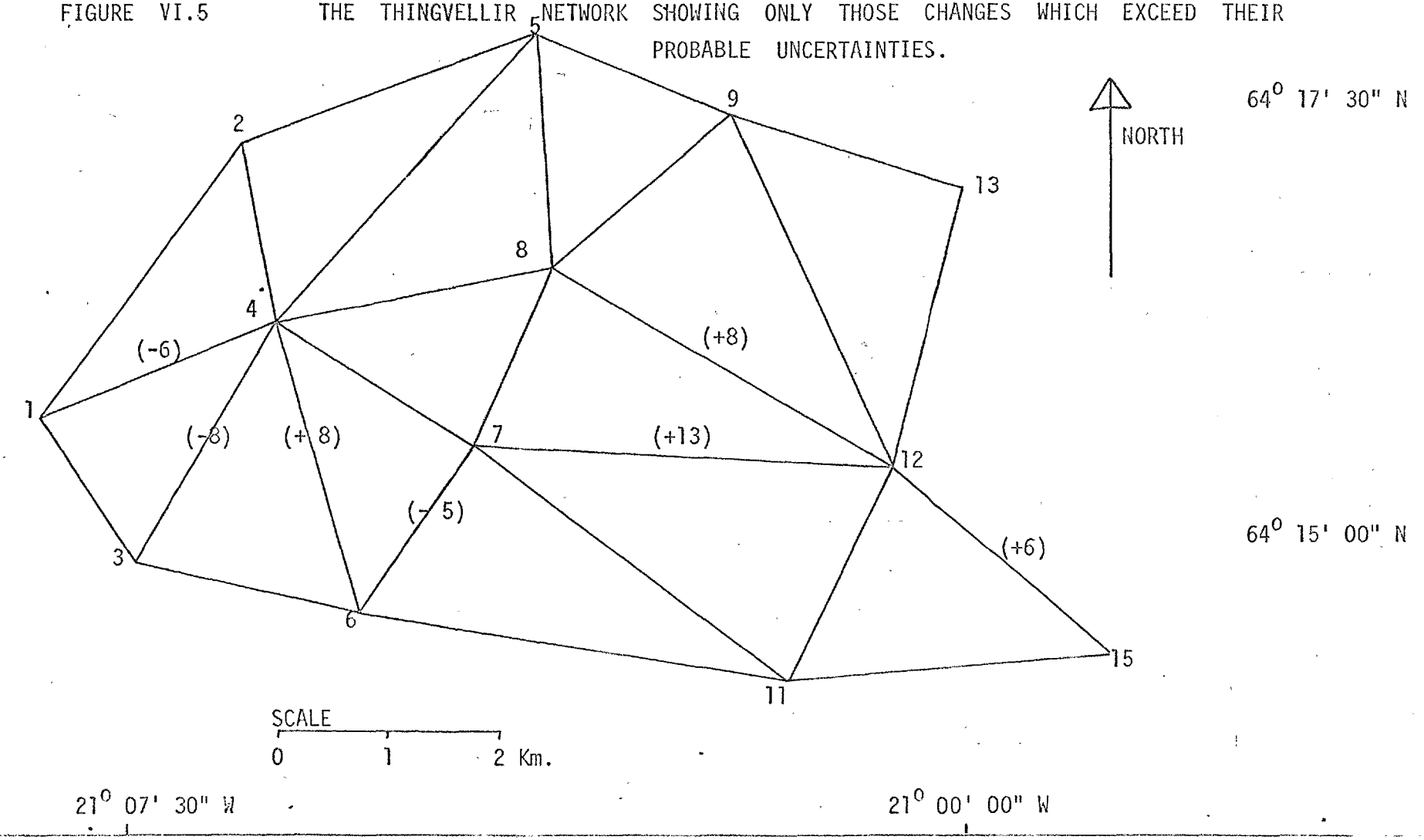
TABLE VI.3 THE OBSERVED DISTANCE CHANGES AT THINGVELLIR 1968 - 1972.

LINE	CHANGE (mm.)	STRAIN (10^{-6})	UNCERTAINTY (mm.)
1 - 1/2	0	0	± 3
1 - 1/4	- 5	- 3.8	±3
2 - 1/2	+ 1	1.1	± 2
2 - 2/5	0	0	± 3
3 - 1	0	0	± 2
3 - 3/4	- 2	- 1.5	±1
3 - 3/6	0	0	± 3
4 - 1/4	- 3	- 2.9	± 2
4 - 2	0	0	± 4
4 - 3/4	- 6	- 4.9	± 3
4 - 4/5	- 5	-2. 9	± 4
4 - 4/6	+ 8	+ 3.6	± 3
4 - 4/7	+ 2	+ 1.5	± 3
4 - 4/8	+ 2	+ 1.5	± 5
5 - 2/5	- 3	- 1.6	± 4
5 - 4/5	+ 2	+ 1.1	± 3
5 - 5/8	0	0	± 3
5 - 5/9	0	0	± 3
6 - 3/6	- 2	-2. 7	± 1
6 - 4/6	+ 1	+ 1.6	± 1
6 - 7	- 5	- 2.6	± 3
6 - 6/11	0	0	± 5
7 - 4/7	- 1	-1.4	± 2
7 - 8	0	0	± 3

TABLE VI.3 (CONTINUED).

LINE	CHANGE (mm.)	STRAIN (10^{-6})	UNCERTAINTY (mm.)
7 - 7/11	0	0	± 6
7 - 7/12	+ 2	+ 1.0	± 3
8 - 5/8	0	0	± 3
8 - 4/8	+ 3	+ 3.3	± 2
8 - 8/9	+ 3	+ 3.9	± 2
8 - 8/12	- 5	- 3.0	± 3
9 - 5/9	0	0	± 2
9 - 8/9	+ 3	+ 2.3	± 3
9 - 9/12	- 2	- 1.6	± 3
9 - 9/13	+ 2	+ 2.4	± 2
11 - 6/11	0	0	± 8
11 - 7/11	0	0	± 6
11 - 11/12	+ 1	+ 1.0	± 3
11 - 11/15	0	0	± 6
12 - 7/12	+ 13	+ 7.4	± 4
12 - 8/12	+ 8	+ 4.0	± 4
12 - 9/12	0	0	± 5
12 - 11/12	+ 1	+ 1.1	± 3
12 - 12/13	+ 3	+ 3.0	± 2
12 - 12/15	0	0	± 3
13 - 9/13	0	0	± 3
13 - 12/13	+ 1	+ 1.0	± 3
15 - 11/15	+ 3	+ 2.2	± 2
15 - 12/15	+ 6	+ 4.6	± 3

FIGURE VI.5 THE THINGVELLIR NETWORK SHOWING ONLY THOSE CHANGES WHICH EXCEED THEIR PROBABLE UNCERTAINTIES.



or other of the large normal faults discussed earlier.

The number of lines which crosses the Almannagjá (or the complex zone which replaces it) perpendicular to its strike is six; in addition there are four lines which cross it parallel to the strike.

On the eastern side, two lines 12 - 15, and 11 - 15, cross the upper fault, and six the lower.

Using the definite changes only (figure VI.5) as indications it becomes possible to look more closely at the other lines which cross the faults in order to try to arrive at a possible overall scheme of displacements. Table VI.4 shows the changes found then across each of the three main faults (Almannagjá in the west, Hrafnagjá and Heithargjá in the east).

TABLE VI.4

LINE	CHANGE (mm.)	UNCERTAINTY (mm.)	COMPONENT OF CHANGE ACROSS GRABEN.
Almannagjá Lines.			
3 - 3/6	0	± 3	0 ± 3
4 - 4/6	+8	± 3	11 ± 4
4 - 4/7	+2	± 3	2 ± 3
4 - 4/8	+2	± 5	3 ± 7
5 - 5/8	0	± 3	0 ± 5
5 - 5/9	0	± 3	0 ± 3
Hrafnagjá Lines.			
11-6/11	0	± 8	0 ± 8
11-7/11	0	± 6	0 ± 6
12-7/12	13	± 4	14± 4
12-8/12	8	± 4	8 ± 4
12-9/12	0	± 5	0 ± 6
13-9/13	0	± 3	0 ± 3
Heithargjá Lines			
12-12/15	0	± 3	0 ± 6
11-11/15	0	± 6	0 ± 6
15-12/15	+6	± 3	12 ± 3
15-11/15	+3	± 2	6 ± 2

The pattern of extensions suggested by this is thus

across	Almannagjá	(northern end)	3	±	3 mm.
		(southern end)	8	±	5 mm.
across	Hrafnagjá		7	±	5 mm.
across	Heithargjá		9	±	4 mm.

As was mentioned above, to the north of station 4 Almannagjá becomes a broad zone of parallel features, most of which is crossed by lines almost parallel to its strike which would not detect extension across the zone. This explains the subdivision of Almannagjá into northern and southern ends.

The important changes in the Heithargjá region take place on lines 15 - 12/15 and 15 - 11/15 which do not actually cross the main fault scarp. Thus the extension observed must have occurred across one or other of the smaller features in that area.

The total extension across the graben has therefore been 24 ± 14 mm. in the period of the measurements, 1968 to 1972, which represents an annual average of 6 ± 3 mm.

In addition to the extension there is also an element of contraction along the graben suggested. This seems to amount to about 1.4 ppm. in the four year period, and may be connected with the breakdown of the single Almannagjá into a broader zone, suggestive of shearing.

Thus, to conclude this section, the Thingvellir graben, one of the most impressive structures of its kind in the world, which has been considered to represent the median valley of a mid-ocean ridge on land, showed a total of 24 ± 14 mm. of extension in the four year measuring period. The direction of this extension is approximately perpendicular to the strike of the graben, or at about N120°E. A small component of contraction on the western side of the graben may be connected with the diffusion of the boundary fault.

SECTION VI.4 COMPARISON OF THE RESULTS FROM THE TRILATERATION SURVEY WITH OTHER OBSERVATIONS FROM THE AREA.

There have been three other geodetic surveys made in the Thingvellir area, from which there are results of two.

The first of these, showing a null result, comes from the distance measure--ments of Decker et al. (1971). These authors describe the results of a single line geodimeter traverse across southern Iceland which was first measured in 1967 and again in 1970, after the eruption of Hekla.

On the Thingvellir section of the line no significant changes between the two measurements were detected, although the distance changes would need to be in excess of about 15 mm. to be resolvable with their results. The results from the last section suggest that the annual rate of extension across the graben is 6 $\pm$ 3 mm., so that in the three years between their surveys 18 mm. of extension might have been expected. The null result of these authors is thus within the limits of the annual extension rate derived from the results of the last section.

The other geodetic work from which results are available is precise levell--ing.

Tryggvason (1968) made measurements on a precise levelling profile across the Thingvellir graben in 1967 and 1968. His results showed that there was subsidence of the graben floor with respect to the eastern and western flanks. This subsidence did not however appear to be related to movements on any of the main faults in the area, and has been explained by him as a general downwarping of a large area of which the levelling profile happens to be a part.

From the results of Bernauer (1943), Tryggvason shows that there has been 75 metres of extension across the graben since its formation. Thingvallahraun, the lava flow of which it forms a part, has been radio-carbon dated by Kjartáns--son at 9130 $\pm$ 260 years B.P. (1964), so that the annual rate of extension across the graben has been at least 8 mm. per year.

This is in good agreement with the measured result of 6 $\pm$ 3 mm. per year given in the last section.

It is worth considering this result (and the geological estimate of Bernauer) in the light of the evidence from sea-floor spreading measurements of Heirtzler et al., Talwani et al., and Vogt et al.

These, as was observed before, all show that the average rate of crustal extension found on the mid-Atlantic ridge both to north and south of Iceland has been 20 mm. per year since the Tertiary, so that neither the current rate of movement at Thingvellir nor the minimum geological estimate can account for the necessary crustal extension. However, there is no reason why the minimum geological estimate should represent the true historical picture. Indeed, if the graben had formed only 3,700 years ago then the mean annual extension rate would be approximately 20 mm. It is impossible to date the formation of the graben, and the only historical evidence is of 0.63 metres susidence during an earthquake in 1789.

On the other hand if the minimum estimate is approximately correct, then it means that throughout post-glacial time there must have been some other axis about which most of the spreading was occurring. This would undoubtedly be the south-central active zone, on which Decker et al. (1971) reported 20 mm. per year of crustal extension between 1967 and 1970, and which has certainly been in existence at least since the beginning of the last ice age (as there are many instances of sub-glacial eruptions in it).

Thus there is no doubt that throughout the existence of the Thingvellir graben there has been another spreading axis active in southern Iceland, one which certainly now is responsible for much the greater part of the observed crustal extension in this part of the world, so that it seems reasonable to suppose that the Thingvellir graben has never been the axis of sea floor spread-ing in Iceland. This is not to be taken however, as saying that the axis of spreading did not once, before the formation of the graben, exist at the same place; at any stage in Iceland's history before ten thousand years ago this might have been true.

SECTION VI. THE TECTONIC SETTING OF THE REYKJANES NETWORK.

The Reykjanes network has already been mentioned in connection with the vertical angle measurements discussed in chapter V. However, at that time its detailed position in the tectonics of Iceland was not described.

The network is situated at the extreme soth-west tip of Iceland, at the end of the Reykjanes peninsula.

The peninsula is a very young feature whose oldest surface rocks are quater--nary basalts which are found on a smaller peninsula to the north of the trilate--ration network, and also farther east, near Reykjavik, Iceland's capital.

The name of the peninsula means smoke-peninsula, which probably refers to the geothermal activity which occurs at many places along its length.

The surface rocks of the peninsula are all recent volcanics, many resulting from fissure eruptions either sub-glacial during the last ice-age, or within the last ten thousand years.

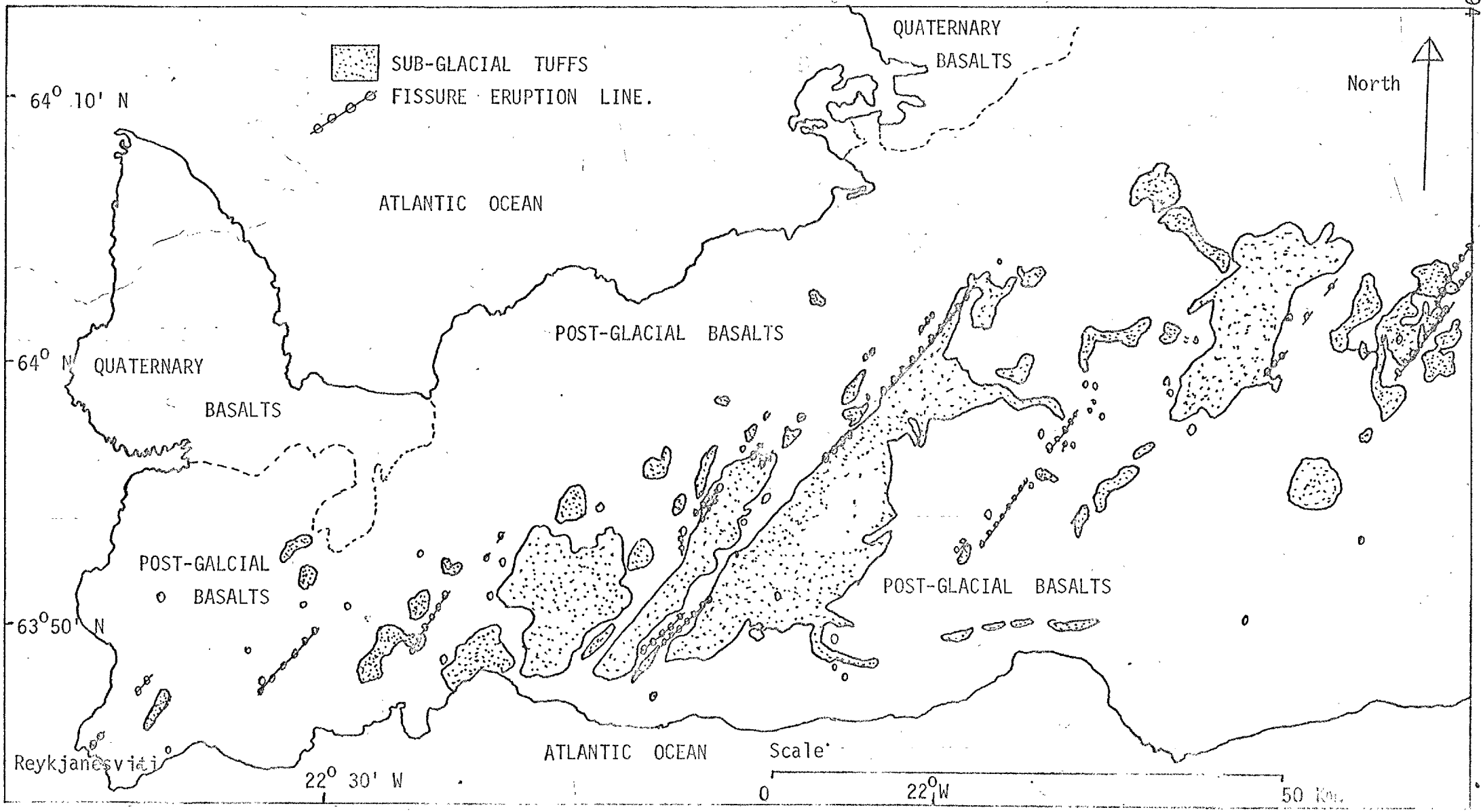
The fissure eruptions, along with other extensional features (e.g. open fissures and normal faults), are arranged in groups which are staggered en echelon the length of the peninsula (figure VI.6). There are seven of these groups of tensional features between Reykjanesviti (the name of the lighthouse at the south-west tip of the peninsula, one kilometre from the trilateration network) and Hengill, which is just south of Thingvellir.

The strikes of the individual groups vary systematically from N45^{o}E at Reykjanesviti to N38^{o}E at Hengill (the strike of the Thingvellir graben it will be recalled was described as N30^{o}E).

Talwani et al. (1971) show from a detailed geophysical survey of the Reykjanes ridge (the name of the local section of the mid-Atlantic ridge), which is structurally continuous with the Reykjanes peninsula, that the en echelon arrangement of apparently tensional groups begins at about 64^{o}N. They surmised this from bathymetric and magnetic profiles in the area offshore of the peninsula,and from the known distribution of historical eruptions (Berninghausen, 1964).

These same authors also showed as a result of the same survey that the

FIGURE VI.6 GEOLOGICAL MAP OF THE REYKJANES PENINSULA (after G. Kjartansson, 1960).



axial magnetic anomaly of the tensional group nearest the peninsula intersected the coastline actually at Reykjanesviti, suggesting that the axis of the ridge passes through the area of the lighthouse, the geothermal field, and the trilat--eration network. This does not agree with the evidence set out in chapter V, based upon the vertical movement results and the micro-earthquake studies, which show that the ridge axis passes somewhat to the north of the lighthouse and geothermal fields.

Sigurgeirsson (1969) published an aeromagnetic map of the Reykjanes peninsula which shows that the central magnetic anomaly found from the ridge studies continues inland along the length of the peninsula, suffering the same en echelon offsets as the fissure eruptions and other tensional groups. However, the significance of this is not certain, as presumably the axial magnetic anomaly reflects the position of more intensely magnetised rock,which might easily be the feeder dyke associated with a linear eruption. Indeed the positions of the magnetic anomalies reflect very closely the lines of the most recent post-glacial linear eruptions.

Ward et al. (1969) found considerable micro-earthquake activity in five places along the peninsula. Each of these corresponds exactly with a geo--thermal field, the significance of which is discussed by Ward and Björnsson (1971).

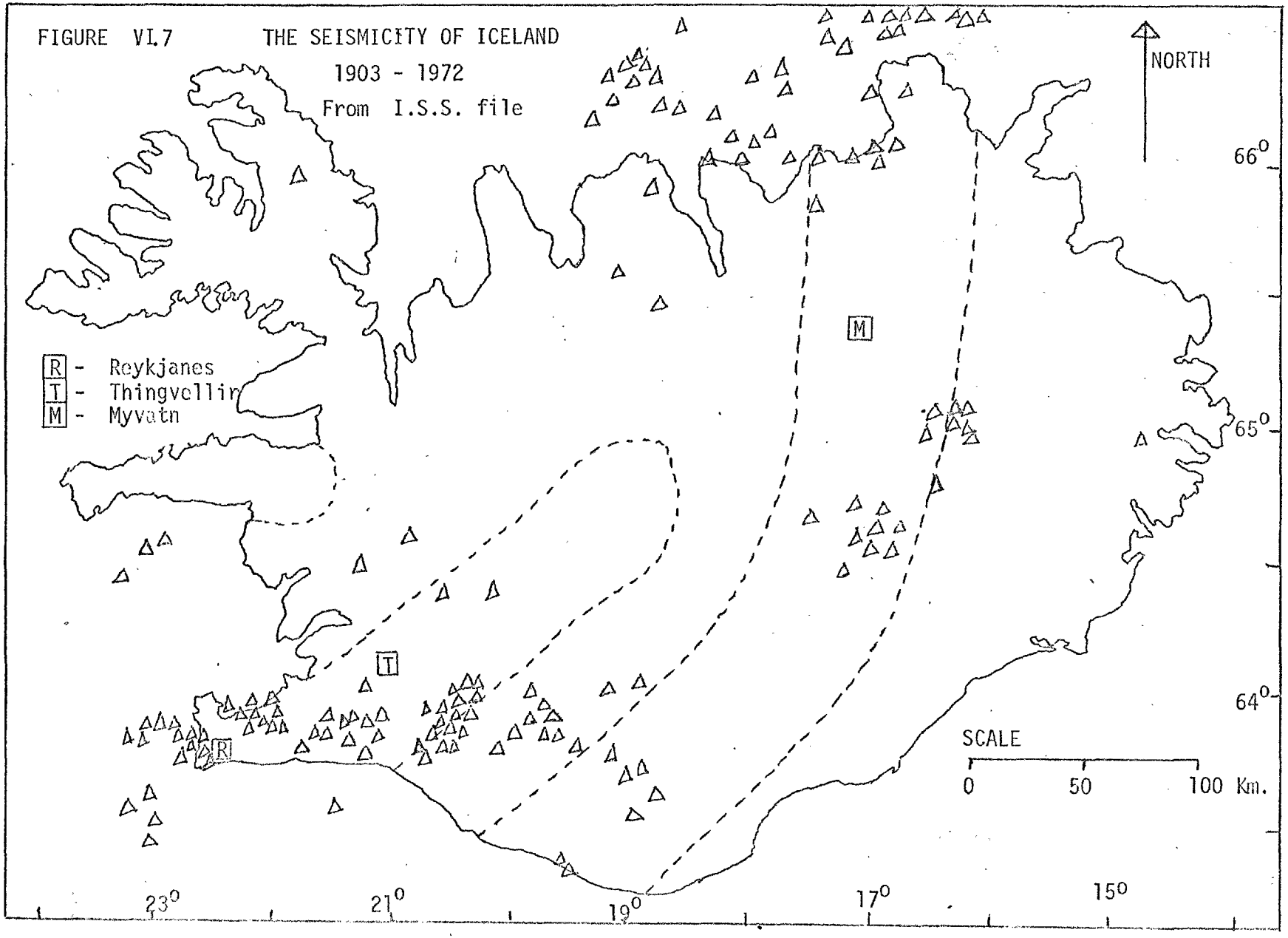
Further studies of the same sort by Klein et al. (1973) show that in two of the areas (one near Reykjanesviti, the other at Krysuvik some twenty kilomet--res away) the activity is confined to fairly narrow zones and tends to occur in swarms of several thousand events within a few days. Fault plane solutions are reported from both of the areas studied by this group, showing almost exclusively normal and left-lateral motion. Solutions of each type show the same extensional axis, namely N135^{o}E.

Larger earthquakes occur along the length of the peninsula (figure VI.7 is an epicentral distribution map drawn from the I.S.S. files), although events of magnitude greater than 4 are rare on the peninsula, and tend to occur, if at all, somewhat to the east.

FIGURE VI.7 THE SEISMICITY OF ICELAND

1903 - 1972

From I.S.S. file



Nakamura (1970) made a detailed investigation of the surface features in one of the extensional groups of the peninsula, the one at the south-west tip in the area of the trilateration network, and showed that all the faulting was indicative of pure extension perpendicular to the strike of the group. This is to say that the local extension axis in the immediate area is directed at N135^{o}E, which is exactly the direction of the extensional axes found from the micro-earthquake survey of Klein et al.

Jónsson (1967) conducted a preliminary survey of the same area from which he concluded that, while it was difficult to believe, all the appearances were that pure extension was responsible for the surface features in the area.

Thus there is quite considerable evidence to suggest that the surface features in this area exhibit pure extension, from which it would be concluded that all the en echelon groups along the peninsula are large-scale versions of the fractures observed in clay by Cloos (1932). This was the interpretation of Tryggvason (1968) who considered that the Reykjanes peninsula is a large-scale left-lateral strike-slip fault. Ward et al. (1969) further interpreted it as a left-lateral transform fault offsetting the sea-floor spreading axis of the mid-Atlantic ridge eastwards to join the south-central active zone in Iceland This will be discussed further after the presentation of the results of the trilateration work.

Before that however, there are two more observations which have a bearing on the interpretation of the tectonic role of the peninsula.

The first of these concerns the incidence of volcanic activity.

Berninghausen (1964) lists all the known historical eruptions in the Icelandic region.

He shows that in the sea off the south-west tip of the Reykjanes peninsula there have been eruptions regularly throughout historical time (which began in Iceland only in about 800 A.D.), and that on the south-central active zone too there have been frequent eruptions in the same time period. Indeed most of the recorded eruptions from the Icelandic mainland have occurred on the south-central zone, with the repetition frequency on average about once every twenty years.

On the Reykjanes peninsula itself however, there have been only three eruptions reported in the historical period, the last in 1510 A.D.

This suggests that the sea-floor spreading activity in Iceland is restricted to the south-central active zone, and that the Reykjanes peninsula, should not be considered, at least primarily, a spreading axis.

The other piece of information which is of interest in the context of the tectonic role of the peninsula concerns the chemistry of the basalts erupted there.

Jónsson observed that the post-glacial activity of the peninsula falls into two phases. In the first shield volcanoes produced olivine-rich basalts; in the second, which might just have lasted into historic time, fissure eruptions produced basalts containing rather less olivine. These fissure eruptions seem also to have produced rather small quantities of lava for their lengths, often several kilometres, certainly at least when compared to the great fissure eruptions of the south-central zone.

The suggestion is thus of a change with time of the nature of the volcanism, from typical oceanic basalts from shield volcanoes, to less typically oceanic basalts from fissures.

Trilateration measurements across the eruptive fissure on Heimaey (on the south-central active zone in Iceland) showed that the fissure represented a shear zone (Brander and Wadge, 1973).

Olivine-rich basalts are very much associated with the extensional tectonics of sea-floor spreading (Gass, 1970), while basalts containing less olivine, the transitional and alkali types, are apparently associated with shear zones.

Thus it seems that the change in volcanic activity of the peninsula suggests a change from purely extensional tectonics to processes involving a greater component of shear.

This is an interesting way of explaining the variation in activity observed, although it should not be considered as definitely proven.

This section can be summarised then, by saying that all the surface features of the Reykjanes peninsula point to there being a series of en echelon tensional

units arranged such as to suggest a deep left-lateral shear zone. Each tensional unit seems to act to some extent as an axis of sea-floor spreading where the earthquake activity takes the form of intense swarms with no major events, in which fault plane solutions indicate both left-lateral strike-slip and normal mechanisms.

Spreading however, is not, as indicated by the comparative lack of current volcanic activity, the primary present tectonic role of the peninsula; it is seen more as a large strike-slip fault from which a certain amount of extrusion has also occurred.

The strike of the peninsula, which is about N80^{o}E, is exactly the direction which would be expected for the left-lateral member of a conjugate set of shear planes formed under the influence of an extensional axis orientated at N135^{o}E and a corresponding compression orientated at N45^{o}E, assuming that the angle of internal friction involved was 20^{o}. Such an angle is within the range usually encountered (Moody and Hill, 1956).

It is within this context that the trilateration results from the network at the extreme south-western end of the peninsula are to be interpreted.

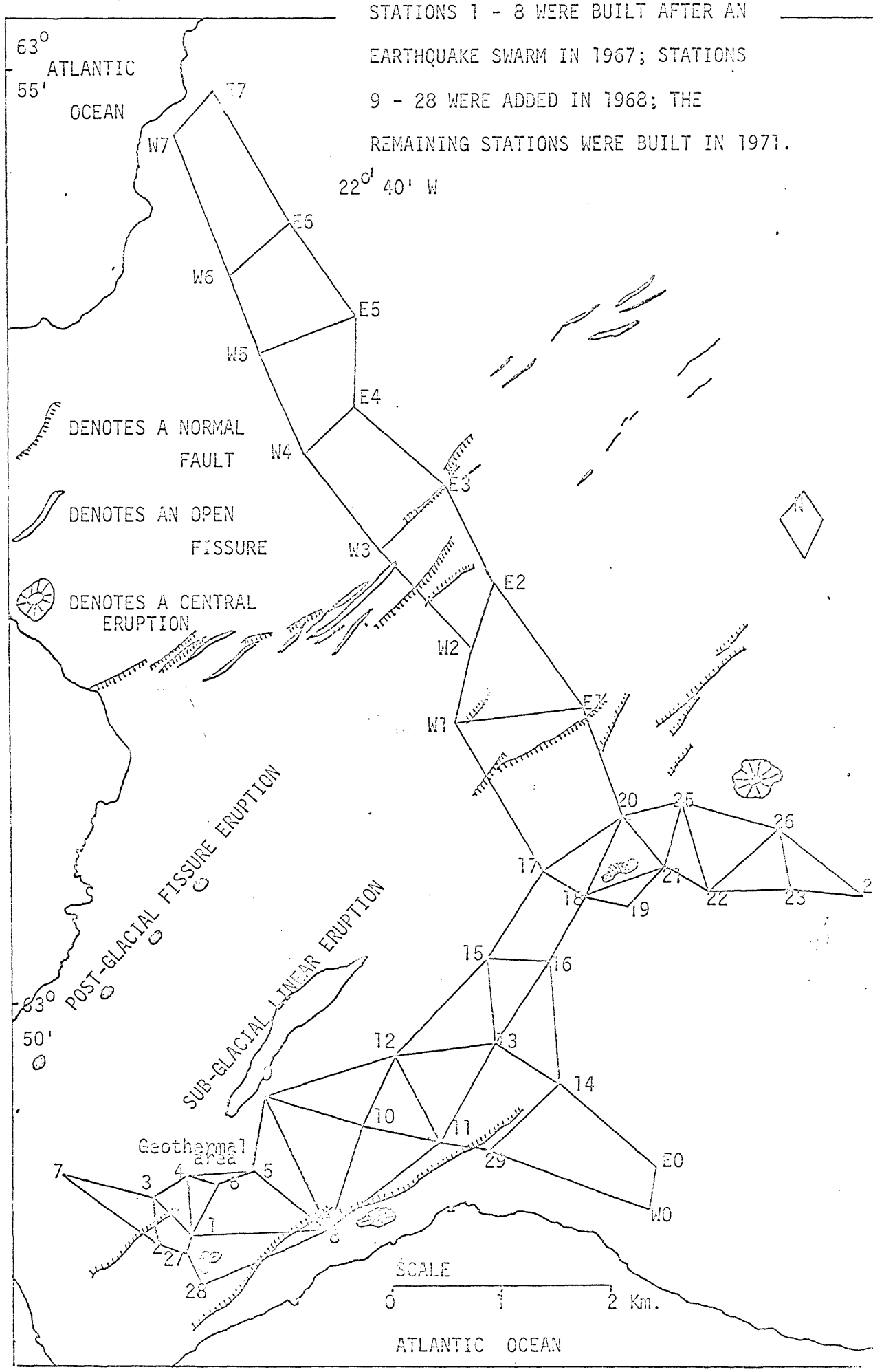
SECTION VI.6 THE INTERPRETATION OF THE TRILATERATION RESULTS FROM THE REYKJANES NETWORK.

The Reykjanes network is illustrated in figure VI.8. It consists of 45 stations, all concrete pillars, arranged approximately in a 'T ', whose cross piece strikes at approximately N35^{o}W.

The network was not all built at the same time, but in three separate stages. Stations 1 - 8 were constructed late in 1967 after a large earthquake swarm and an accompanying massive increase in the geothermal activity had brought about fears of a new eruption in the area. These proved groundless, and the earthquake activity died away within a week, leaving the intensified geothermal activity.

During these events Ragnar Stefánsson (pers. comm. to Ward et al., 1969) noted between five and eight centimetres of horizontal movement (sense unspeci-

FIGURE VI.8 THE COMPLETE REYKJANES NETWORK. STATIONS 1 - 8 WERE BUILT AFTER AN EARTHQUAKE SWARM IN 1967; STATIONS 9 - 28 WERE ADDED IN 1968; THE REMAINING STATIONS WERE BUILT IN 1971.



-fied). Also during the swarm, the western side of a fault near Reykjanesviti (figure VI. 8) dropped several centimetres.

New surface fracturing related to the increased geothermal activity consisted of short approximately north-south en echelon fractures which can be seen well still on days of high humidity and low pressure when the steam from them is particularly visible.

These fractures are indicative of left-lateral shear in an approximately N30^{o}E direction (assuming as before for this area, a 20^{o} angle of friction).

As a result of these events an exploratory drilling project was undertaken in 1968 and 1969 (Björnsson et al., 1972), in the course of which some eight steam wells were drilled in a zone five hundred metres wide striking about N50^{o}E for one kilometre. Two of these wells have been left open to the atmosphere since drilling.

Stations 9 - 28 were built in 1968 to extend the coverage of the network, and the remaining seventeen stations were constructed in 1971 to cover the area of most intense surface faulting and to tie the network to the relatively unfractured area to the north west (figure VI.8).

The older stations of the network can be seen to be arranged somewhat irregularly, particularly around the geothermal area, although the 1971 stations are arranged as a series of double-braced quadrilaterals.

The lines on the pre-1971 network have all been measured at least five times, and many of them as often as eleven times. The 1971 lines have been measured only twice.

The graphs of length against time (in years) are shown for all the older lines in Appendix E. Straight lines have been fitted to all of these,except three which do not seem to show linear behaviour. The changes derived from these fitted straight lines are shown in table VI.5, in addition to the effect of the observed vertical movement (see chapter V), the net horizontal change, and the horizontal strain.

The net horizontal changes are shown also in figure VI.9.

Choice of analysis technique for these changes was not easy. It was consider-

FIGURE VI.9 THE HORIZONTAL CHANGES OBSERVED ON THE REYKJANES NETWORK BETWEEN 1968 AND 1972, IN MILLIMETRES.

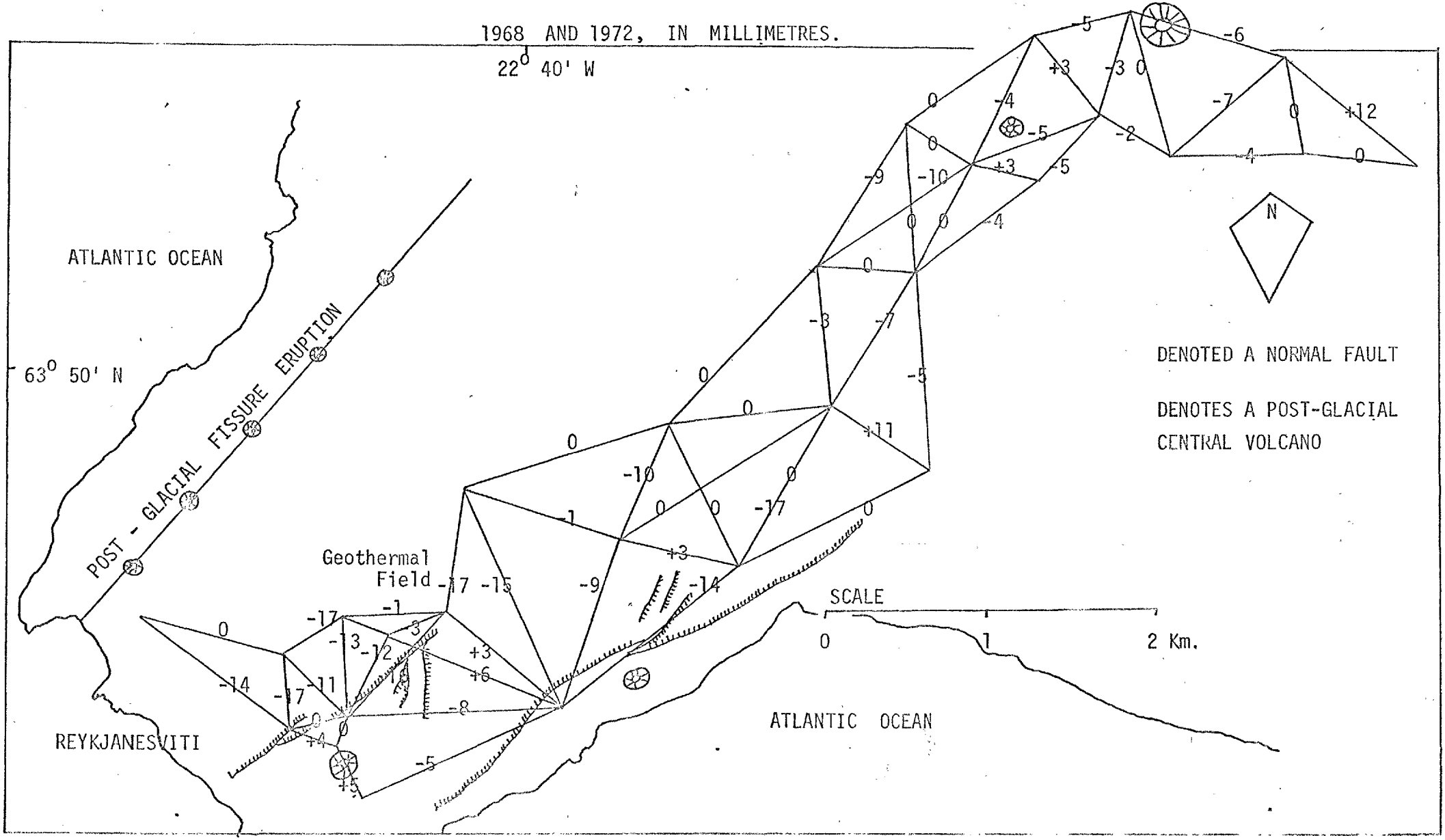


TABLE VI.5 THE DISTANCE CHANGES OBSERVED AT REYKJANES BETWEEN 1968 AND 1972.

LINE	OBSERVED CHANGE	VERTICAL EFFECT	NET CHANGE	STRAIN(10^{-6})
1 - 2	- 3 mm.	- 3 mm.	0	0
1 - 3	- 12mm.	-1 mm.	-11 mm.	-21.4
1 - 4	-16 mm.	- 3 mm.	-13 mm.	-19.6
1 - 5	-18 mm.	- 2 mm.	-16 mm.	-20.2
1 - 6	-13 mm.	- 1 mm.	-12 mm.	-23.4
8 - 1	-10 mm.	- 2 mm.	- 8 mm.	- 5.7
1 - 27	0	0	0	0
2 - 3	-15 mm.	+ 2 mm.	-17 mm.	-42.0
2 - 7	-14 mm.	0	-14 mm.	-13.6
2 - 27	- 1 mm.	+ 5 mm.	+ 4 mm.	+11.5
3 - 4	-17 mm.	0	-17 mm.	-30.5
3 - 6	-15 mm.	0	-15 mm.	-21.2
3 - 7	0	0	0	0
3 - 27	- 8 mm.	- 1 mm.	- 7 mm.	-17.5
4 - 5	- 1 mm.	0	- 1 mm.	- 1.9.
4 - 6	- 9 mm.	0	- 9 mm.	-25.6
5 - 6	- 3 mm.	0	- 3 mm.	-10.0
5 - 8	+ 5 mm.	+ 2 mm.	+ 3 mm.	+ 2.9
6 - 8	+ 8 mm.	+ 2 mm.	+ 6 mm.	+ 4.7
5 - 9	-17 mm.	0	-17 mm.	-28.9
8 - 9	-15 mm.	0	-15 mm.	-11.3
10- 9	- 1 mm.	0	- 1 mm.	- 1.1
10 - 8	- 9 mm.	0	- 9 mm.	- 8.7
10- 11	+ 3 mm.	0	+ 3 mm.	+ 3.8

TABLE VI.5 (CONTINUED).

LINE	OBSERVED CHANGE	VERTICAL EFFECT	NET CHANGE	STRAIN (10^{-6})
11 - 8	- 14 mm.	0	- 14 mm.	- 9.6
12 - 10	- 10 mm.	0	- 10 mm.	- 9.4
12 - 9	0	0	0	0
12 - 13	0	0	0	0
12 - 15	0	0	0	0
13 - 10	0	0	0	0
13 - 11	- 17 mm.	0	- 17 mm.	- 16.4
13 - 14	+ 11 mm.	0	+ 11 mm.	+ 13.8
13 - 15	- 3 mm.	0	- 3 mm.	- 3.3
13 - 16	- 7 mm.	0	- 7 mm.	- 6.0
14 - 11	0	0	0	0
14 - 16	- 5 mm.	0	0	- 4.2
15 - 16	0	0	0	0
17 - 15	- 9 mm.	0	- 9 mm.	- 8.0
17 - 16	0	0	0	0
17 - 18	0	0	0	0
18 - 15	- 10 mm.	0	- 10 mm.	- 6.9
18 - 16	0	0	0	0
18 - 19	+ 3 mm.	0	0	+ 9.1
19 - 16	- 4 mm.	0	0	- 4.4
20 - 17	0	0	0	0
20 - 18	- 4 mm.	0	- 4 mm.	- 4.6
20 - 25	- 5 mm.	0	- 5 mm.	- 8.0
21 - 20	+ 2 mm.	0	+ 2 mm.	+ 2.8

TABLE VI.5 (CONTINUED).

LINE	OBSERVED CHANGE	VERTICAL EFFECT	NET CHANGE	STRAIN (10^{-6})
21 - 18	- 5 mm.	0	- 5 mm.	- 6.8
21 - 19	- 5 mm.	0	- 5 mm.	- 9.0
21 - 22	- 2 mm.	0	- 2 mm.	- 3.6
21 - 25	- 3 mm.	0	- 3 mm.	- 4.4
23 - 22	- 4 mm.	0	- 4 mm.	- 6.9
23 - 24	0	0	0	0
23 - 26	0	0	0	0
25 - 22	0	0	0	0
26 - 22	- 7 mm.	0	- 7 mm.	- 8.4
26 - 24	+ 12 mm.	0	+ 12 mm.	+ 9.7
25 - 26	- 6 mm.	0	- 6 mm.	- 6.7
28 - 8	- 13 mm.	- 3 mm.	- 10 mm.	- 7.3
28 - 27	+ 5 mm.	0	+ 5 mm.	+ 16.4

-ed desirable that, in view of the highly fractured nature of the ground surface, analysis of the changes should not be based upon the assumption of homogeneous strain. But as changes occur throughout the network it was found impossible to choose an axis from which to establish displacement vectors which did not suffer considerably from the problems of error accumulation. Thus almost all the changes have, after all, been analysed according to the assumptions of homogeneous strain. The results of the analysis for the original network are shown in table VI.6

The 1971 network distance measurements are given in table VI.7, with, as was done for the Mývatn results, a comment as to the significance of the observed changes. As before the significance criterion is taken to be the sum of the expected errors from the two measurements, which a change must exceed to be considered significant. Figure VI.10 illustrates the significant changes found on the 1971 network, which have also been analysed for homogeneous strain, the results being given in table VI.8.

Figure VI.11 shows the parameter of shear (in ppm.) calculated from the changes observed on the original twenty eight station network. It can be seen from the figure that there is some shear over almost all the network, but that it is generally larger towards the southern end, particularly around the geothermal field. At the north-eastern end of the original network the changes were found to be most satisfactorily explained by individual movements of stations 26 and 24, which will be discussed later.

In the light of the fault-plane solutions derived from the micro-earthquake studies of the region (Klein et al., 1973), and of the general description of the tectonics of the Reykjanes peninsula given in the last section, the sense of the observed shear is taken to be left-lateral, although there is unfortunately no way of determining this from the measurements (at least when the pattern of changes is as complex as it is here).

The average value of the observed shear over all the triangles of the original network which are not within the geothermal field (for reasons which will be considered later these triangles are excluded from the general analysis) is 15.9 ppm., an annual rate of 4 ppm.

Figure VI.12 illustrates the shear and dilatation parameters obtained from

TABLE VI.6 THE RESULTS OF THE HOMOGENEOUS STRAIN ANALYSIS OF THE REYKJANES CHANGES, 1968 - 72.

TRIANGLE	SHEAR (10^{-6})	DILATATION (10^{-6})	BEARING OF MAX. EXT.
1 - 2 - 3	31.8	-54.0	N77°E
2 - 3 -27	55.6	-32.2	N97°E
2 - 3 - 7	79.0	-77.0	N115°E
1 - 3 - 4	14.7	-49.3	N157°E
1 - 4 - 6	11.3	-50.4	N178°E
3 - 4 - 6	14.9	-57.8	N 99°E
1 - 3 - 6	2.8	-44.7	N101°E
4 - 5 - 6	48.6	-47.4	N84°E
1 - 5- 6	48.2	- 0.5	N114°E
1 - 5 - 8	23.8	-16.7	N134°E
1 - 6 - 8	32.2	-16.2	N131°E
5 - 6 - 8	21.3	-12.7	N112°E
5 - 8 - 9	33.0	-20.2	N108°E
1 -28 - 8	24.0	9.3	N164°E
8 - 9 - 10	14.7	-10.1	N 81°E
8 - 10 -11	21.0	- 0.4	N131°E
9 - 12 -10	18.3	-15.3	N 87°E
12 - 13 - 10	36.3	2.5	N101°E
10 - 13 - 11	22.6	-13.1	N 85°E
10 - 11 - 12	16.4	- 2.6	N122°E
11 - 12 - 13	24.2	- 6.7	N124°E
12 - 15 - 13	5.7	- 3.9	N 65°E
13 - 15 - 16	9.8	-3.0	N127°E
11 - 13 - 14	21.4	15.7	N130°E

TABLE VI.6 (CONTINUED).

TRIANGLE	SHEAR (10^{-6})	DILATATION(10^{-6})	BEARING OF MAX. EXT.
13 - 16 - 14	11.0	- 2.5	N114°E
15 - 17 - 16	17.3	0.6	N136°E
15 - 18 -16	26.8	12.6	N150°E
15 - 17 - 18	8.7	- 7.5	N122°E
16 - 18 - 19	16.1	7.3	N147°E
17 - 20 - 18	11.8	- 5.5	N 86°E
18 - 20 - 21	10.9	- 5.2	N145°E
18 - 21 - 19	21.0	0.8	N141°E
2o - 25 - 21	6.1	-14.9	N154°E
21 - 25 - 22	6.7	- 3.9	N131°E
25 - 26 - 22	LOCAL DISTURBANCE OF STATION 26		
22 - 26 - 23	"	" " "	" "
26 - 24 - 23	"	" " "	" "

TABLE VI.7 THE DISTANCE MEASUREMENTS ON THE 1971 EXTENSION AT REYKJANES.

LINE	1971	1972	CHANGE(mm.)	SIGNIFICANT
W 0-E 0	548.1702	548.1717	+ 1.5	YES
29 -W0	1320.0308	1320.0327	+ 1.9	NO
29 -14	1021.7276	1021.7282	+ 0.6	NO
E 0-14	1176.8061	1176.8085	+ 2.4	NO
W 0-14	1393.6718	1393.6730	+ 1.2	NO
29 -E 0	1514.4551	1514.4543	- 0.8	NO
29 - 11	580.4624	580.4626	+ 0.2	NO
29 - 13	1045.1817	1045.1810	- 0.7	NO
W 1-17	1633.4307	1633.4353	+ 4.6	YES
E 1-W 1	1017.5008	1017.5000	- 0.8	NO
E 1-20	1087.1488	1087.1539	+ 5.1	YES
E 1-17	1603.0647	1603.0667	+ 2.0	NO
W 1-20	1727.2822	1727.2823	0	NO
W 2-W 1	726.9629	726.9628	0	NO
W 2-E 2	662.3607	662.3610	+ 0.3	NP
E 2-E 1	1439.9351	1439.9342	- 0.9	NO
E 2-W 1	1373.1120	1373.1141	+ 2.1	NO
W 2-E 1	1150.9472	1150.9440	- 3.2	YES
W 2-W 3	1325.8792	1325.8760	- 3.2	NO
E 3-W 3	765.5409	765.5408	0	NO
E 2-E 3	1040.1073	1040.1047	- 2.6	YES
W 2-E 3	1576.4125	1576.4054	- 7.1	YES
E 2-W 3	1114.5682	1114.5659	- 2.3	NO
1130W 3	1130.5154	1130.5140	- 1.4	NO

TABLE VI.7 (CONTINUED)

W 4-E4	659.1329	659.1318	- 1.1	NO
E 4-E 3	1111.9754	1111.9756	0	NO
E 4-W 3	1367.1677	1367.1725	+ 4.8	YES
W 4-W 5	1070.0622	1070.0647	+ 2.7	NO
E 5-W 5	973.5849	973.5820	- 2.9	YES
E 4-E 5	892.6624	892.6618	- 0.6	NO
W 4-E 5	1426.9682	1426.9677	- 0.5	NO
E 4-W 5	1049.0661	1049.0661	0	NO
W 6-W 5	810.0890	810.0916	+ 2.6	YES
W 6-E 6	711.7771	711.7773	0	NO
E 6-E 5	1056.5522	1056.5533	+ 1.1	NO
E 6-W 5	1236.4527	1236.4518	- 0.9	NO
W 6-E 5	1252.1159	1252.1202	+ 4.3	YES
W 6-W 7	1402.2367	1402.2398	+ 3.1	NO
E 7-W 7	574.8179	574.8197	+ 1.8	YES
E 6-E 7	1427.3308	1427.3306	0	NO
W 6-W 7	1722.7830			
E 6-W 7	1359.6887	1359.6886	0	NO

Figure VI.10 THE DISTANCE CHANGES ON THE 1971 REYKJANES EXTENSION, BETWEEN 1971 AND 1972.

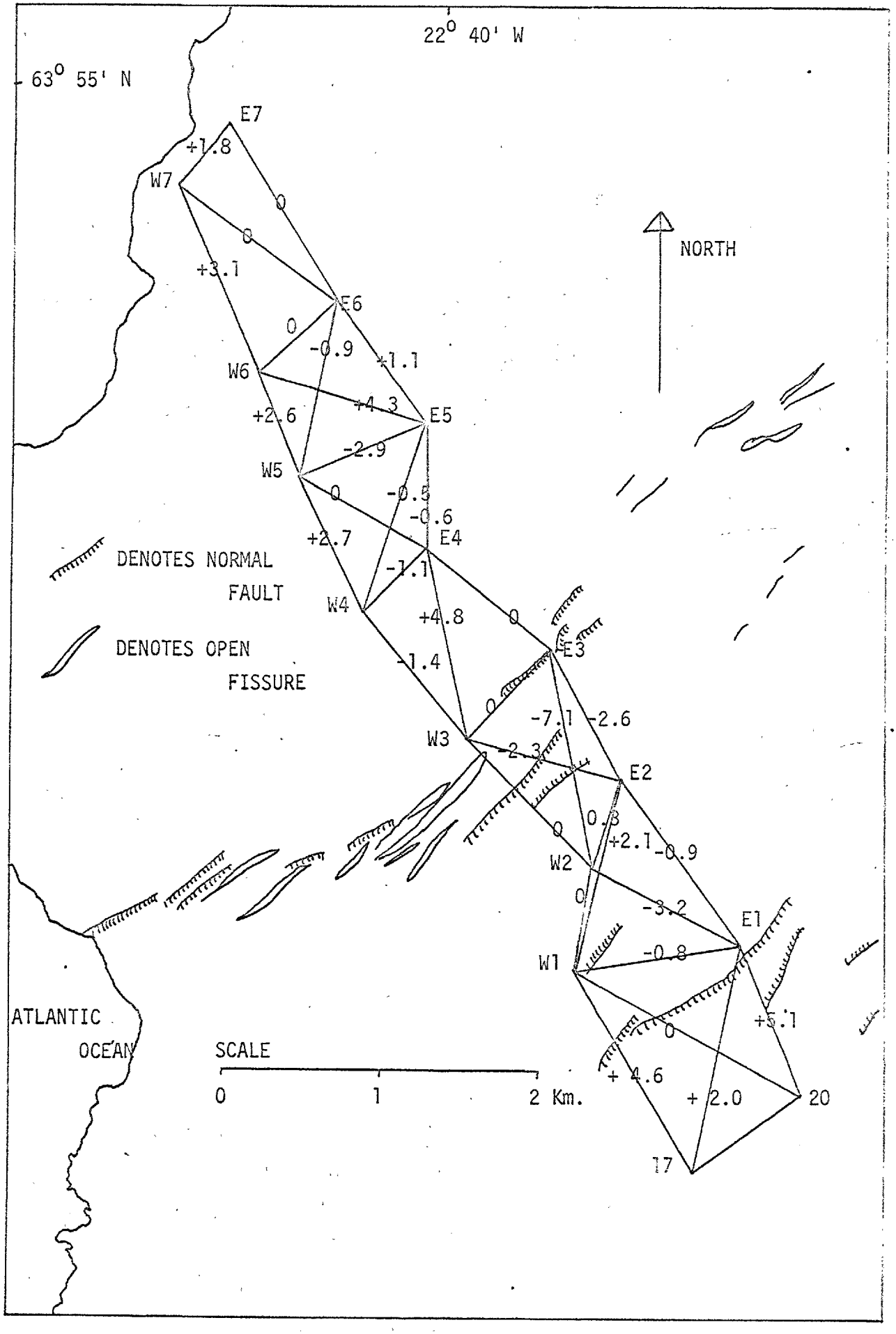


TABLE VI.8 RESULTS OF THE HOMOGENEOUS STRAIN ANALYSIS OF THE CHANGES ON THE REYKJANES EXTENSION.

TRIANGLE	SHEAR (10^{-6})	DILATATION (10^{-6})	BEARING OF MAX. EXT.
17 - 20 - E 1	5.4	3.4	N142°E
17 - 20 - W 1	6.8	3.3	N 68°W
17 - E 1- W 1	5.2	- 4.2	N185°E
20 - E 1-W 1	5.8	- 0.4	N19 °W
W 1- E 1- E 2	4.4	- 1.4	N 92°E
W 1- E 1- W 2	5.2	-0. 6	N195°E
W 1- E 2- W 2	3.6	- 2.6	N187°E
E 1- E 2- W 2	15.2	-12.1	N190°E
W 2- E 2- E 3	9.1	-0 .1	N 53°E
W 2- E 2- W3	2.5	- 2.5	N44° E
W 2- E 3- W 3	11.2	1.5	N 90°E
W 3- E 3- E 2	2.9	- 2.5	N 25°E
W 3- E 3- E 4	13.6	4.9	N 78°E
W 3- E 3- W 4	13.0	-4.7	N 5°E
W 4- E 4- E 5	5.1	- 4.8	N190°E
W 4- E 4- W 5	5.1	- 0.3	N163°E
W 4- E 5- W 5	4.1	- 2.1	N151°E
E 4- E 5- W 5	5.3	-11.0	N158°E

FIGURE VI.11 THE VALUES OF THE SHEAR (IN PPM.) PARAMETER OBTAINED FROM THE HOMOGENEOUS STRAIN ANALYSES OF THE CHANGES OBSERVED ON THE ORIGINAL REYKJANES NETWORK.

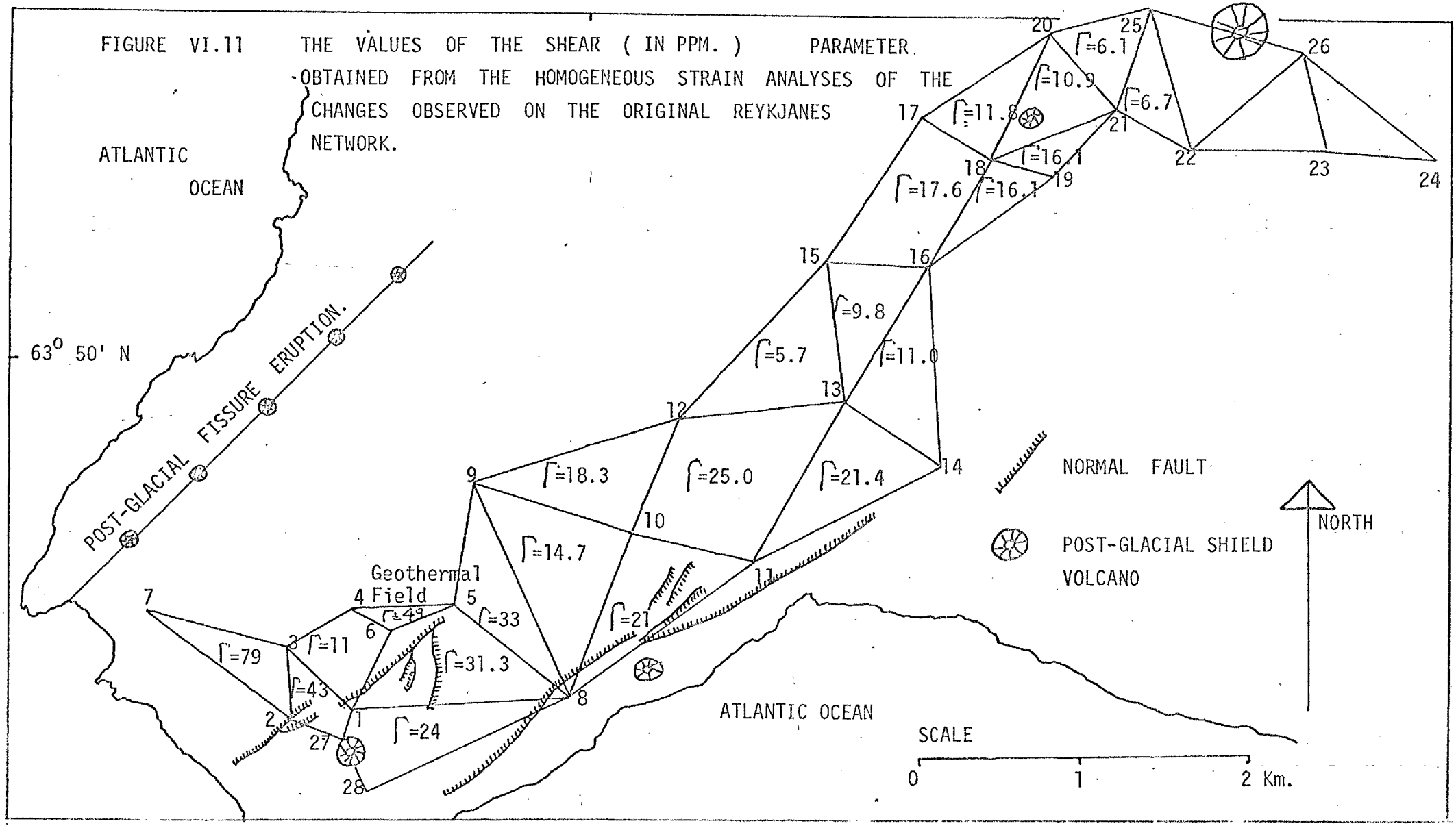
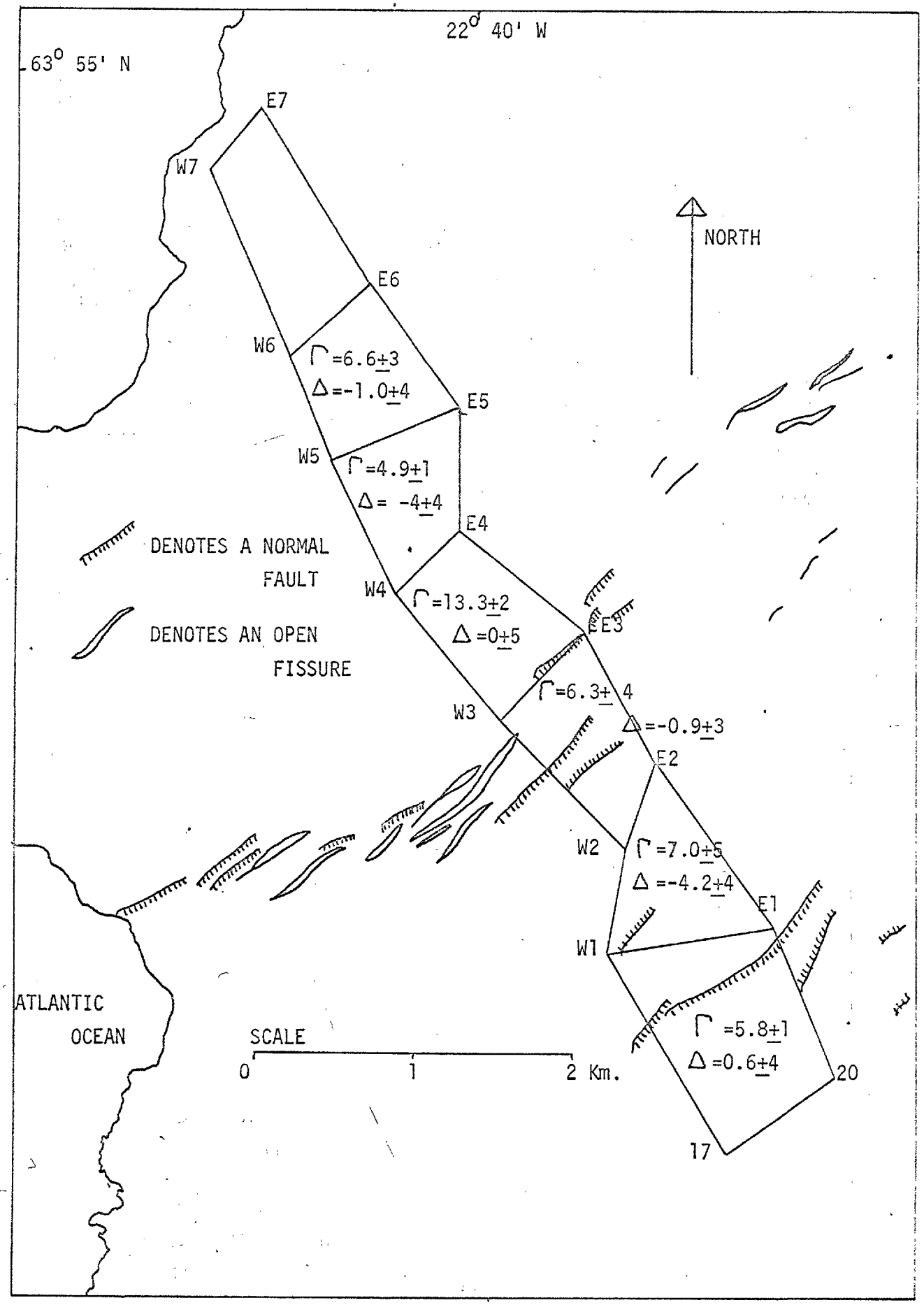


FIGURE VI.12 THE MAGNITUDES OF THE SHEARS AND DILATATIONS INFERRED FROM THE HOMOGENEOUS STRAIN ANALYSIS OF THE CHANGES ON THE 1971 REYKJANES EXTENSION.



the homogeneous strain analysis of the changes observed on the 1971 network. This shows that the shear found in each quadrilateral is about 7.5 ppm., a rather higher yearly rate than was found for the quadrilaterals of the original network.

From figures VI.11 and VI.12 it can be seen that the zone of shear is limited to the south-east by the large normal fault, and that in the north-west it ext--ends one quadrilateral beyond the region of surface faulting. Its total width thus turns out to be 4 kilometres.

The width of the micro-earthquake activity was found by Klein et al. to be about 2 kilometres, which is not greatly different, and certainly suggests that the zone of current activity (and therefore presumably the boundary between the North-American and European plates) is, in relation to the dimensions of the plates, extremely narrow. This is what has been found from other results from other parts of the world, particularly the San Andreas fault zone in California, where ninety per cent of the movement is in a zone about ten kilometres wide. Also the widths of the median rift zones of mid-ocean ridges are typically about ten kilometres.

Assuming the 16 ppm. average for the shear found over the triangles away from the geothermal field on the original network, and a one kilometre width for the network (it strikes almost exactly along the local tectonic direction), the total shear movement found on it during the four years of measurement, 1968 - 1972, is 16 mm., 4 mm. per year.

The 1971 network shows a total width across the tectonic strike of three kilometres, so that the total shear movement found on it is about 22.5 mm. in the one year, 1971 - 72.

Thus the total rate of movement (shear) found seems to be 26.5 mm. per year.

The uncertainty estimates from the 1971 network are given on figure VI.12 and suggest that the uncertainty in the estimate of the total shear movement is $\pm$ 15 mm. for the 1971 network. The uncertainty in the estimates from the orig--inal network is discussed in the next section of this chapter, which shows that the individual values of the shear parameter are accurate to $\pm$ 3 ppm. Thus the uncertainty in the estimated rate of movement over the four years on the original

network is ± 3mm., from which it is seen that the total uncertainty in the rate of shear movement across the four kilometre wide zone is ± 16 mm.; this is rather less than the estimate of that movement, showing that the latter should be considered significant.

The second parameter of the homogeneous strain analysis which will be considered is the dilatation. This is shown for the 1971 network on figure VI.12, and for the original network on figure VI.13.

There is no significant dilatation in any of the quadrilaterals of the 1971 network, which will not be discussed further.

A large number of the triangles of the original network show negative values of the dilatation, although there are positive values along the whole length of the south-eastern fault (which was discussed above as the boundary of the zone of shear).

Extremely large negative dilatation is found in an elongated region striking approximately north-east from, and including, the geothermal field.

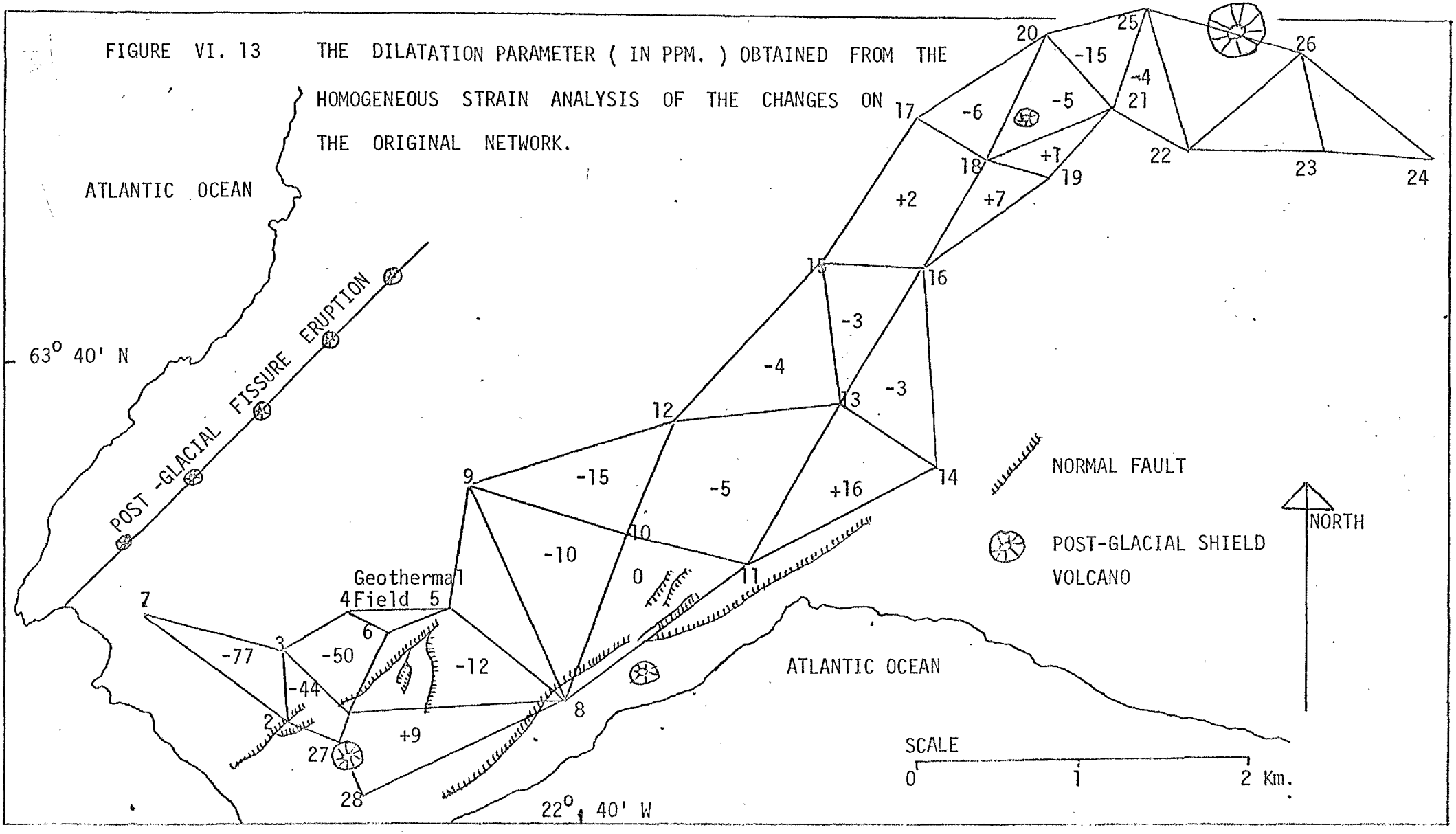
That there is positive dilatation associated with the south-east fault can only mean that there has been extension on it, in addition to the shear movement already discussed. The magnitude of this extension is however, not very large, about 1 mm. per year.

Negative dilatation can only imply compression. Pure shear movement shows no area change (Appendix B), although simple shear does involve a decrease in area. Simple shear is not easy to understand geologically, so that it is felt that the strong spatial correlation between the geothermal field (especially the area in which the steam holes were drilled) and the area of negative dilatation suggests that there is a causal relationship involved.

Large vertical and horizontal subsidences have been reported from oil fields in several places throughout the world, so that similar effects might be expect-ed from exploited geothermal fields where a fairly large mass-discharge rate has been effected by drilling.

In the case of the Wairakei geothermal field in the Taupo volcanic zone of New Zealand, the expected vertical deformation has been observed (Bolton, 1973).

FIGURE VI. 13 THE DILATATION PARAMETER (IN PPM.) OBTAINED FROM THE HOMOGENEOUS STRAIN ANALYSIS OF THE CHANGES ON THE ORIGINAL NETWORK.



The total vertical subsidence found at Wairakei has been about 3.3 m. since exploitation of the field began in 1956, an annual rate of about 200 mm. per year.

Unfortunately there are no horizontal measurements from the region.

Chapter V of this thesis discussed the results of repeated vertical angle surveys in the region of the geothermal field at Reykjanes, which suggested that the centre of the field had subsided in the five years between the surveys by about 130 mm., an annual rate of about 25 mm.

The mass discharge rate from the Wairakei field is at the moment about 170 kg. $sec.^{-1}$ and the total mass removed since 1955 is about 6×10^{11} kg. (Bolton, 1973).

The current mass discharge rate from one of the two open wells at Reykjanes is 65 kg. $sec.^{-1}$ (Björnsson et al., 1972). The other is somewhat smaller, so that the total discharge rate is probably of the order of 100 kg. $sec.^{-1}$ The total mass removed from this field since 1968 is about 9×10^{9} kg.

It seems perfectly possible that the observed vertical deformation at Reykjanes results directly from the removal of water from the high temperature aquifer, in much the same way as has been observed at Wairakei, despite the fact that the ratio of vertical movement:mass discharge is an order of magnitude higher at Reykjanes than at Wairakei.

It also seems then perfectly possible that the large negative dilatation observed in the geothermal area results too from the removal of water from the aquifer, although this effect has not been observed before.

Another possible explanation of the observed negative dilatation on the original network is that a shift of the spreading axis to the south-central active zone (which was shown in the last section to be much more volcanically active than the Reykjanes peninsula) has put the peninsula into a state of compression.

This explanation is not favoured because it would entail compression over the whole of the network, which the observed positive dilatation on the south-east fault shows is not the case.

The third parameter arising from the homogeneous strain analysis is the

bearing of the extensional principal strain. This is shown in figures VI.13 and VI.14 for the original and 1971 networks respectively.

Figure VI.15 is a histogram of these directions (drawn from the original network results, although a glance at the directions from the 1971 network results shows that the same effect is observed there also).

This histogram shows that the directions fall into two distinct groups.

The first is very well-defined at N85^{o}E, the second is also well-defined at N130^{o}E. The first peak seems to have a very small standard deviation, about 8^{o}, whereas that of the second peak is about 20^{o}. These standard deviations will be discussed further in the analysis of the uncertainty in the values of the homogeneous strain parameters.

The spatial distribution of the members of the two peaks is very interesting (figure VI.13). It seems very much as though the lower valued extensional bearings are associated with the geothermal field and some parts of the north-western side of the original network, while the triangles away from the geother--mal area all belong to the latter group of directions.

The second direction, N130^{o}E, corresponds extremely well with the extension--al direction inferred both from the geological studies of Nakamura (1970), and from the micro-earthquake studies of Klein et al. (1973). It also exactly corresponds to the direction of sea-floor spreading inferred from the magnetic results of Heirtzler et al. (1966), and Talwani et al. (1971), so that it seems very much as though this direction is the regional tectonic extensional direction. It is true too that those triangles which show positive dilatation also show a N130^{o}E extensional direction (e.g. the triangles bordering on the south-east fault), so that the south-east fault can be assumed to be interpret--ed as a large normal fault related to the regional extension in the area. It should also be noted that (chapter V) most of the observed vertical movement in the area was across this fault.

The second peak in the distribution of directions of extension is made the subject of a separate section of this chapter, and will follow shortly.

It is now necessary to summarise the findings of this section, and to

FIGURE VI.13 THE DIRECTIONS OF THE AXES OF MAXIMUM EXTENSION DERIVED FROM THE HOMOGENEOUS STRAIN ANALYSIS OF THE REYKJANES CHANGES.

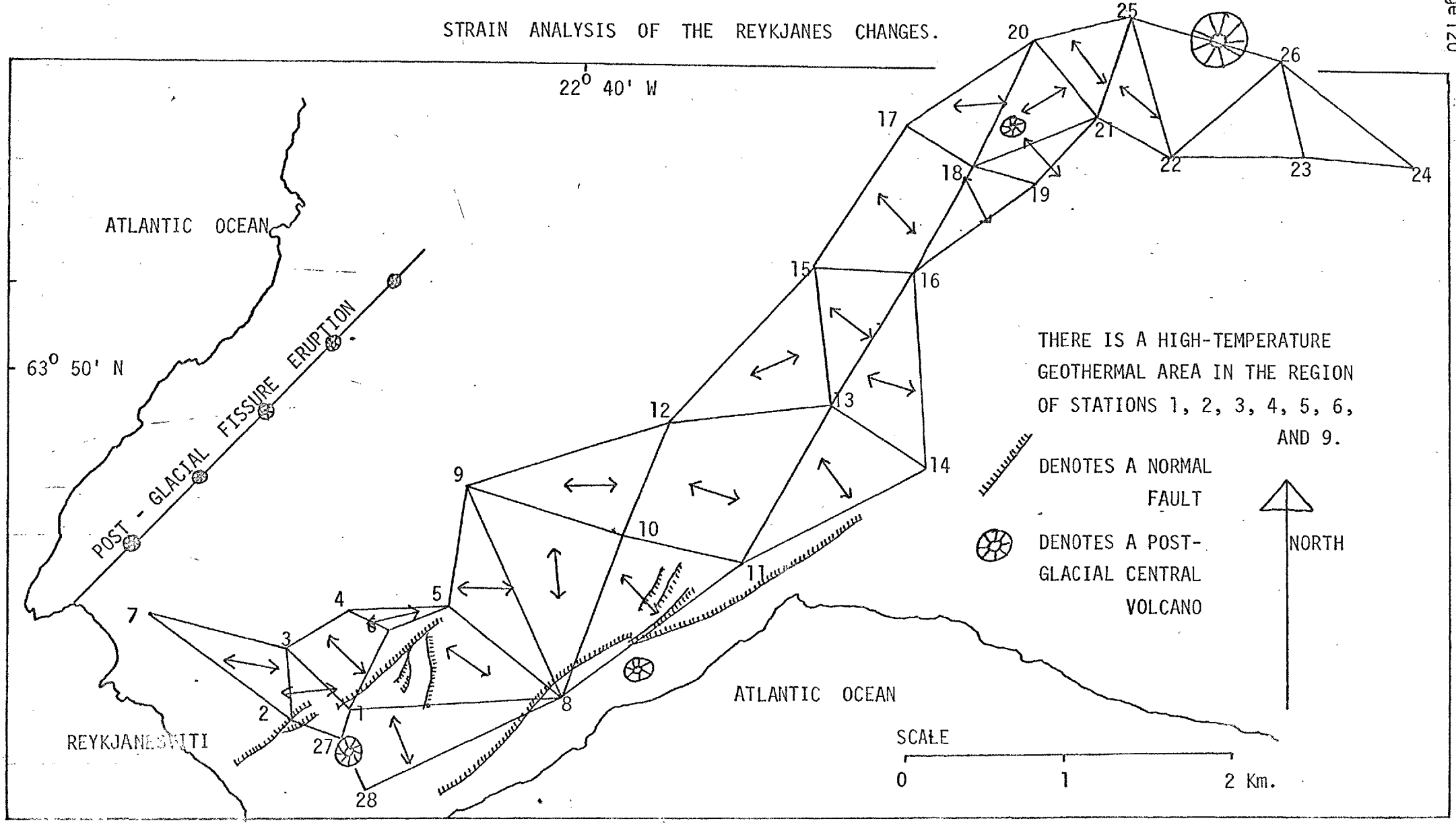


FIGURE VI.14 DIRECTIONS OF AXES OF MAXIMUM EXTENSION INFERRED FROMM MOMOGENEOUS STRAIN ANALYSIS OF THE CHANGES ON THE 1971 REYKJANES EXTENSION.

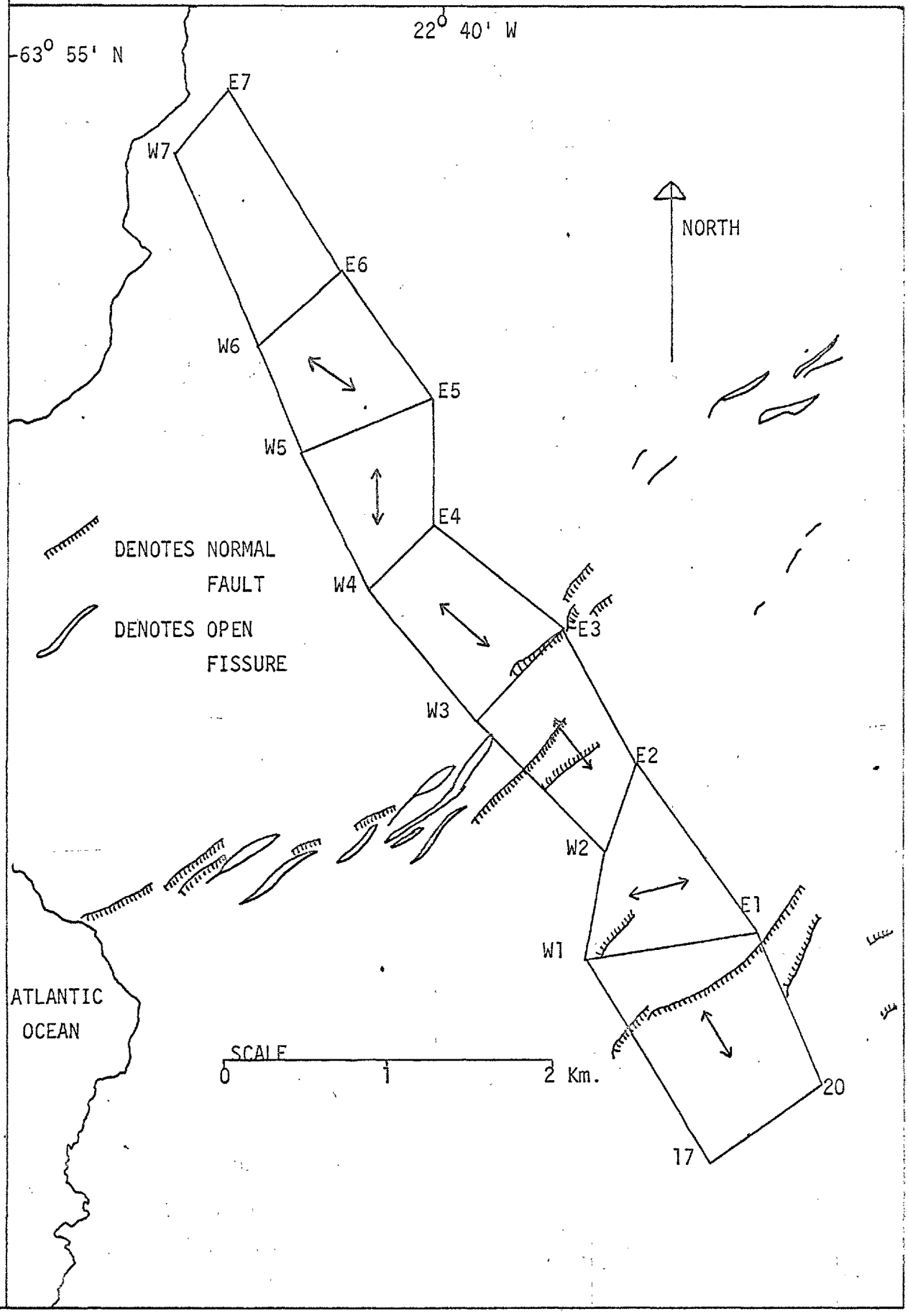
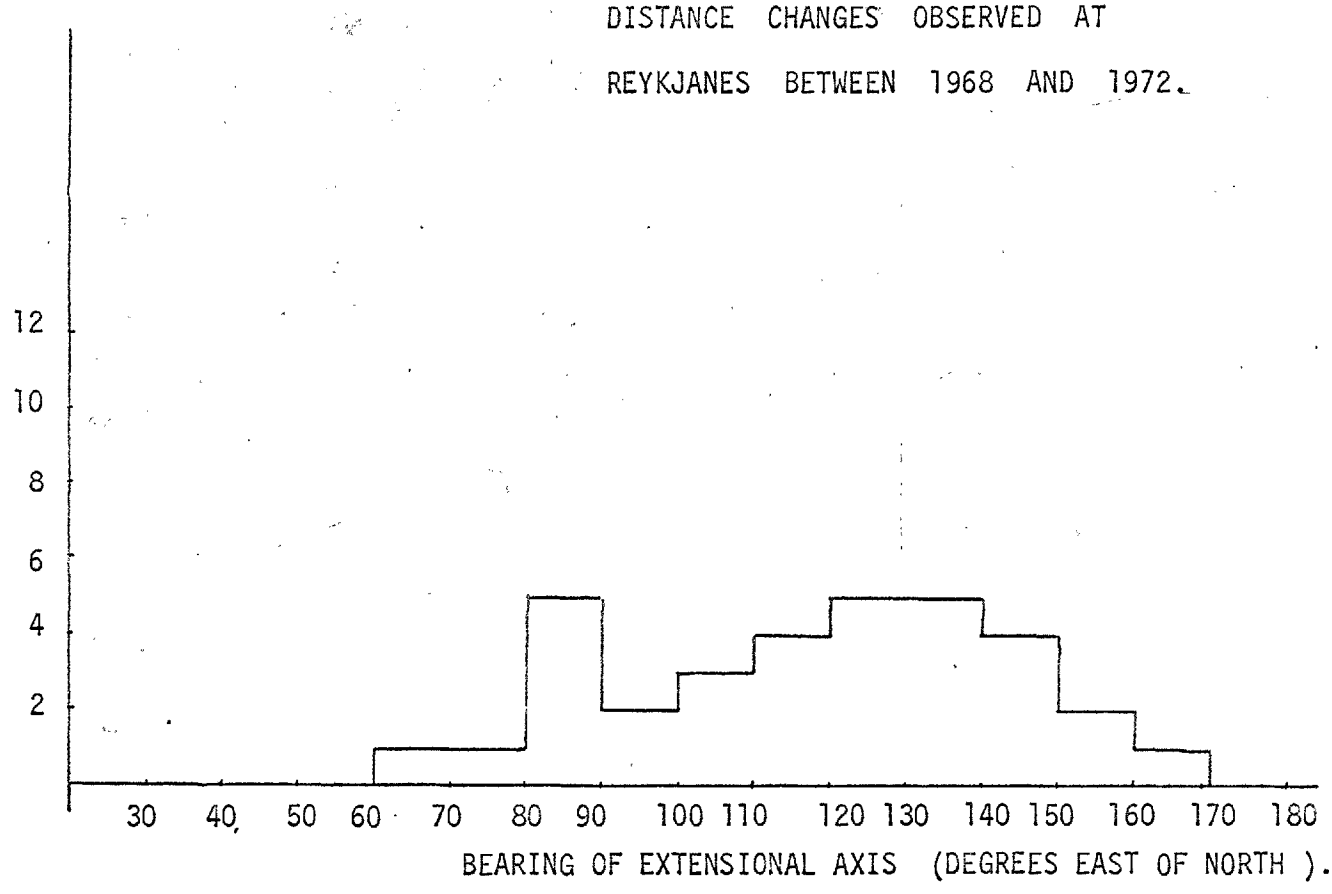


FIGURE VI.15 HISTOGRAM SHOWING THE DISTRIBUTION OF THE BEARINGS OF THE MAXIMUM EXTENSION AXES DERIVED FROM THE HOMOGENEOUS STRAIN ANALYSES OF THE DISTANCE CHANGES OBSERVED AT REYKJANES BETWEEN 1968 AND 1972.



The distribution shows two peaks: the first, at N85^{o}E, is identifiable with the surface faulting: the second, at N130^{o}E, is identifiable with the tectonic trends of the region.

compare them with the findings of the last section which discussed the results of other work and the tectonism of the Reykjanes peninsula.

The results of the distance measurements show that shear is the dominant mechanism on the part of the Reykjanes peninsula studied.

Positive dilatation, which would be associated with sea-floor spreading and crustal extension is found in significant amounts in only one place, across a large normal fault which also shows considerable vertical movement (chapter V).

The shear is distributed across a zone about 4 kilometres wide, whose strike is not very well defined by these results, although as the south-eastern border of the shear zone is the large normal fault on which positive dilatation was found and this strikes at N45^{o}E, the strike of the shear zone must be similar.

The north-western boundary of the shear zone approximately corresponds with the north-western limit of the surface faulting, but might extend a little beyond it.

The larger part of the shear movement (which amounts to 26 $\pm$ 16 mm. per year across the entire zone) takes place within a graben to the north of the geothermal field (figures VI.8 and V.2), which the vertical angle results suggest is subsiding at a rate of about 25 mm. per year. Within the graben one group of faults in particular seems to account for a large proportion of the shear (see figure VI.12), indeed almost half of the annual total.

Considerable negative dilatation (- 50 ppm. in four years), vertical subsidence of about 130 mm. in five years, and an anomalous direction of maximum extension are associated with a geothermal field which has been producing a hot brine and steam mixture at a rate of about 100 kg. sec.$^{-1}$ for the last four years. This result is directly comparable with geodetic observations from another high productivity geothermal field in New Zealand. The anomalous extension direction associated with this field suggests a faulting direction different from that of the main tectonics of the region.

The principal tectonic direction of the region which governs the non-geothermal shear and also the small amount of extension observed is extension at N130^{o}E $\pm$ 20^{o}, which direction is completely in agreement with the geologically derived extension direction, fault-plane solutions from micro-earthquake studies

in the area, local directions of sea-floor spreading, and the direction of extension required if, as is indicated by the seismic and volcanic evidence, the Reykjanes peninsula is considered to be a left-lateral shear zone.

The similarity between the area of the network and the other tensional groups of the peninsula suggests that the findings from the one should be applicable to all, and that therefore shear should be the dominant mechanism along the entire peninsula, in which case the peninsula should indeed be consid--ered a left-lateral shear zone, with a small component of extension.

According to the original definition of a transform fault (Wilson, 1965), the Reykjanes peninsula cannot be one. Transform faults should lie on small circles of the pole of rotation governing the relative motions of the plates concerned. In this case the pole of rotation is at 68^{o}N 137^{o}E (Pitman and Talwani, 1968) so that transform faults should strike at N100^{o}E (Klein et al., 1973). The strike of the Reykjanes peninsula is, as has been mentioned before, N80^{o}E so that it cannot be considered a true transform fault, and must show a certain amount of spreading as well, as has indeed been observed.

However, it is significant that the direction of the Reykjanes peninsula is as would be expected from the normal structural geological analysis of a stress system whose extensional principal component is at N135^{o}E, i.e. is parallel to the direction of local sea-floor spreading. This perhaps shows that the processes of plate tectonics are not in any way opposed to the normal consider--ations of structural geology, but are as much controlled by them as are smaller scale problems. This leads to interesting possibilities for analysing the stress systems operating in complex regions such as Iran and the south Pacific.

SECTION VI.7 CONSIDERATION OF THE ACCURACY OF THE STRAIN PARAMETER ANALYSIS.

In the last section a very large number of results of analyses of the distance measurements in terms of homogeneous strain was presented.

Of these there were some, in the double-braced quadrilaterals of the 1971 Reykjanes network, that were presented along with estimates of their accuracy.

These estimates were all derived from the scatter of the values obtained from the four different triangles of which a double-braced quadrilateral is composed.

For the triangles of the original network no estimates of the accuracy of the values of the three strain parameters was given, although it was noted that the spread of the values of the direction of maximum extension about the two peaks was such as to suggest that the standard deviation of the 130^{o} group was about 20^{o}, while that of the 85^{o} group was about 8^{o}.

These values of the different standard deviations will now be discussed.

The formulae from which the three parameters are derived are

$$\tan 2\emptyset = \frac{(e_a - e_b).\sin(b + c).\sin(b - c) - (e_b - e_c).\sin(a + b).\sin(a - b)}{(e_a - e_b).\cos(b + c).\sin(b - c) - (e_b - e_c).\cos(a + b).\sin(a - b)}$$

$$\Gamma = \frac{2\,(e_a - e_b)}{\cos(2a - 2\emptyset).\cos(2b - 2\emptyset)}$$

$$\Delta = 2e_a - \Gamma.\cos(2a - 2\emptyset)$$

where a,b, and c are the bearings of three directions from a fixed reference (e.g. due north); $\emptyset$ is the bearing of the extensional principal strain from the same reference; e_a, e_b, and e_c are the strains in the three directions; Γ and Δ are the shear and dilatation respectively.

These equations are derived from the simultaneous solution of the three equations for e_i given in chapter IV.

Uncertainties in the measured distances influence the values of $\emptyset$, Γ and Δ through the parameters e_i.

Estimates of the uncertainties in the values of the parameters e_i are obtained (when more than two measurements are available) from the range of

possible fits to the distance-time graphs shown (for Reykjanes original network) in Appendix E.

It so happens that the short lines, on which a large scatter of the distance results would entail a large uncertainty in the strain, are also those which have been measured most frequently, so that the total distance changes are better defined than on the longer ones.

The uncertainty in the strain measured on line 1 - 3 at Reykjanes is $\pm$ 3 ppm. (the line is 513 m. long), which compares with the uncertainty on the strain measurement of line 1 - 3 at Thingvellir (1620 m. long), $\pm$ 2 ppm.

Thus,for the purposes of estimating the errors in the homogeneous strain analysis, the uncertainty in the values of e_i has been assumed constant at $\pm$ 3 ppm.

Using this value and the principle of the superposition of errors in a typical triangle (here assumed to be equilateral), the estimate of the uncertainty in the direction of maximum extension is found to be 10^{o} for the situation where the total strains on each line are of the order of 25 ppm. (the lines around the geothermal field at Reykjanes), and 22^{o} on the rest of the original network, where the total strains have not been so large.

The uncertainties resulting from this in the estimates of the shear and dilatation parameters turn out to be $\pm$ 2 ppm. and $\pm$ 3 ppm. respectively for each case.

These uncertainties are quite large, but rarely approach the actual values obtained for the parameters, so that the interpretation of the results is not affected by this, except that some of the smaller values of the dilatation from triangles away from the geothermal field should not be considered very meaningfull.

SECTION VI.8 CONSIDERATION OF THE CHANGES OBSERVED AT THE NORTH END OF THE ORIGINAL REYKJANES NETWORK.

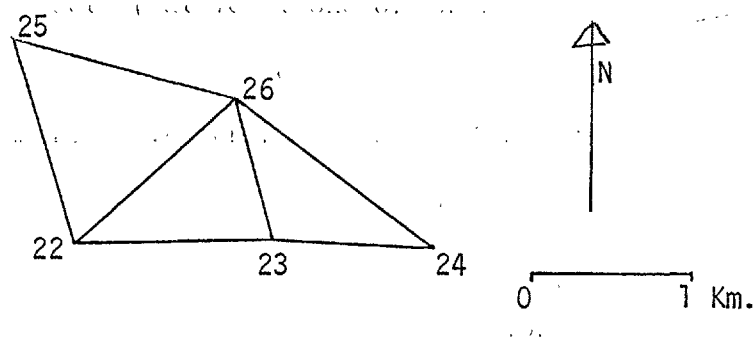
It was mentioned in the section dealing with the main presentation of the Reykjanes results that certain of the changes observed at the north-eastern end of the original Reykjanes network are best explained by movements of two of the stations there in a discrete fashion. Strain analysis has not been conducted in that part of the network because these movements are not deemed to represent tectonic effects (at least one of them probably does not, although the other may).

The table below summarises the changes found at the north-eastern end of the network.

LINE	CHANGE (mm.)
23 - 24	0 before 1972, then suddenly + 6
23 - 26	0
26 - 22	- 7
26 - 24	+ 12
26 - 25	- 6

The number of changes associated with station 26 is noticeable.

The figure below is a detail of the network in the area.



Assuming that stations 22, 23, and 25 have remained fixed, it is possible to solve the displacement vector solution for station 26, in which case the movement of that station is 7.5 mm. at N100^{o}W, and the changes on the various lines involved are

23 - 26	0
26 - 22	-6.8
26 - 25	-6.4
26 - 24	+3.6

from which it is seen that the movement of the one station neatly explains all the observed changes associated with it except that of line 26 - 24, on which there remain yet 8.4 mm. extension unaccounted.

This 8.4 mm. is certainly of the same order of magnitude as the other change associated with station 24, the sudden 6 mm. increase of line 23 - 24 which occurred between the 1971 and 1972 measurements. If it can be assumed that the extra 8.4 mm. on line 26 - 24 occurrred suddenly in the same period (for which there is no particular evidence one way or the other) then both changes would be explained by a sudden movement of station 24 by about 9 mm. in the direction N150°E.

It can be seen from any of the figures illustrating the original Reykjanes network that station 24 lies a little to the south-east of the north-eastward extension of the large normal fault which forms the southern boundary of the zone of shear. This fault has already been shown from the strain analysis in the last section to have been associated with shear and extensional movements during the period of measuring, and the fact that the possible displacement of station 24 is in the direction N150°E, which is very like the regional extensio-nal direction found, suggests that this displacement is related to the movement on the large fault.

The movement was sudden, and may have been the result of an earthquake swarm. However, its average value over the four years is two millimetres per year, which is very similar to the rate of 1 mm. per year extension estimated from the strain analysis for the large fault.

The movement of station 26 however, is not so easily comprehended, indeed as it bears no apparent relation to any other process observed on the network, it has been assigned to the class of non-tectonic disturbance.

These isolated displacements, or at least that of station 24, corroborate the strain analysis results to some extent, and provide further weight to the suggestion that extension across the peninsula is a great deal smaller than shear along it.

SECTION VI.9 DISCUSSION OF THE N85°E PEAK IN THE HISTOGRAM OF MAXIMUM EXTENSION DIRECTIONS FROM THE REYKJANES NETWORK.

It will be recalled that figure VI.15, the histogram of extensional direct--ions found from the homogeneous strain analysis of the results from the origin--al Reykjanes network, showed two distinct peaks.

The one, at N130°E, has been associated with the regional tectonics of the area and shown to agree well with the direction of sea-floor spreading found in the region and with the extensional axes derived from other observations.

The second has been shown to be associated with the geothermal field, and as will be seen from figure VI.14, is found also on the 1971 network in one quadrilateral. The line joining this quadrilateral and the geothermal field strikes at N30°E.

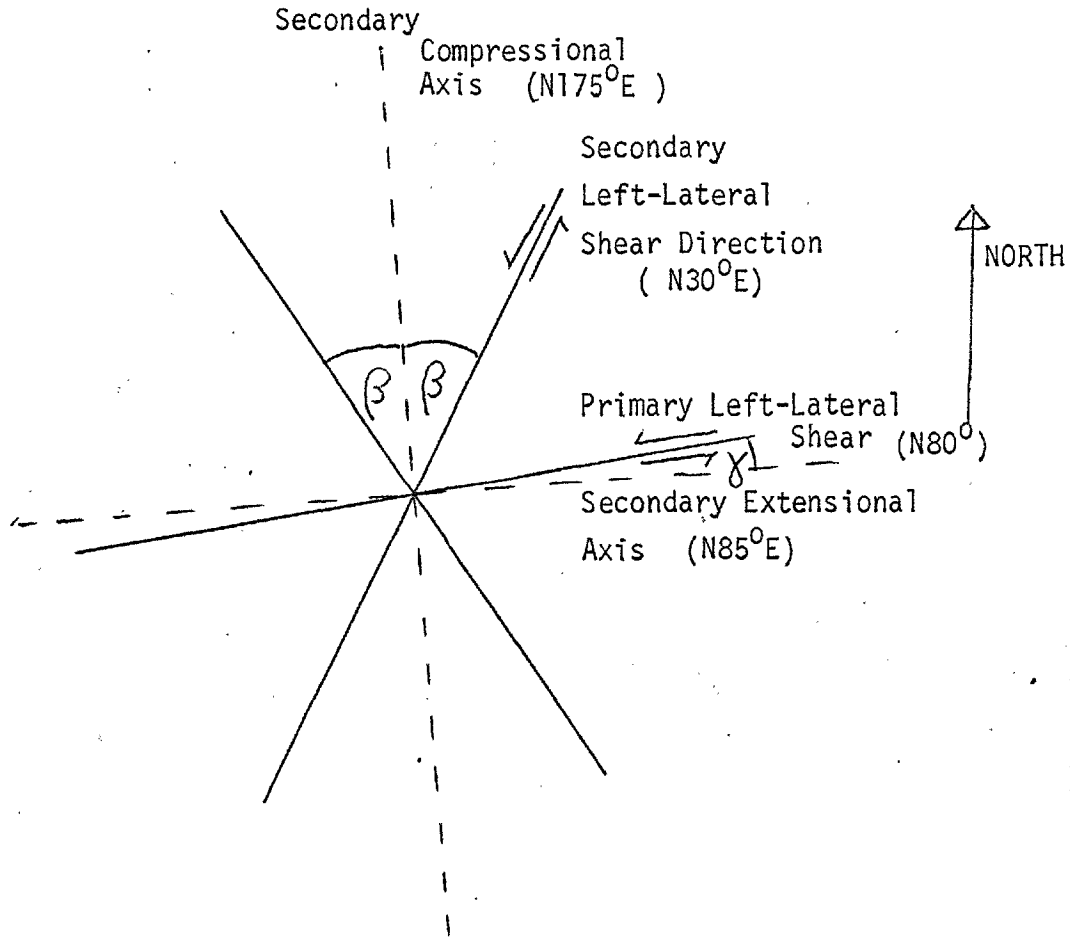
Some sections ago, in the introduction to the tectonics of the Reykjanes area, it was mentioned that during the earthquake swarm that accompanied the great increase in the geothermal activity at Reykjanes, a series of en echelon north-south fractures opened. These were very noticeable because of the steam issuing from them.

It was also observed that such a fracture system is indicative of left-lateral faulting on a zone striking approximately at N30°E, exactly the strike of the zone showing the N85°E extensional axis discussed above. Indeed extension at N85°E (together with the usual orthogonal compression) would be expected, in a medium whose angle of internal friction is 20°, to produce left-lateral shear planes at N30°E. Thus all these facts seem to be self-consistent.

The problem then is to relate this group of observations to the regional structure which is defined, as has been shown, by an extensional axis at N130°E ($\pm$ 20°) producing shear and a little extension along the Reykjanes peninsula in a N80°E direction.

Figure VI.16 shows an analysis of these directions based upon the observatio--ns of secondary faulting on the San Andreas zone by Moody and Hill (1956).

FIGURE VI. SECONDARY FAULT ANALYSIS OF OBSERVED REYKJANES SYSTEM.



This analysis is conducted according to the system suggested by Moody and Hill (1956).

The angle β is the angle of shear, meaning the angle between the maximum compressive stress and the actual shear planes.

The angle γ is the angle of tension, meaning the angle between the secondary maximum extensional axis and the primary shear planes.

Moody and Hill suggest that typical values for β are between 25° and 35°, with 30° most often encountered.

They suggest too that γ varies between 5° and 15°.

The values of each used in this analysis are 5° and 35°, with the primary left-lateral shear direction N80°E.

Using these values, the direction of secondary left-lateral shear is N30°E, exactly as would be expected from the field observations.

The secondary extensional axis inferred above agrees exactly with the results of the homogeneous strain analysis.

The primary shear direction, here (unlike the San Andreas) is left-lateral at N80°E. It gives rise to a secondary extensional axis at N85°E, probably as a result of dragging of the surface layers.

The angle of this secondary extension relative to the primary shear is shown by Moody and Hill to vary from place to place between 0° and 15°, so that the angle of 5° used here is well within the possible range. This value for the angle was chosen because it fits the observations.

The angle of internal friction which has been used here is also within the range of values given by Moody and Hill, although at 20° it is rather less than their 'typical' value of 30°. It too has been chosen for this analysis because it fits the observations, both of the primary shear direction in relation to the regional stress, and of the secondary shear direction in relation to the secondary stress.

Thus it seems very probable that the faulting which occurred in 1967 result--ing in the great increase in the geothermal activity of the area was entirely secondary to the major shear zone of the Reykjanes peninsula.

It is worth comparing this observation with information from other Icelandic geothermal fields.

Ward and Björnsson (1971) show a map of the Hveragerthi geothermal field (their figure 6) which shows that the field strikes approximately at N22°W. If this were assumed to represent a secondary right-lateral shear zone then the primary shear would be left-lateral at N98°E (assuming the same solid constants as for the Reykjanes area). As this field occurs further east along the Reykjan--es zone (in fact beyond the eastern end of the peninsula), this would presumably represent the same shear zone as has been found from the distance measurements.

Krýsuvík is another thermal area on the Reykjanes peninsula, more or less mid-way between Hveragerthi and the trilateration network. Here the geothermal activity seems to strike at about N30°E, so that the situation is similar to that at the trilateration area.

The numerous other geothermal sites in Iceland have not been investigated

in detail by this author so that how well-established the principle is cannot be definitely stated, but the indications are interesting.

It may be remembered that quadrilateral 1 of the Mývatn network showed a peculiar (relative to the other observations in the area) direction of maximum extension.

This anomalous direction, N146^{o}E, does not however, bear any obvious relat--ion to the primary direction in the area, which was found to be N60^{o}E, and therefore remains unexplained.

Presumably though, in those places where the secondary faulting idea seems to fit the observations, there is only geothermal activity because the secondary faulting has broken the ground sufficiently for the hot water, which is found in fairly deep aquifers (usually about one kilometre below ground), to rise under hydrostatic pressure (Elder, 1965).

It could also be that the observed association of micro-earthquake activity with geothermal zones (Ward and Björnsson, 1971) also reflects this secondary faulting, although the mechanisms for events from these zones do not support this idea (Klein et al., 1973).

CHAPTER VII. SYNTHESIS OF THE GEODETIC RESULTS AND CONSTRUCTION OF AN OVERALL TECTONIC PATTERN FOR ICELAND.

In the last chapter the geodetic results from various parts of Iceland were presented and interpreted in the light of local structural observations.

This chapter is divided into three sections dealing with the south, the north, and then the whole island.

SECTION VII.1 THE TECTONICS OF SOUTHERN ICELAND.

The results from the Reykjanes peninsula showed predominantly shear, left-lateral along a N80^{o}E striking zone about four kilometres wide, on which the total annual movement amounted to 25 $\pm$ 16 mm.

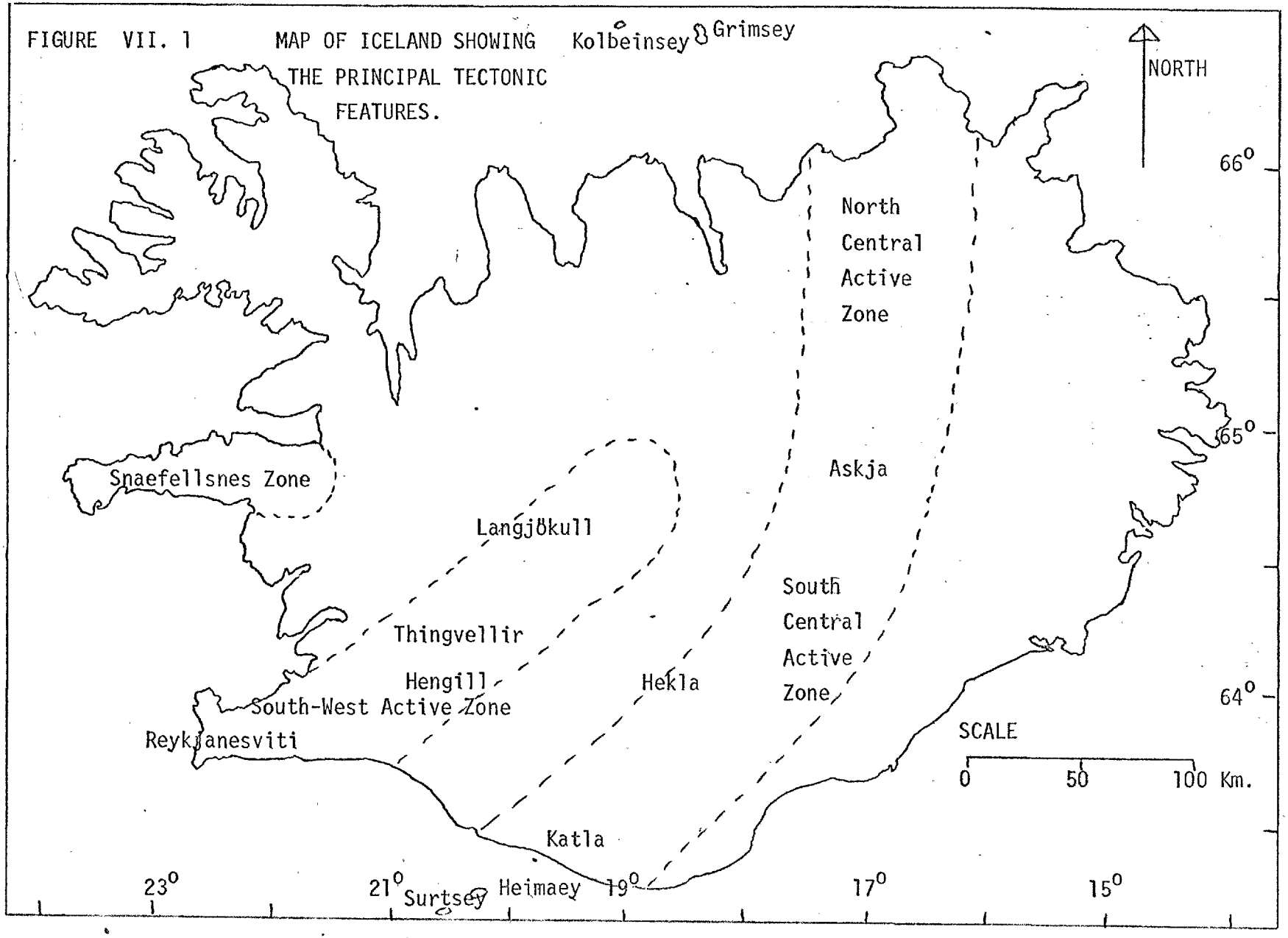
At the surface this shear zone is evidenced by a series of en echelon tensional groups (including fissure eruption axes which were probably responsible for building up the peninsula) which continue eastwards along the peninsula as far east as Hengill (figure VII.1). Here the en echelon arrange-ment of fissure eruptions ceases.

The results from Thingvellir, which is a few kilometres N35^{o}E of Hengill, show mainly extension perpendicular to the strike of the graben, which is N30^{o}E, with a little contraction perpendicular to it. The extension rate is 6 $\pm$ 3 mm. per year, and the contraction is about 1 ppm. per year, although it is not known precisely how far this operates and therefore how much it represents in actual shortening.

Figure VII.1 shows that the western zone of post-glacial activity continues northwards from Thingvellir along a N30^{o}E direction. This line would take it beneath the Langjökull ice sheet. No historical activity has been reported from anywhere along this line, although there is a small zone of micro-earthquakes on the south-western side of the ice sheet.

There have been recent eruptions (probably not historical) immediately north of Langjökull (Piper, 1973b), some of which have been produced by fissur-es striking N05^{o}W and showing en echelon arrangements indicative of sinistral

FIGURE VII. 1 MAP OF ICELAND SHOWING THE PRINCIPAL TECTONIC FEATURES.



shear.

From there post-glacial activity dies out completely, although the zone striking N05°W from this point was active during early quaternary time (Ward, 1971) and was very likely the northern axis of crustal extension.

Thus the axis of post-glacial activity which passes through at N30°E peters out to the north of Langjökull (after undergoing another change of direction). The northern end of the axis will be discussed in the next section dealing with northern Iceland.

Hengill marks the end of the well-defined en echelon arrangement of eruptive fissures of the Reykjanes peninsula, and thus, it might be supposed, the end of the N80°E striking left-lateral shear zone.

However, the geological map of south-central Iceland (Kjartánsson, 1960) shows that the rivers Thjórsá and to some extent Hvitá have curious step-like courses whose longer sections, the treads, all strike around N45°E.

It is proposed that these tread-like sections of the courses represent the continuation of the en echelon structure of the Reykjanes peninsula (and thus of the shear zone) eastwards to join the south-central zone of post-glacial activity a little to the north of Hekla.

Taken alone this evidence for the continuation eastwards of the shear-zone is not compelling, but considered in conjunction with the distribution of epice-ntres given by the I.S.S. (figure VII.2) , it is thought to bear some weight.

This extension of the shear zone was first proposed by Ward et al. (1969) who considered that the entire zone east from Reykjaneviti was a transform fault offsetting the mid-Atlantic ridge eastwards to the south-central zone of post-glacial activity.

Ward (1971) later rejected this idea, principally because of the lack of surface evidence for such a fault, and changes the strike of the proposed fracture zone (which he considered to be about 80 km. wide) to N100°E, which goes neatly under-water and has the additional advantage of being the pure shear direction indicated by the Pitman and Talwani (1971) pole of rotation for this part of the Atlantic. This shear zone would then intersect the south-central

active zone to the south of Surtsey and Heimaey, both of which have been recently volcanically active (Thórarinsson, 1967 ; Thórarinsson et al., 1973).

However, there is chemical evidence (Jakobsson, 1966, 1972, and 1973) and geodetic evidence (Brander and Wadge, 1973) to exclude both these recent eruptions from the true extensional axis of the south-central active zone.

There is also evidence to exclude Hekla from the main extensional axis of southern Iceland, thus allowing the intersection of the shear zone with the extensional axis to occur to the north of Hekla.

This evidence is primarily structural, concerned with the strike of the Hekla fissure, with earthquake fractures (Tryggvason, 1967), and with observed surface faults (Tómasson, 1967).

The strike of the Hekla fissure is seen from the geological map (Kjartansson 1960) to begin at N65^{o}E, although it curves rapidly round to N45^{o}E (the overall trend of the south-central active zone) as it continues northwards. Although there appears to be no evidence of en echelon arrangement of the eruptive centres on it, this fissure has the same initial strike as the Surtsey eruption, inter-preted by Brander and Wadge as being a left-lateral shear zone.

Likewise Katla, although ice-covered so that positive analysis is difficult, seems to lie on a fissure whose initial strike is N18^{o}E, before swinging round like Hekla's, to the general N45^{o}E trend.

This strike is very similar to that of the Heimaey fissure on which distance measurements were made by Brander and Wadge during its eruption, showing it to be a zone of right-lateral shear.

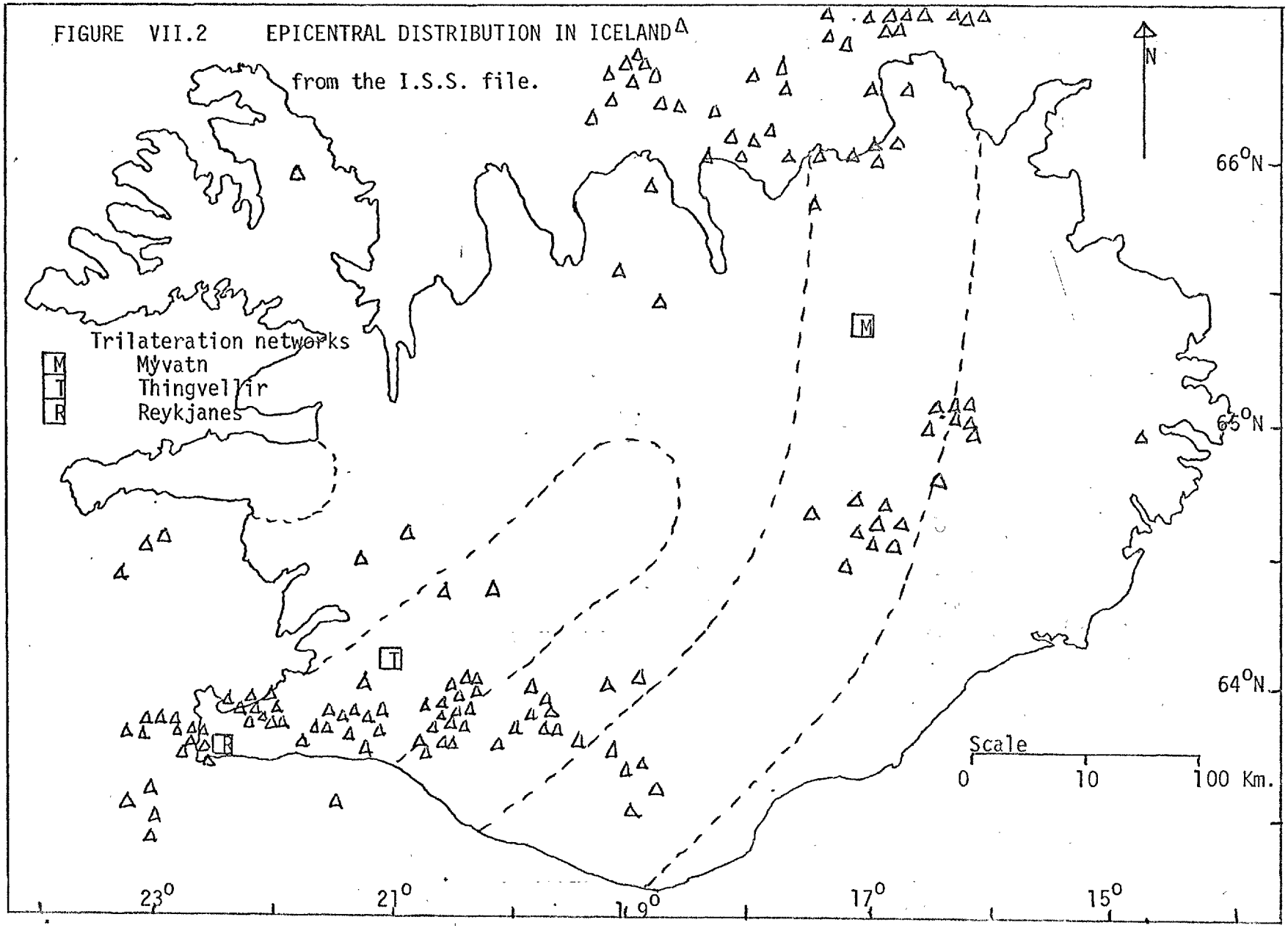
Tryggvason (1967) showed that the surface break of the 1912 earthquake, which was thirty kilometres long and occurred just west of Hekla, was a zone of en echelon segments indicative of right-lateral shear on a plane striking a few degrees east of north.

Tómasson (1967) identified several surface faults at Búrfell (during the course of the construction of the power station there) which is a few kilomet-res north-west of Hekla as being left-lateral and striking ENE.

Thus the whole area from Surtsey north-eastwards to just north of Hekla

FIGURE VII.2 EPICENTRAL DISTRIBUTION IN ICELAND

from the I.S.S. file.



includes both left- and right-lateral shear planes, which suggests that it is an area of pure shear showing both extension at N45^{o}W and orthogonal compression, whose magnitudes are equal.

There is chemical evidence for this region's being a shear zone as well. Gass (1972) shows that volcanic products from shear zones are of the alkali basalt type, as has been shown conclusively to be the case for both Surtsey and Heimaey (Jakobsson, 1966, 1972, and 1973). Jakobsson (1972) classes the basalts from Hekla and Eldgjá (another eruption in the same region) as transitional between the alkali-rich shear zone type, and the olivine-rich tholeiites from extensional axes. Olivine-rich tholeiites occur on the south-central zone to the north of Hekla.

Thus the tectonics of southern Iceland seem to be governed by a left-lateral shear zone extending eastwards at a strike of N80^{o}E from Reykjanesviti to a few kilometres north of Hekla, which (from the trilateration results) shows 25 $\pm$16 mm. per year left-lateral displacement (with, at its extreme western end,a very small amount of crustal extension); an axis of extension striking at N30^{o}E which joins the shear zone approximately half way along its length and shows extension at about 6 mm. per year (with a small amount of contraction along its strike); a second extension axis (the south-central zone north of Hekla) on which Decker et al. (1971) measured 63 $\pm$ 31 mm. extension perpendicular to the strike in three years; and a zone showing equal amounts of extension across its axis and contraction parallel to it which lies south of the intersection of the shear zone with the major extension axis.

Each of these zones of deformation is illustrated symbolically in figure VII.3.

SECTION VII.2 THE TECTONICS OF NORTHERN ICELAND.

Northern Iceland has been greatly less well-studied than the south, and most of the work that has been done has already been summarised in the section considering the trilateration results from the Mývatn network.

There are however, two further areas that have been studied in some detail, from which the results have some bearing on the total tectonic situation.

The first of these is the area immediately north of Langjökull mentioned in the last section as having been studied by Piper (1973 b).

As observed above, he found that the tectonics of the area are dominated by N05°W trending fissures, some of which show en echelon structure indicative of left-lateral shear.

It was also noted before that the zone which strikes at N05°W from Langjökull to the coast is considered to have been the northern axis of crustal extension during early quaternary time.

Faults showing a similar tectonic direction to those found by Piper are found on the north-east of Langjökull too, and presumably belong to the same structural group (K.Saemundsson, 1967).

Otherwise information from northern Iceland is limited to two observations of east-west striking fissures, one to the east of Langjökull (H.Sigurdsson, 1971), the other the eruptive fissure of the 1961 Askja eruption, and to the interpretation of the Snaefellsnes volcanic zone given by H.Sigurdsson (1971).

Nothing is known of the east-west fissures.

The Snaefellsnes volcanic zone has not been mentioned yet at all in this thesis, although it has been shown on every map of the island as an area of post-glacial volcanism.

It is the westernmost peninsula of Iceland and has been volcanically active throughout post-glacial time, with the most recent eruption dated at about A.D. 900.

The peninsula is dominated by the 1400 m. high stratovolcano Snaefell, which occupies the centre of a zone of quaternary volcanic cones extended in a north-west direction.

At the eastern end volcanic activity has occurred on two parallel lines which strike at N108^{o}E. Of these the easterly one shows the more recent activity.

H.Sigurdsson (from whose 1971 paper all the above observations have been taken) interpreted the zone as one of right-lateral shear, which he assumed to be a part of the proposed dextral transform fault striking due east and connect--ing the Langjökull post-glacial active zone to Askja and the north central active zone. This transform fault has been the subject of some debate since its first proposal, and has now been rejected as a result of the complete lack of evidence for it, except on the Snaefellsnes zone.

Thus the tectonics of the north seem to be governed principally by the north-central zone of post-glacial activity, which, from the trilateration results and the structural analysis of the Tjörnes Fracture Zone given in section VI.2, has been seen to be a north-south trending fracture zone showing predominantly extensional movement in an east-west direction of about 5 mm. per year. However, it also shows a certain amount of left-lateral motion.

Otherwise the role of the various structures in north Iceland is not espec--ially clear, although it is hoped that after the next section a great unifying pattern will emerge.

SECTION VII.3 STRUCTURAL SYNTHESIS OF ICELAND.

Figure VII.3 is a symbolic map of the features which have been discussed in the last two sections.

All the structures shown are in the correct spatial orientation, and the dimensions of the larger structures are approximately correct. The smaller fractures, e.g. the Snaefellsnes, Langjökull, and Askja fractures have been exaggerated.

Directions of motion are not to scale, and in the case of the mid- Atlantic ridge, the South Central Zone, and the Tjörnes Fracture Zone, may not be indications of the complete movement.

If the Reykjanes zone is taken to be a zone of almost pure strike-slip movement, and the mid-Atlantic ridge (which has been extended north of the intersection with the Reykjanes peninsula in order to include the magnetic anomaly found in Reykjavik harbour by Talwani et al. (1971)) is assumed to show pure extension, then the only reconciliation between these structures is a pole of rotation at 65^{o}N 21^{o}E, as is shown on figure VII.3.

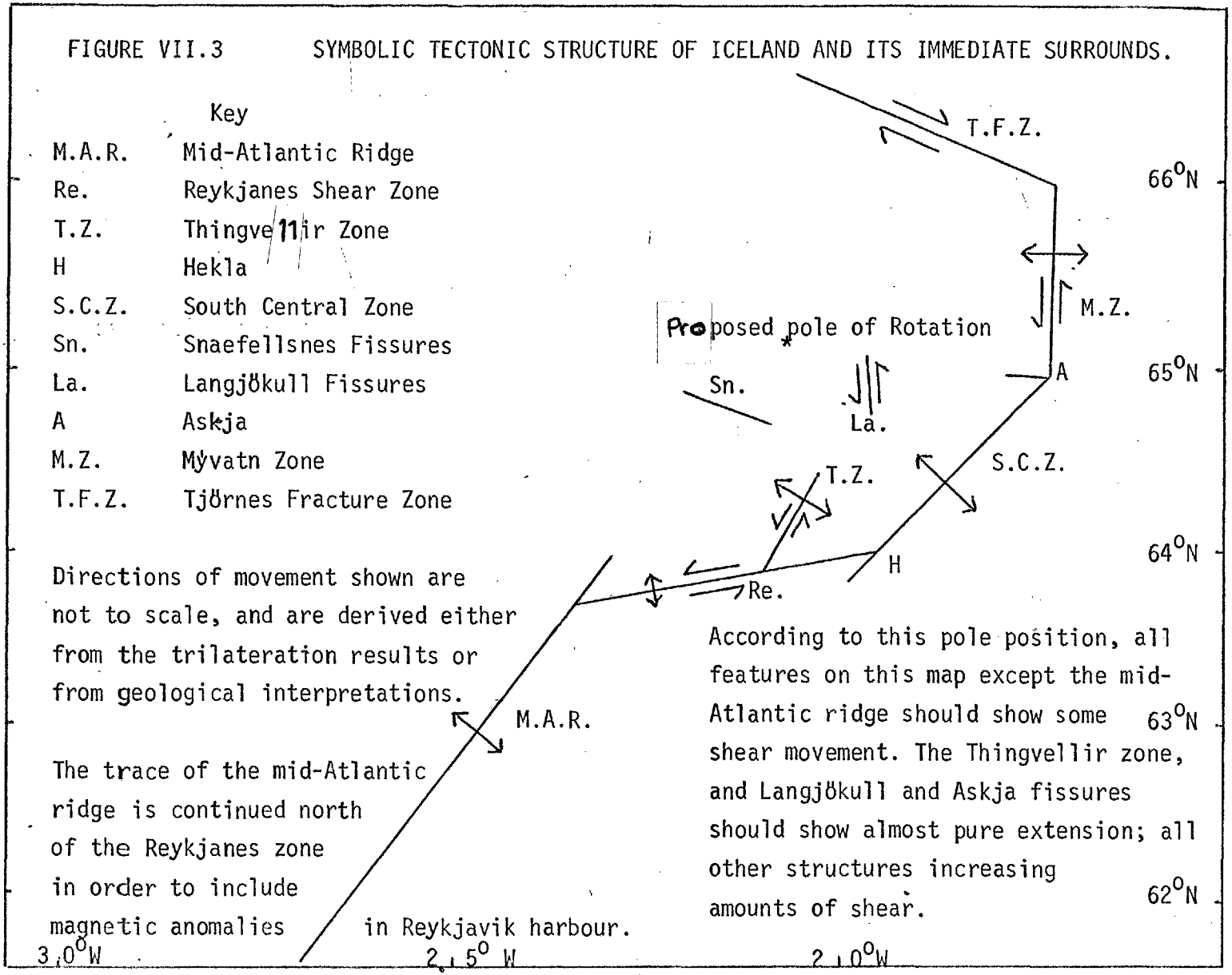
It can be seen from the figure (remembering that zones of pure strike-slip movement lie on small circles about the pole of rotation and that zones of pure spreading are sectors of great circles through the pole) that the Snaefellsnes fissures (whose strikes are at N108^{o}E) should show almost pure strike-slip movement with very little extension. This is supported in a qualitative way by the observations from there, although no estimate can be made from the purely geological observations of the quantities involved.

However, the suggestion of Sigurdsson that the two fissures in eastern Snaefellsnes represent a dextral shear zone is not thought to be such a good representation of the observations (especially with regard to the eastward continuation of such a zone) as is the proposed rotation pole.

Likewise, the Langjökull zone would be only slightly extensional, which is once again in qualitative agreement with the geological observations.

The Askja fracture, however, would lie almost on a great circle through the pole, so that extension would be its predominant movement, as is suggested by

FIGURE VII.3 SYMBOLIC TECTONIC STRUCTURE OF ICELAND AND ITS IMMEDIATE SURROUNDS.



the continued volcanic activity from that mountain.

This pole position would also explain the rotation along the strike of the Reykjanes peninsula of the various tensional groups discussed in chapter VI, and more importantly, the lack of extrusive activity on the eastern section of the Reykjanes shear zone, which can be seen to lie even more than the west--ern part along a small circle about the pole.

The Thingvellir zone strikes very near to a great circle direction, which is in agreement with the observed extension across the zone, although a little shear would also be expected, just as is observed.

The Mývatn zone would be expected to show a combination of extension and shear, with the component of extension increasing northward. It can only be said that the trilateration results of chapter VI agree generally speaking with this conclusion.

The Tjörnes Fracture Zone should show almost pure strike-slip movement along its entire length, just as has been proposed for it, and the Kolbeinsey ridge, which is not shown on figure VII.3, should show pure extension, just as has been proposed for it.

The main breakdown of the proposed pole is the South Central Zone, which ought to show considerable strike-slip movement.

There is no evidence for this (the geodetic results of Decker et al.(1971) were not sufficiently refined to make any definite proposal as to which direct--ion their observed movements were in), and only the chemical evidence against it. Also the stub of the south central zone including Hekla and the area to the south of it has been shown to be predominantly a shear zone, but there the chemistry reflects this.

Thus, until more refined geodetic work has been conducted in the south central area this proposed pole of rotation should not be dismissed as being contrary to observations, especially as it explains, apparently excellently, all the other tectonic features of the country.

CONCLUSIONS

In the abstract the ultimate aim of this thesis was proclaimed as the establishment of of a coherent, unifying tectonic picture of Iceland.

In all honesty it cannot be stated that this has been completely achieved since the quantitative effects of the postulated pole of rotation have not been investigated. However, suggesting such a pole is a new idea arising from the observation of shear movements on two of the post-glacial active zones which were hitherto considered to represent pure extension.

It is hoped that further work on the South Central Zone will show whether or not shear movements exist there too.

However, despite the incomplete attainment of the projected goal, this thesis has shown that trilateration measurements can be made to work, and that provided certain precautions are observed regarding the conditions in which they are attempted, the results can be of high accuracy.

The design of networks, a point not sufficiently appreciated at the beginn--ing of the Icelandic work, can be seen from the fact that most of the movement detected on the Reykjanes zone is occurring on the 1971 network to be of the utmost importance.

From the practical point of view, probably the most interesting results are those relating to the geothermal field at Reykjanes, which show that geothermal activity and secondary faulting are very considerably linked, and also that an exploited geothermal field shows much the same behaviour at the surface (in terms of horizontal and vertical ground deformation) as exploited oil fields. This result must therefore be considered by engineers designing the installations and services of the producing geothermal fields which will surely soon be providing much of the world's energy requirements.

One interesting possibility is that the observed surface effect of the mass discharge from a geothermal field is some indication of the capacity of the field.

But one of the most satisfying parts of this thesis has been tying in the various structural geological observations with the trilateration results. The

secondary faulting analysis provided one of the supreme moments in the interpre--tation, as did the discovery that the large normal fault at Reykjanes showed both vertical and horizontal movements in a sensible direction. These are the two instances of non-mathematical proof of the technique, which between them are considered to validate the entire approach.

It would be encouraging to the author to think that the techniques which have been introduced and shown to work in this thesis might be applied to some advantage in the wider context of the great social and economic upheavals caused by catastrophic ground movements, whether seismically or volcanically derived.

A start has been made on this work with the first measurements, from which the results are highly encouraging, of a very long trilateration network (emb--odying all the principles of good network design laid down in chapter II) in the Imperial Valley of Southern California. Some of the results of this work are briefly mentioned in the thesis (the statement about the width of the plate boundary comes from the Californin results).

This work has also been begun in Iran, mainly in the east, where after only two measurements several millimetres of displacement have been observed on the fault responsible for the great 1968 earthquake in which 12,000 people died.

The thesis makes reference to published work by Brander and Wadge, which describes the results of these measurements on the erupting Heimaey fissure earlier this year. It is possible that the network established for those measur--ements might be periodically remeasured in order to provide warning of any renewal of activity.

On Sicily too these measurements have been made at regular intervals since the last eruption of Mt. Etna ceased. Assuming that a new eruption is not far away and that another measurement is possible there, then very valuable results regarding the surface deformations during the eruption cycle will have been obtained.

Thus it is thought that despite the lack of attainment of the proclaimed goal, this thesis does provide sufficient evidence of tangible results to be of some value.

APPENDICES.

APPENDIX A

ILLUSTRATION OF THE DISPLACEMENT VECTOR SOLUTION TECHNIQUE.

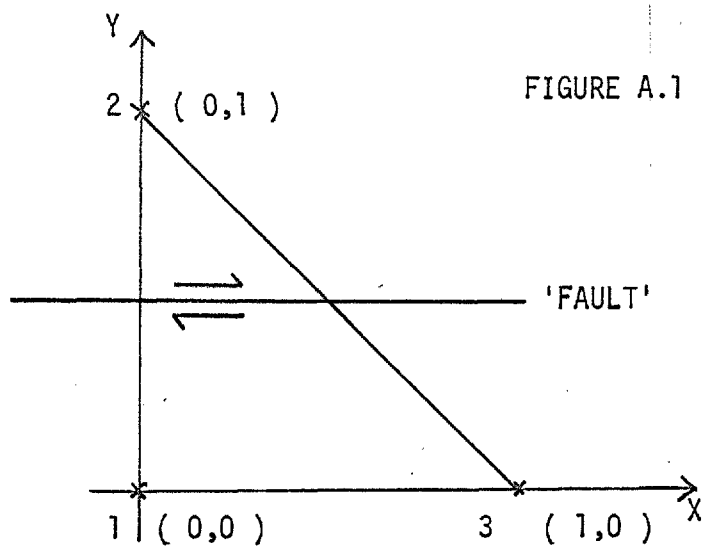


FIGURE A.1

Figure A.1 shows the model used. Stations 1, 2, and 3 form an isosceles triangle whose apex is station 1, the origin.

The co-ordinates of the stations are

(0,0), (0,1), (1,0).

A'fault' crosses the figure at y = 0.5; displacement occurs on this fault such that station 2 is displaced 10^{-4} in the positive X-dirction. (The scale used here corresponds to 10 mm. movement in a 100 m. distance; a great deal by the normal standards of this work.) The displacement of this station may thus be written (10^{-4},90^{o}), where the reference direction is +Y.

Table A.1 lists the old and new distances, and the changes.

LINE	OLD LENGTH	NEW LENGTH	CHANGE
1 - 2	1	1.0000000049	$+4.9\times10^{-9}$
2 - 3	1.41421356	1.4141428534	-7.1×10^{-5}
3 - 1	1	1	0

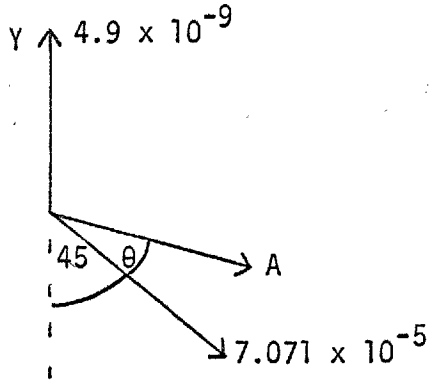
Thus applying the analysis technique described in Chapter IV., and taking stations 1 and 3 as stationary,

component of $\underline{Z}_2$ towards 1 = -4.9×10^{-9}

component of $\underline{Z}_2$ towards 3 = 7.071×10^{-5}

where $\underline{Z}_2$ is the displacement vector of station 2.

Figure A.2 shows the vector diagram for this problem.



From this it may be seen that

$$A.\cos\theta = 7.071 \times 10^{-5}$$

$$A.\cos(135-\theta) = 4.9 \times 10^{-9}$$

$$A.\cos 135.\cos\theta + A.\sin 135.\sin\theta = 4.9 \times 10^{-9}$$

$$A.\sin 135.\sin\theta = 4.9 \times 10^{-9} + 7.071^2 \times 10^{-6}$$

$$A.\sin\theta = \frac{4.9 \times 10^{-9} + 7.071^2 \times 10^{-6}}{.7071}$$

dividing by $A.\cos\theta = 7.071 \times 10^{-5}$

$$\tan\theta = 1$$

$$\theta = 45^{o}$$

$$A = 10^{-4}$$

Referring to the vector diagram (figure A.2) shows that this implies displacement in the positive X-direction of 10^{-4}, exactly as originally assumed.

APPENDIX B

ILLUSTRATING THE STRAIN-PARAMETER SOLUTION FOR A SQUARE UNDERGOING STRIKE-SLIP DEFORMATION.

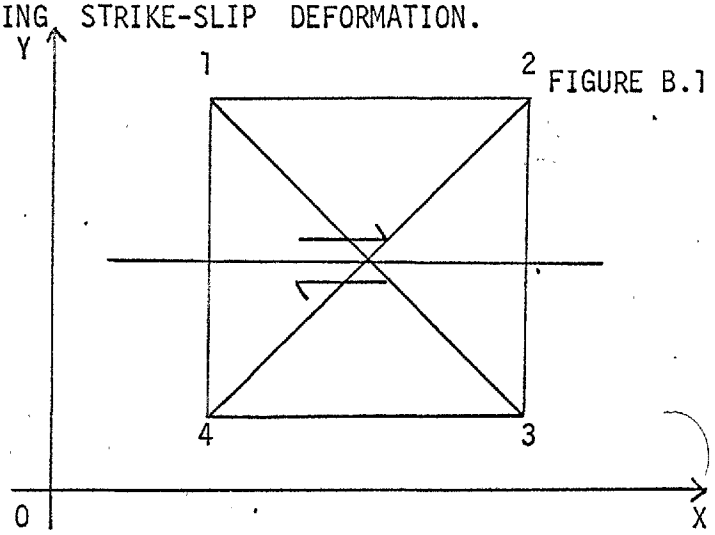


FIGURE B.1

Figure B.1 shows a square of unit side cut in half by a 'fault' parallel to the X-axis.

Stations 1 and 2 each move 10^{-4} right-laterally along the fault

The change on line 1 - 2 = 0

on line 3 - 4 = 0

on line 1 - 4 = 4.9×10^{-9}

on line 1 - 3 = -7.071×10^{-5}

on line 2 - 3 = 4.9×10^{-9}

on line 2 - 4 = 7.071×10^{-5}

Applying the strain-parameter solution described in chapter IV. to each of the four triangles gives the following results:

TRIANGLE	SHEAR ($\times 10^5$)	DILATATION ($\times 10^5$)	DIRECTION OF MAX. EXTENSION
4 - 1 - 2	14.1	0	45^o
1 - 2 - 3	14.1	0	225^o
4 - 1 - 2	14.1	0	45^o
4 - 2 - 3	14.1	0	45^o

APPENDIX C

ILLUSTRATING THE STRAIN-PARAMETER SOLUTION FOR A SQUARE UNDERGOING PURE EXTENSION

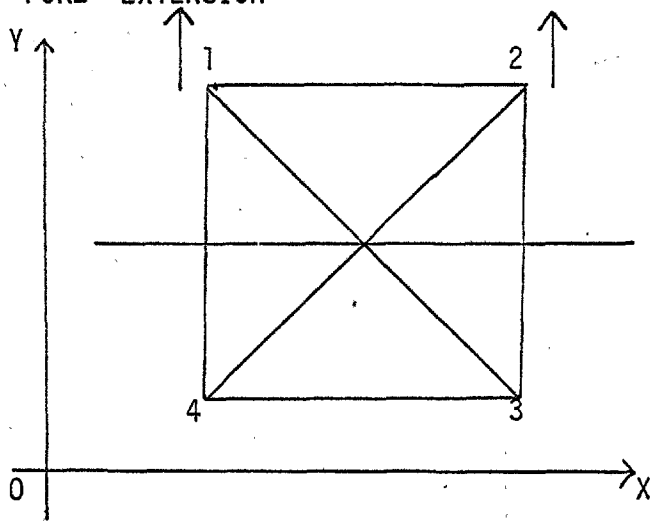


Figure C.1 shows a square of unit side cut by a tension fissure parallel to the X-axis

Stations 1 and 2 each move 10^{-4} in the +Y direction.

The change on line 1 - 2 = 0

on line 3 - 4 = 0

on line 1 - 4 = 10^{-4}

on line 2 - 3 = 10^{-4}

on line 1 - 3 = 7.071×10^{-5}

on line 2 - 4 = 7.071×10^{-5}

Applying the strain parameter solution to the four triangles gives the following results;

TRIANGLE	SHEAR ($\times 10^4$)	DILATATION ($\times 10^4$)	ANGLE OF MAX. EXTENSION
1 - 2 - 3	1.08	1.00	169^o 45'
4 - 1 - 3	1.08	1.00	-11^o 15'
4 - 1 - 2	1.08	1.00	11^o 15'
4 - 2 - 3	1.06	1.00	11^o 45'

where the angles are measured clockwise from +Y.

These results indicate that the calculated shear, which was zero in the original model, must alternate between left- and right-lateral in order to average zero.

APPENDIX D. THE DISTANCE - TIME GRAPHS FOR THINGVELLIR.

In the following twenty five pages the distance against time graphs for all the lines measured at Thingvellir are shown.

On each, time is measured in years from the beginning of 1968, the name of the line and its approximate (whole number length) are shown in the top right-hand corner, and the excess of the length over a whole number of metres is shown as the ordinate.

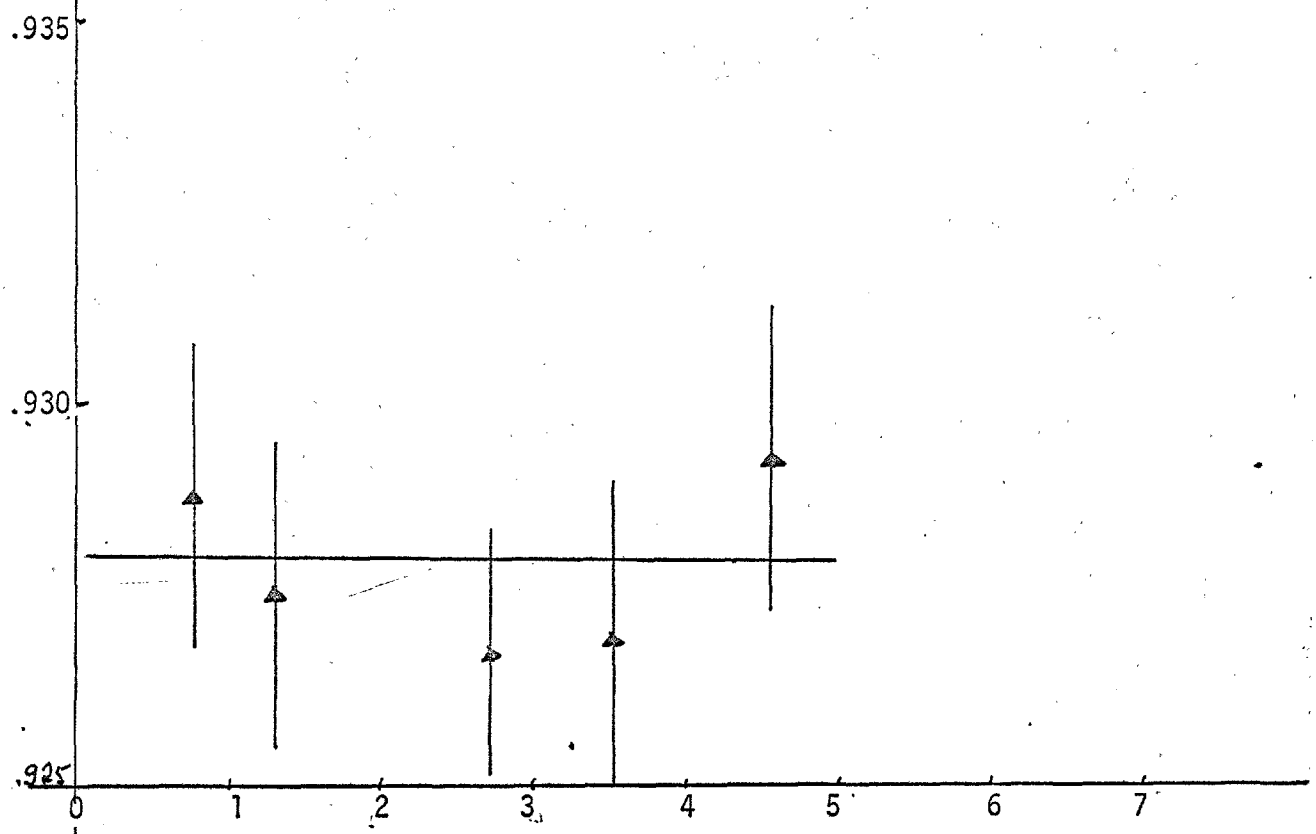
Straight lines have been fitted to all of the distance-time graphs.

The error bars shown associated with each plotted point are derived from the square root of the sum of the squares of the expected error for the length of line concerned and the standard deviation of the readings from which the measure--ment is derived. The expected error is given by the formula of chapter III, and is usually very much larger than the standard deviation. Indeed only in the 1968 measurement (when the effects of unsuitable atmospheric conditions were not appreciated) is the standard deviation a significant part of the error bar.

The results of these measurements are discussed in chapter VI.

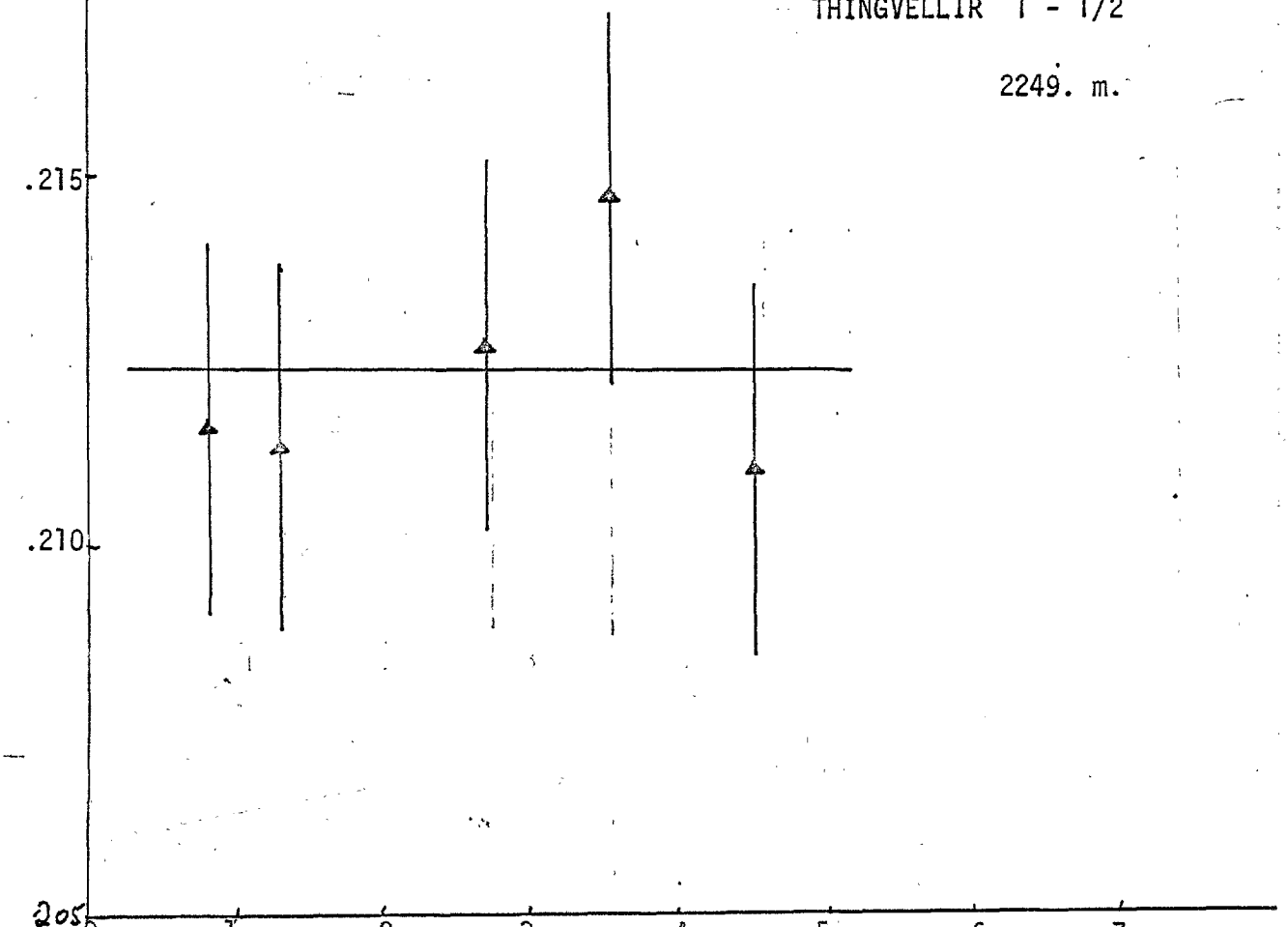
THINGVELLIR 3 - 1

1620 m.



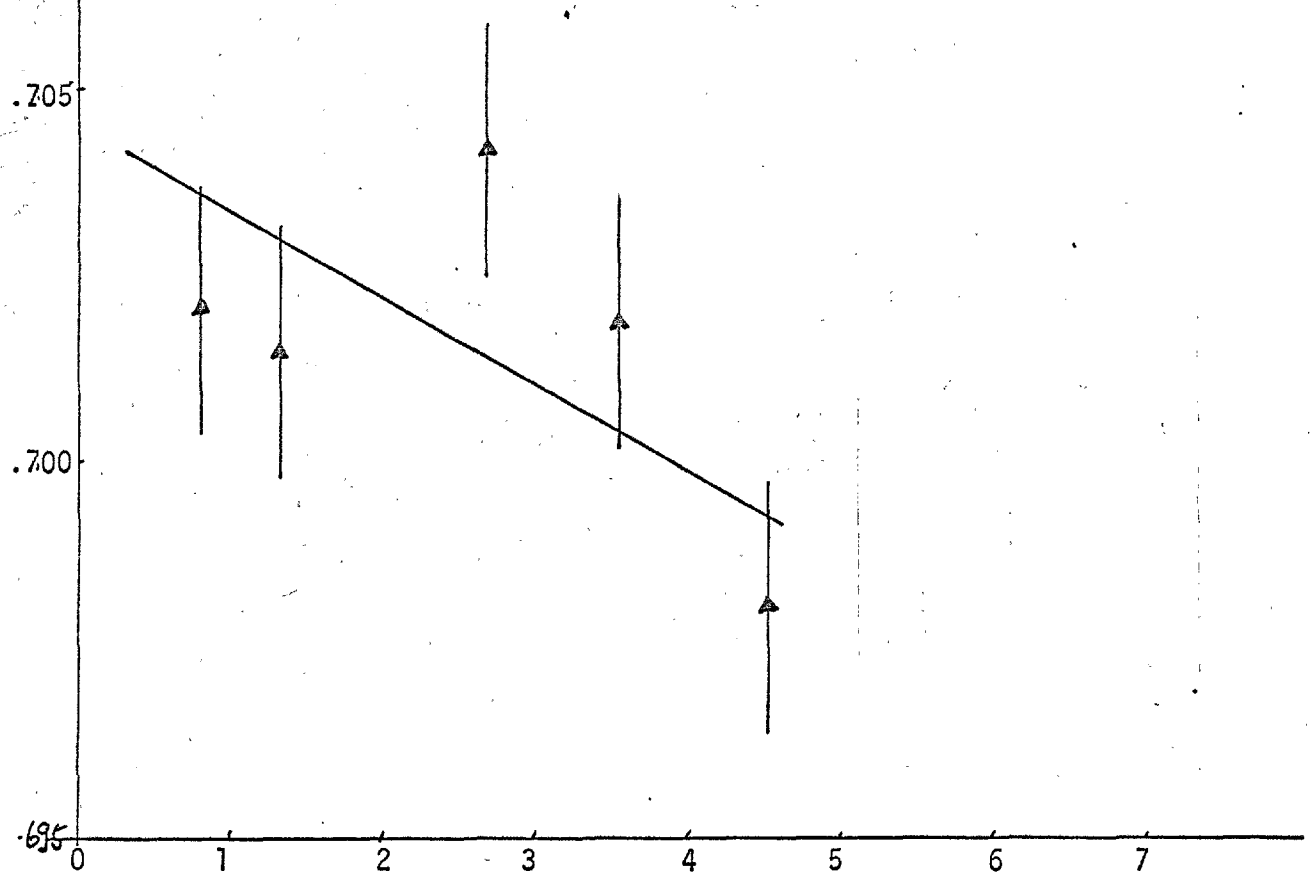
THINGVELLIR 1 - 1/2

2249. m.



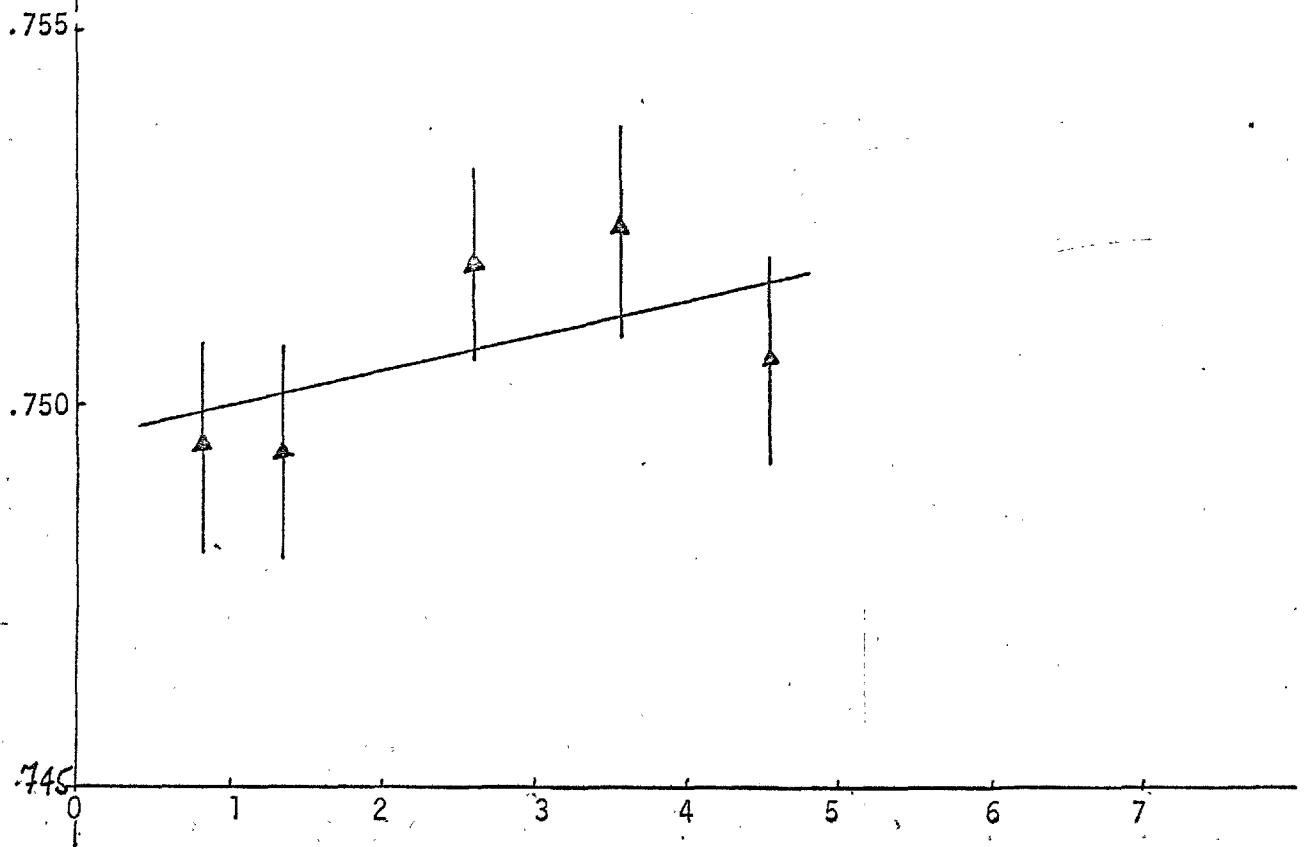
THINGVELLIR 1 - 1/4

1312. m.



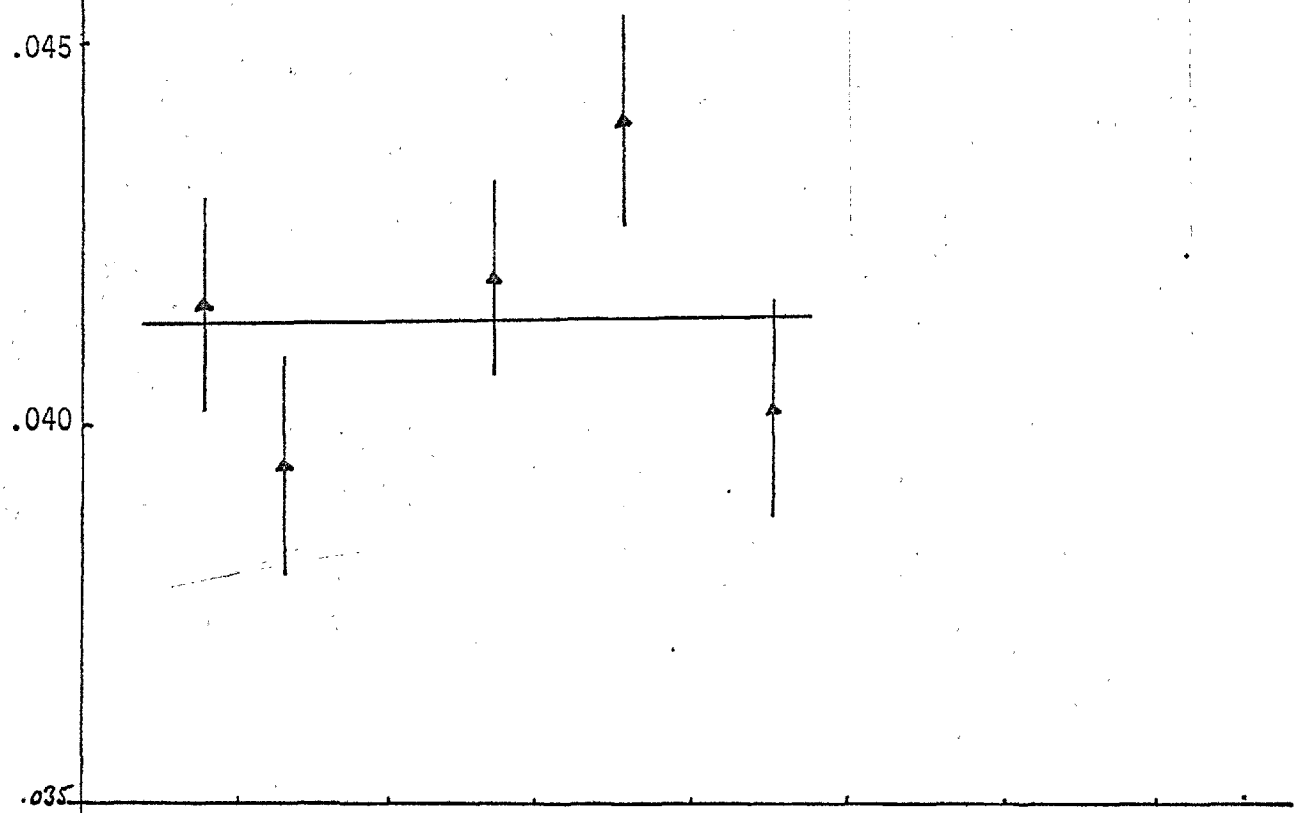
THINGVELLIR 2 - 1/2

914. m.



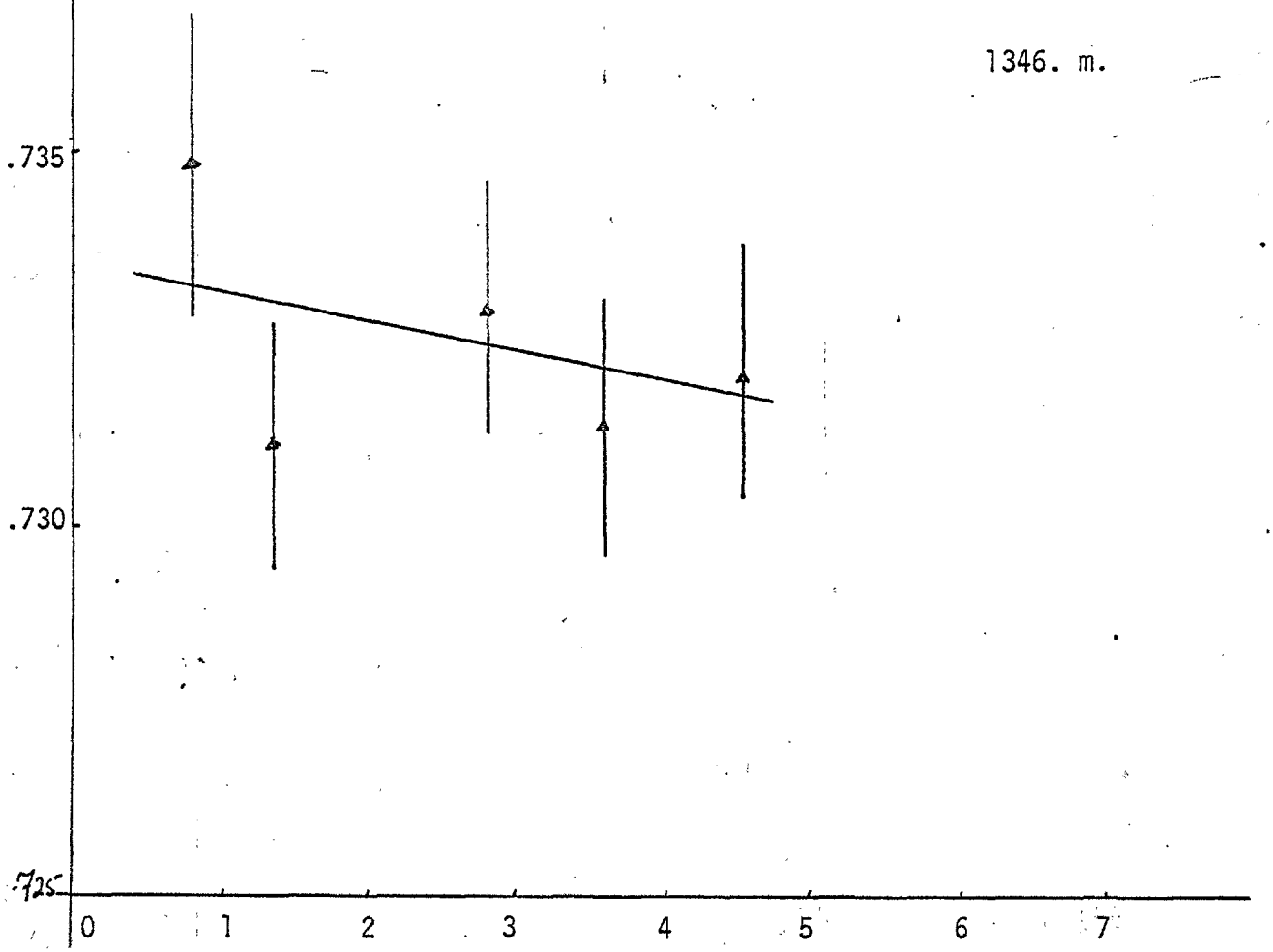
THINGVELLIR 2 - 2/5

963. m.



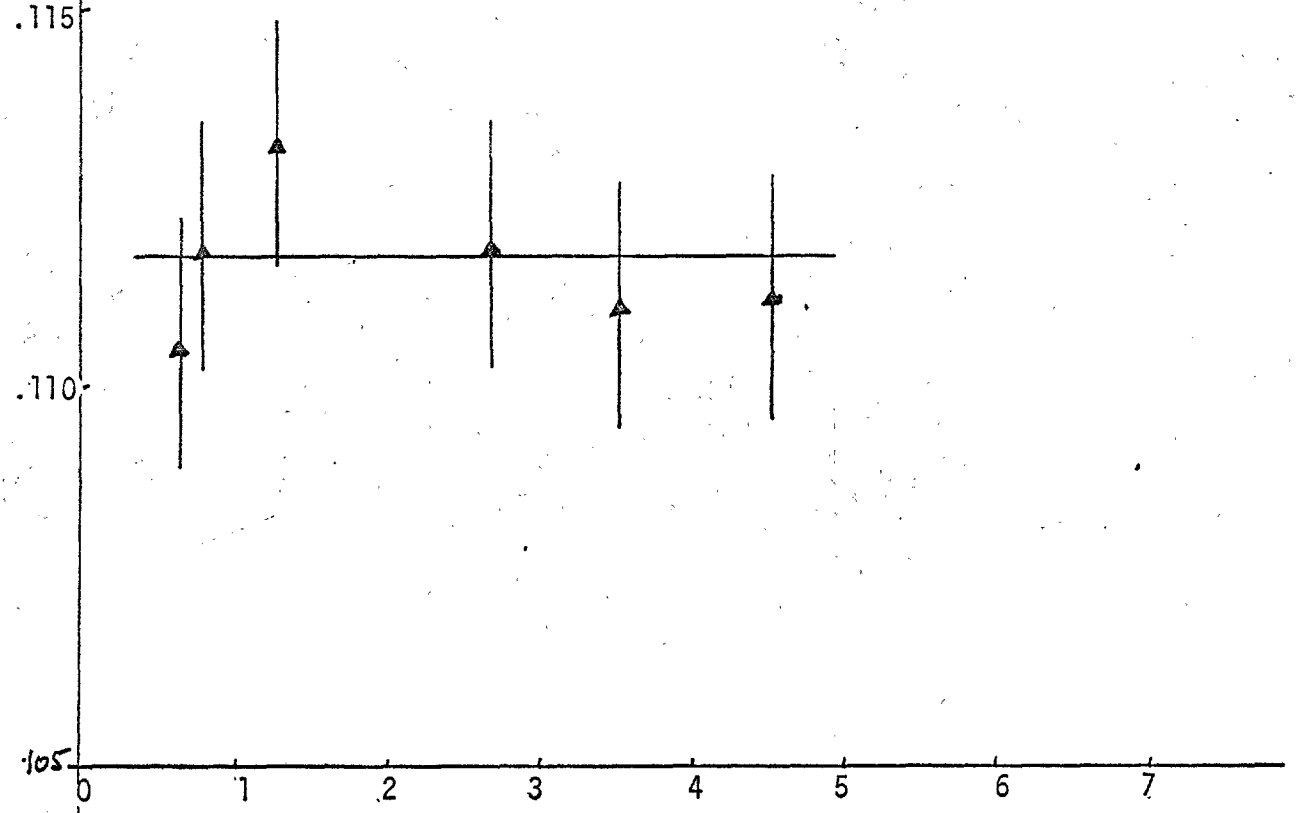
THINGVELLIR 3 - 3/4

1346. m.



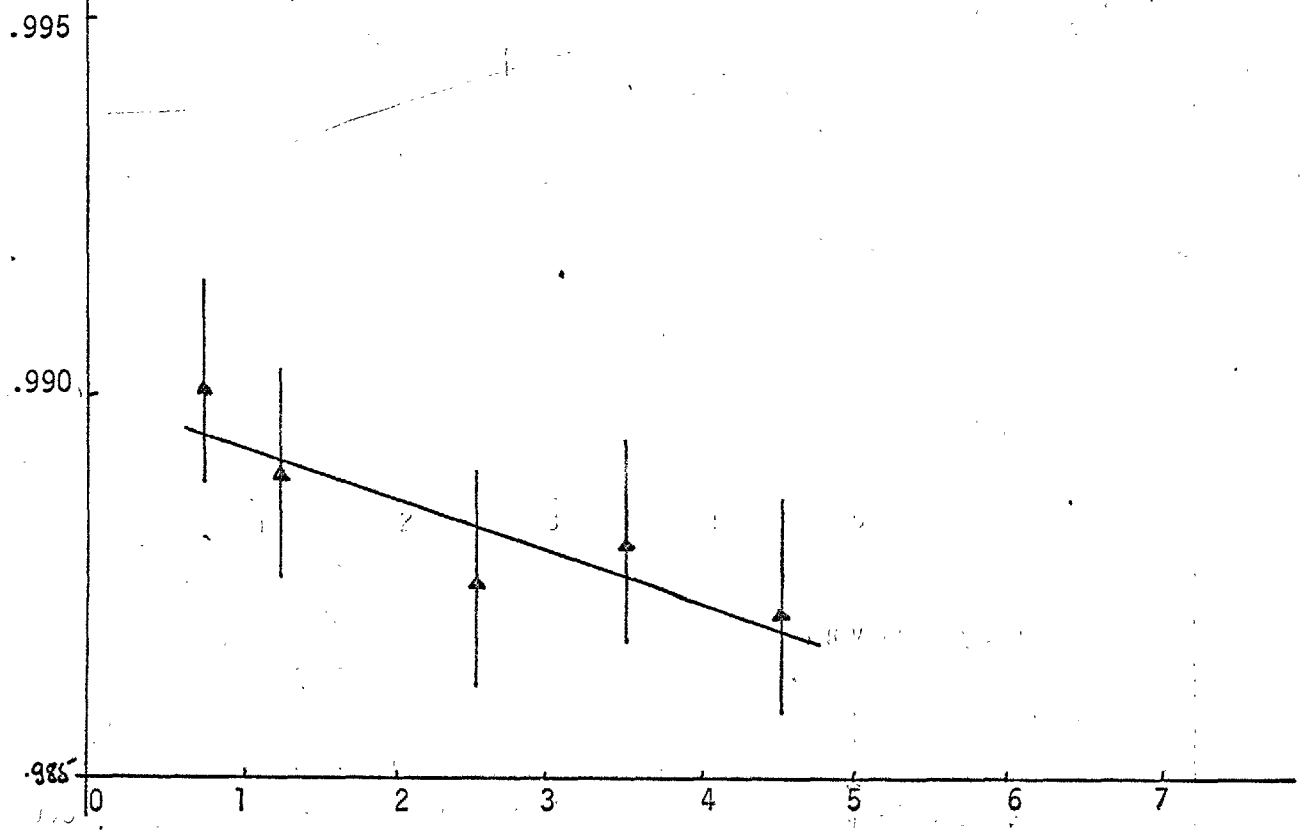
THINGVELLIR 3 - 3/6

1220. m.



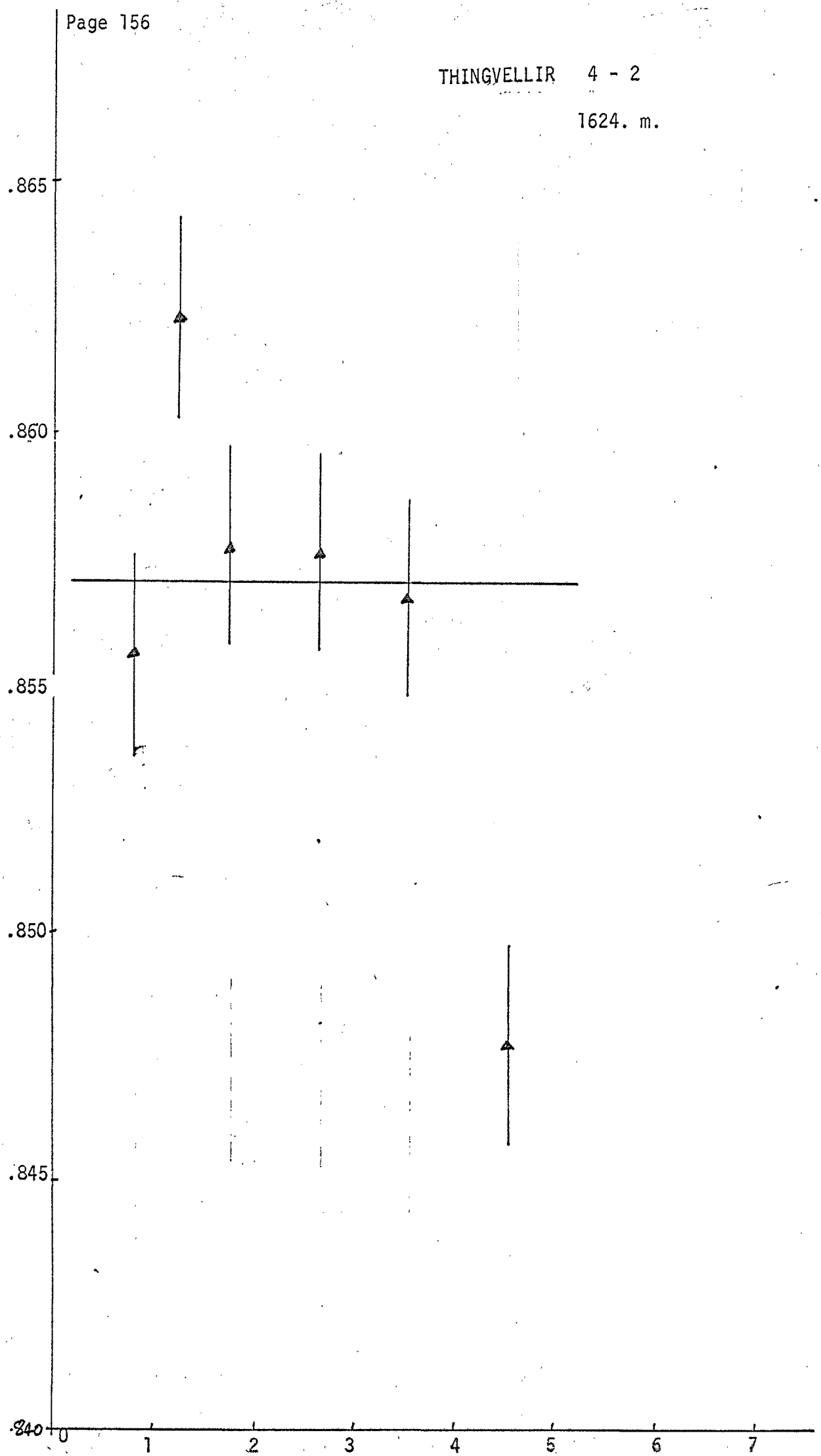
THINGVELLIR 4 - 1/4

1036. m.



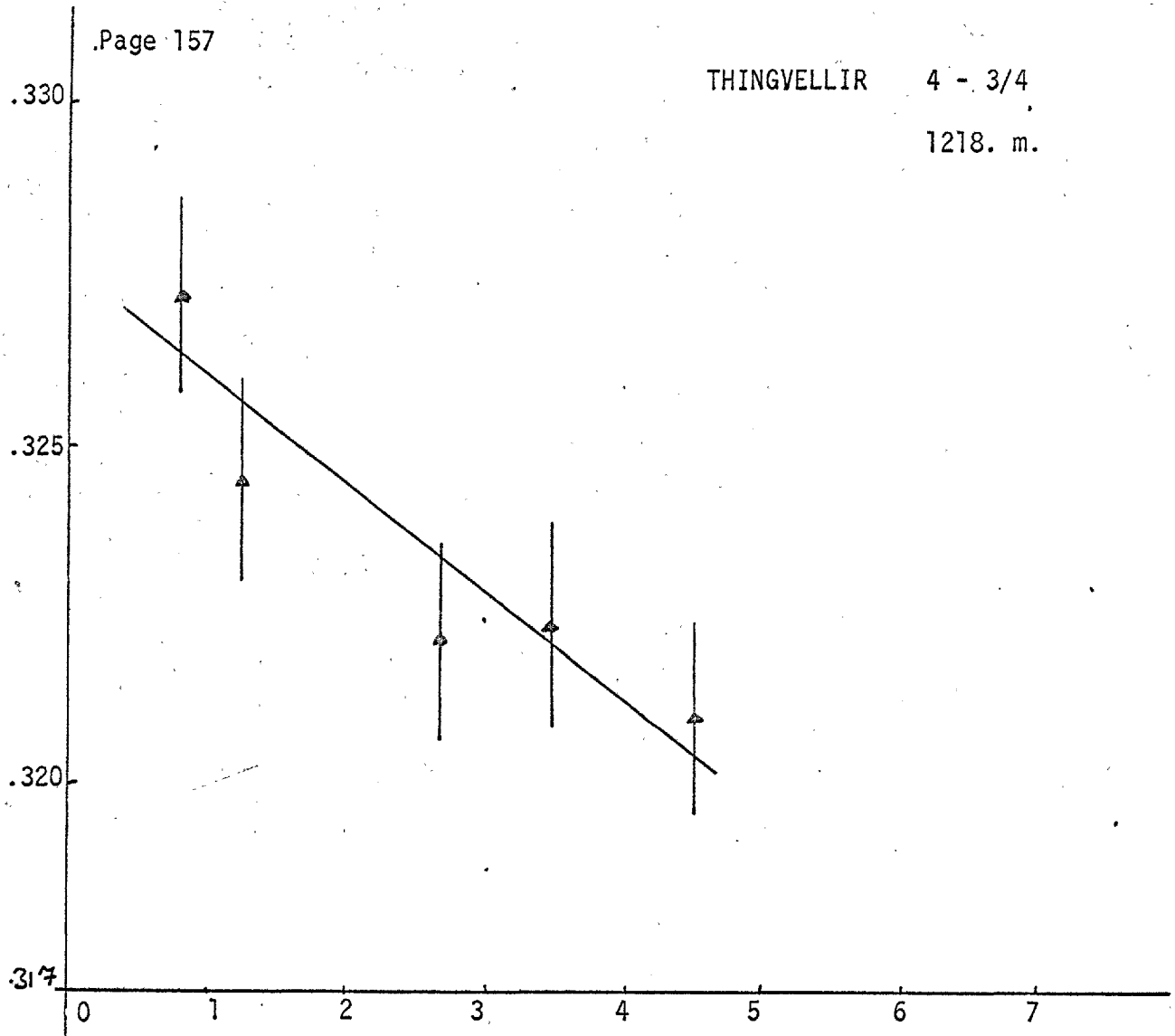
THINGVELLIR 4 - 2

1624. m.



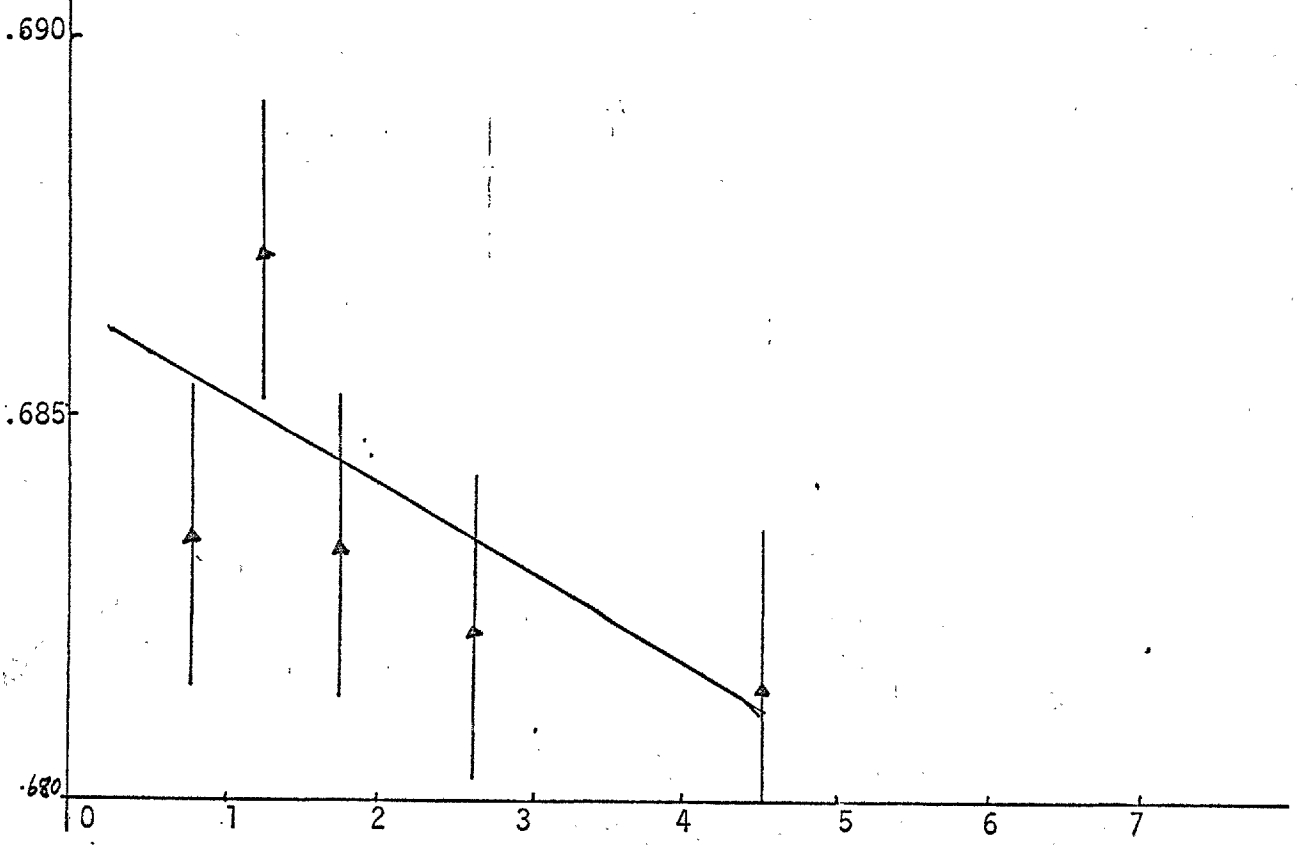
THINGVELLIR 4 - 3/4

1218. m.



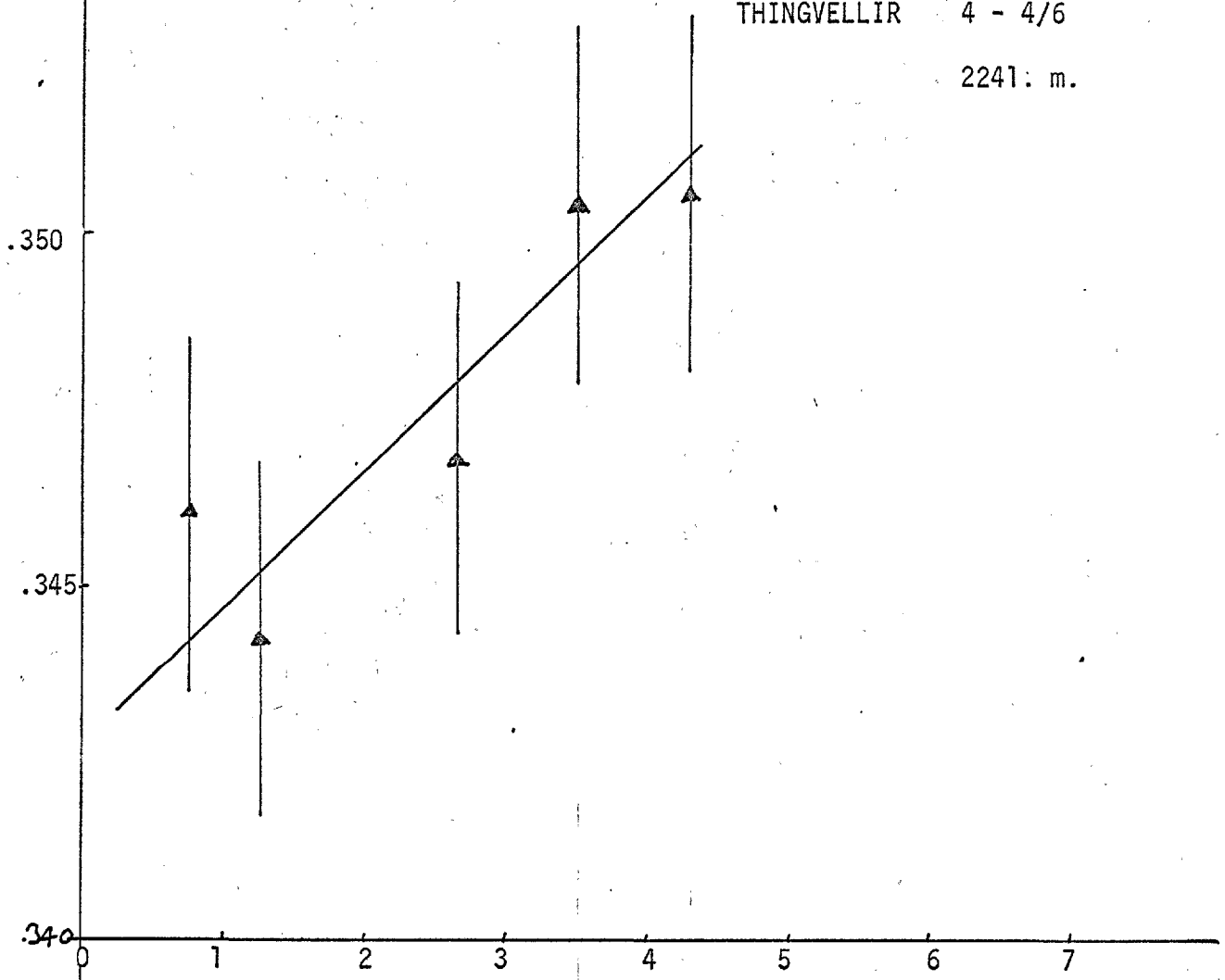
THINGVELLIR 4 - 4/6

2241. m.



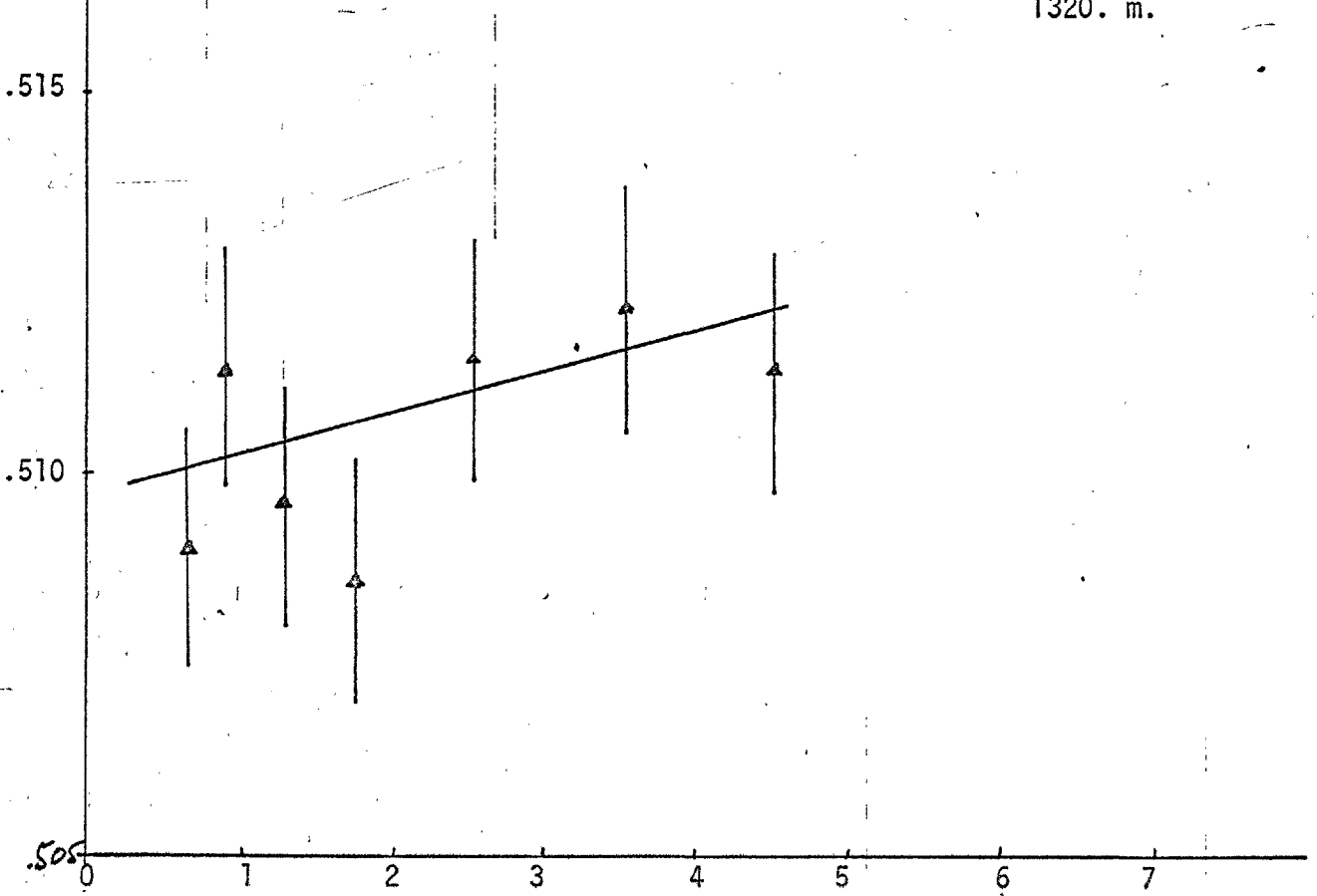
THINGVELLIR 4 - 4/6

2241. m.



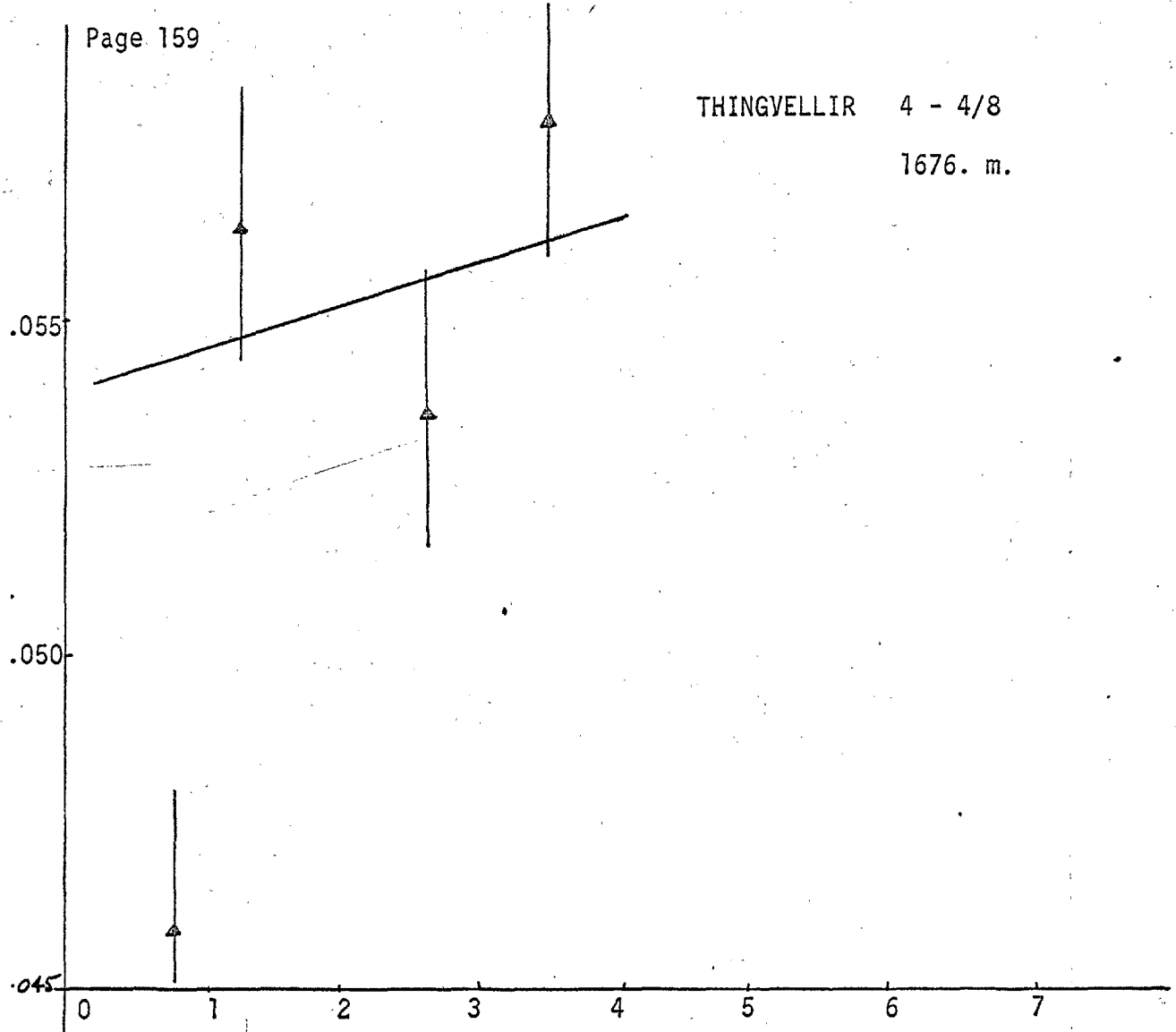
THINGVELLIR 4 - 4/7

1320. m.



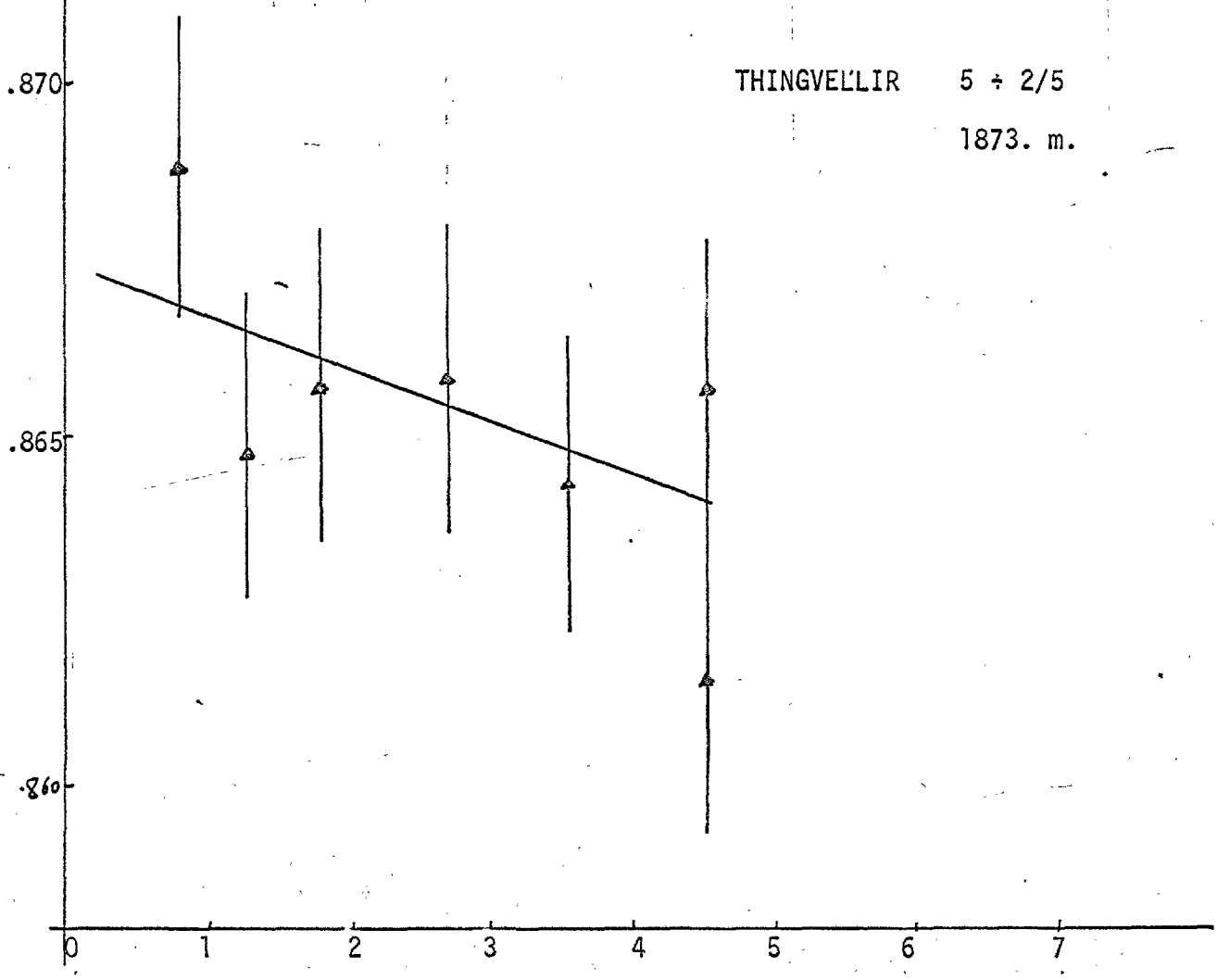
THINGVELLIR 4 - 4/8

1676. m.



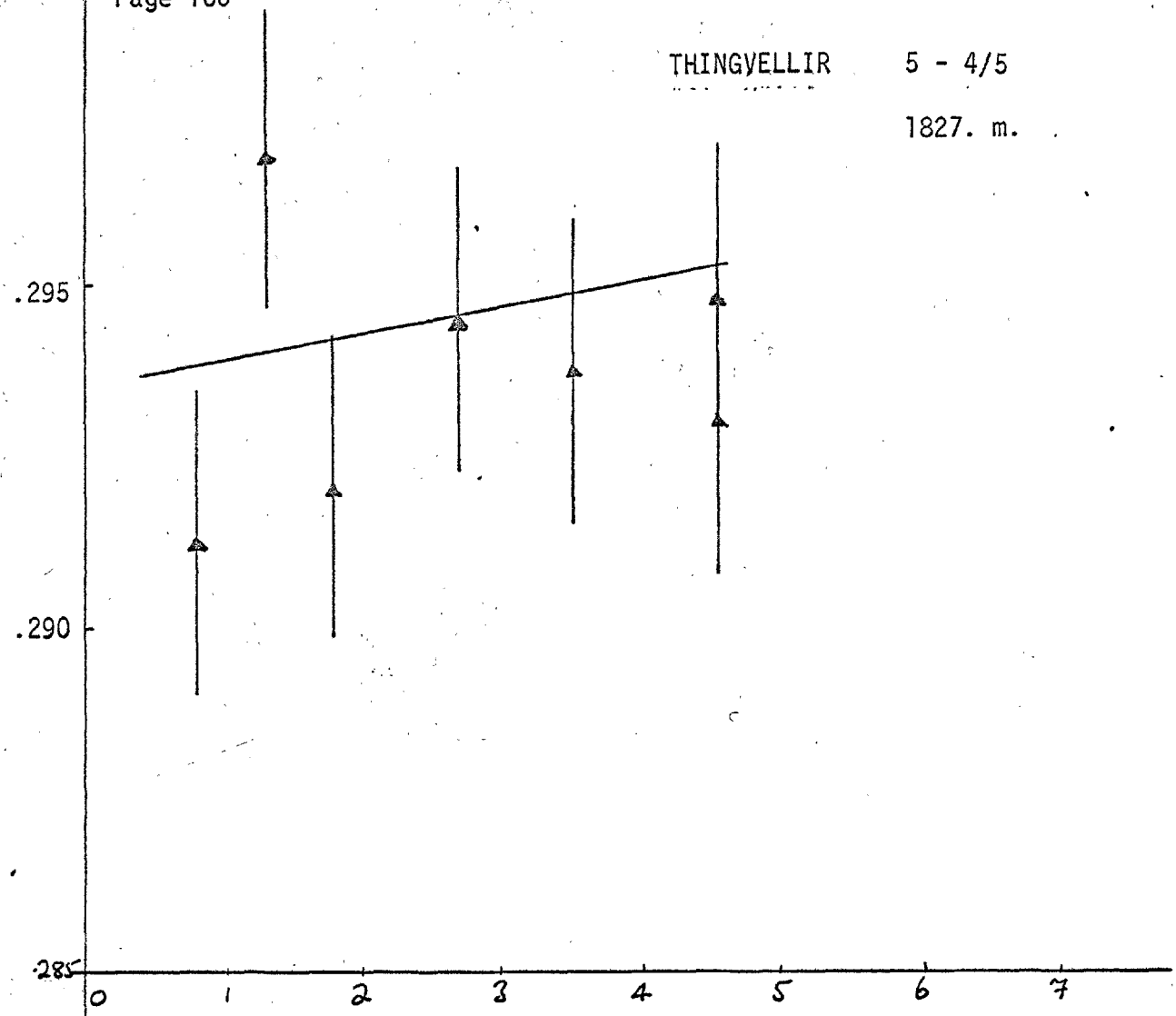
THINGVELLIR 5 ÷ 2/5

1873. m.



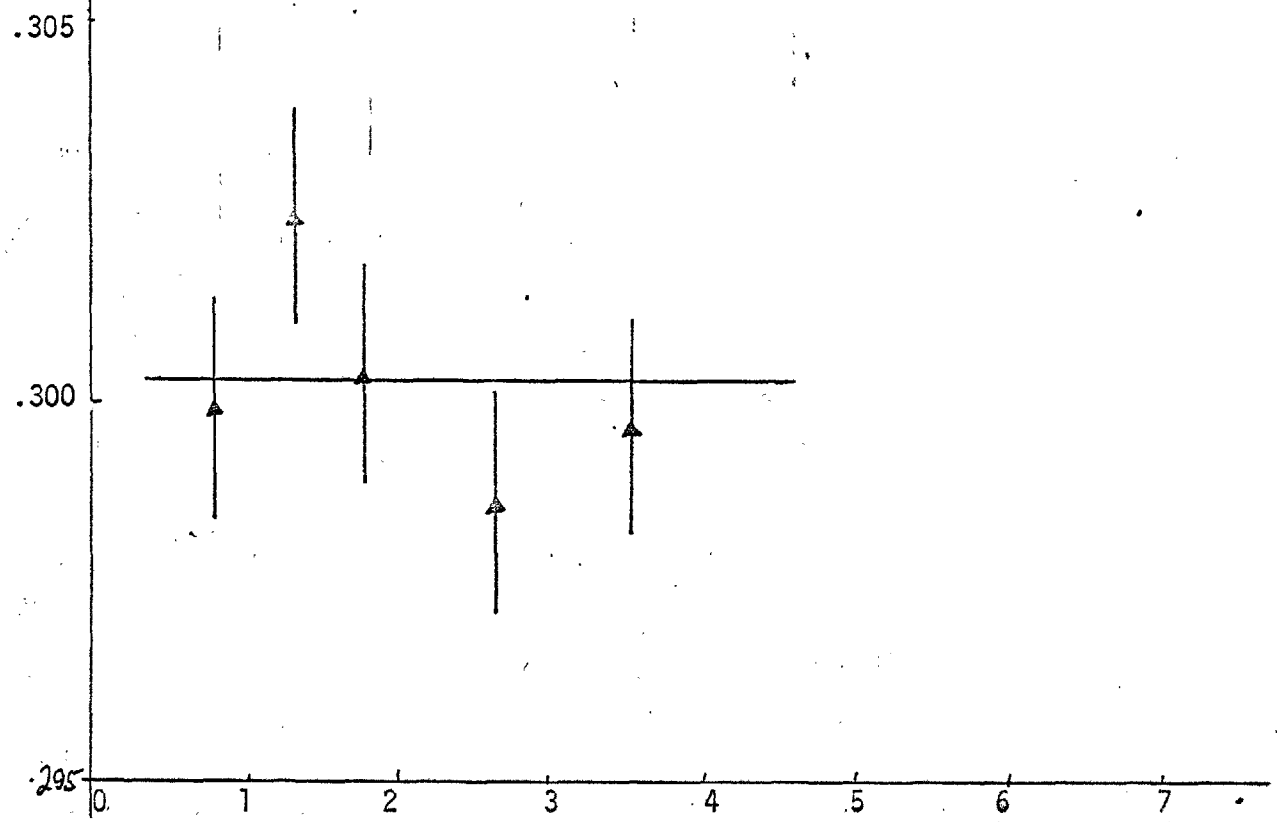
THINGVELLIR 5 - 4/5

1827. m.



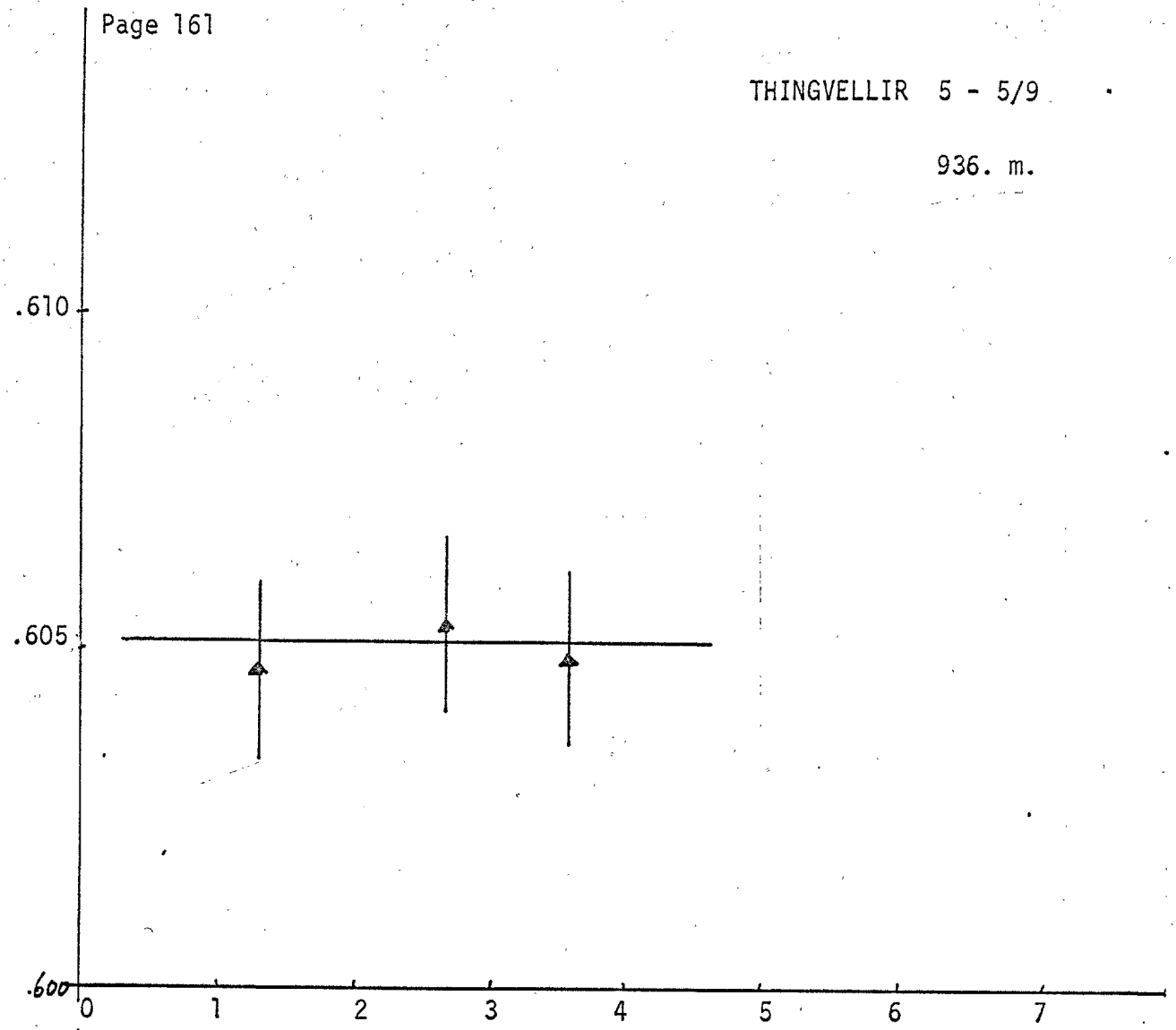
THINGVELLIR 5 - 5/8

1095. m.



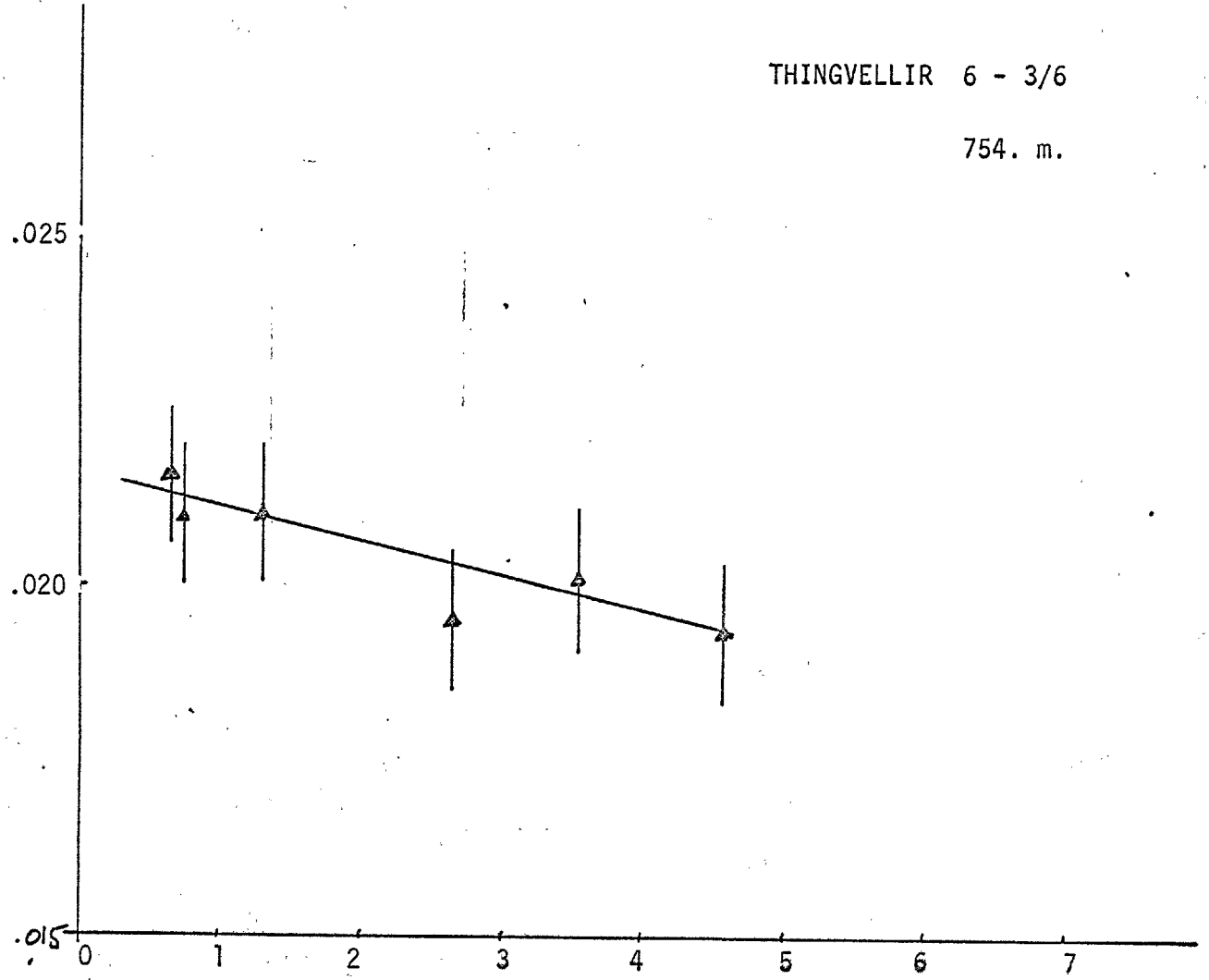
THINGVELLIR 5 - 5/9

936. m.



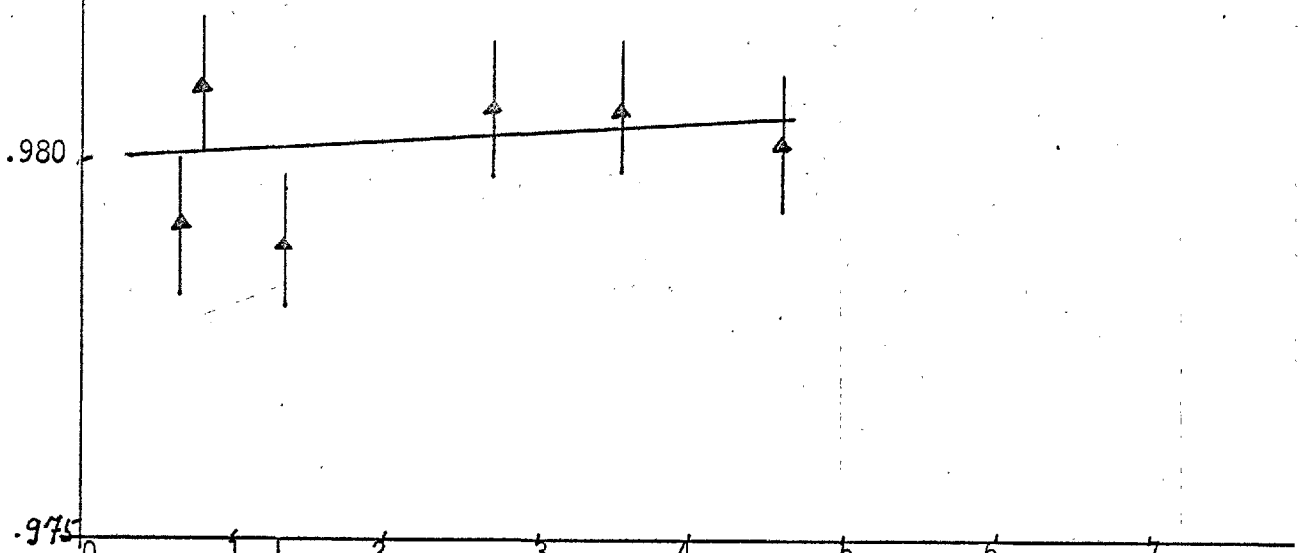
THINGVELLIR 6 - 3/6

754. m.



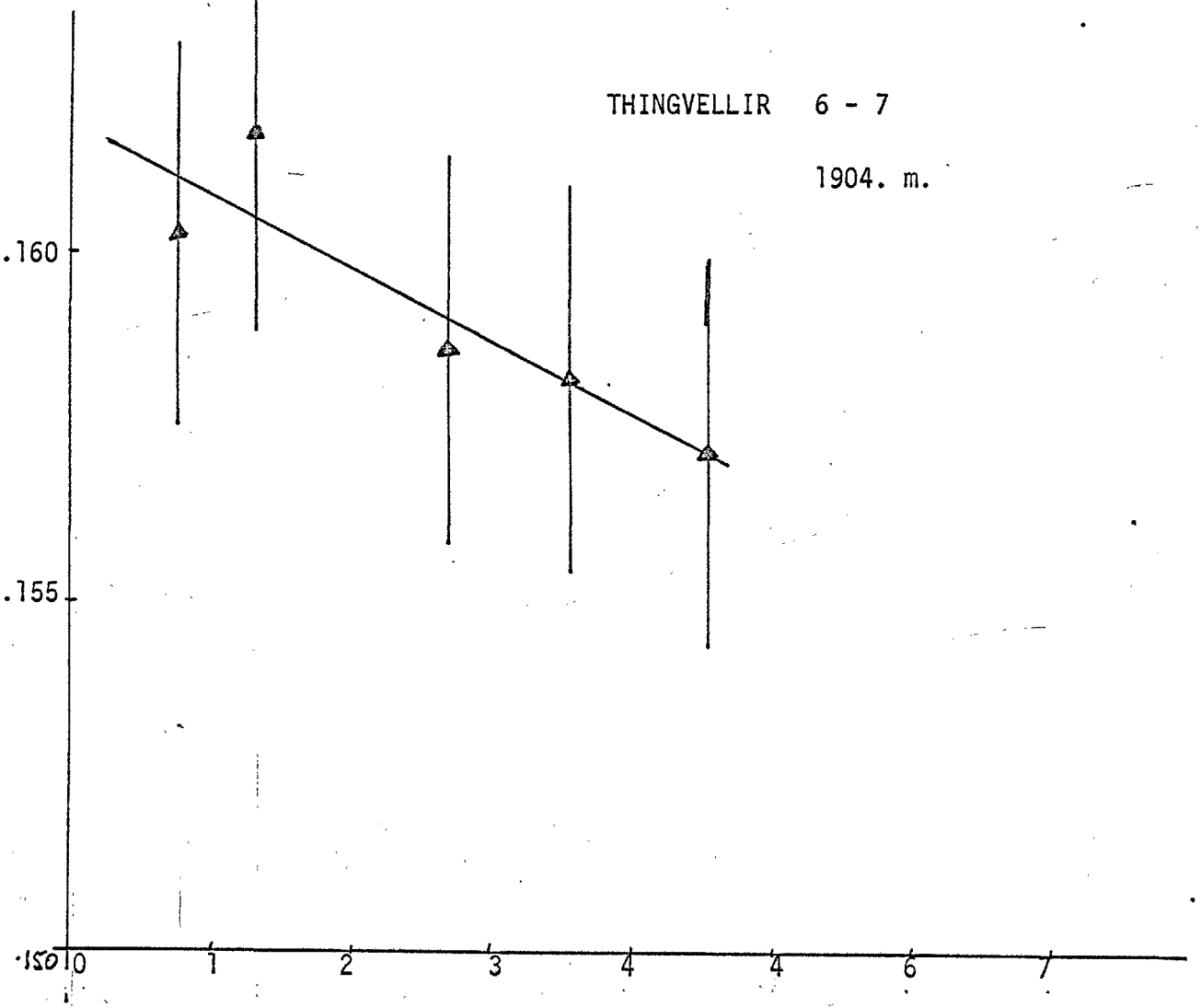
THINGVELLIR 6 -4/6

610. m.



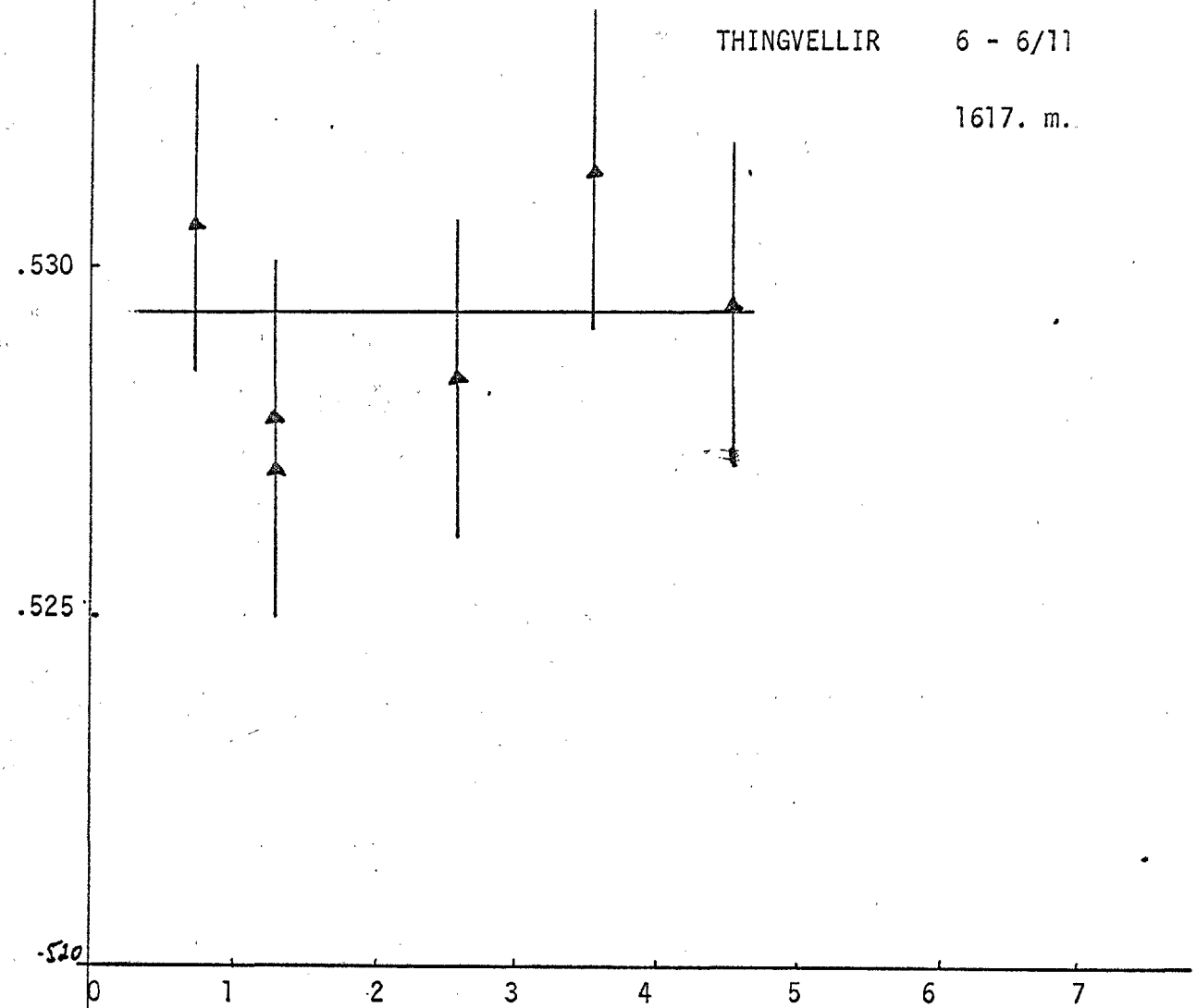
THINGVELLIR 6 - 7

1904. m.



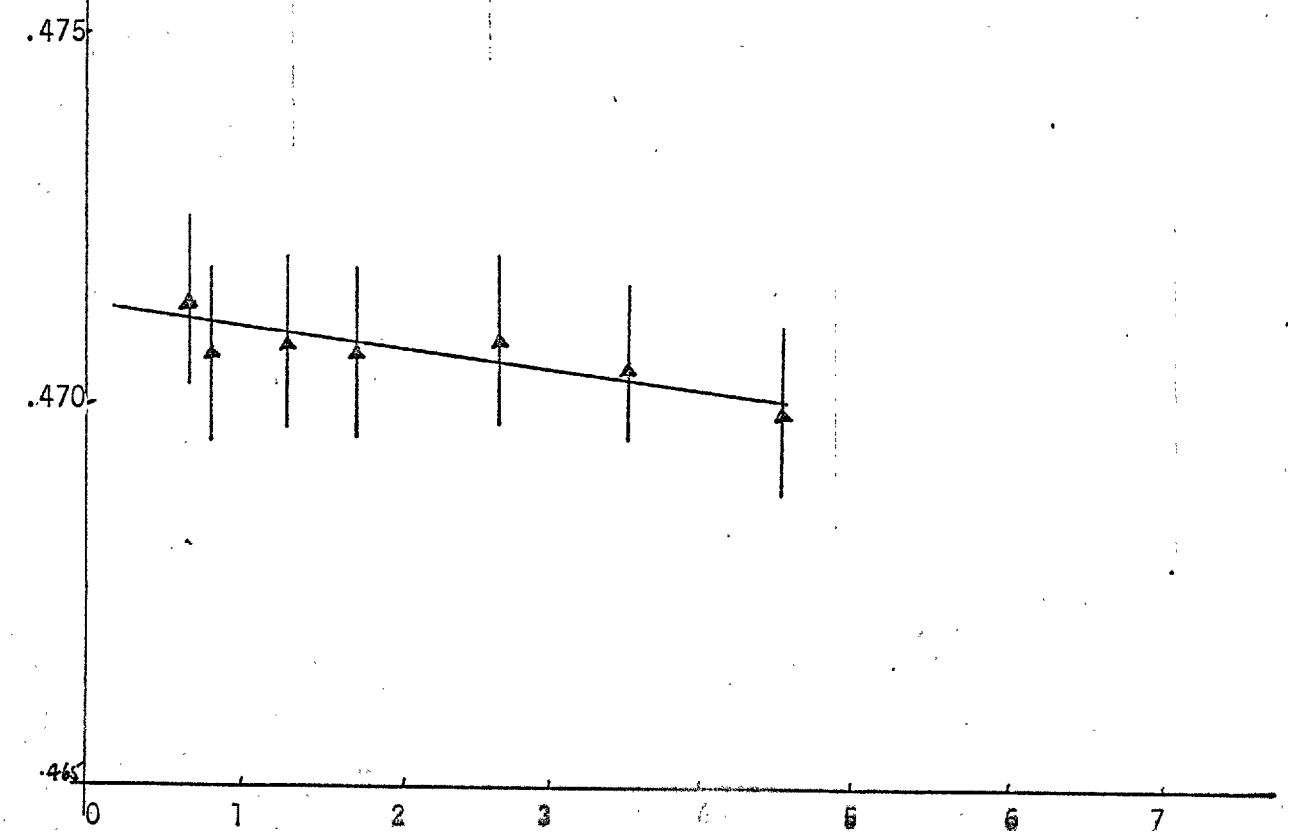
THINGVELLIR 6 - 6/11

1617. m.



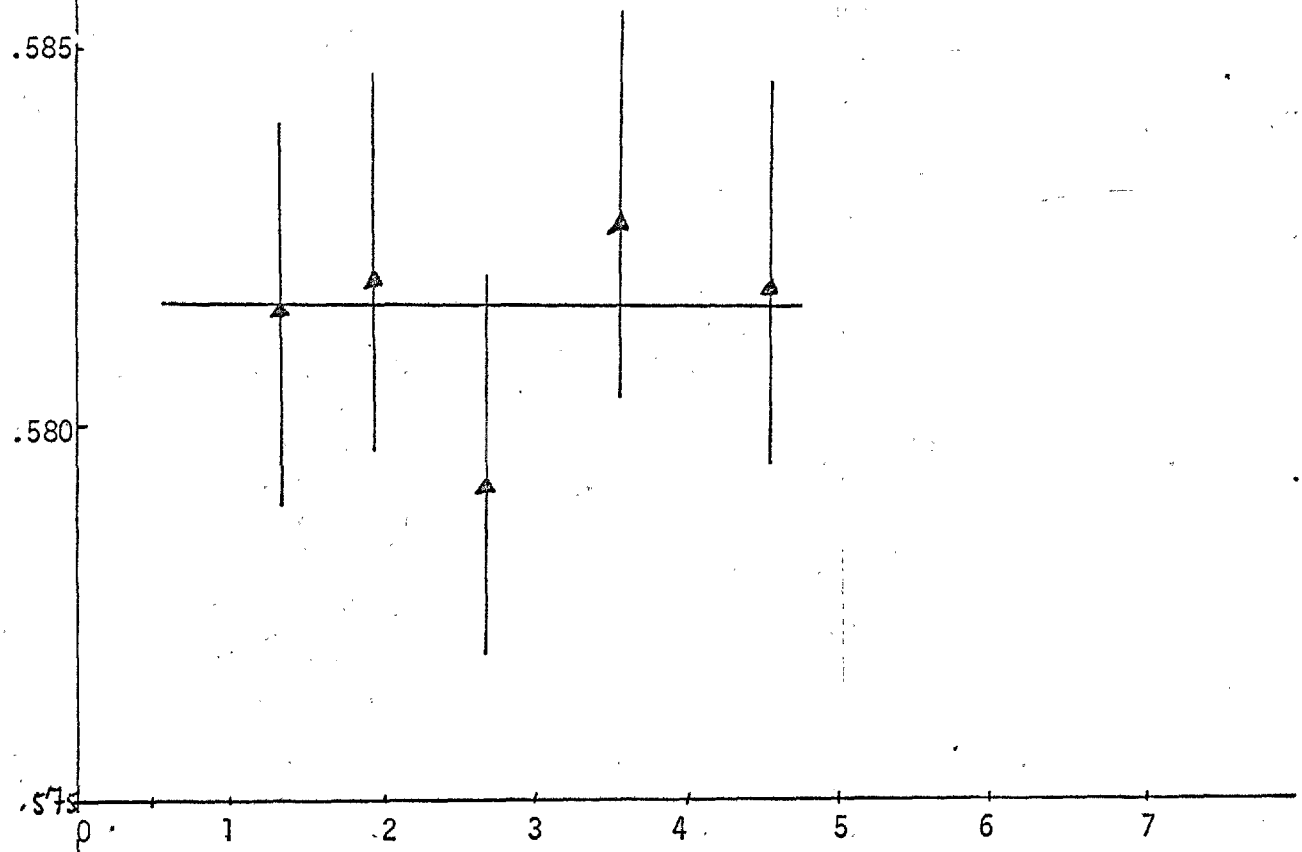
THINGVELLIR 7 - 4/7

722. m.



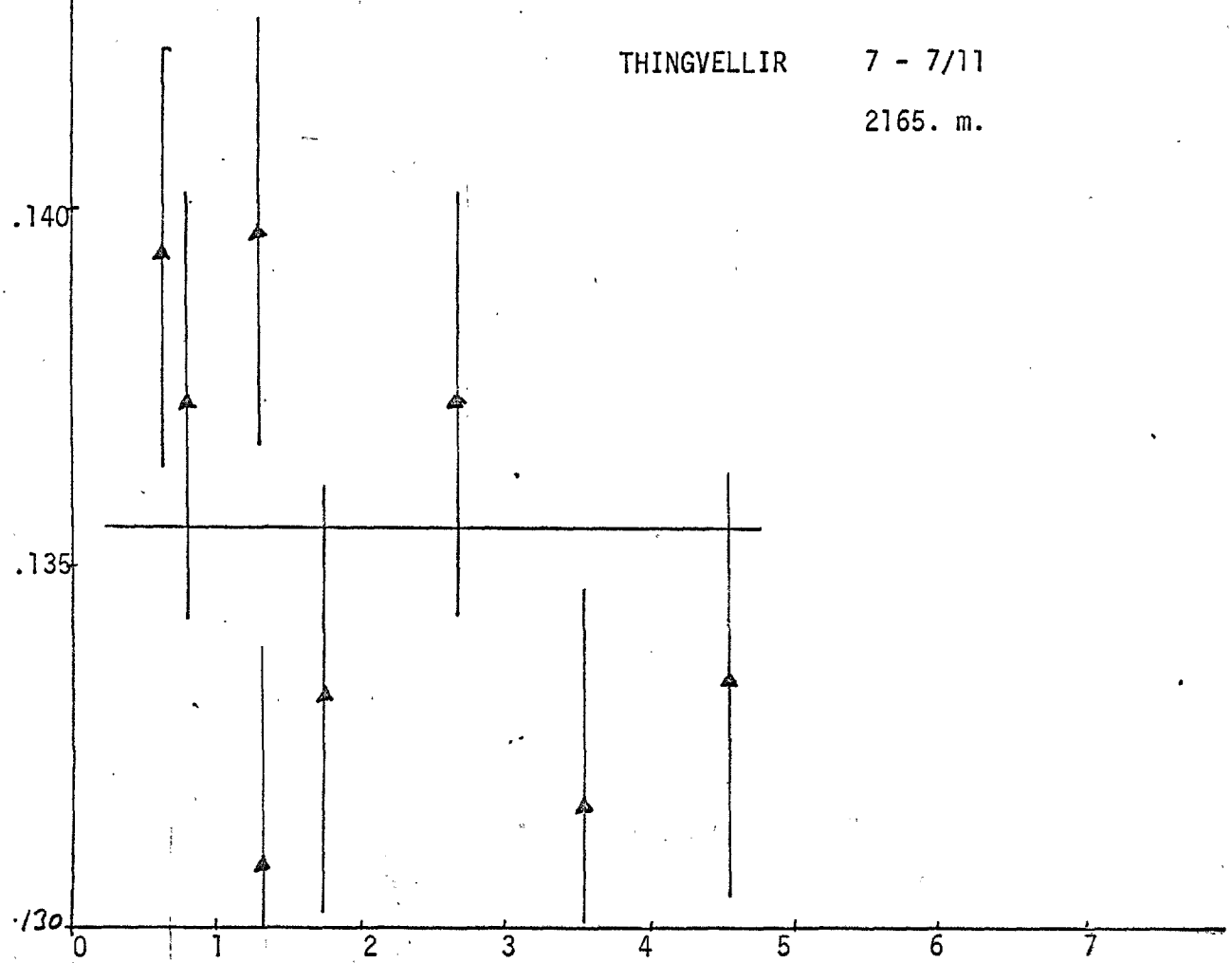
THINGVELLIR 7 - 8

1734. m.



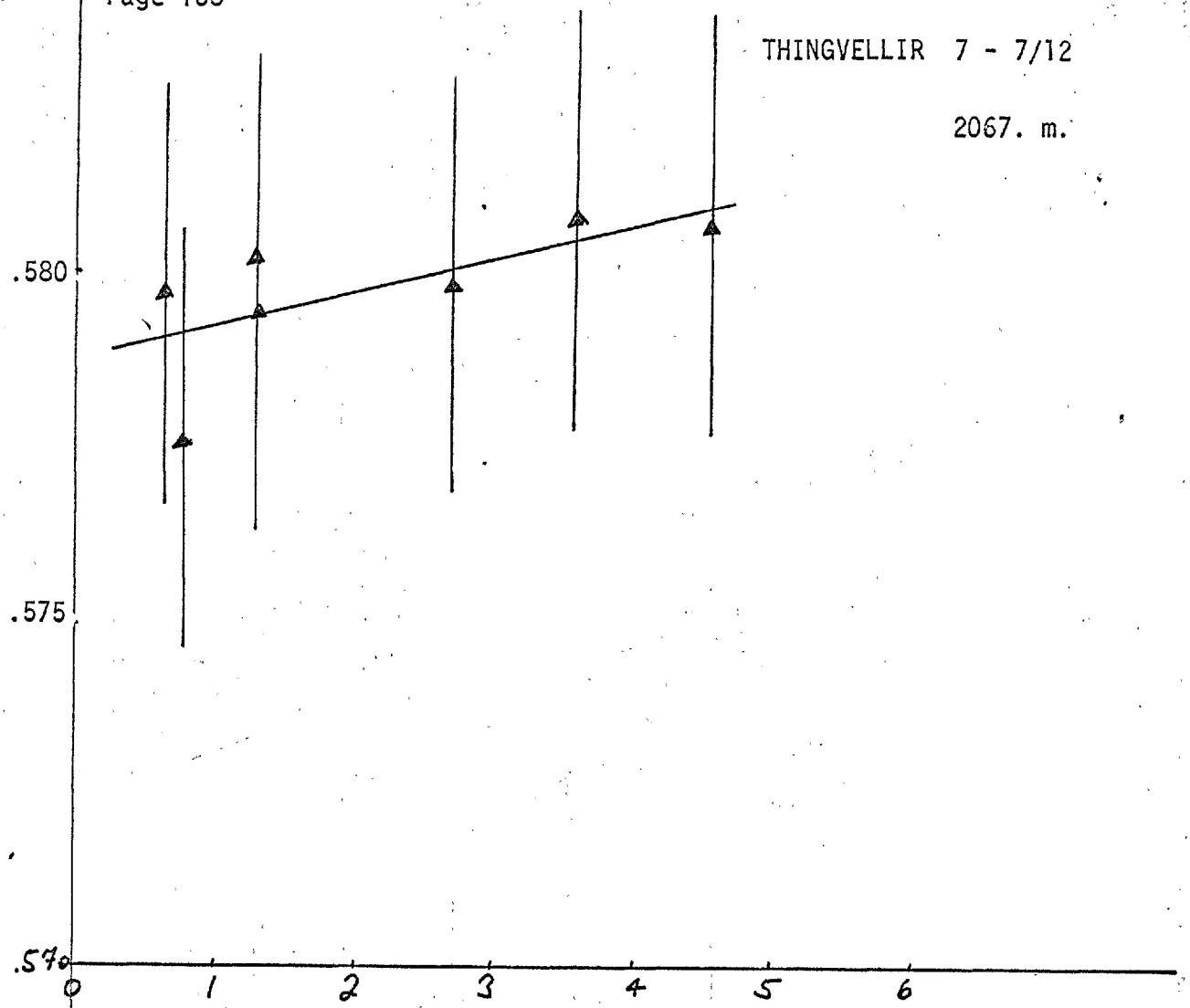
THINGVELLIR 7 - 7/11

2165. m.



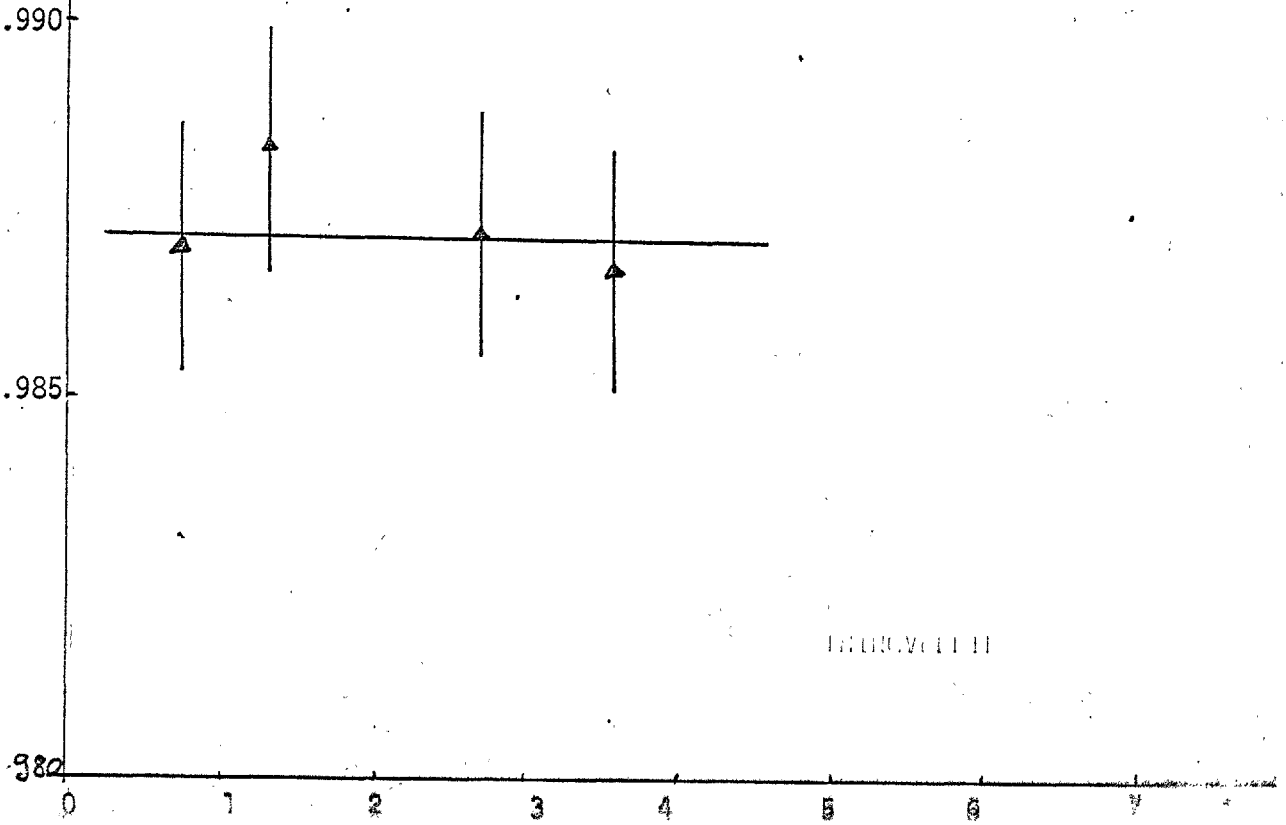
THINGVELLIR 7 - 7/12

2067. m.



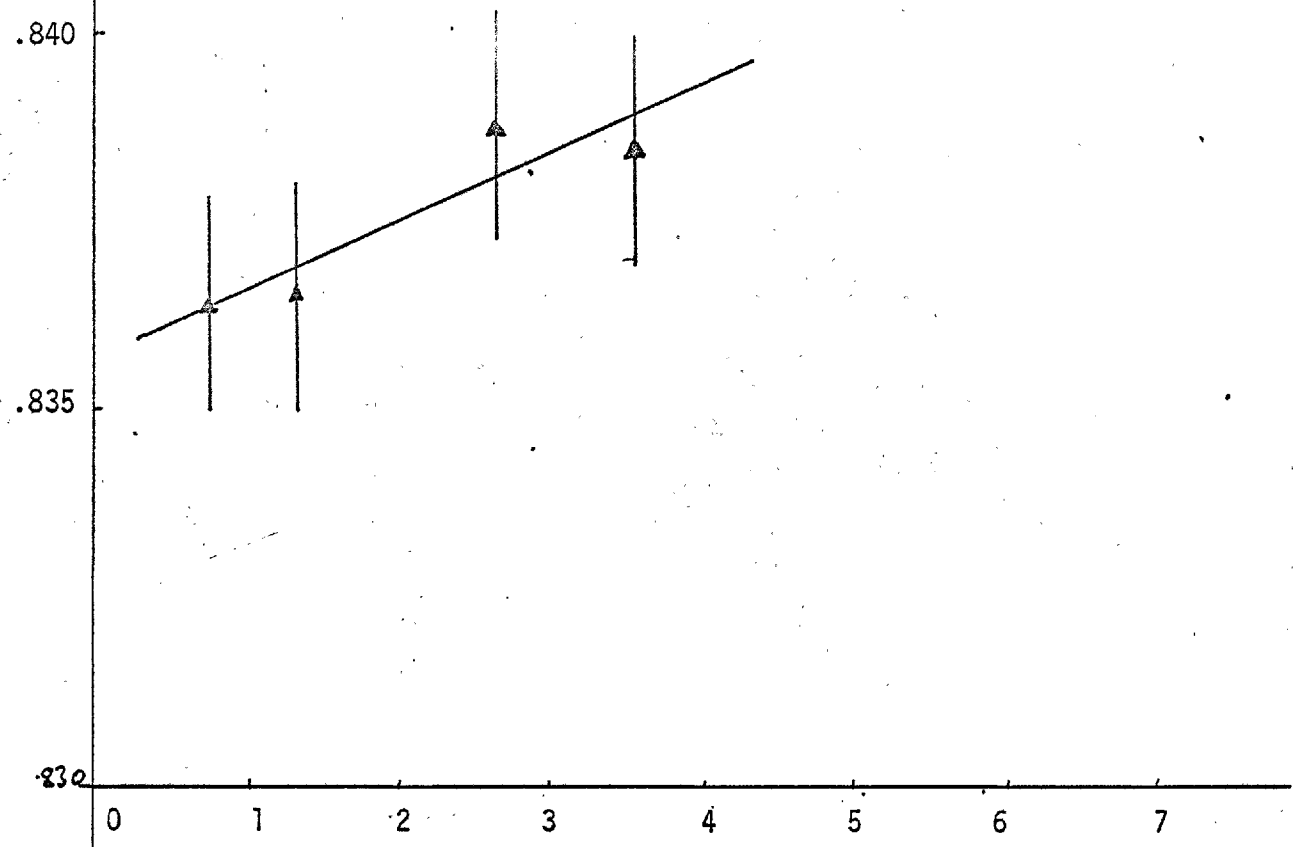
THINGVELLIR 8 - 5/8

1140. m.



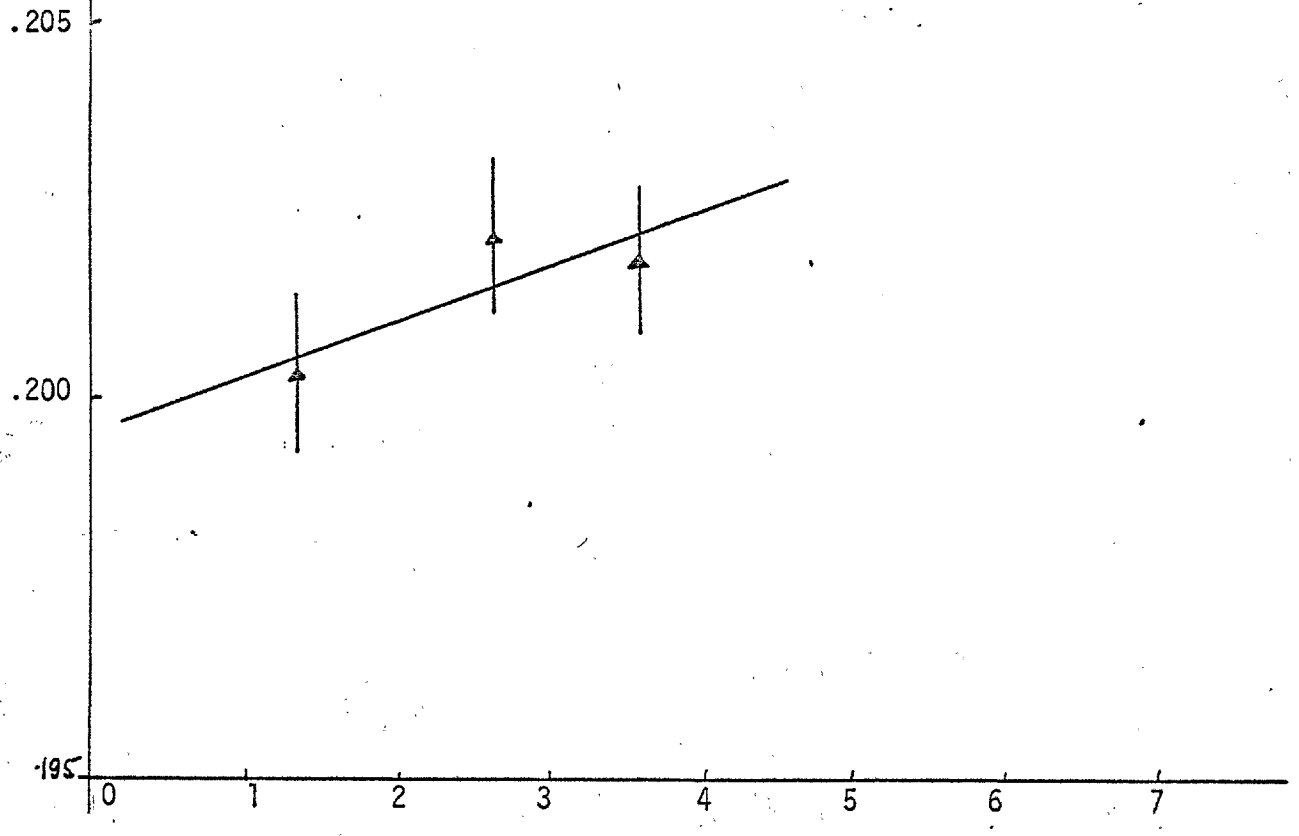
THINGVELLIR 8 - 4/8

921. m.



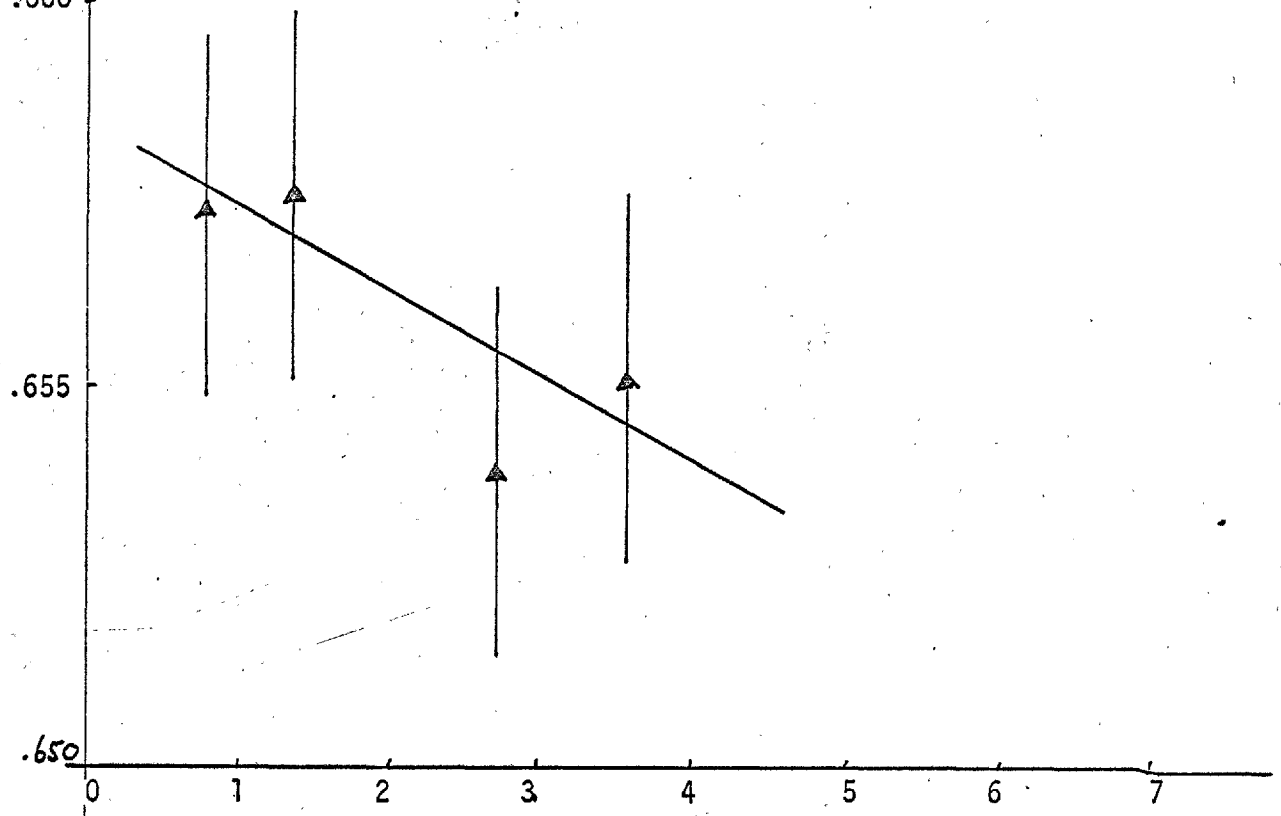
THINGVELLIR 8 -8/9

771. m.



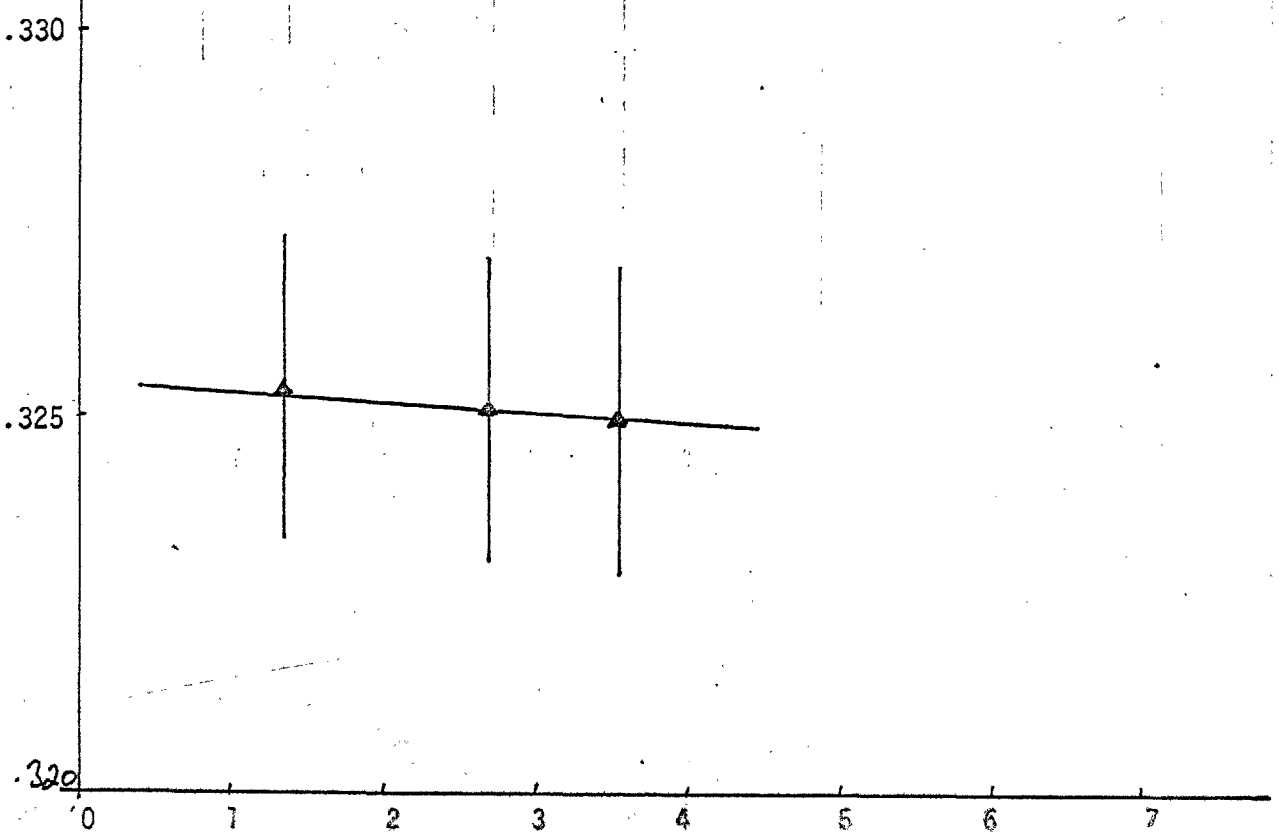
THINGVELLIR 8 - 8/12

1648. m.



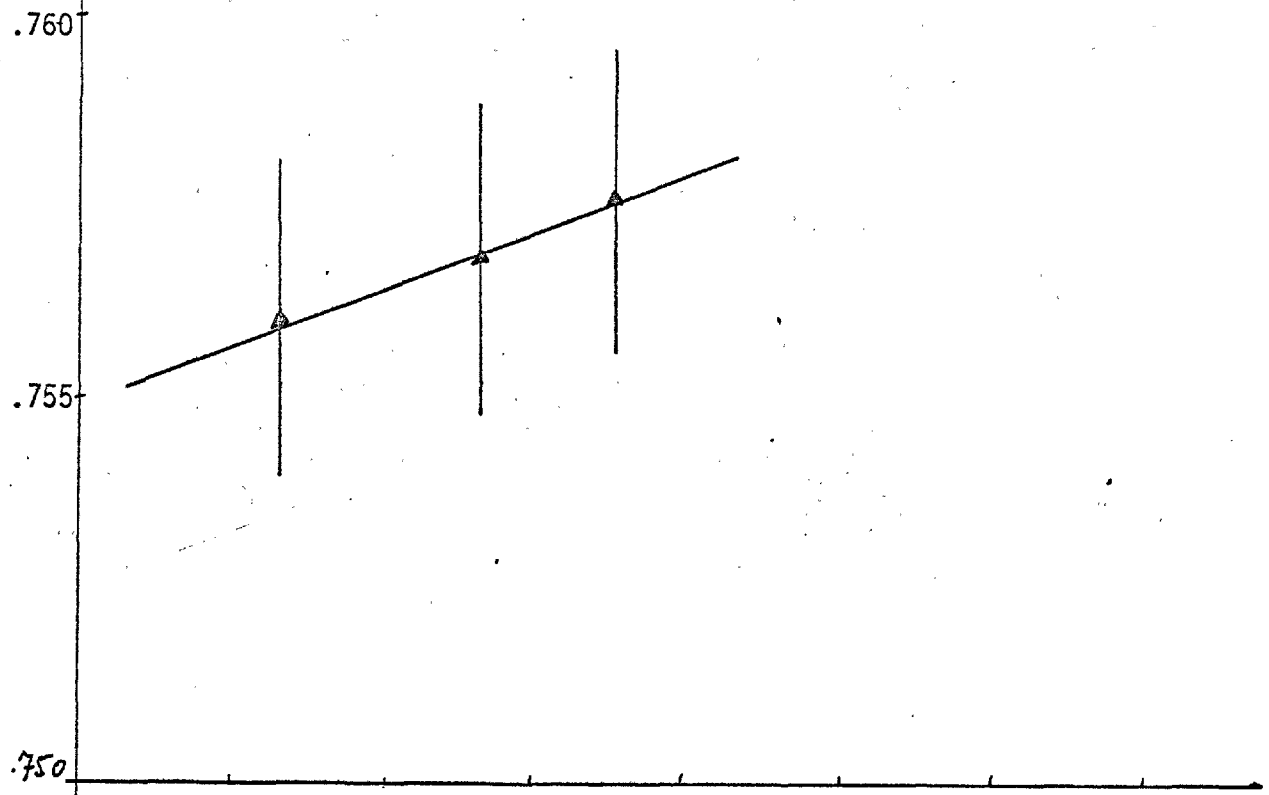
THINGVELLIR 9 - 5/9

1303..m.



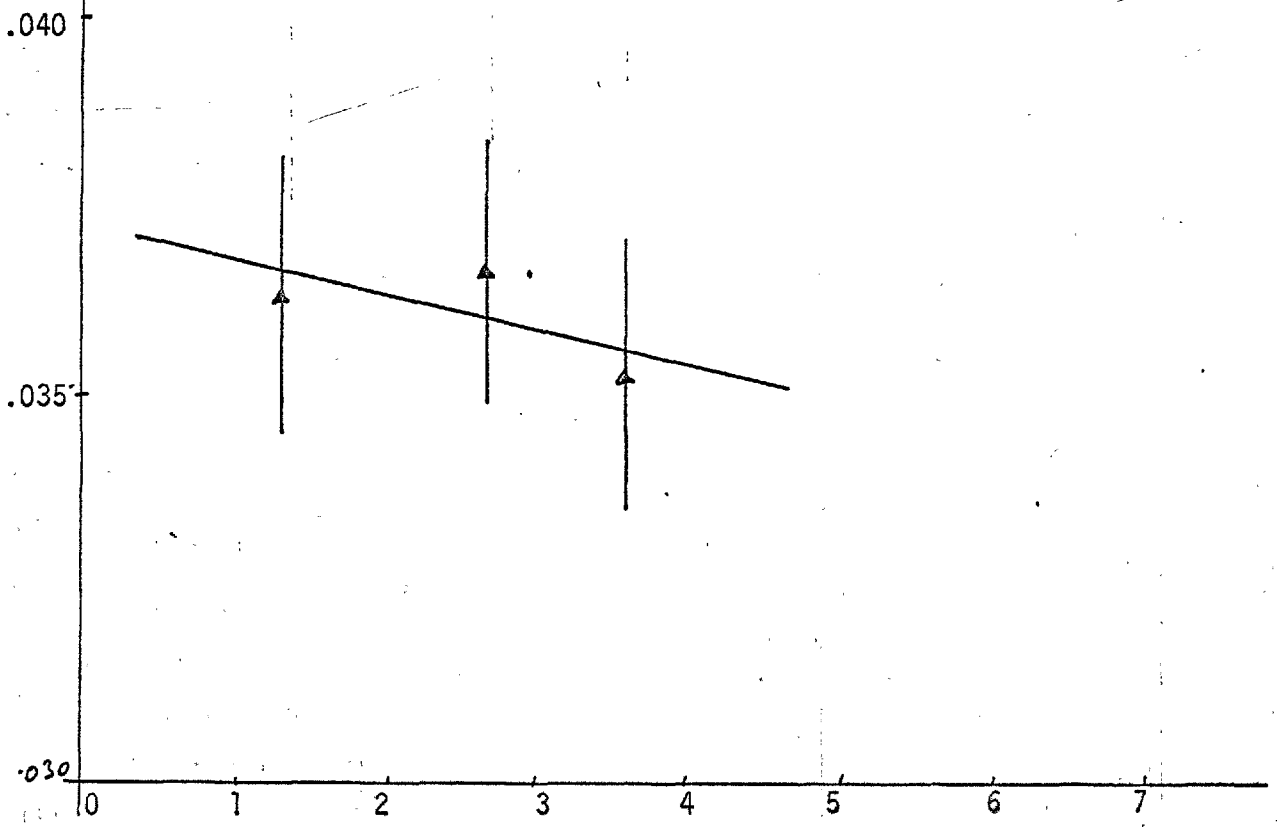
THINGVELLIR 9 -8/9

1326. m.



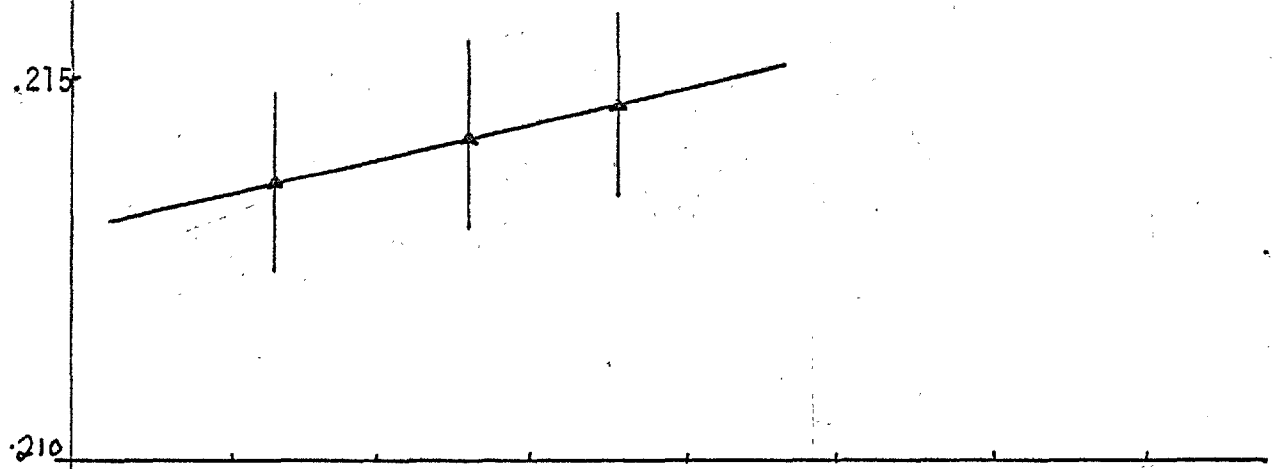
THINGVELLIR 9 - 9/12

1247. m.



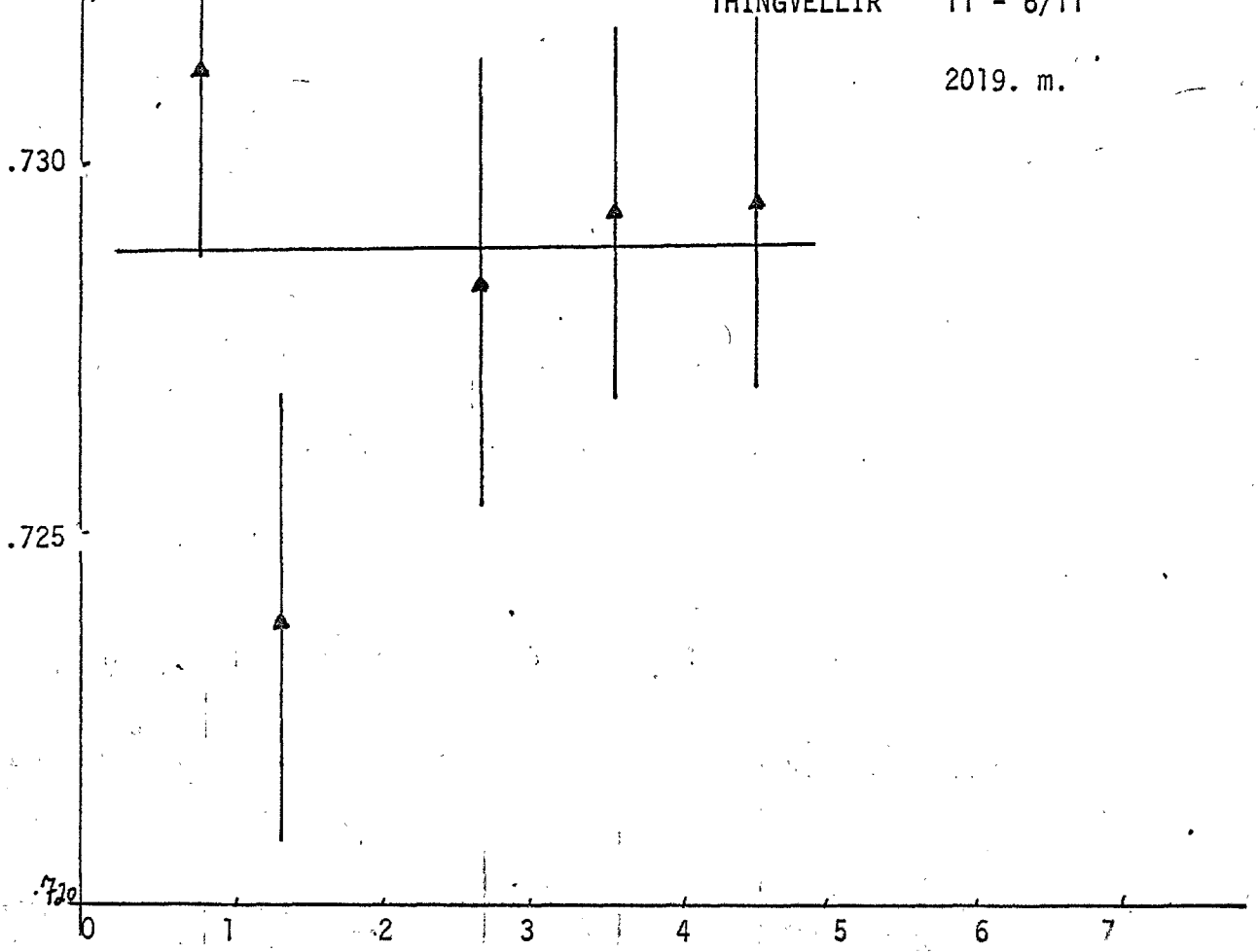
THINGVELLIR 9 - 9/13

817. m.



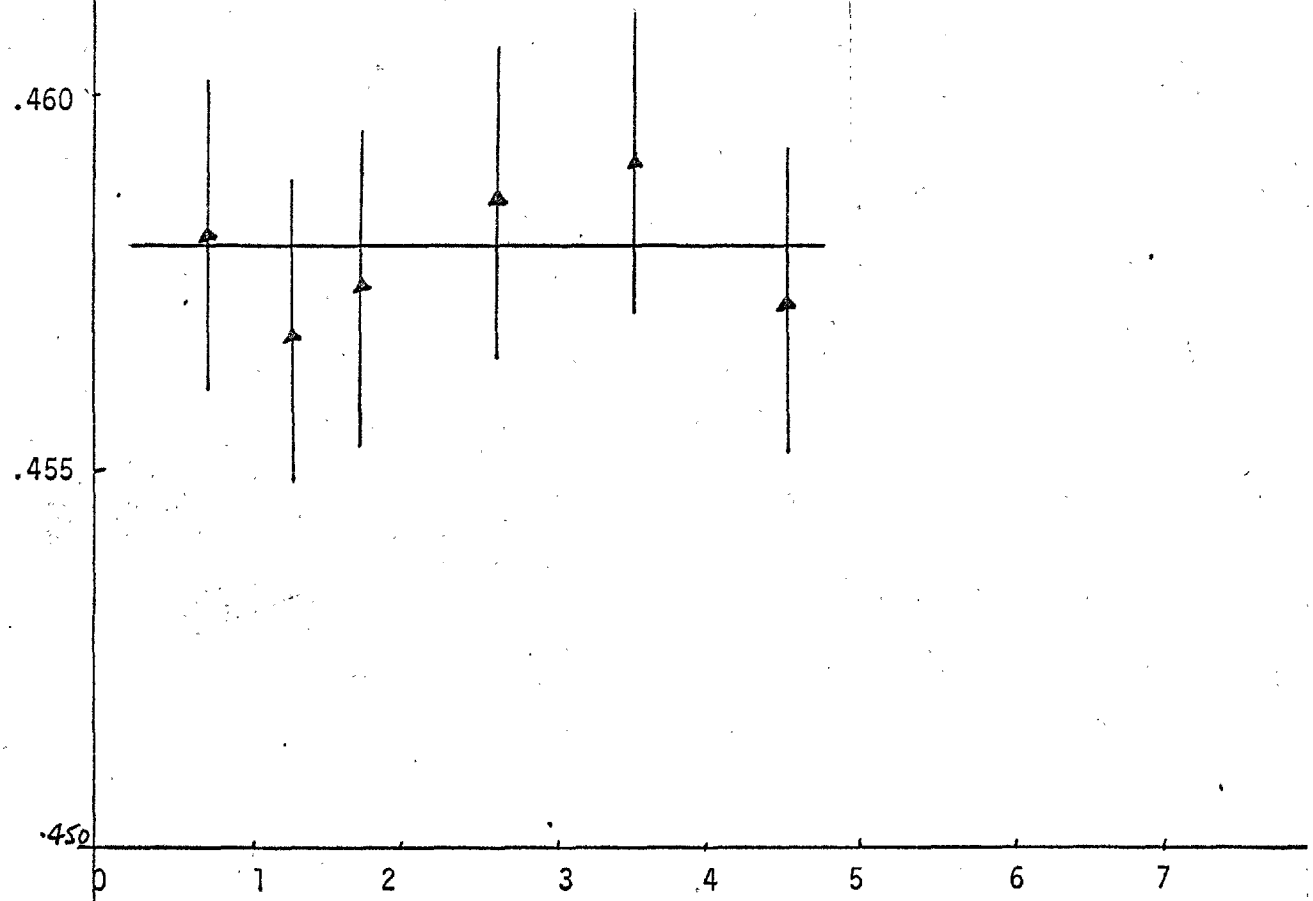
THINGVELLIR 11 - 6/11

2019. m.



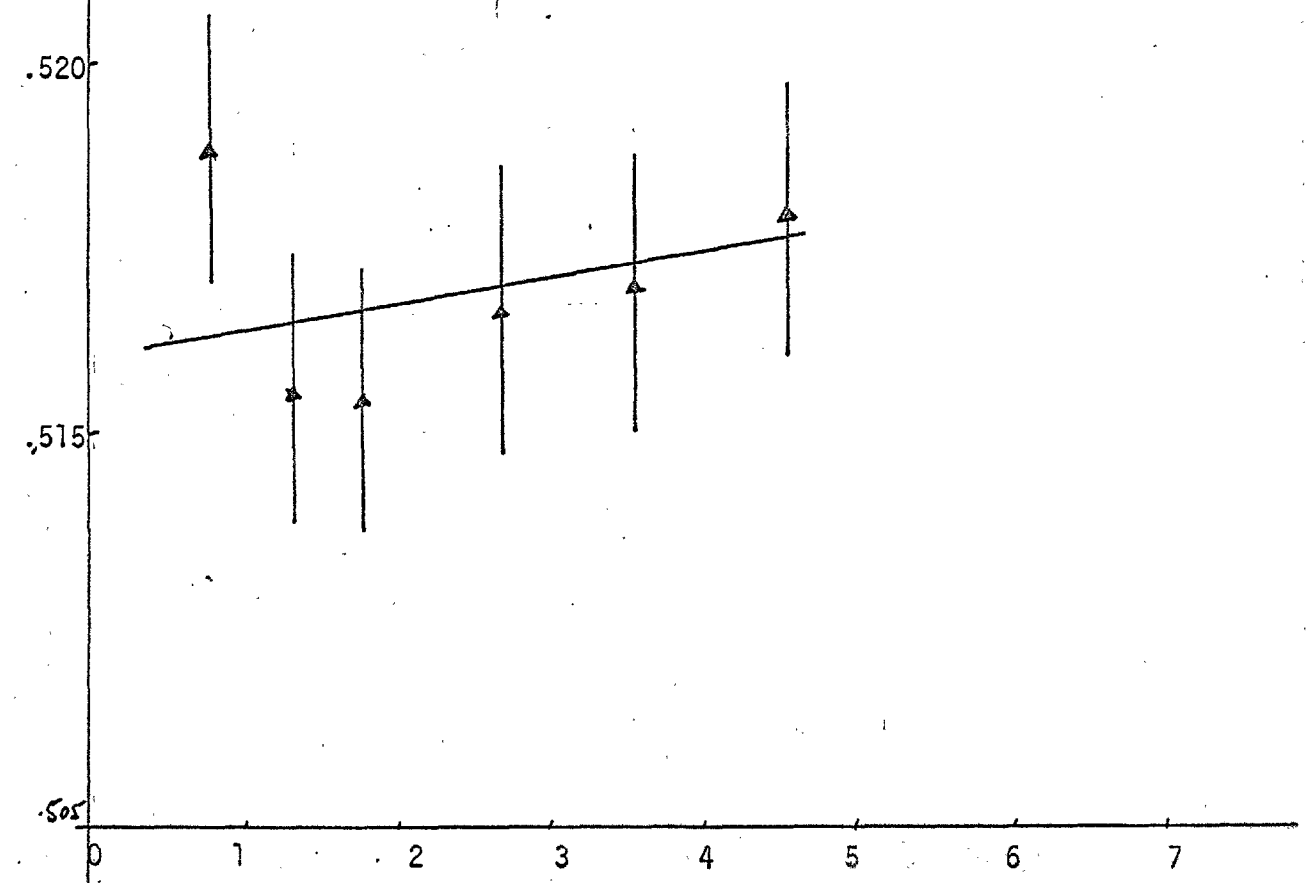
THINGVELLIR 11 - 7/11

1387. m.



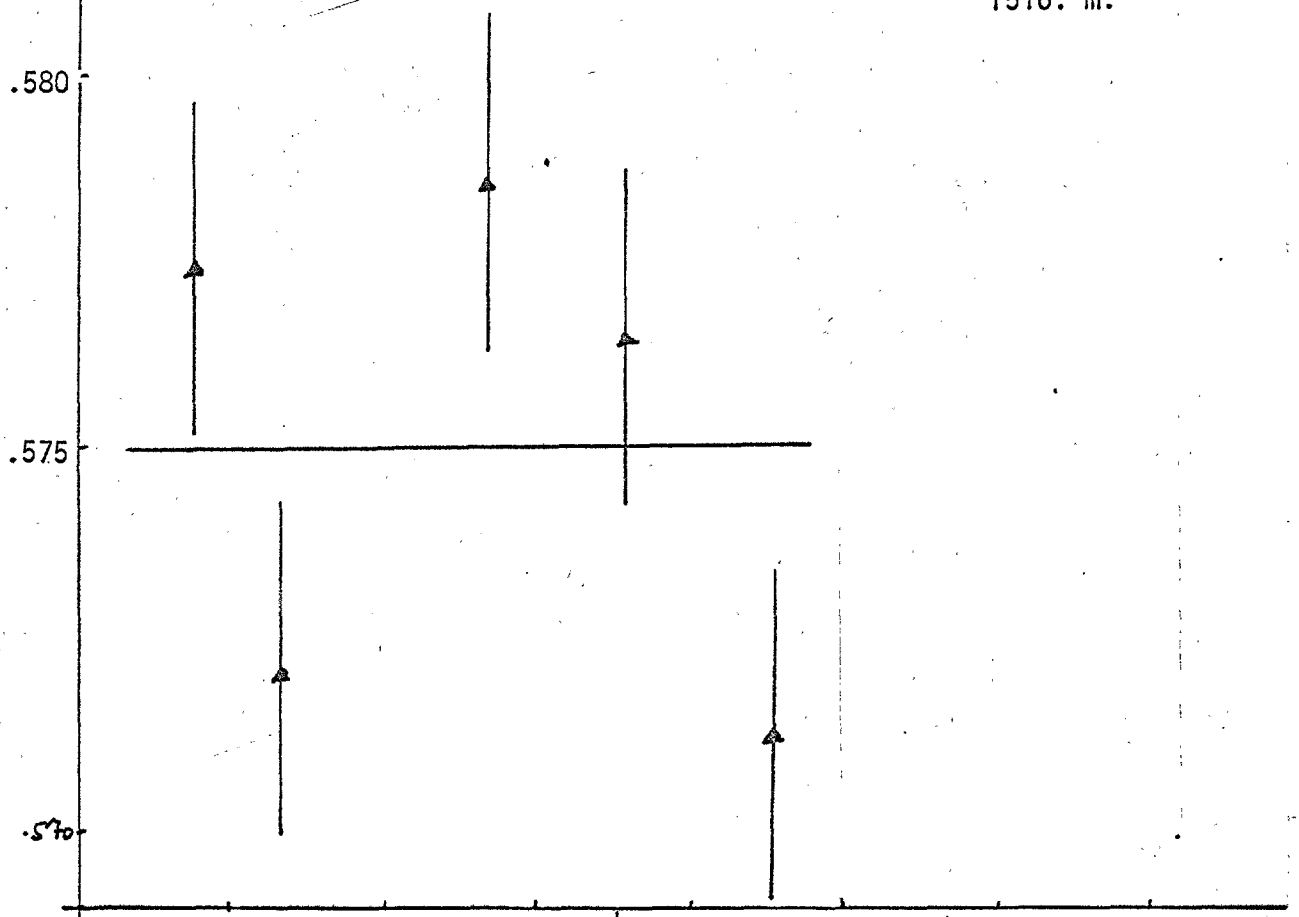
THINGVELLIR 11 - 11/12

1261. m.



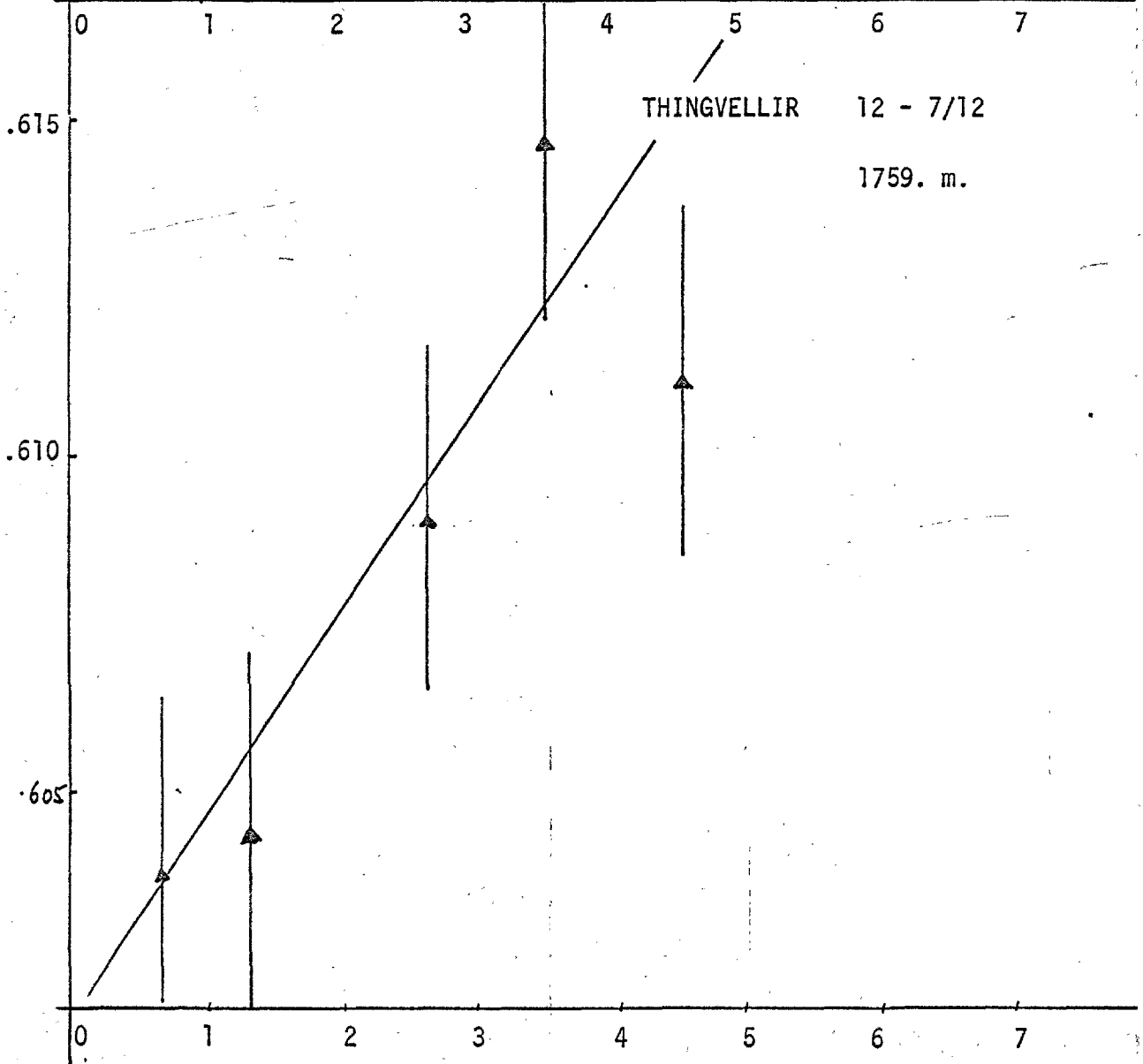
THINGVELLIR 11 - 11/15

1516. m.



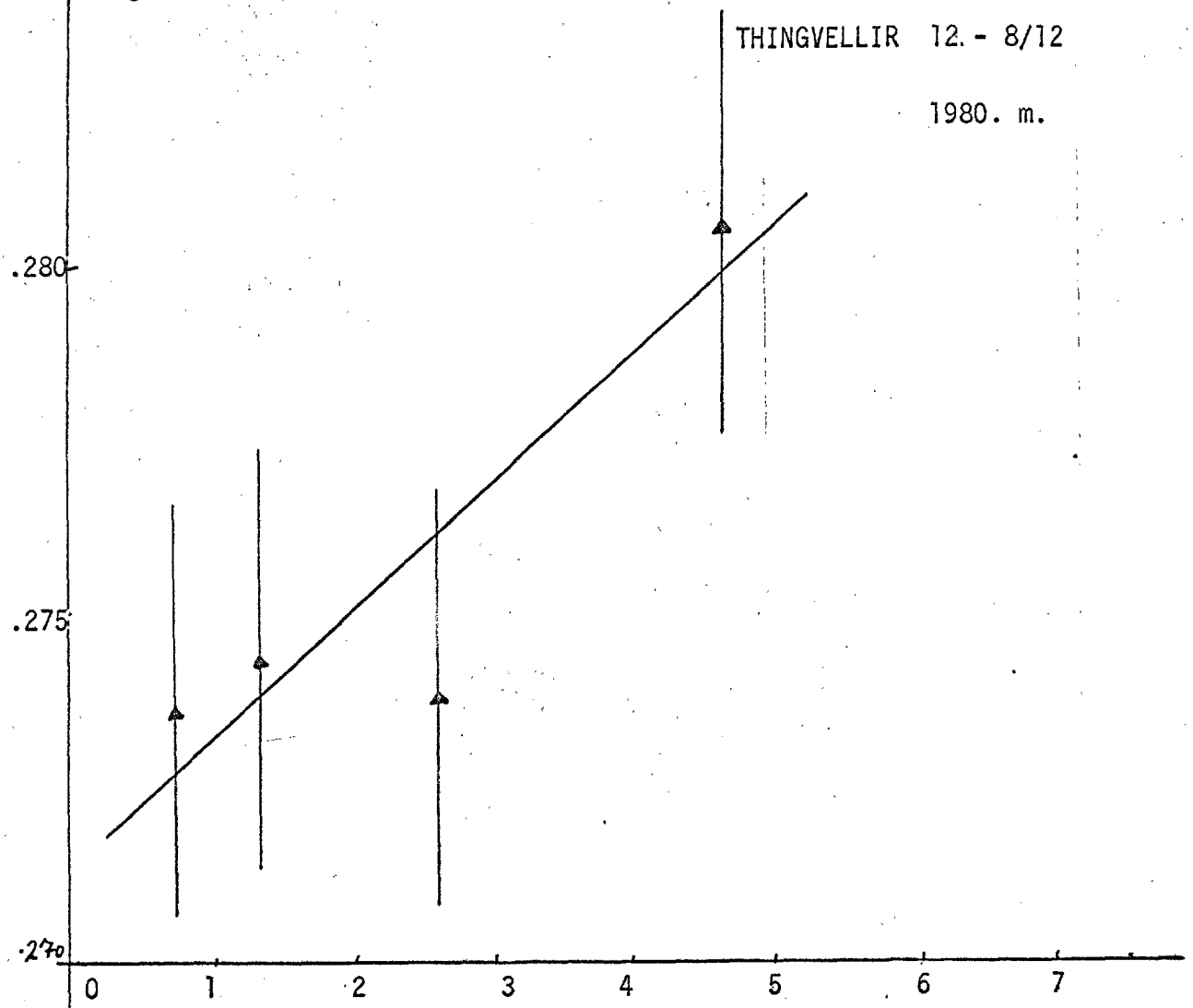
THINGVELLIR 12 - 7/12

1759. m.



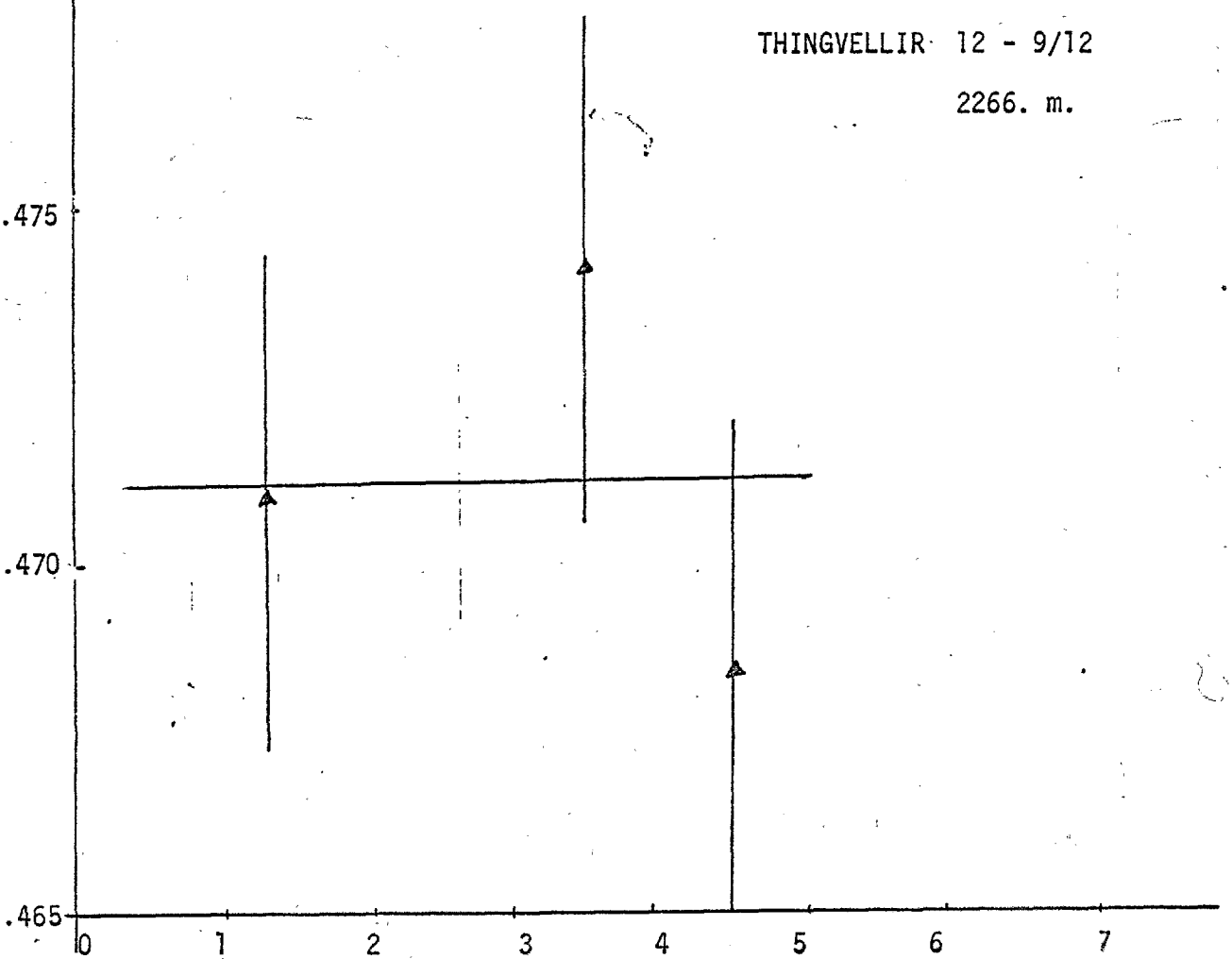
THINGVELLIR 12. - 8/12

1980. m.



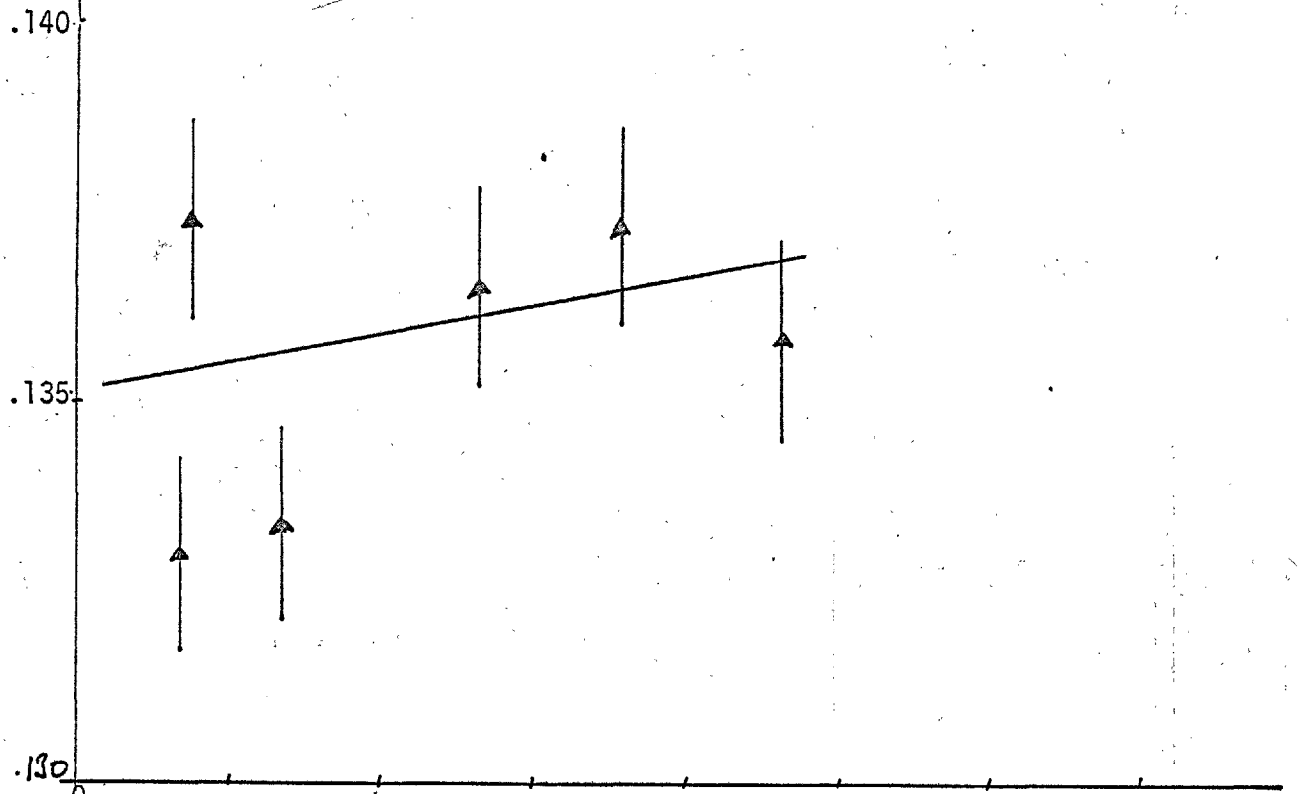
THINGVELLIR 12 - 9/12

2266. m.



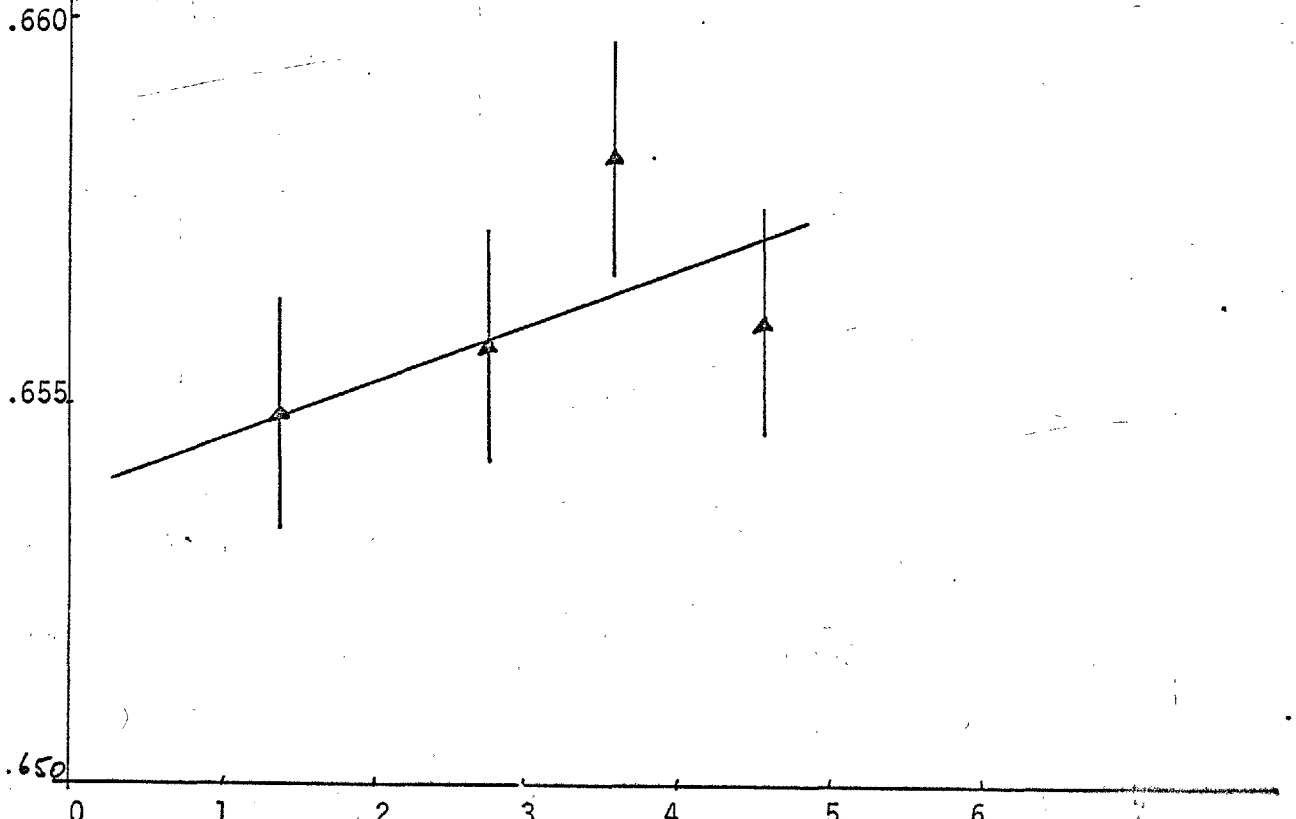
THINGVELLIR 12 - 11/12

894. m.



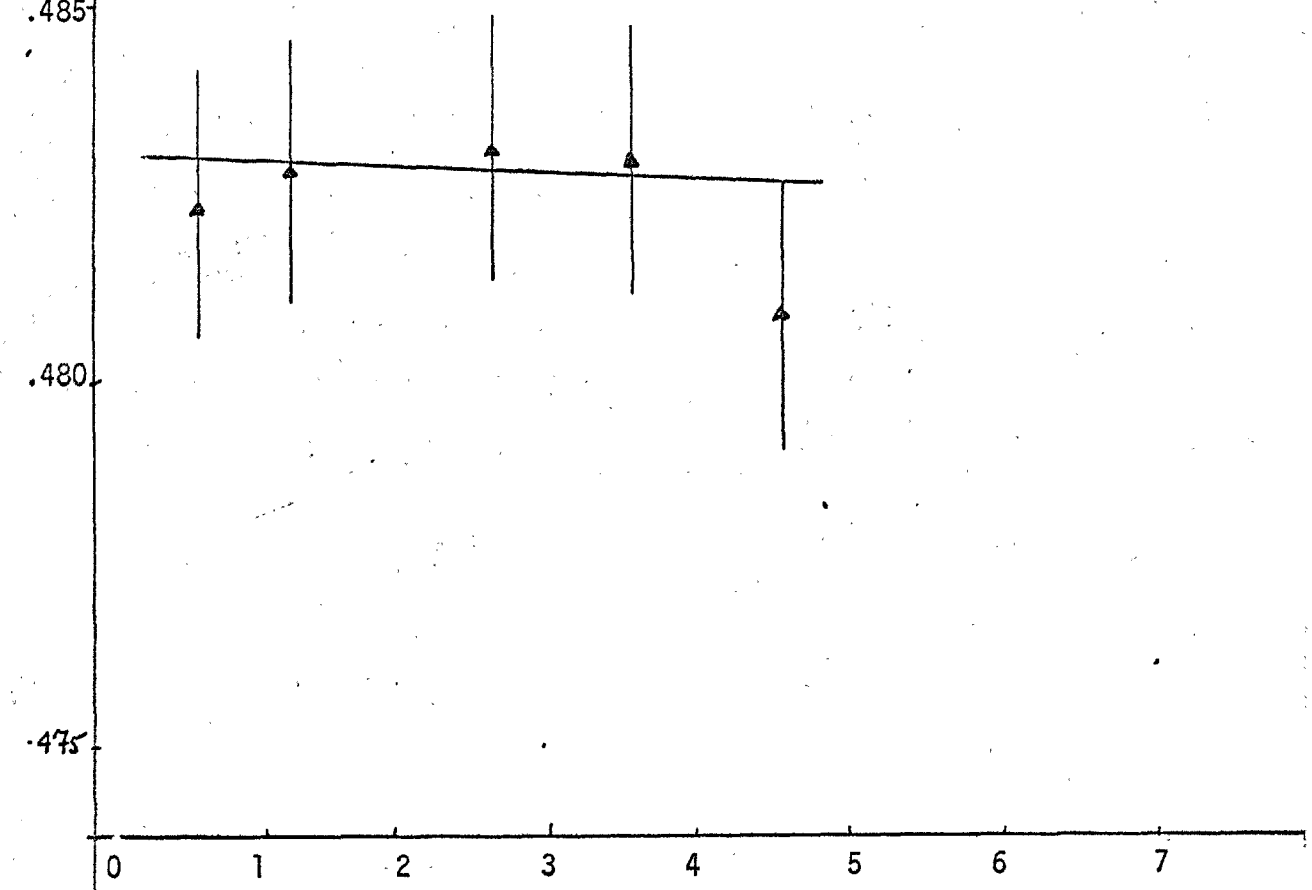
THINGVELLIR 12 - 12/13

998. m.



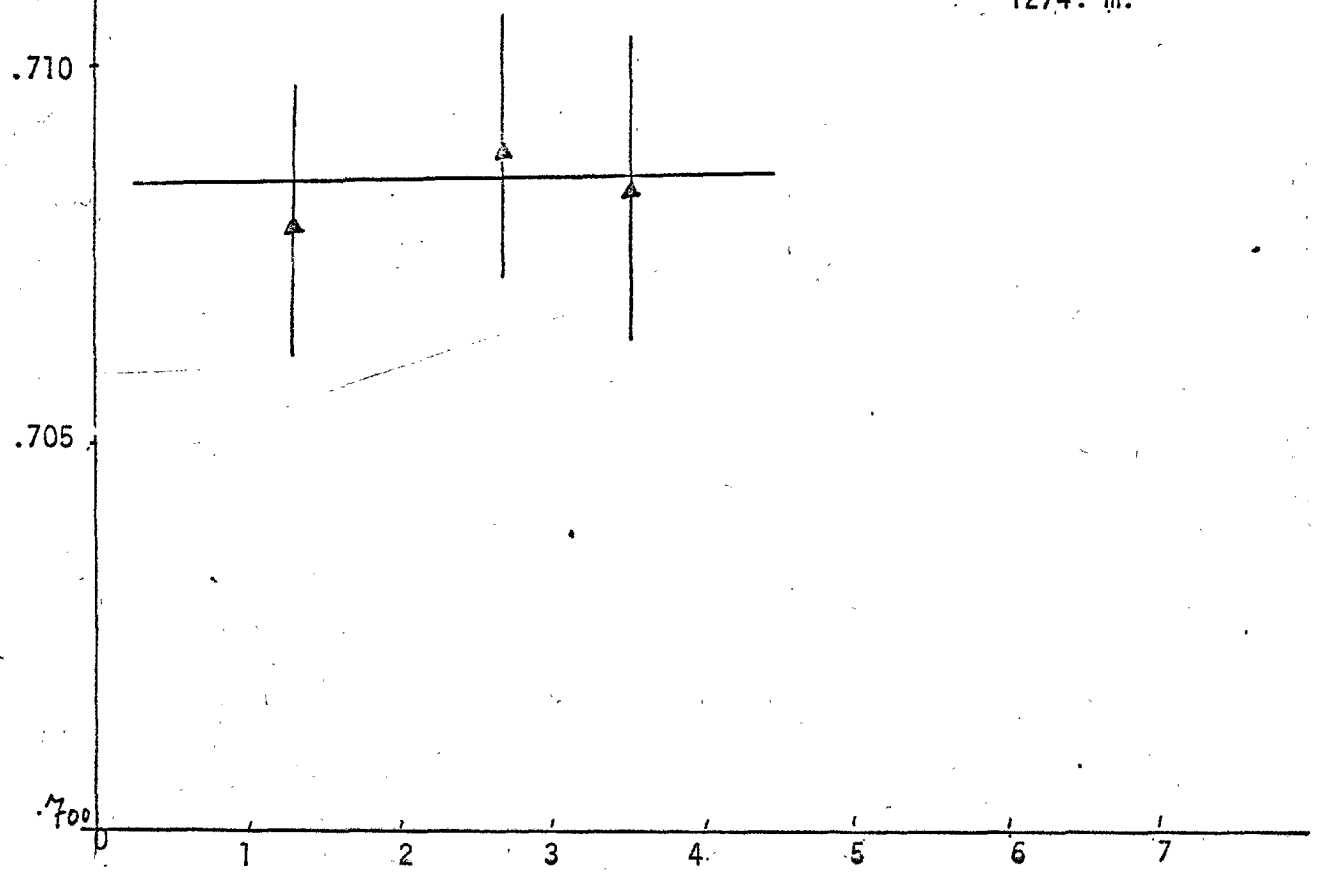
THINGVELLIR 12 - 12/15

1224. m.



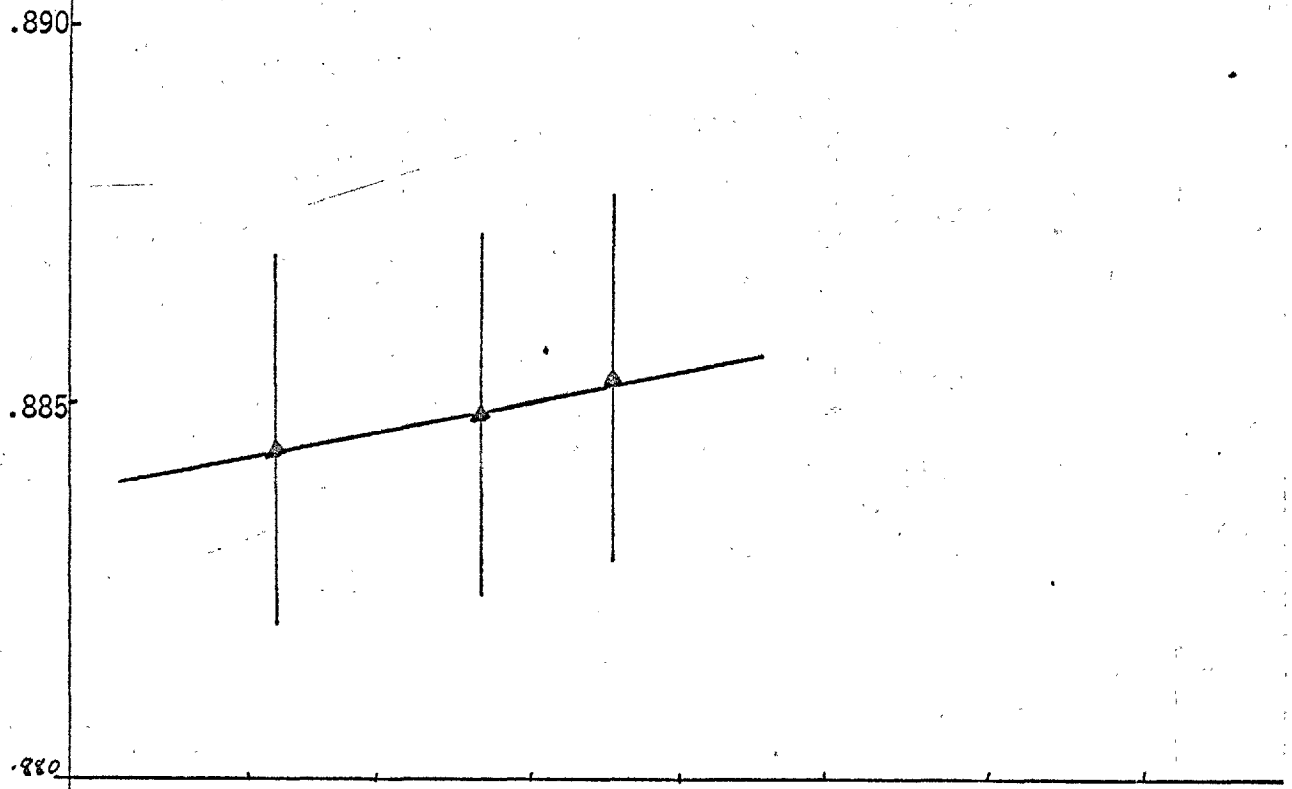
THINGVELLIR 13 - 9/13

1274. m.



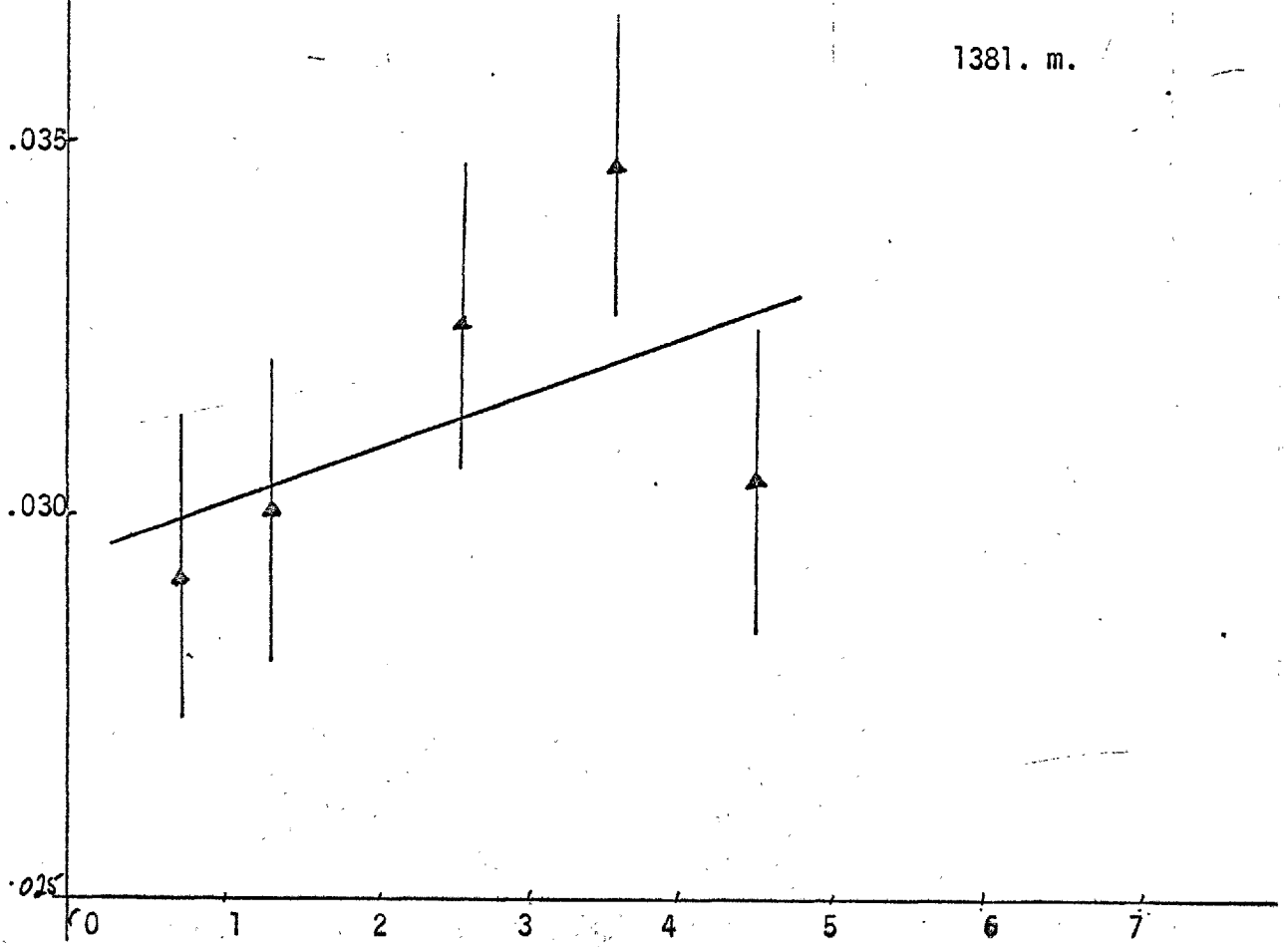
THINGVELLIR 13 - 12/13

1612. m.



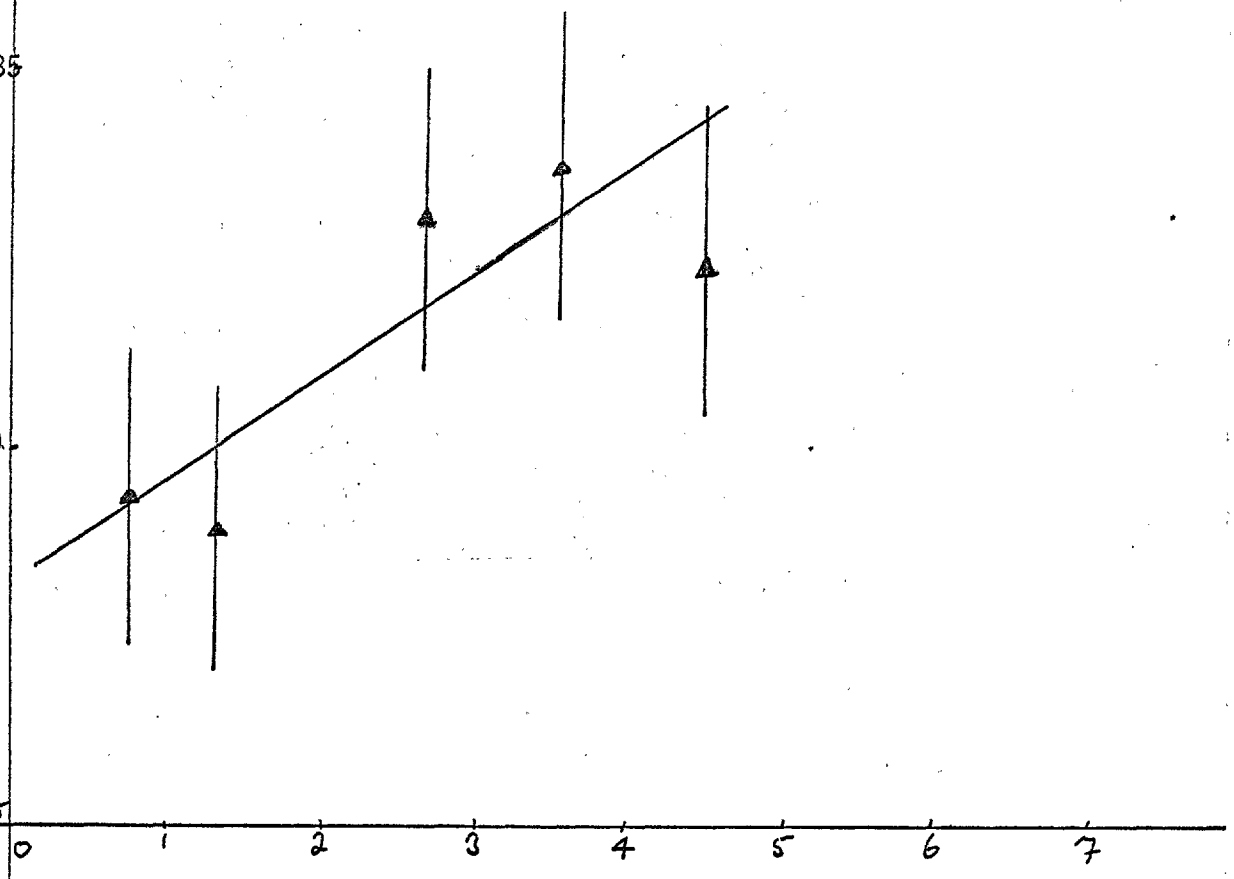
THINGVELLIR 15 - 11/15

1381. m.



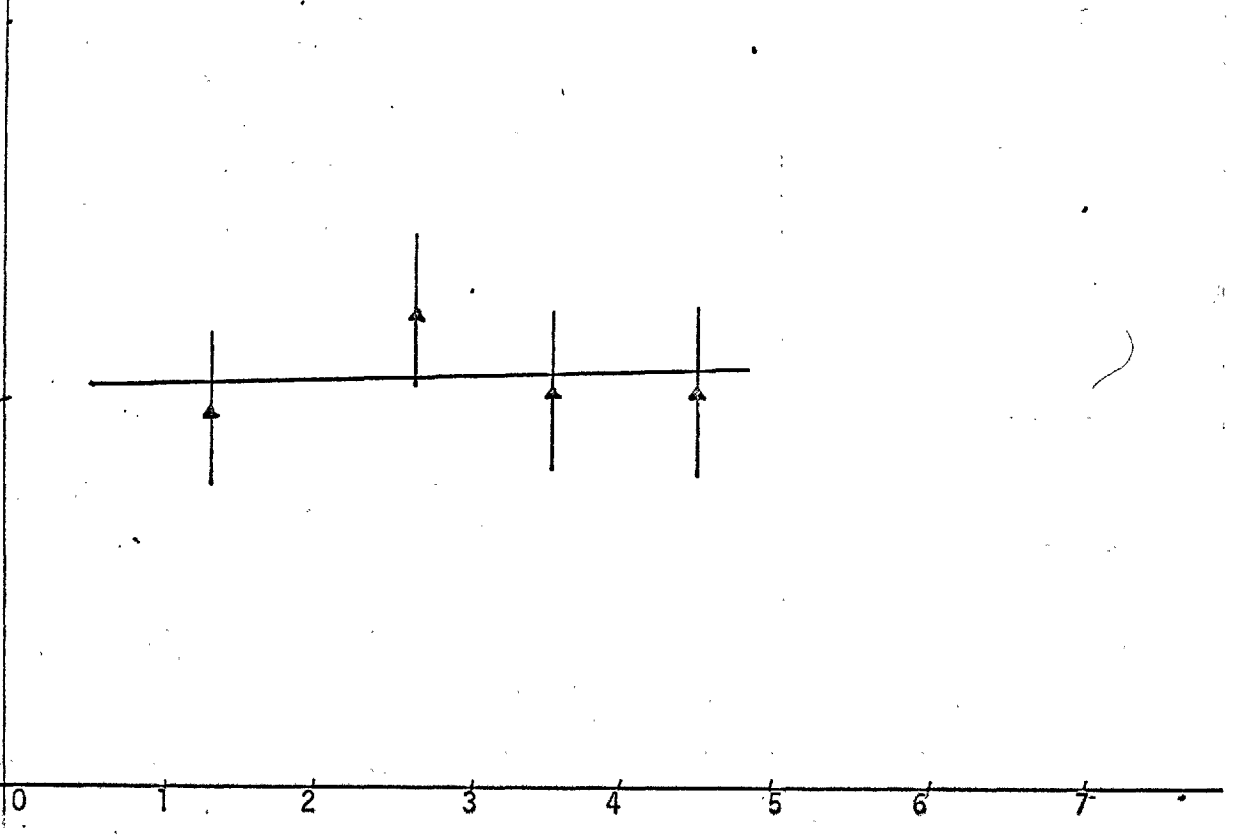
THINGVELLIR 15 - 12/15

1310. m.



THINGVELLIR 15 - 15/16

679. m.



APPENDIX E THE DISTANCE - TIME GRAPHS FOR THE REYKJANES MEASUREMENTS.

The following forty five pages show the distance-time graphs for the lines of the original network at Reykjanes.

On each the whole number distance and line name are shown on the top right-hand corner; the ordinate expresses the excess in the measured distance over an integral number of metres.

Time is measured in years from the beginning of 1968.

On some curves it will be seen that two different symbols are employed.

Small triangles indicate that the line was measured in the direction given by the line name; small circles indicate that the line was measured in the reverse reverse direction.

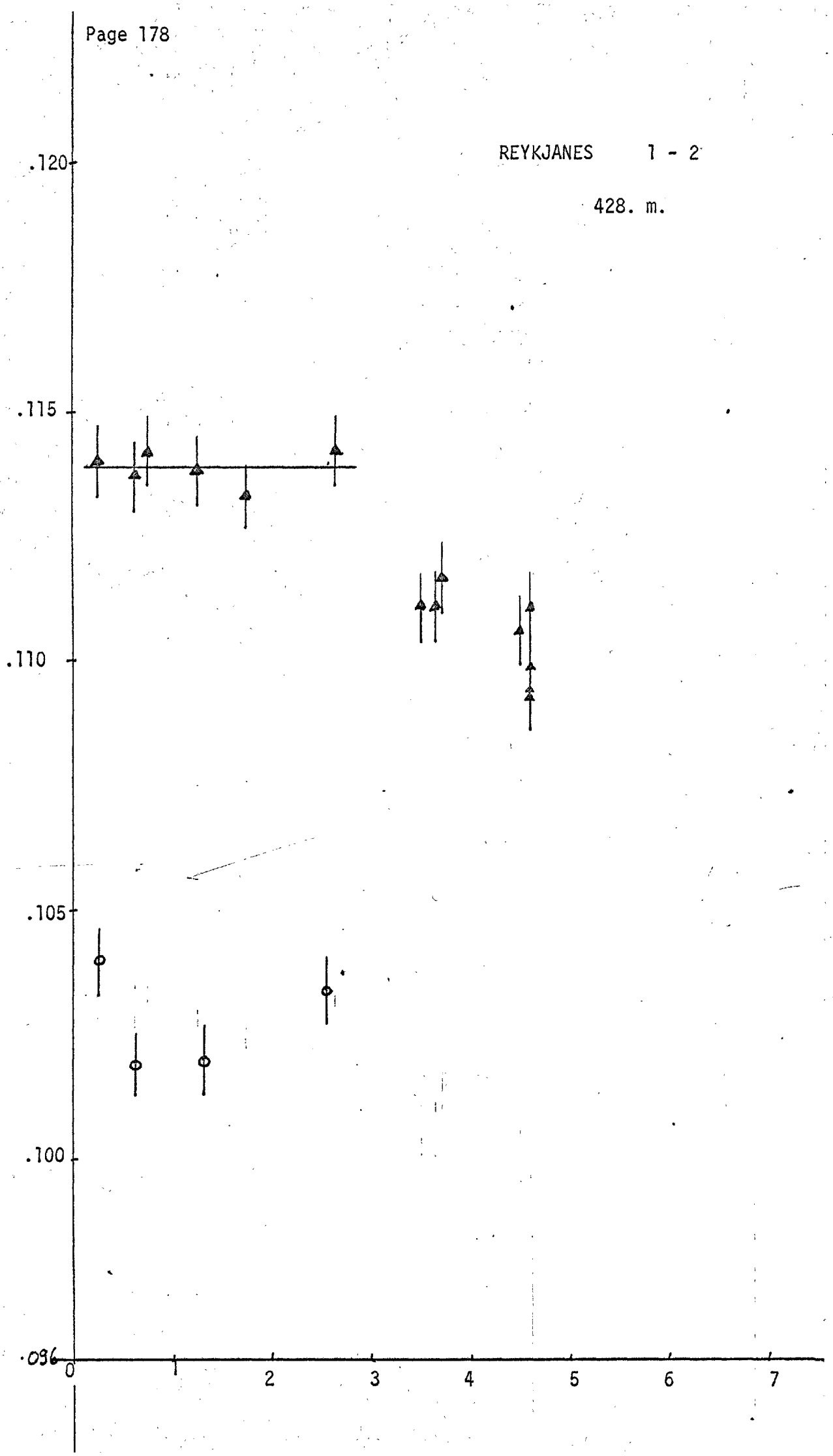
Error bars are the square root of the sum of the squares of the expected error for the length of line concerned (as given in chapter III) and the standard deviation of the group of readings from which the measurement was deriv--ed.

Straight lines have been fitted to the plots of almost all the lines. In only one or two cases does there appear to be no justification for fitting a straight line to the results.

These distance measurements are interpreted in chapter VI.

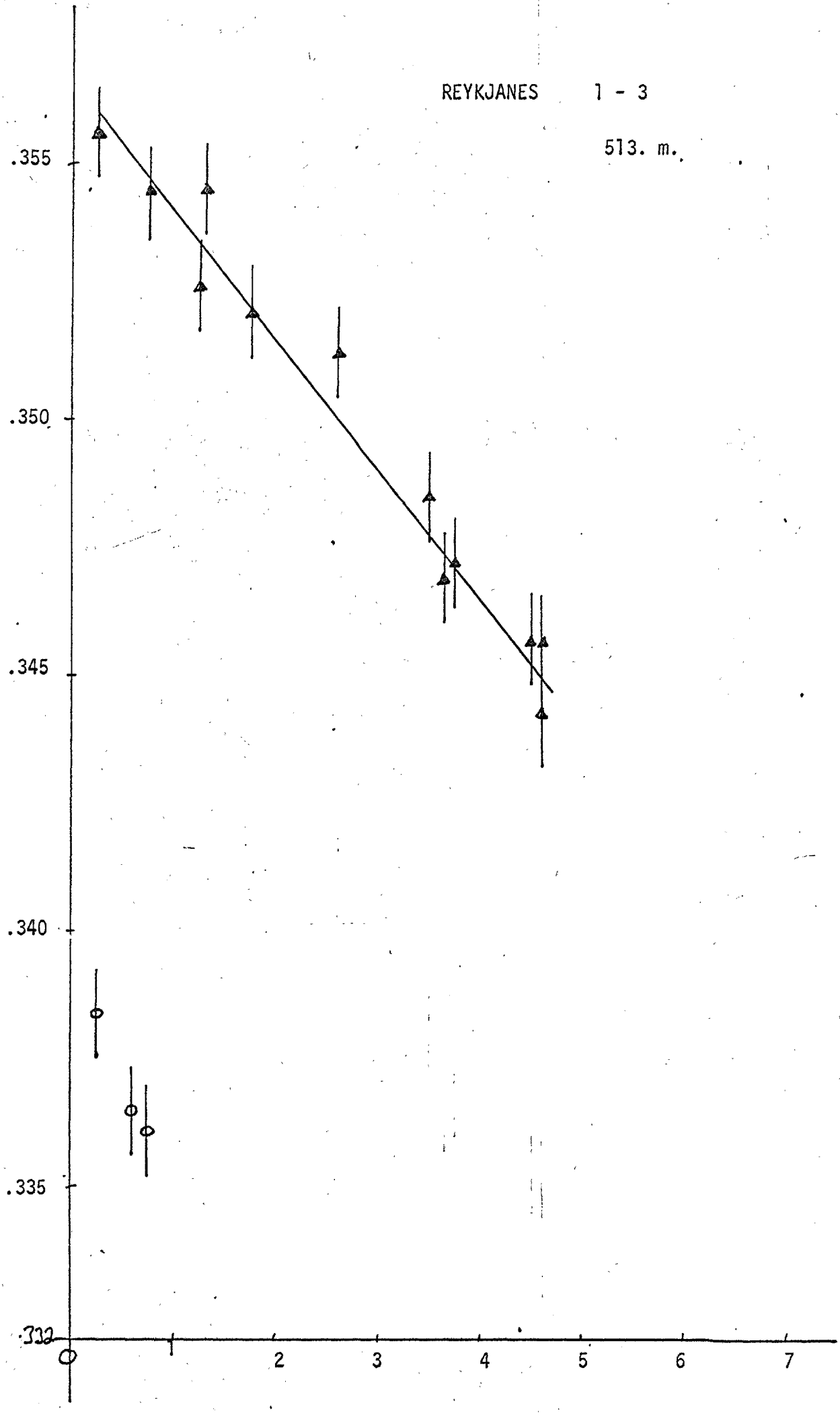
REYKJANES 1 - 2

428. m.



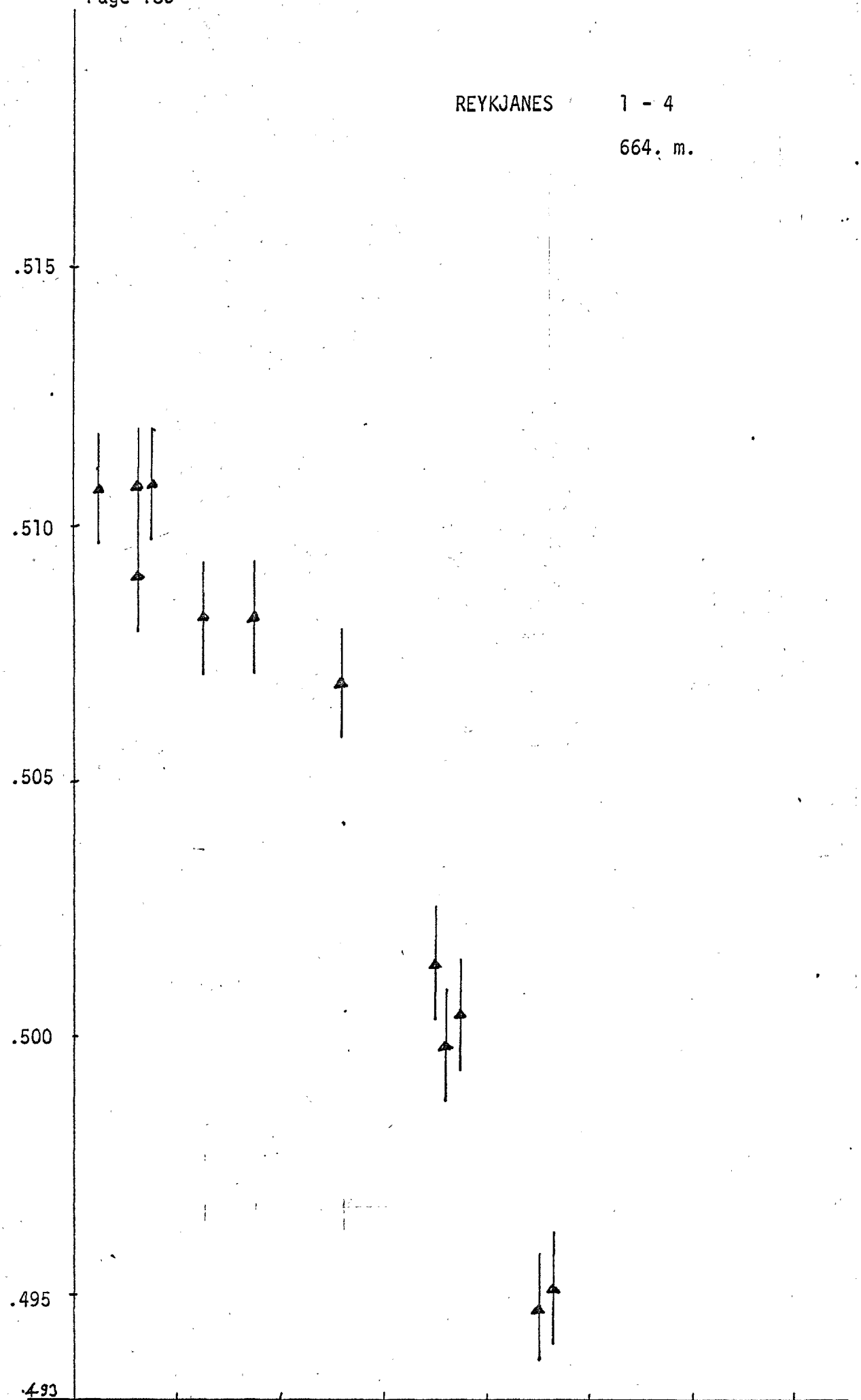
REYKJANES 1 - 3

513. m.



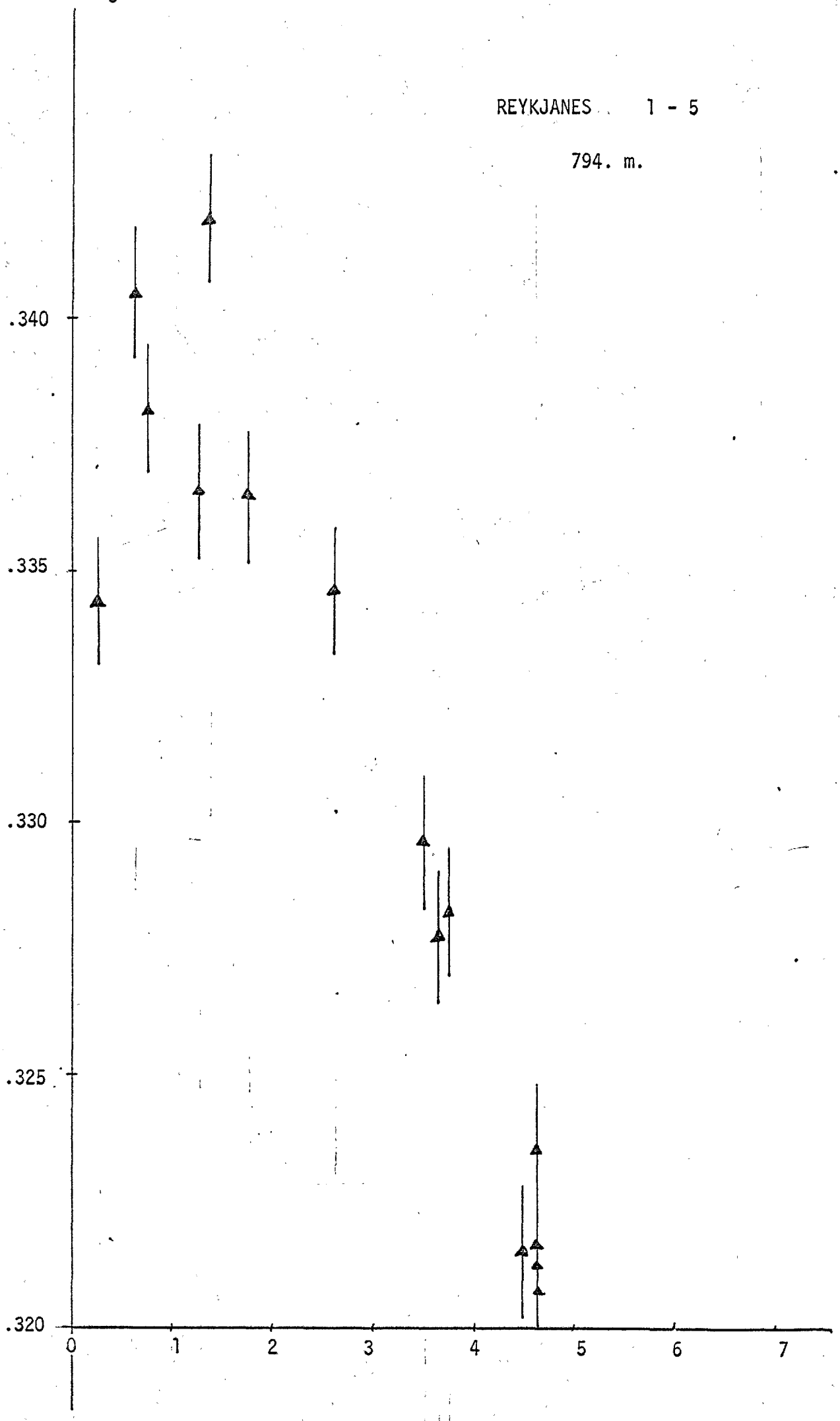
REYKJANES 1 - 4

664. m.



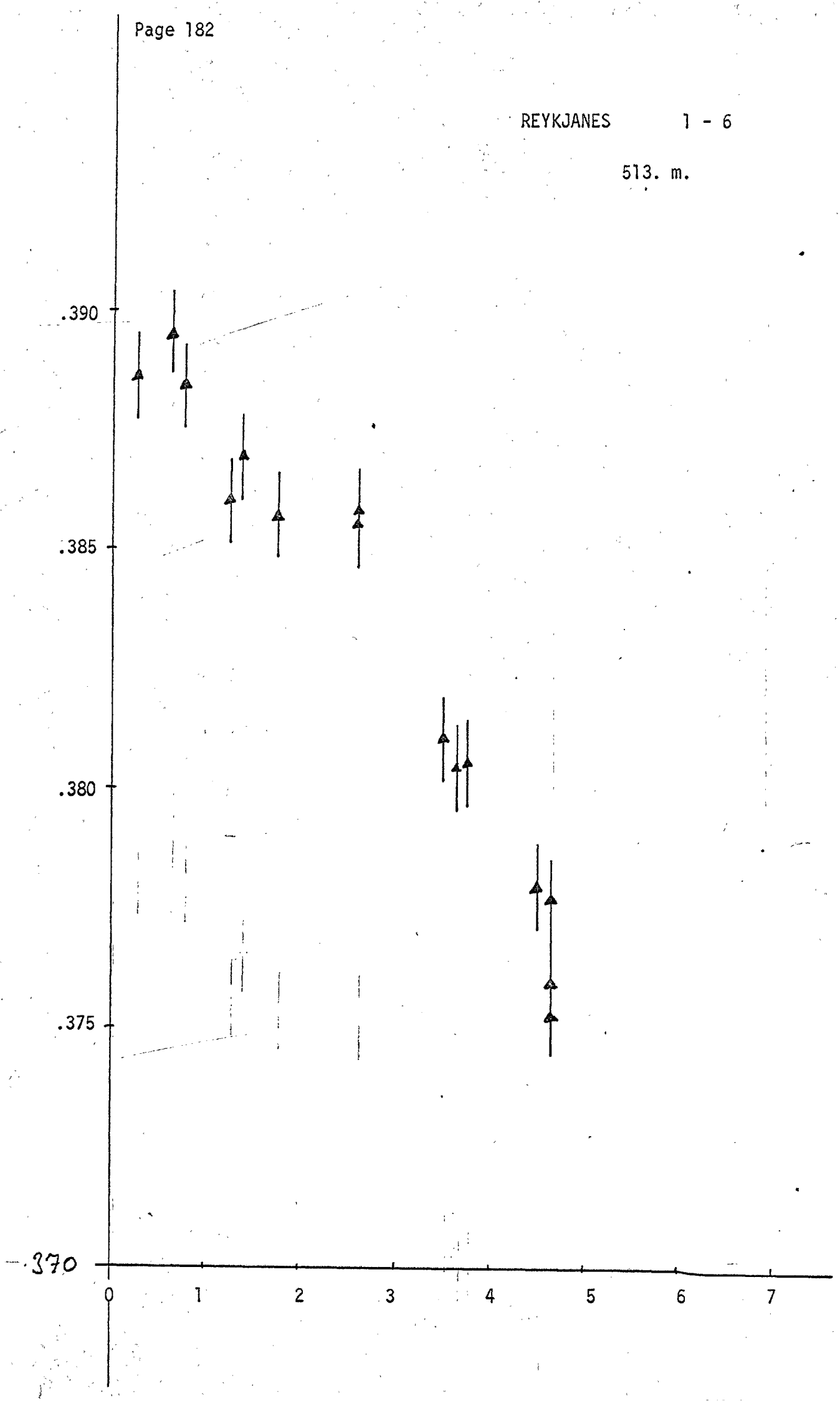
REYKJANES 1 - 5

794. m.



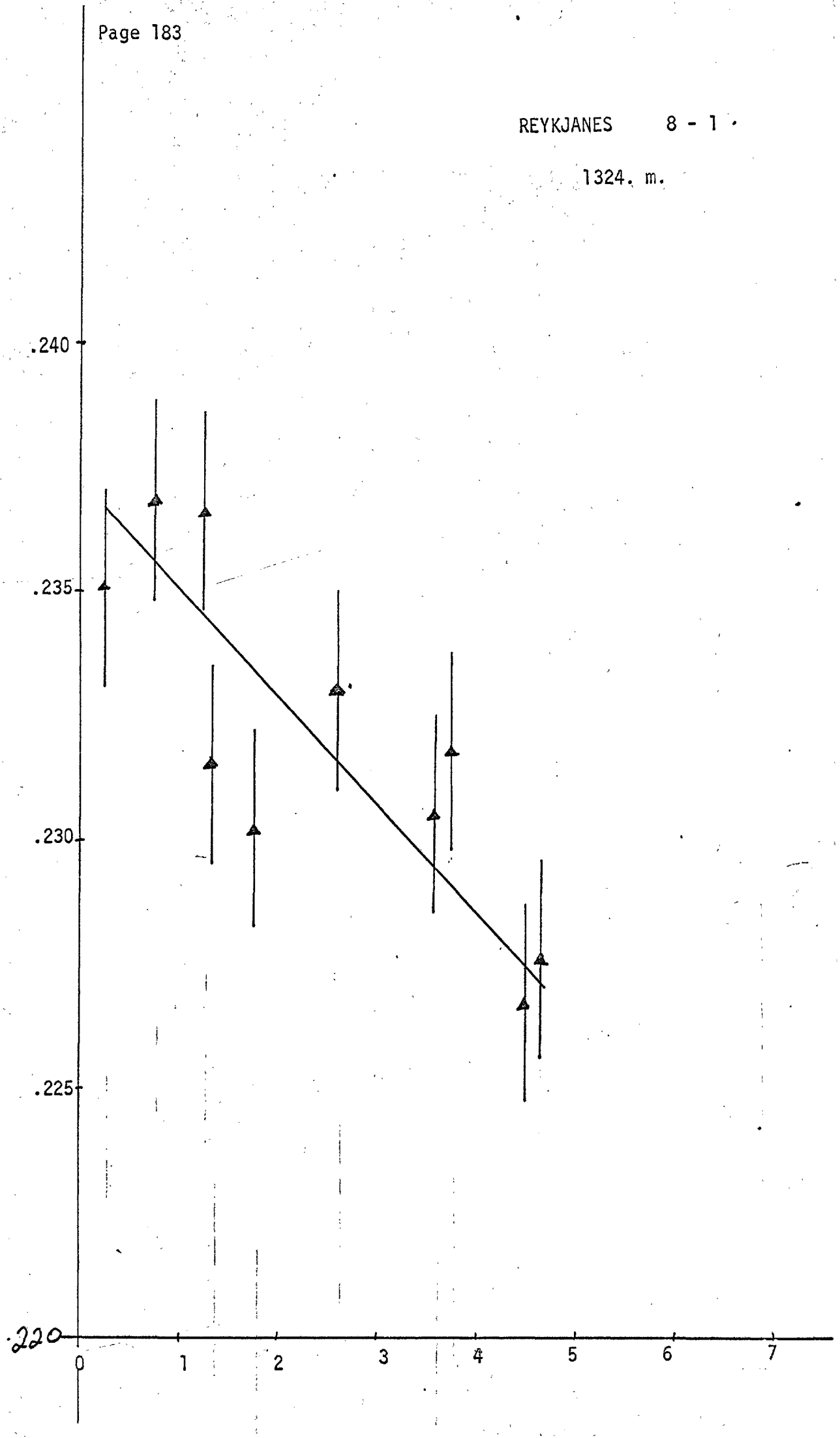
REYKJANES 1 - 6

513. m.



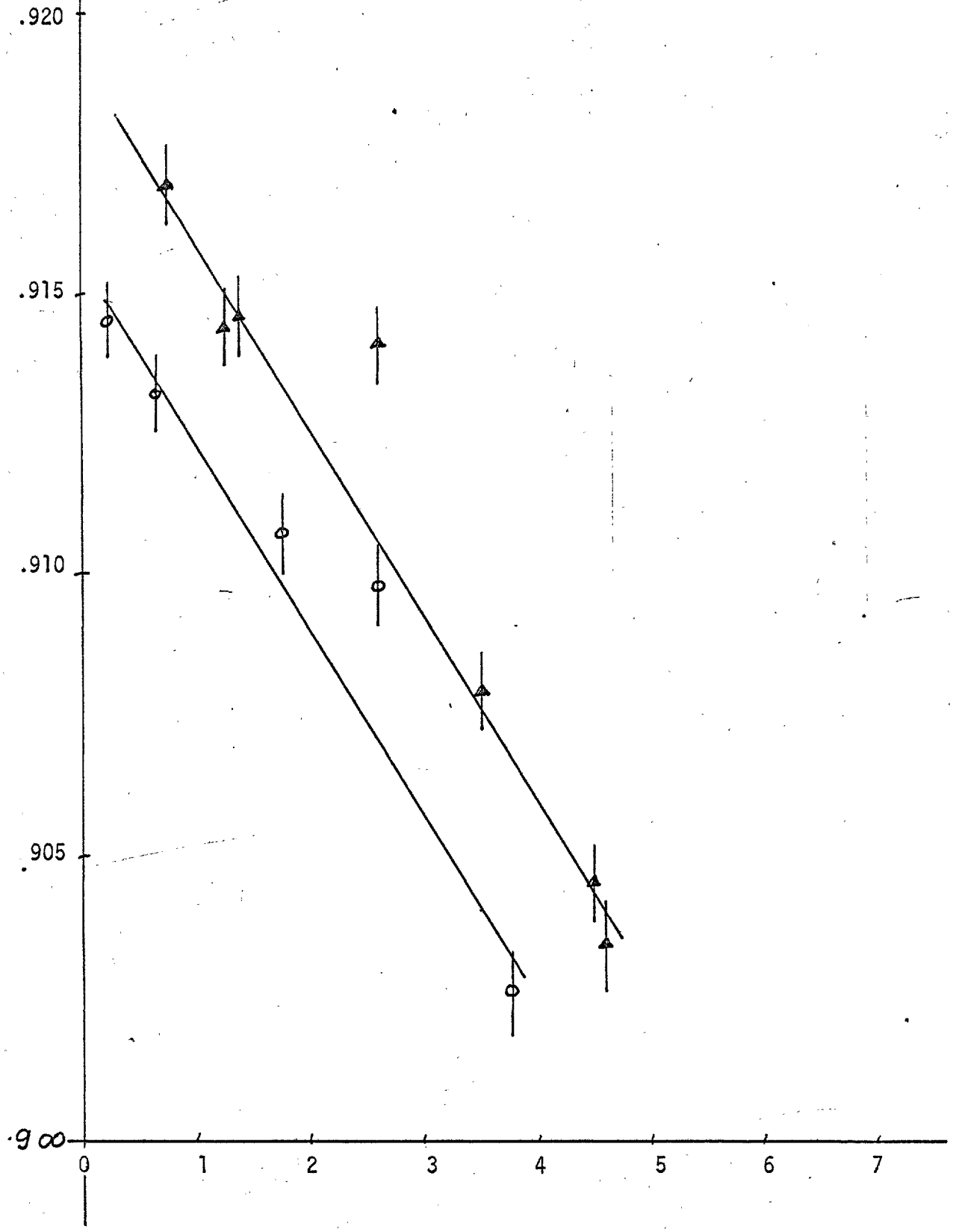
REYKJANES 8 - 1

1324. m.



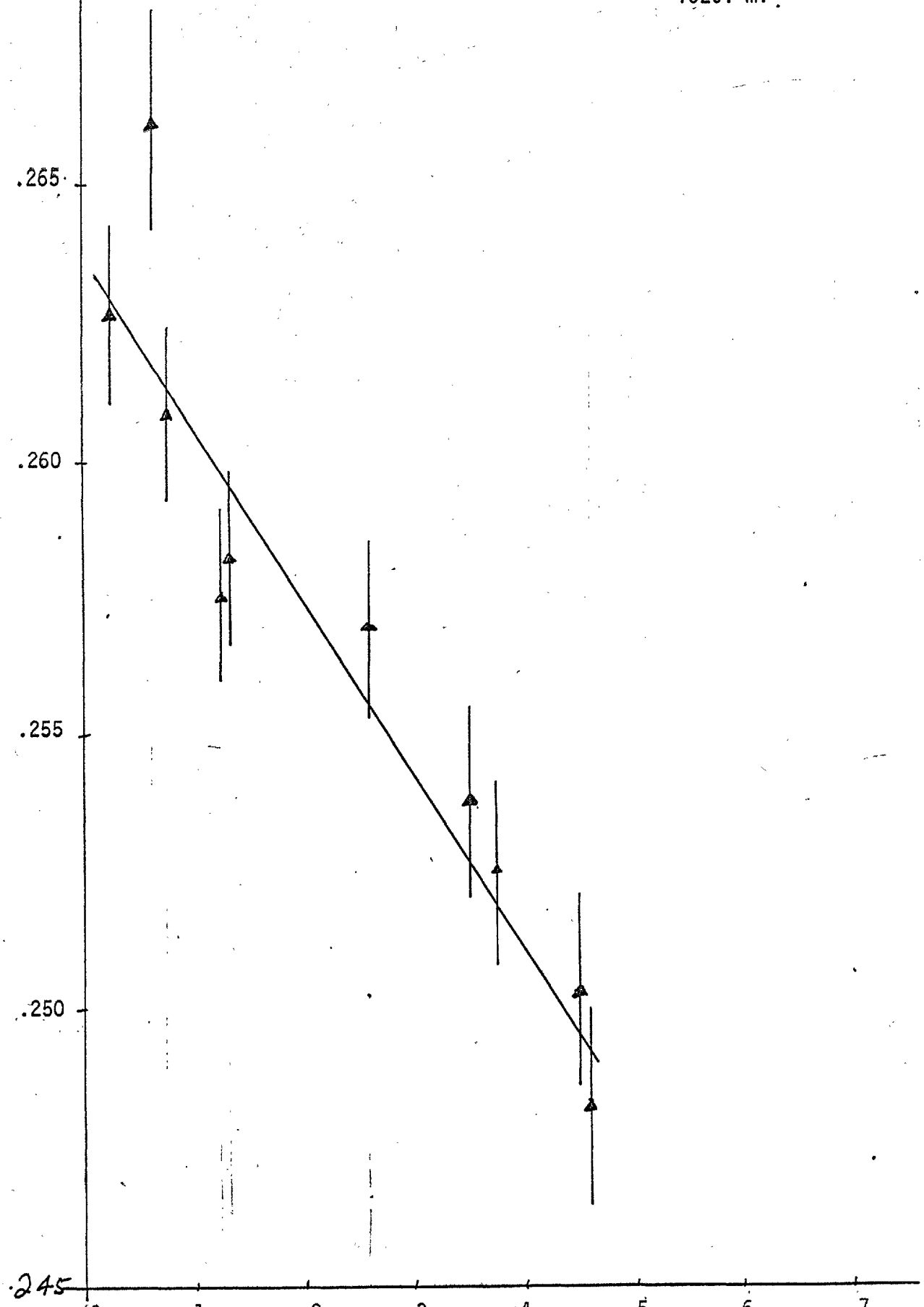
REYKJANES 2 - 3

405. m.



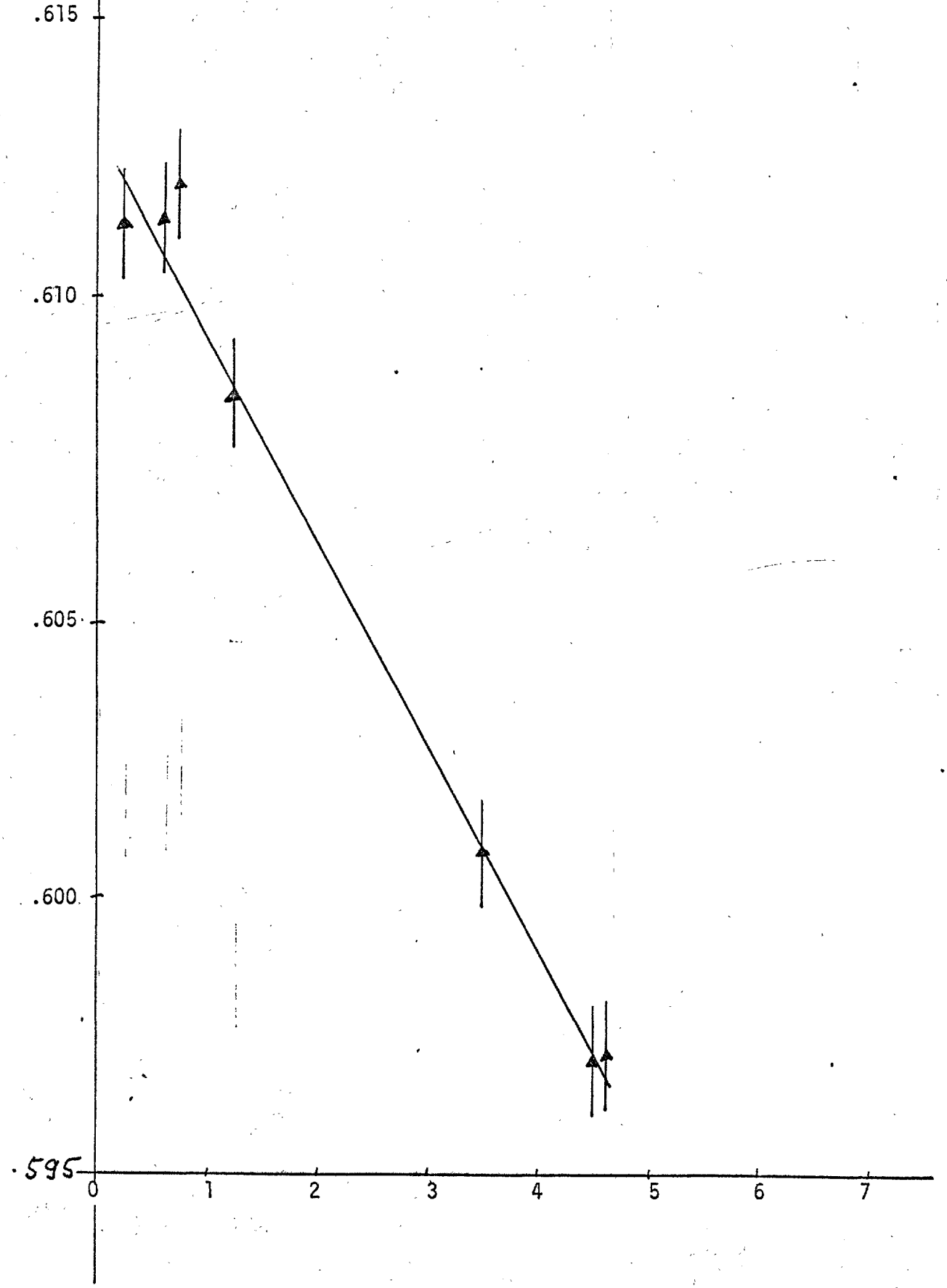
REYKJANES 2 - 7

1026. m.



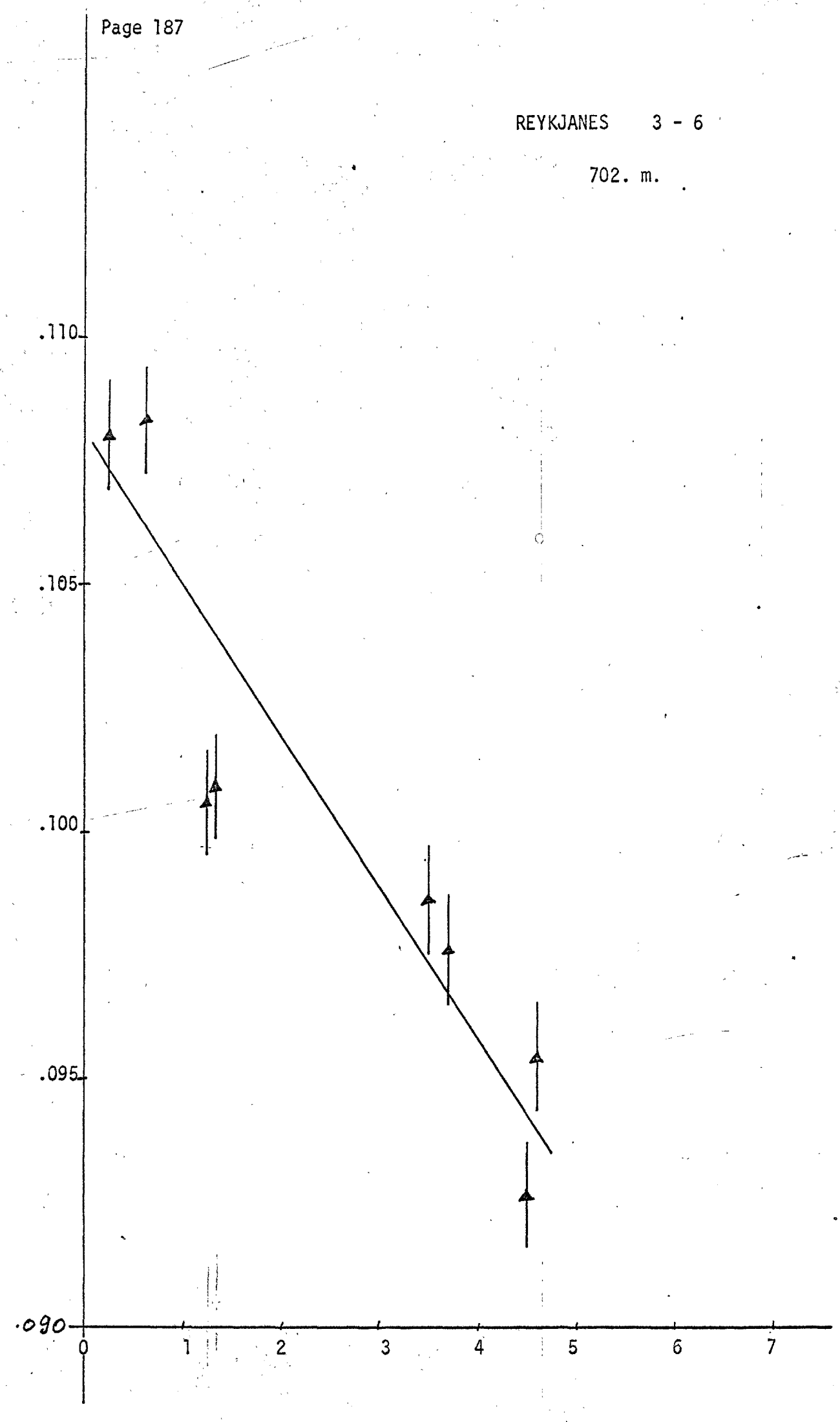
REYKJANES 3 - 4

557. m.



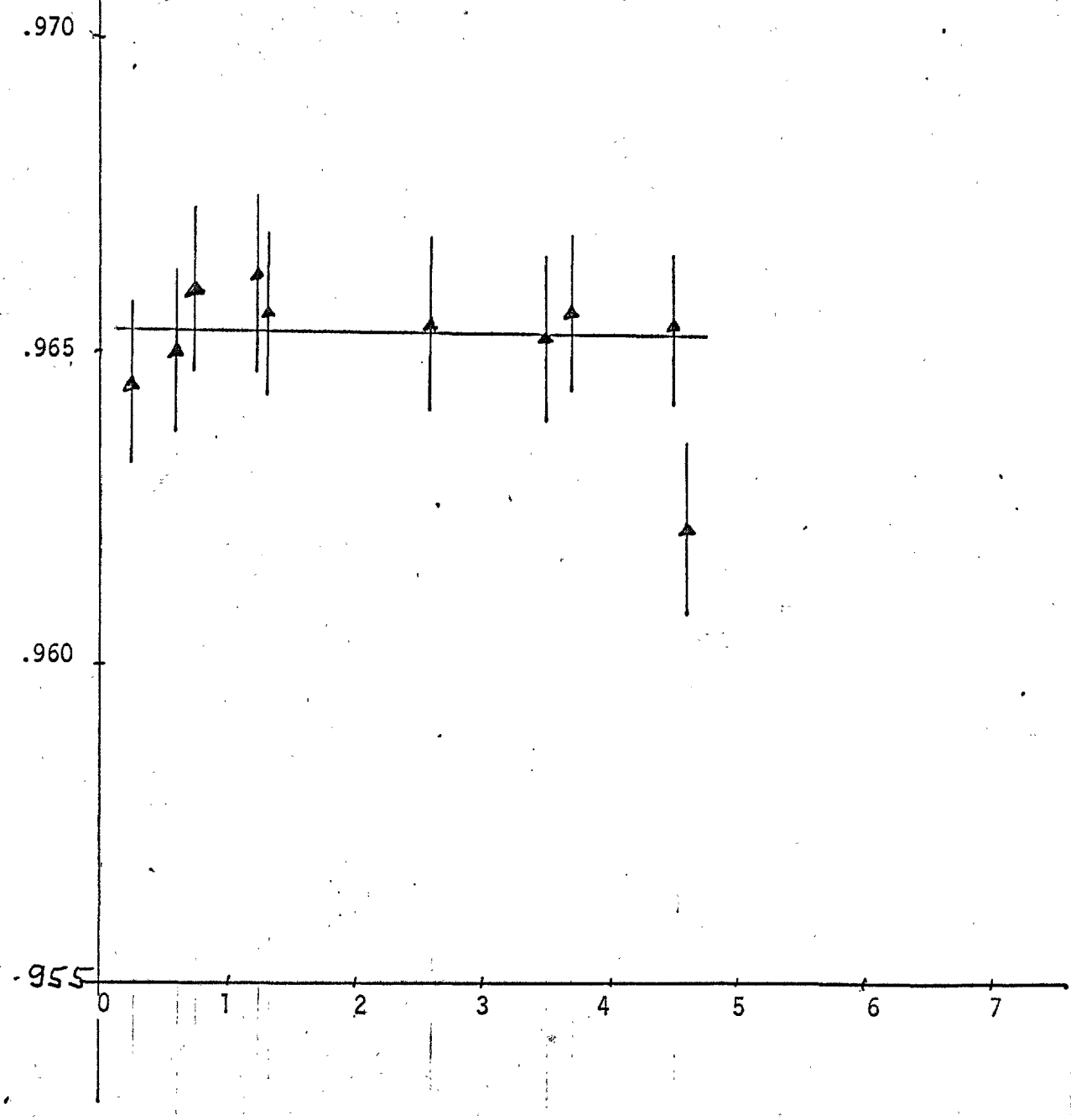
REYKJANES 3 - 6

702. m.



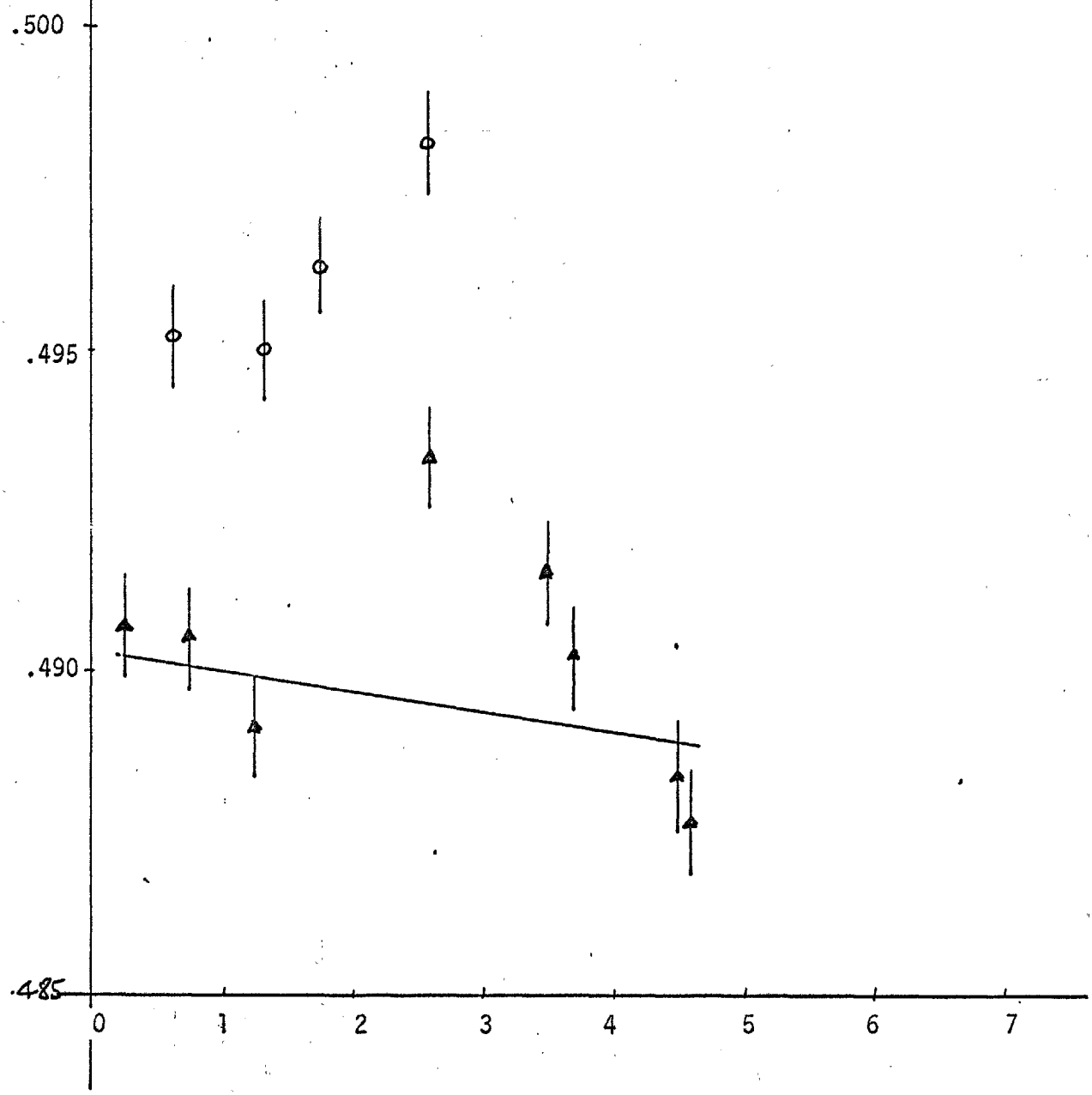
REYKJANES 3 - 7

747. m.



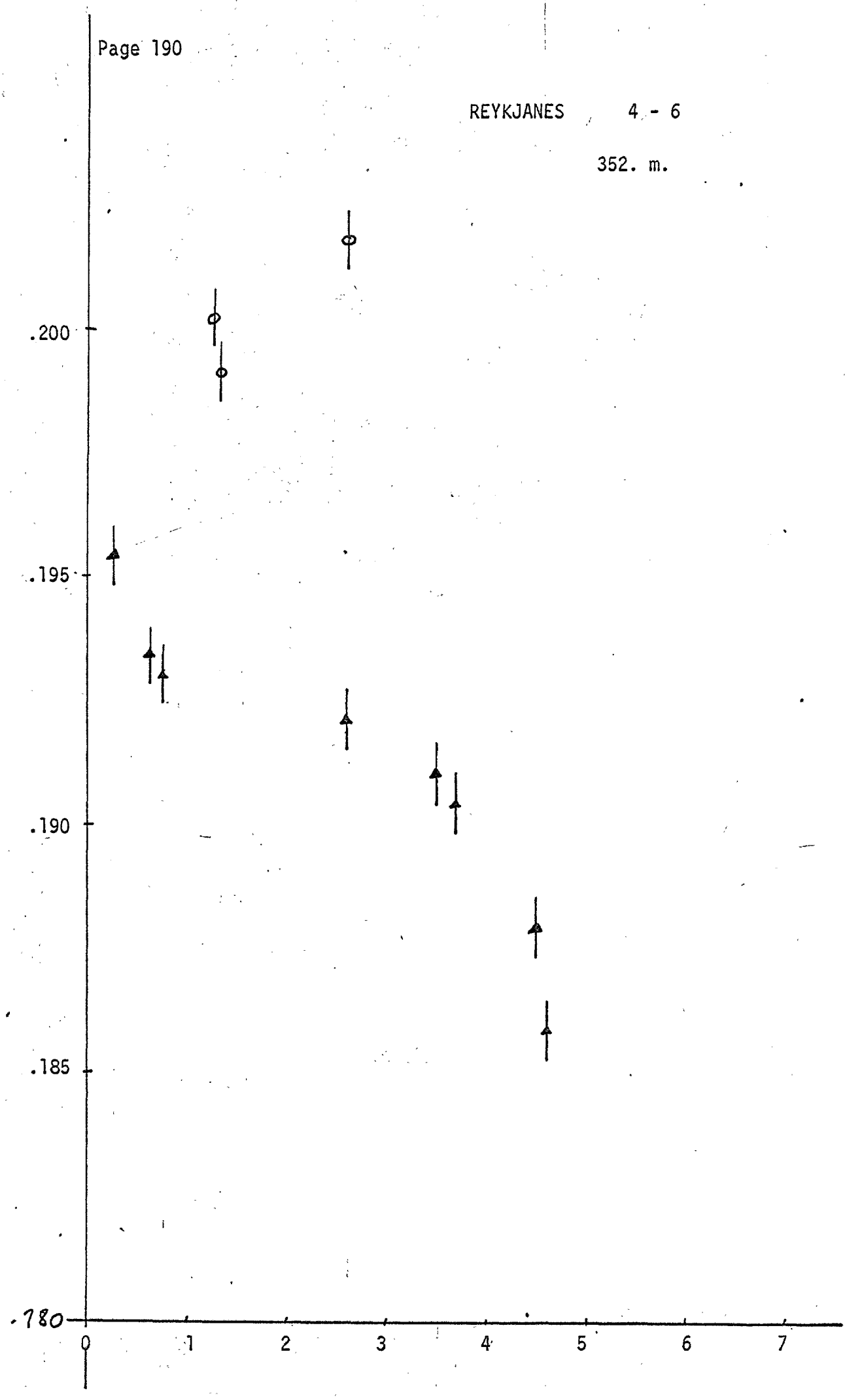
REYKJANES 4 -5

530. m.



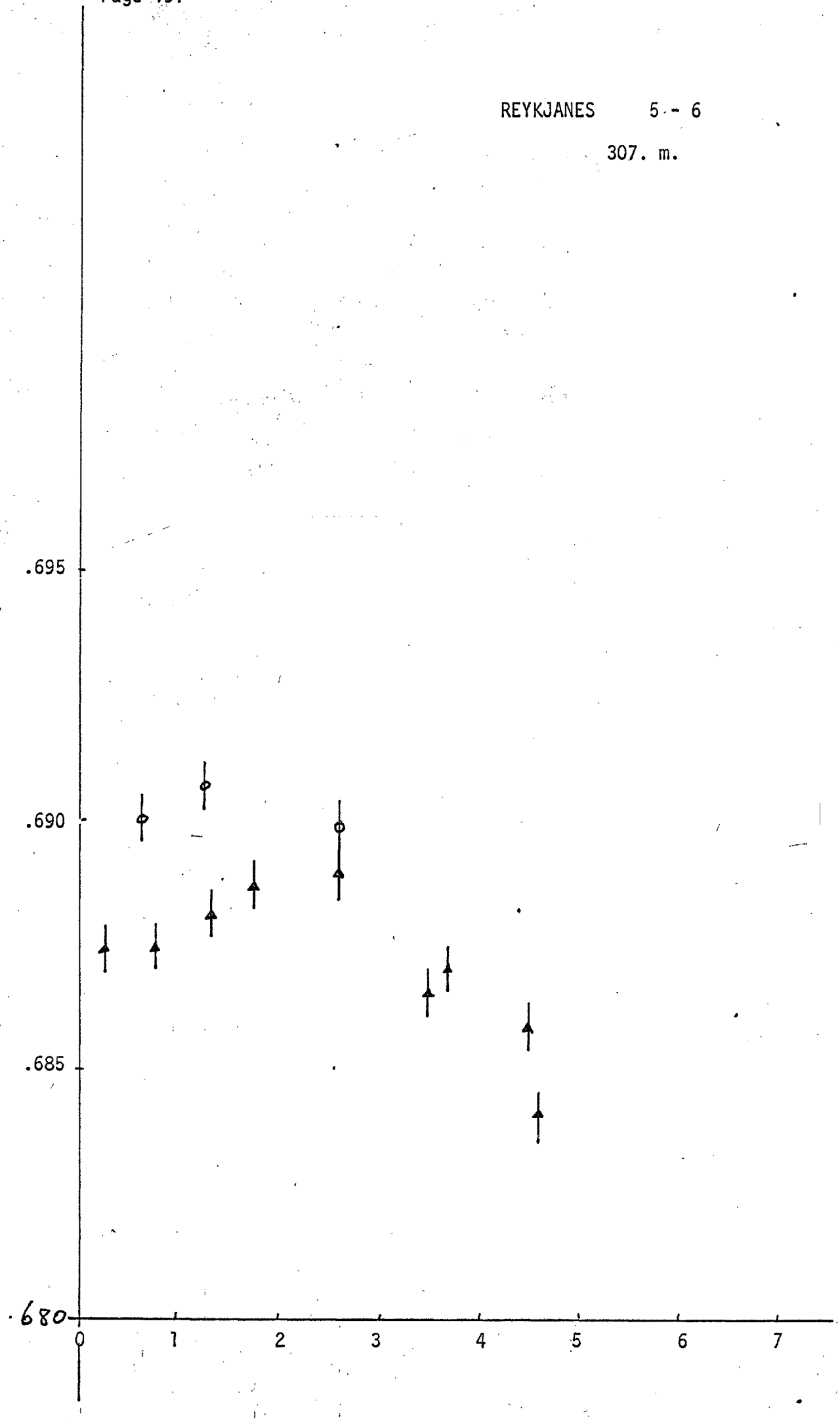
REYKJANES 4 - 6

352. m.



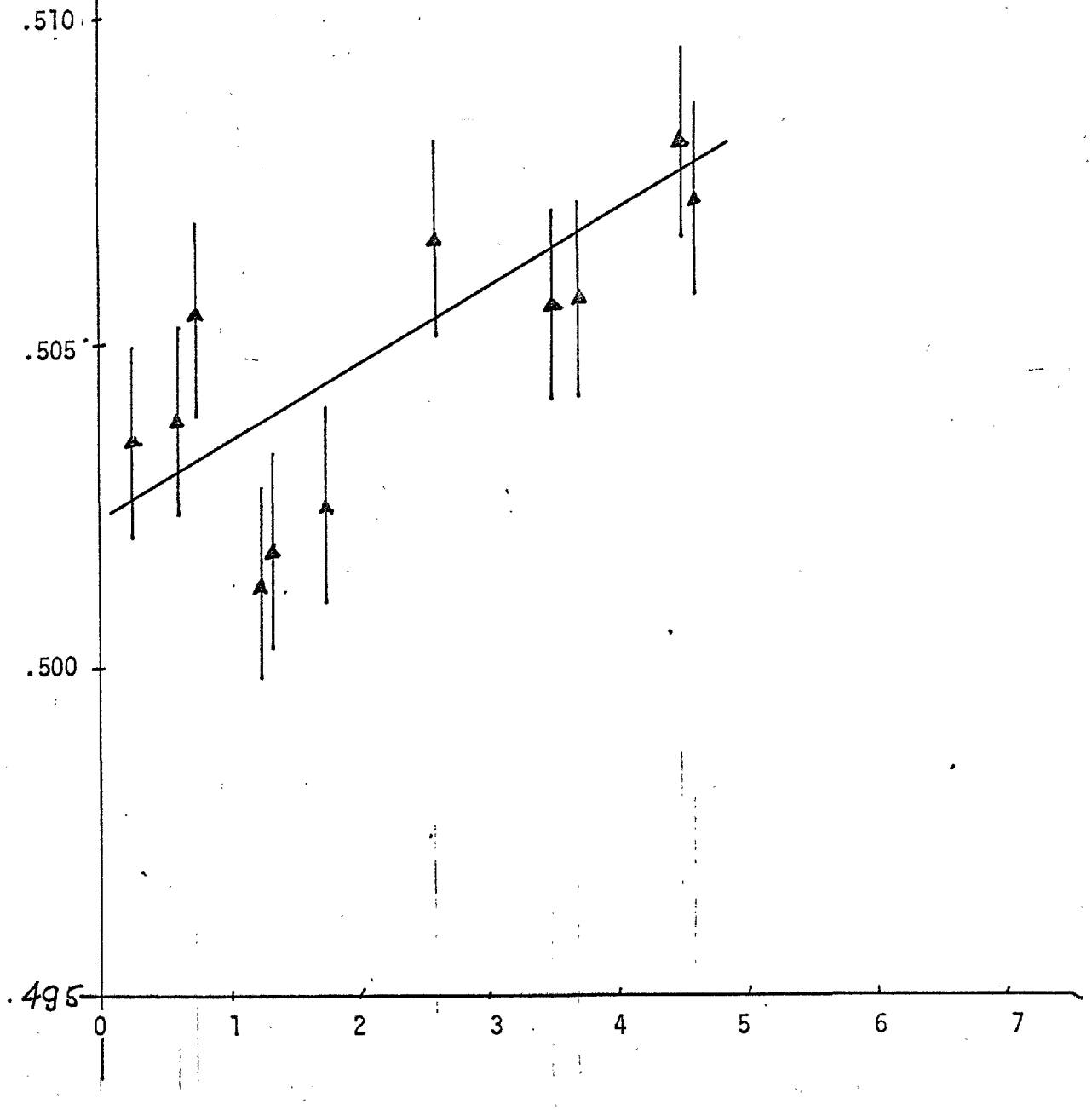
REYKJANES 5 - 6

307. m.



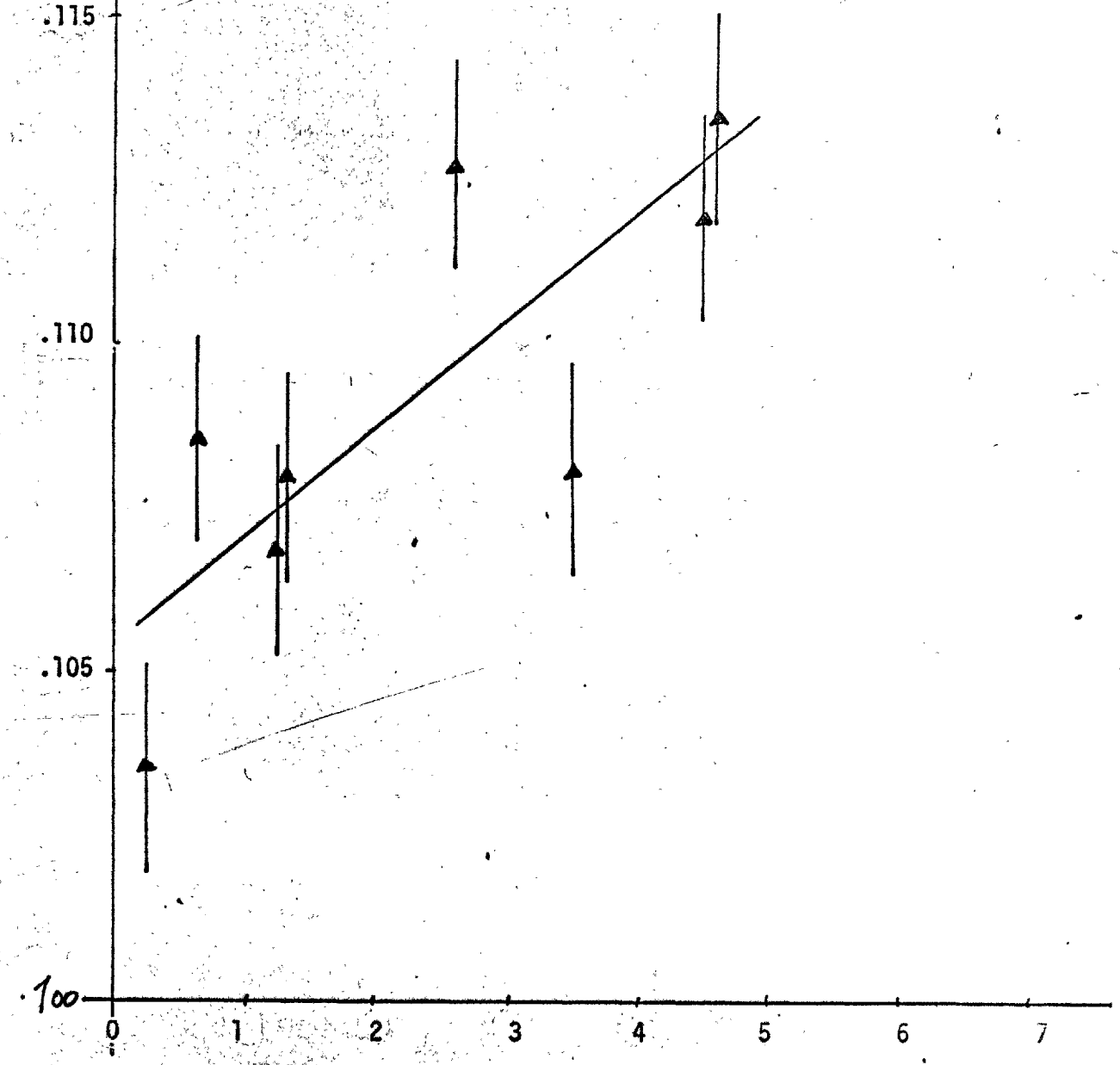
REYKJANES 5 - 8

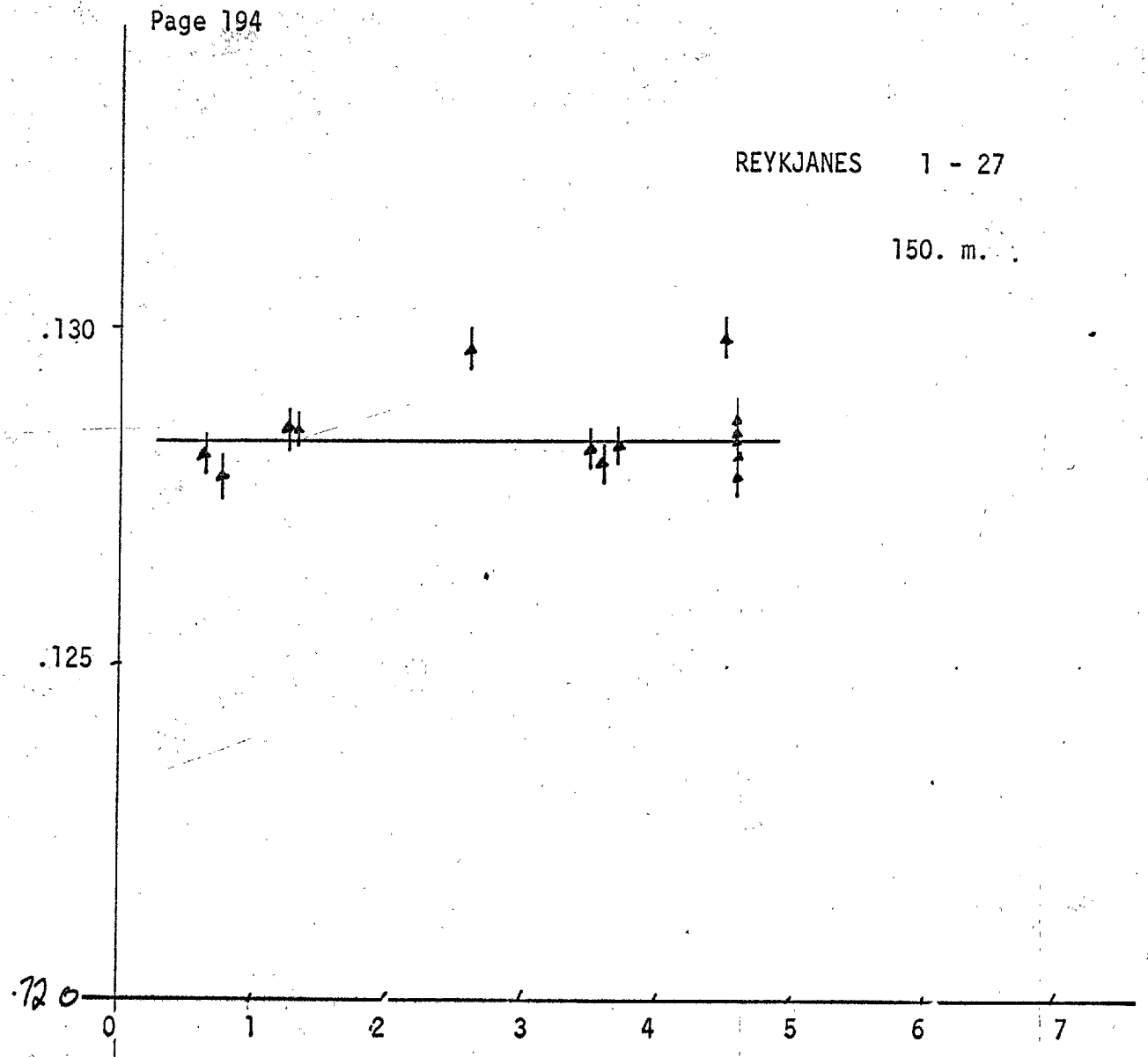
1025. m.

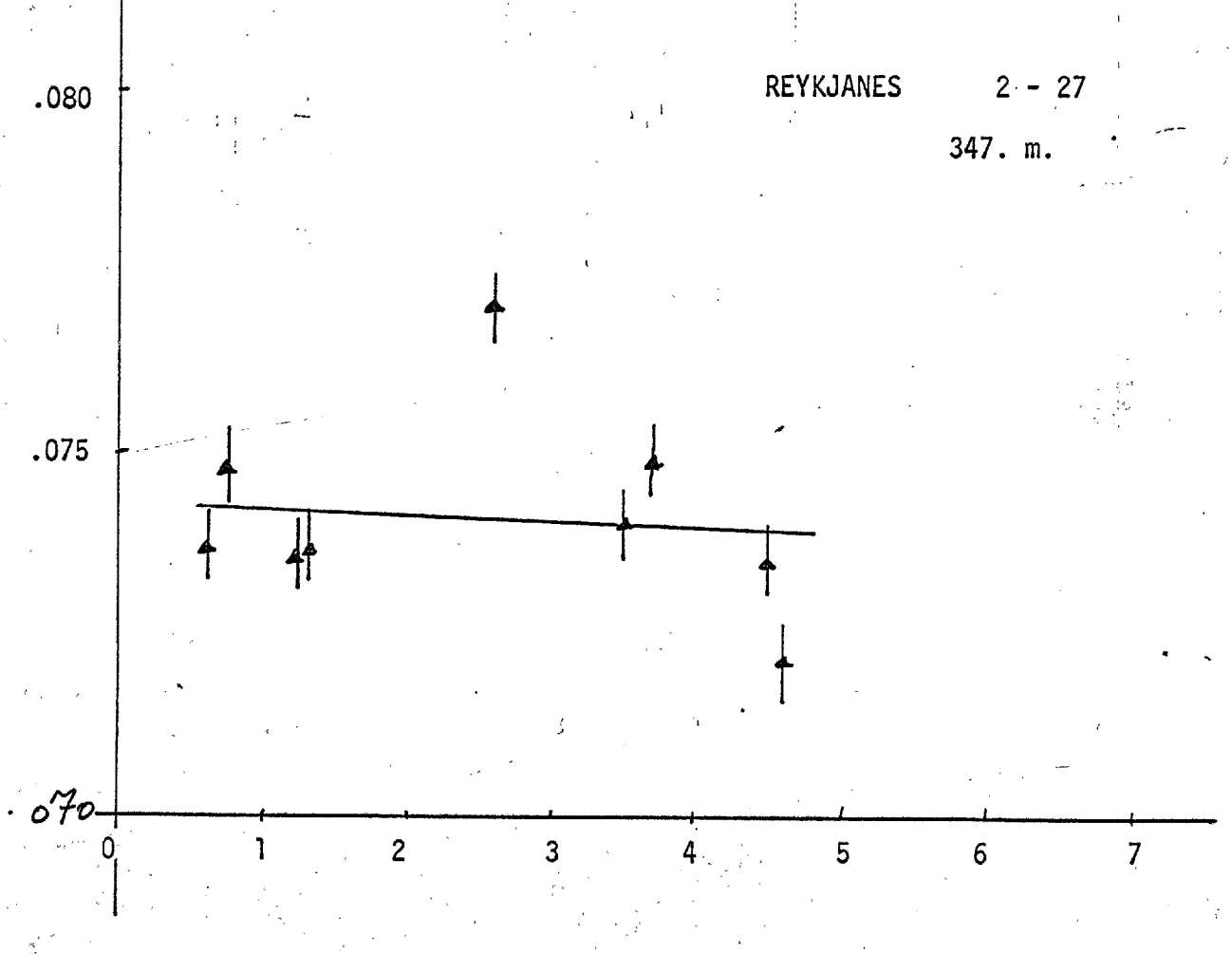


REYKJANES 6 - 8

1161. m.

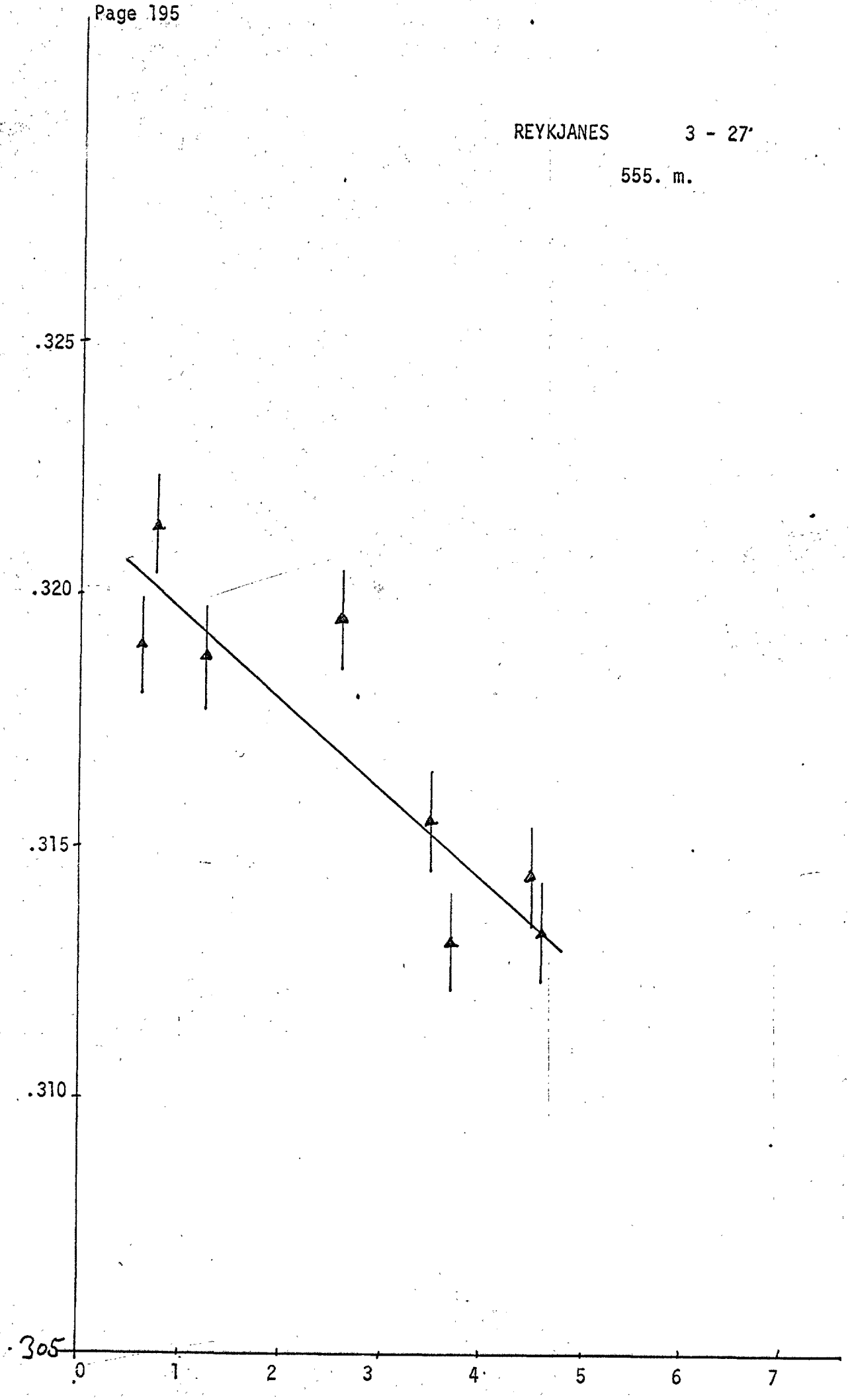



REYKJANES 1 - 27
150. m.
.130
.125
.120
0
1
2
3
4
5
6
7


REYKJANES 2 - 27
347. m.
.080
.075
.070
0
1
2
3
4
5
6
7

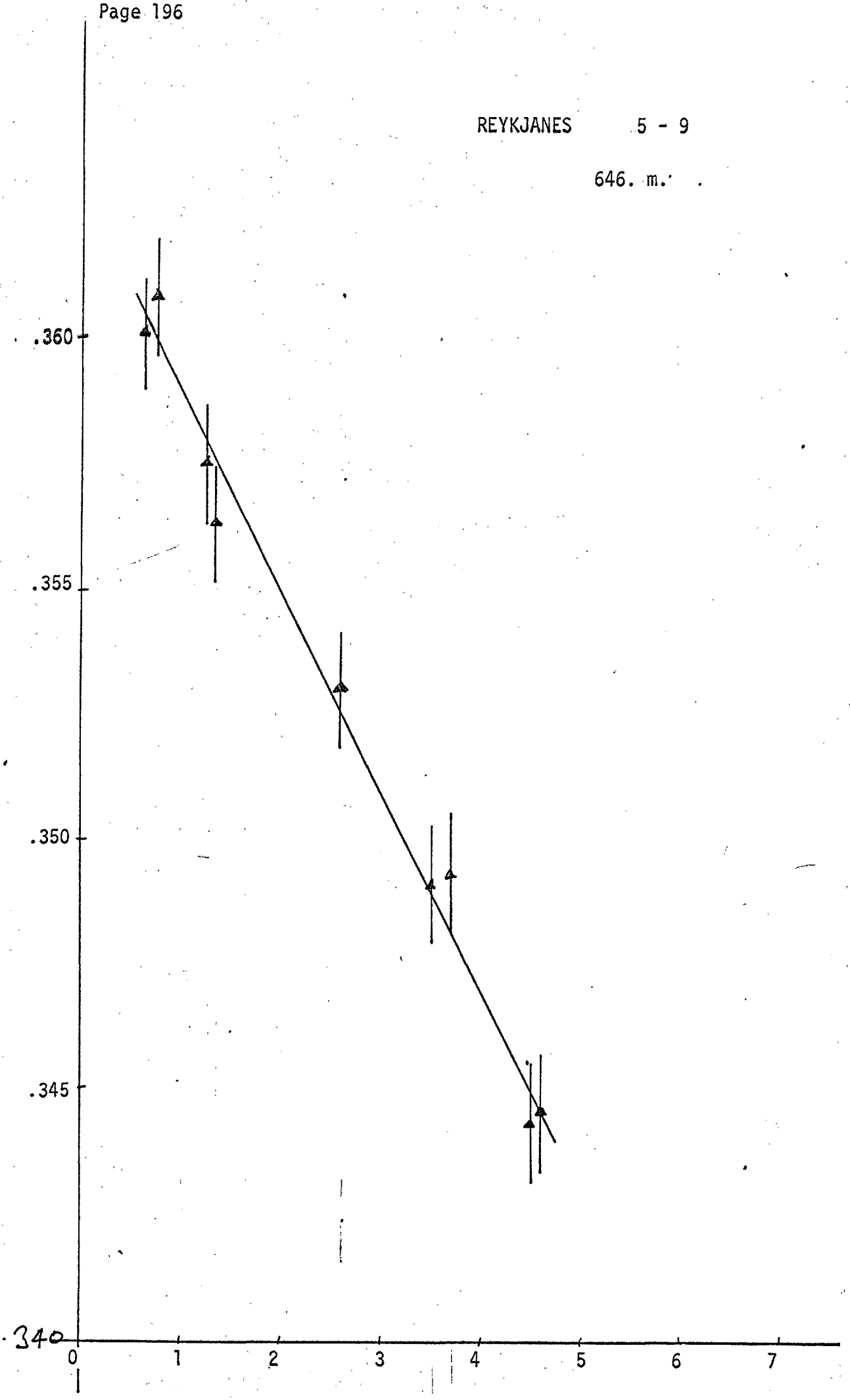
REYKJANES 3 - 27'

555. m.



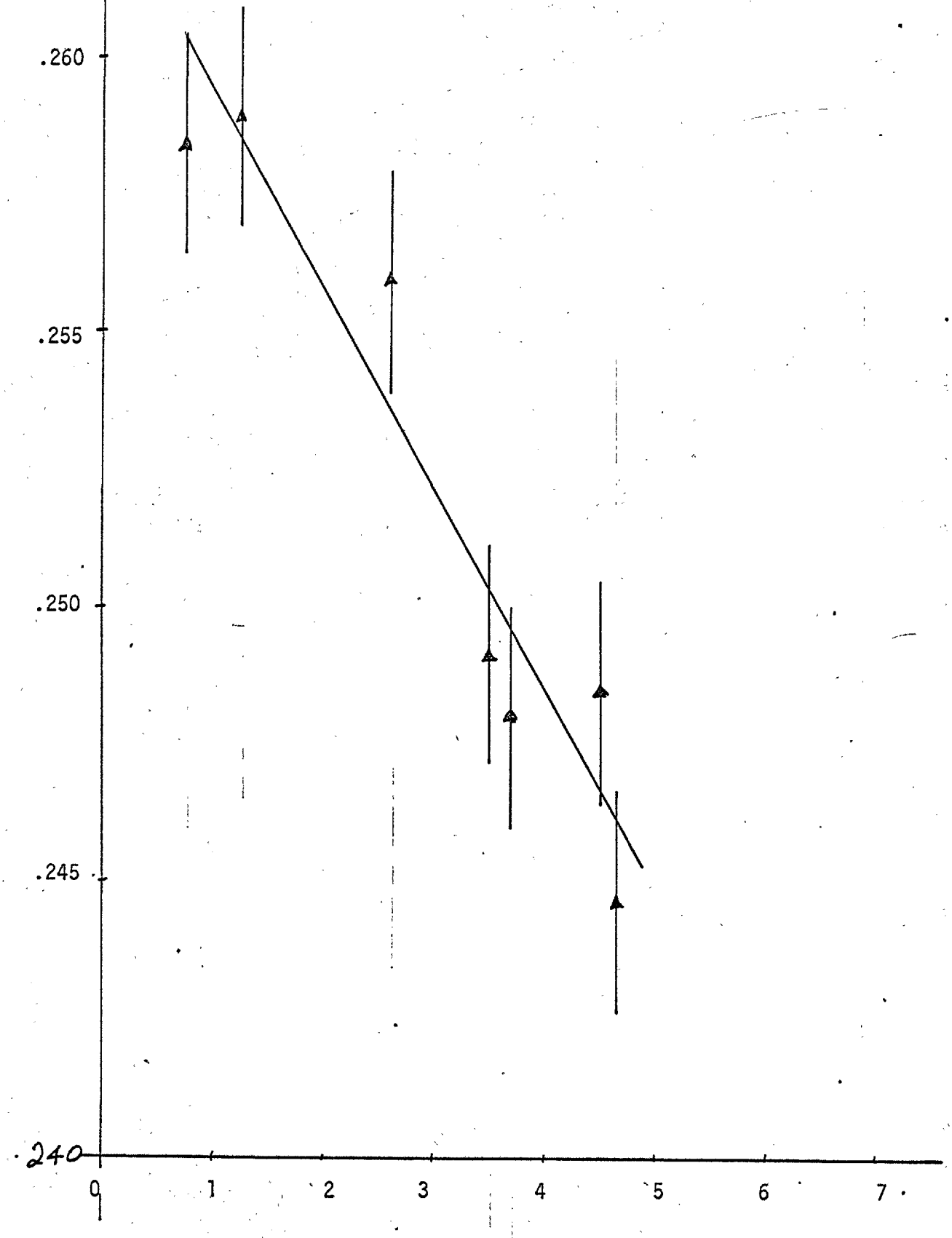
REYKJANES 5 - 9

646. m.



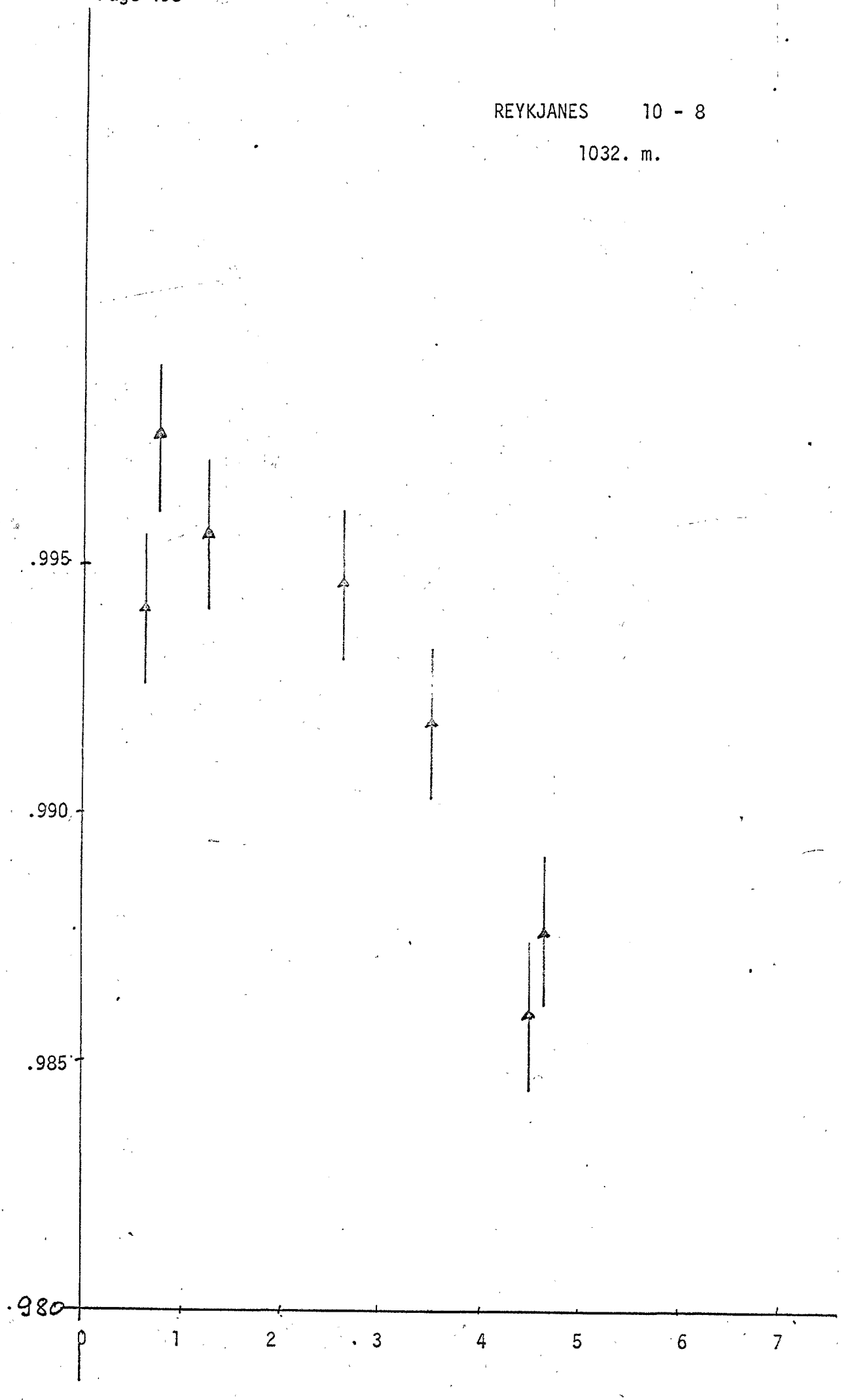
REYKJANES 8 - 9

1330. m.



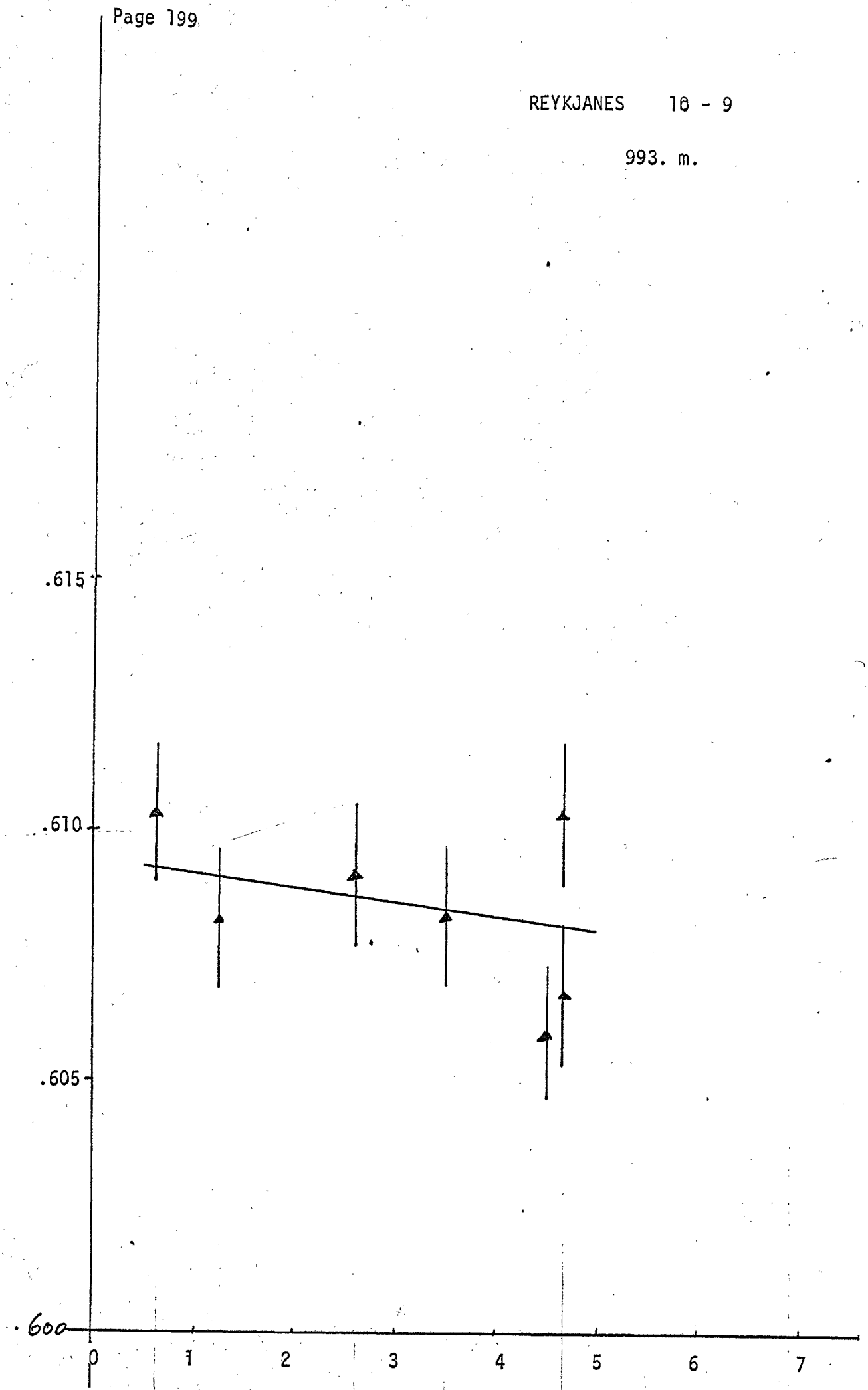
REYKJANES 10 - 8

1032. m.



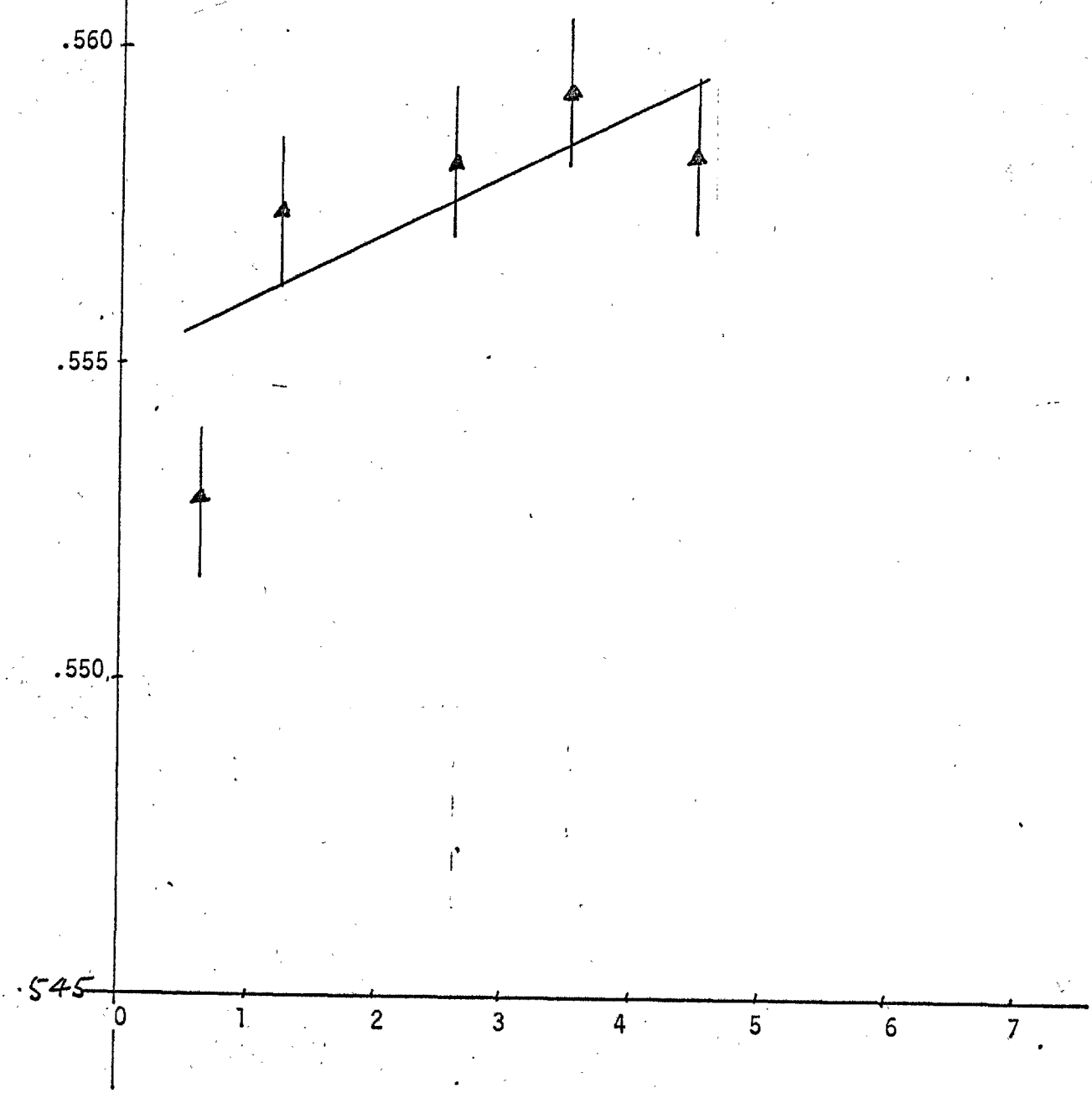
REYKJANES 16 - 9

993. m.



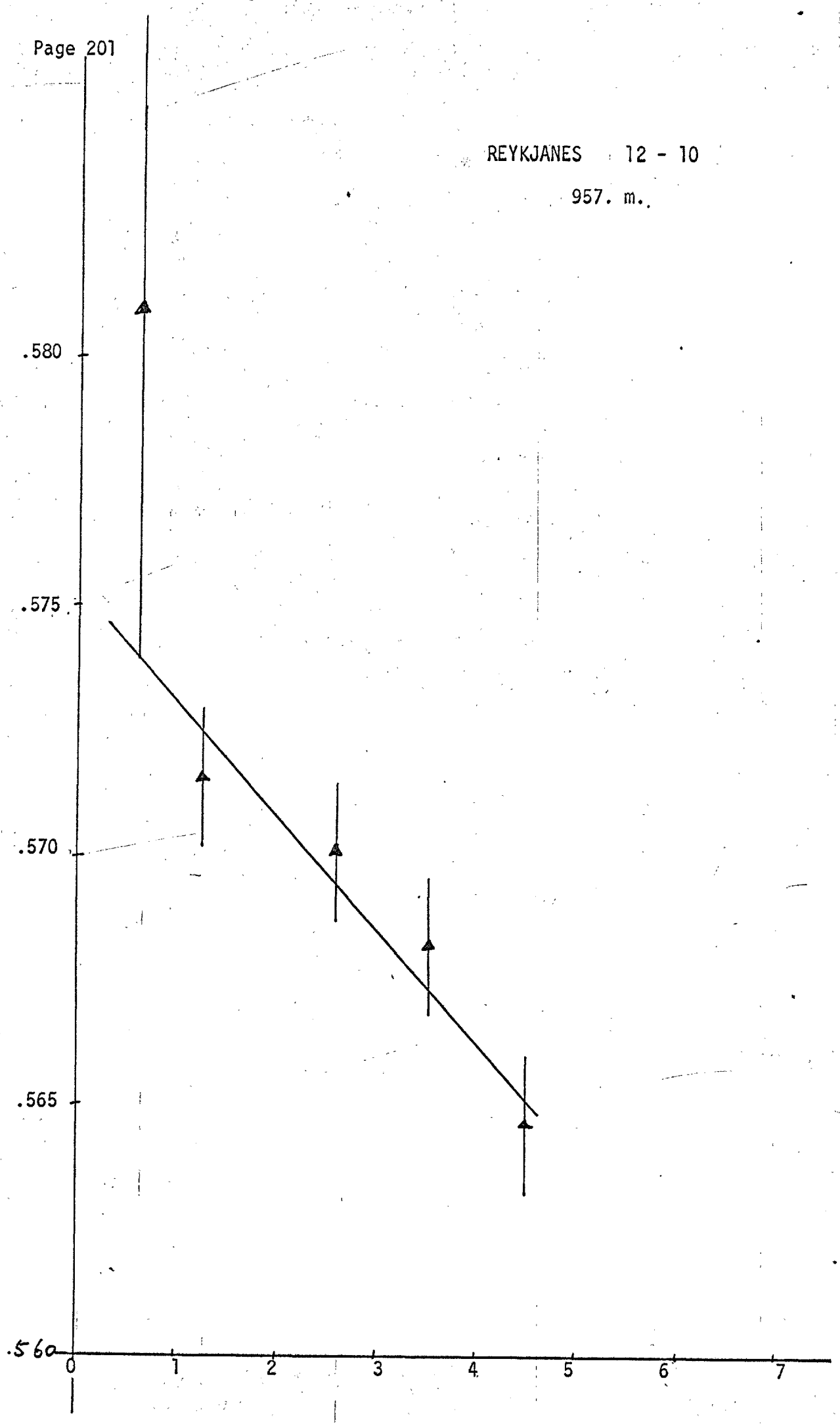
REYKJANES 10 - 11

781. m.



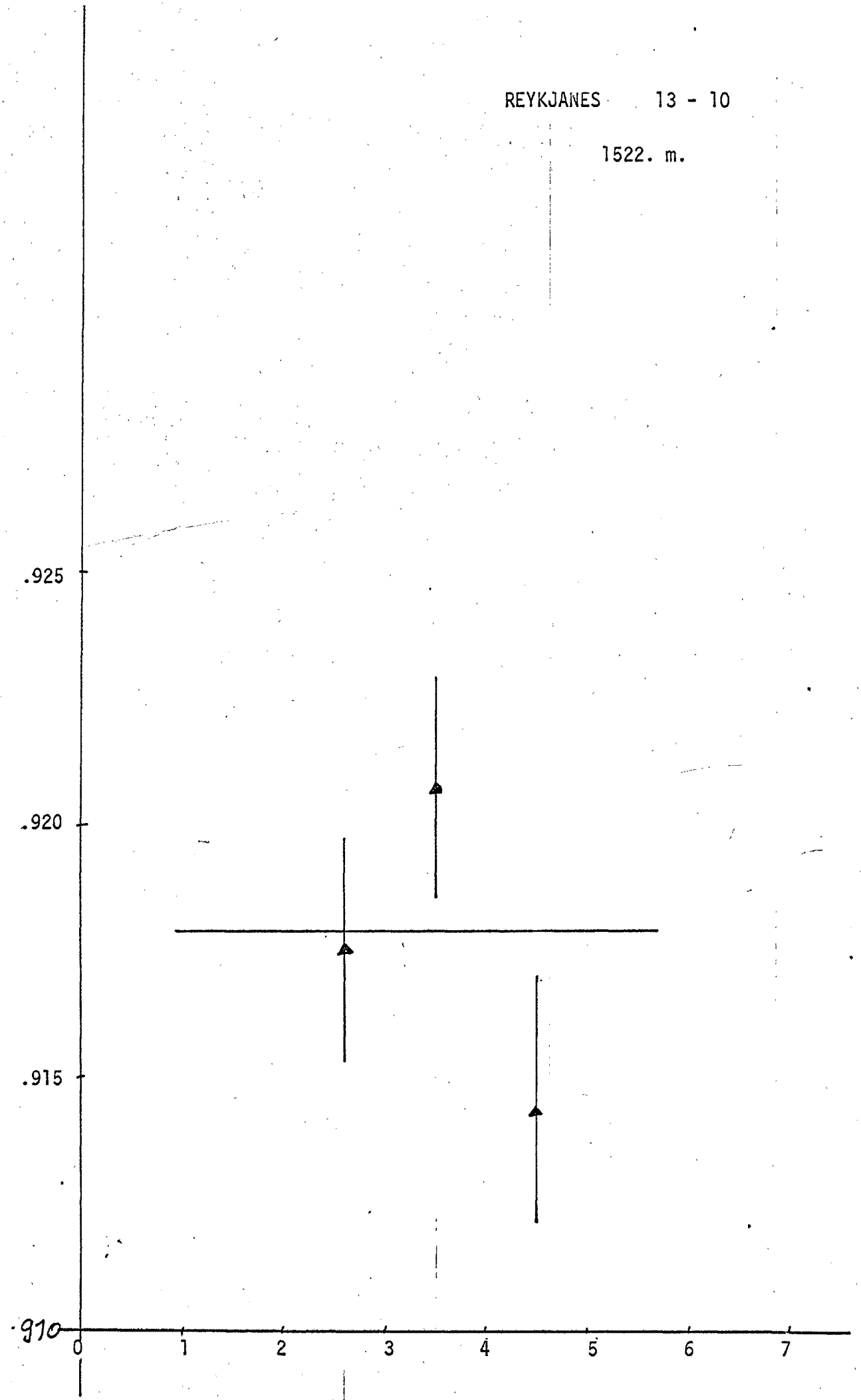
REYKJANES 12 - 10

957. m.



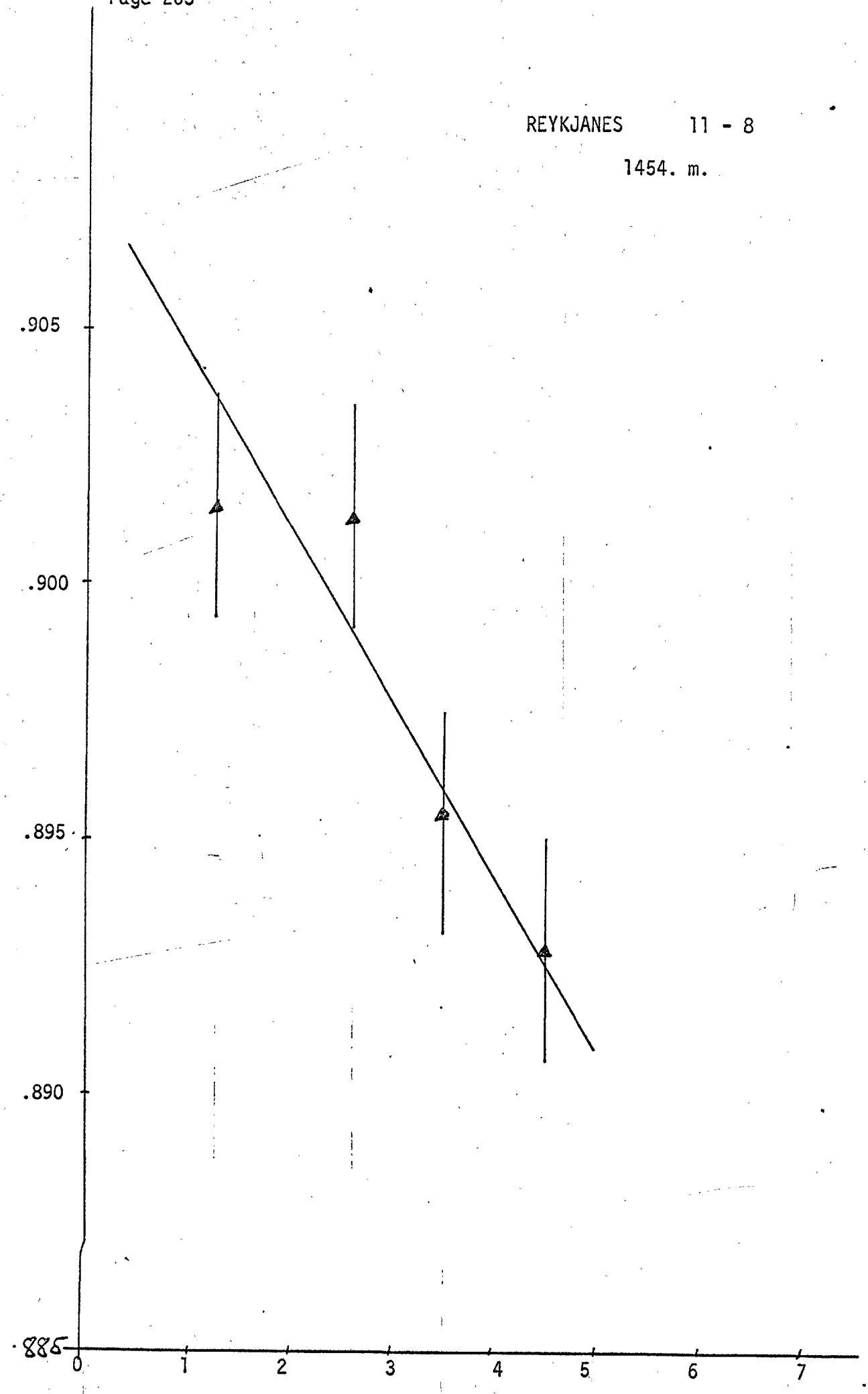
REYKJANES 13 - 10

1522. m.



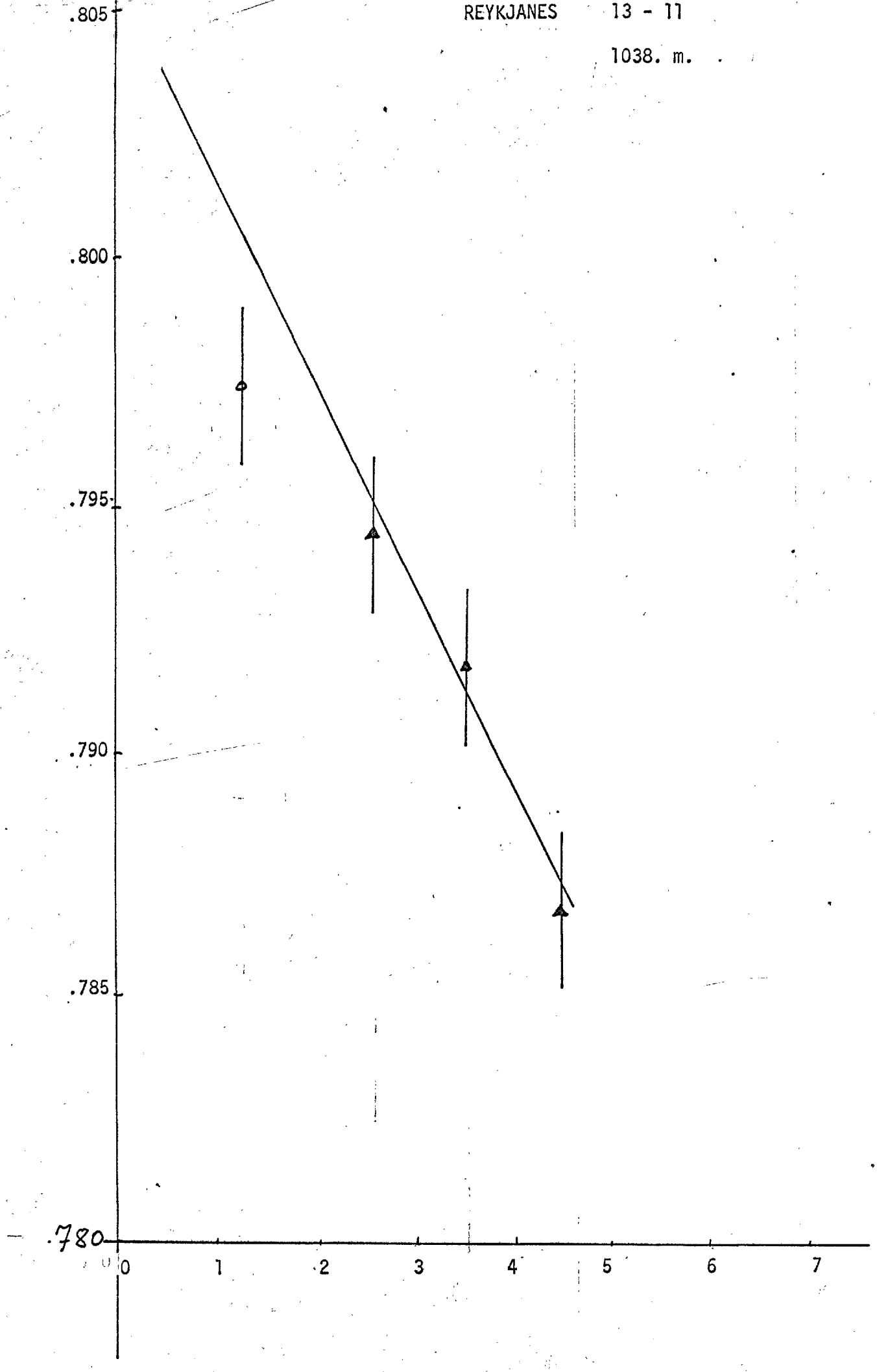
REYKJANES 11 - 8

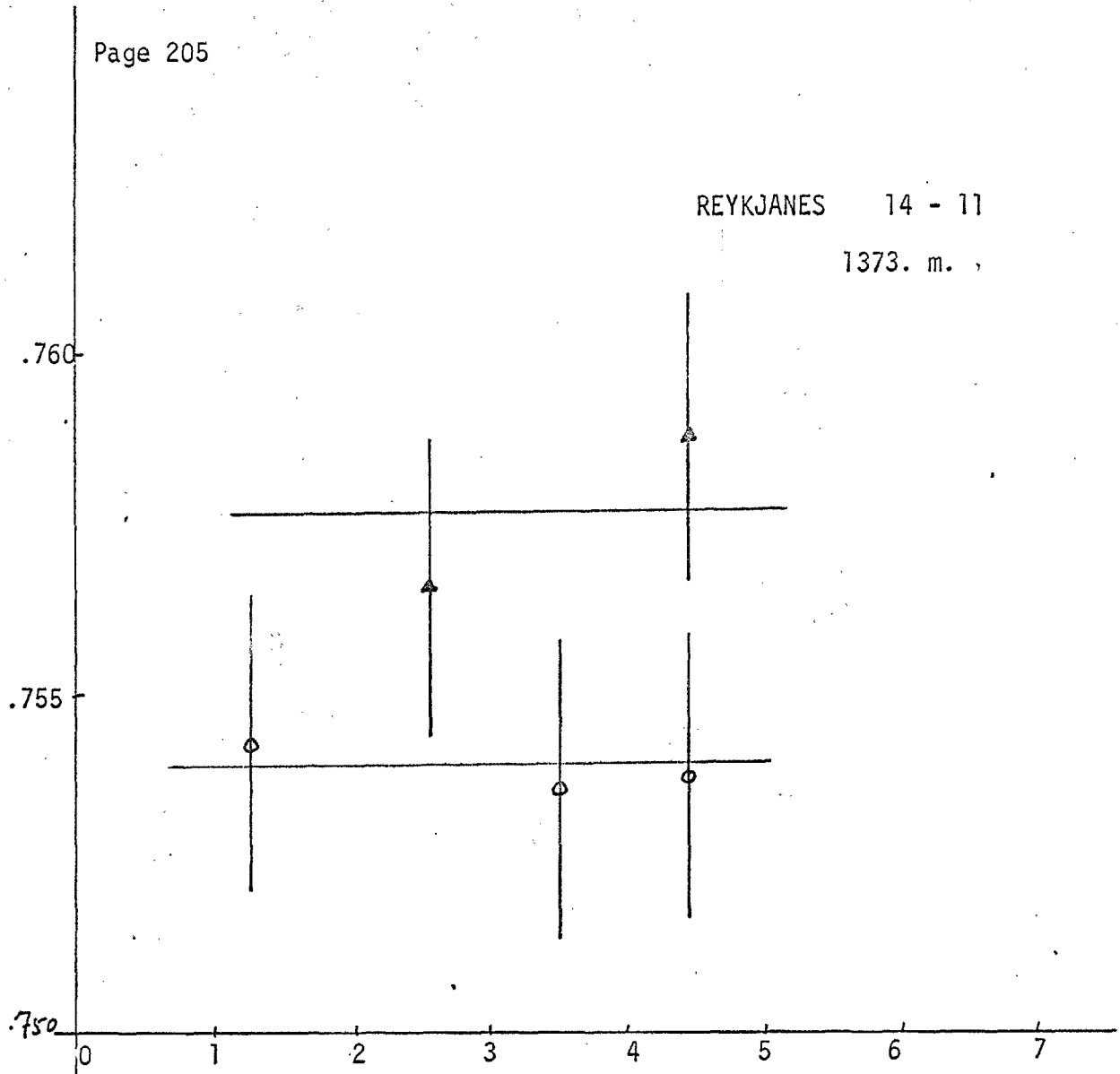
1454. m.

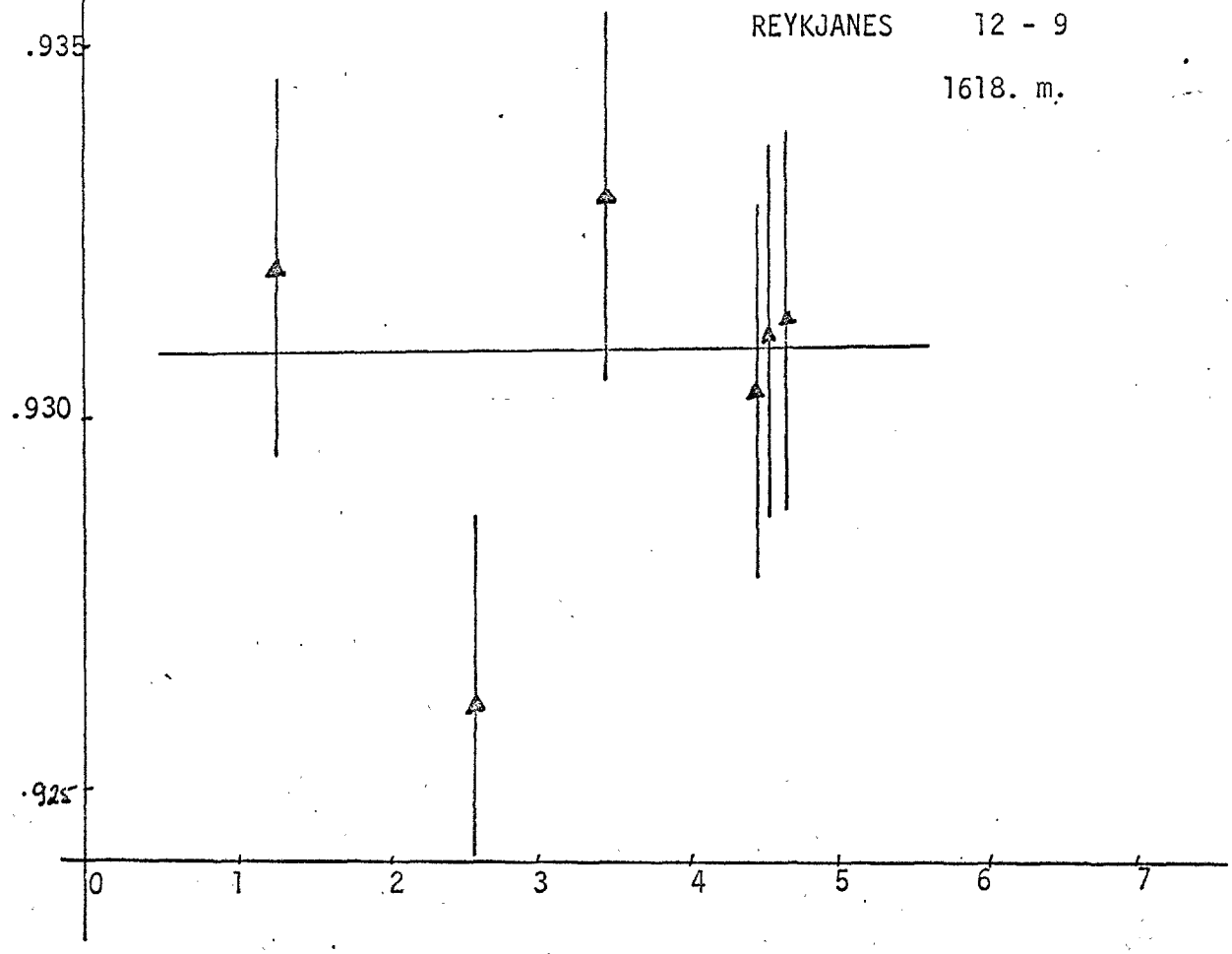


REYKJANES 13 - 11

1038. m.

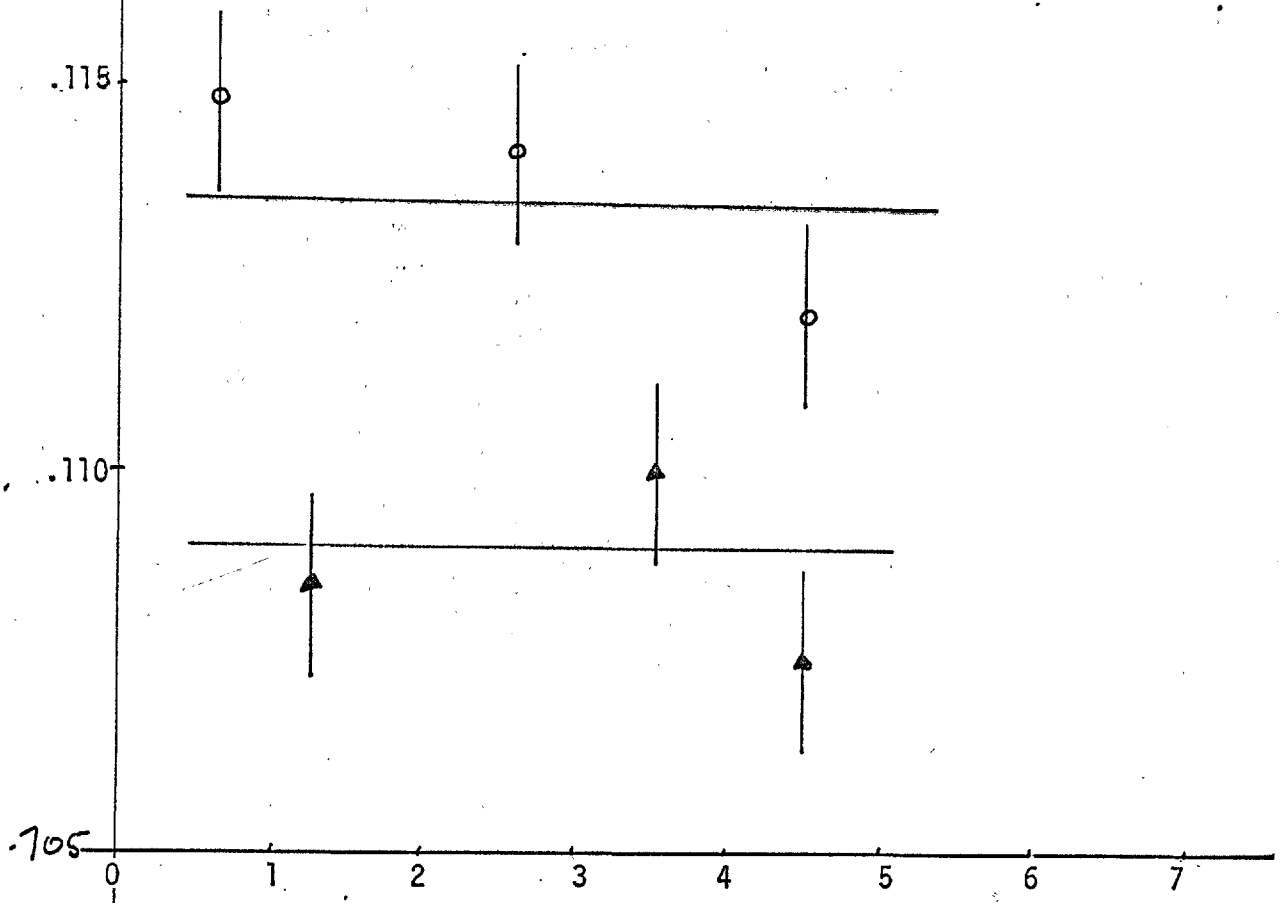



REYKJANES 14 - 11
1373. m.
.760
.755
.750
0
1
2
3
4
5
6
7


REYKJANES 12 - 9
1618. m.
.935
.930
.925
0
1
2
3
4
5
6
7

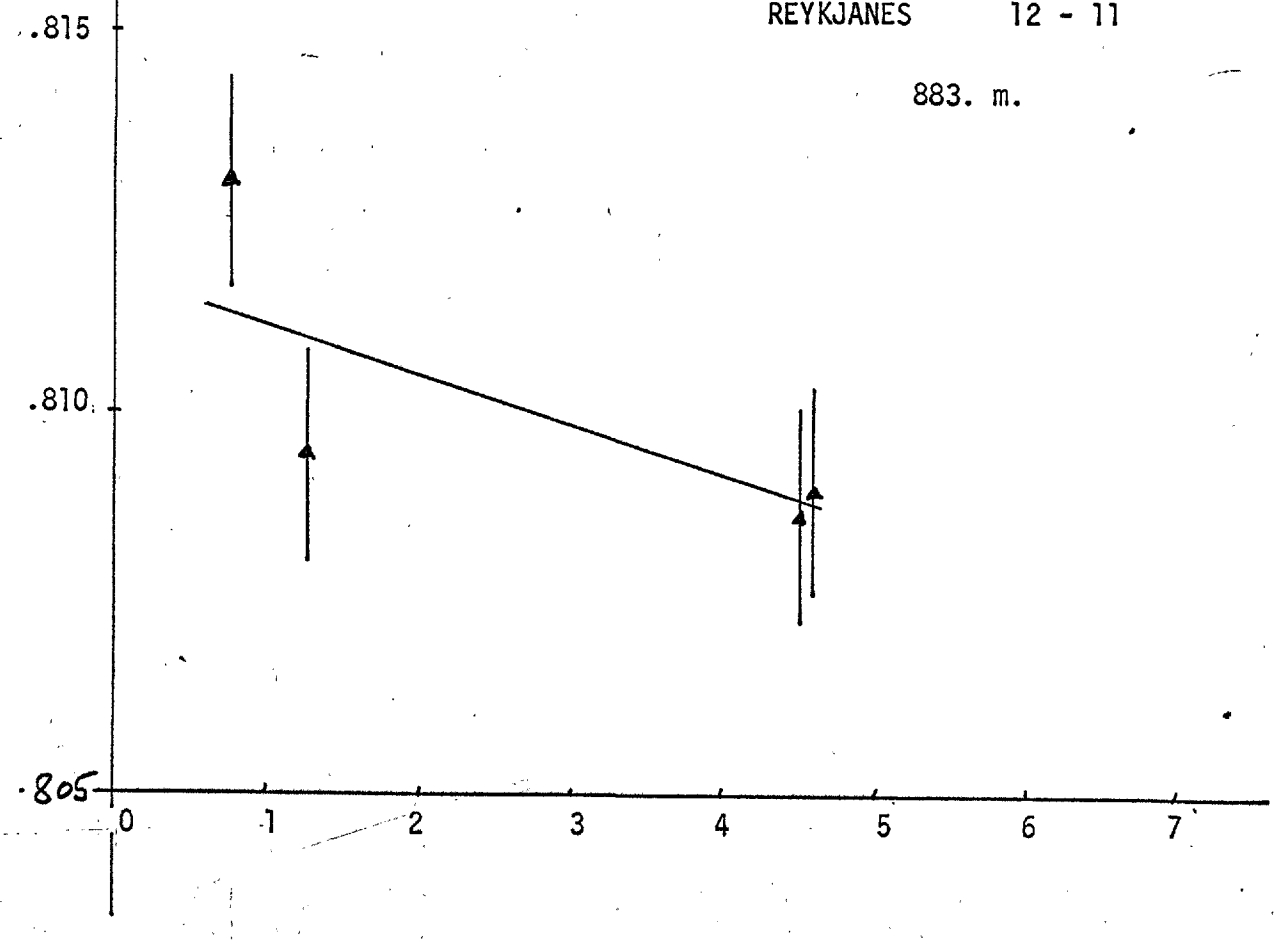
REYKJANES 12 - 13

718. m.



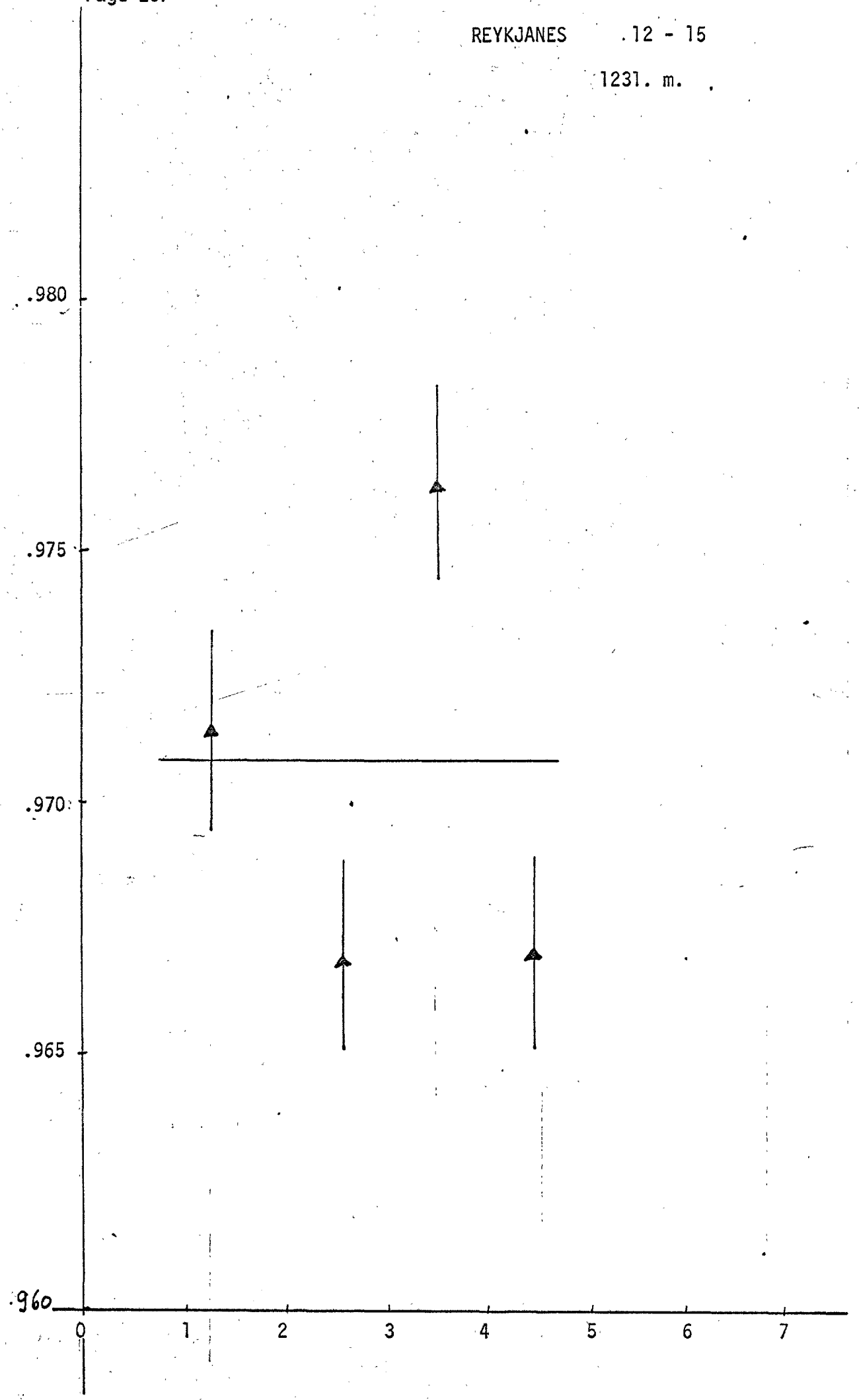
REYKJANES 12 - 11

883. m.



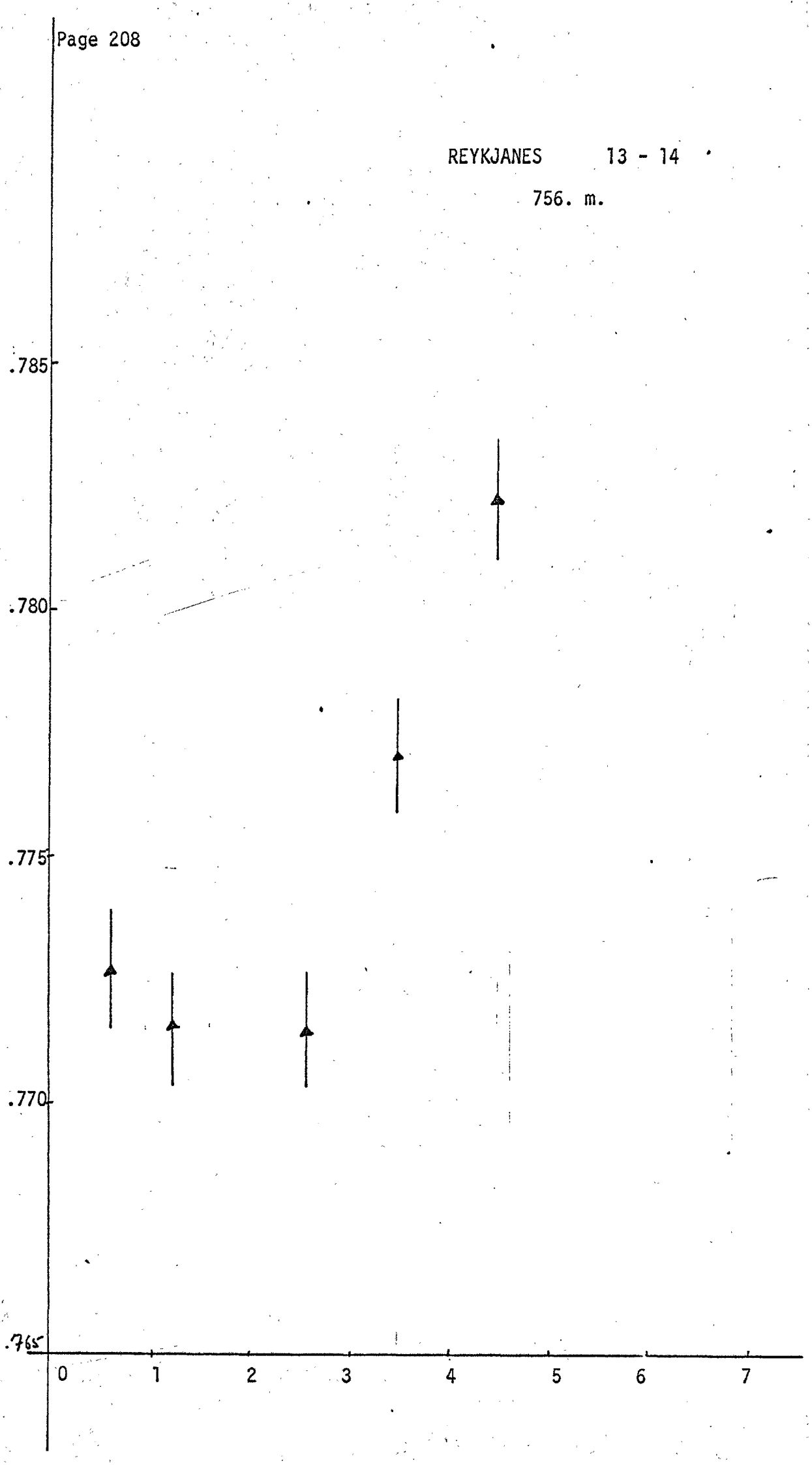
REYKJANES .12 - 15

1231. m.



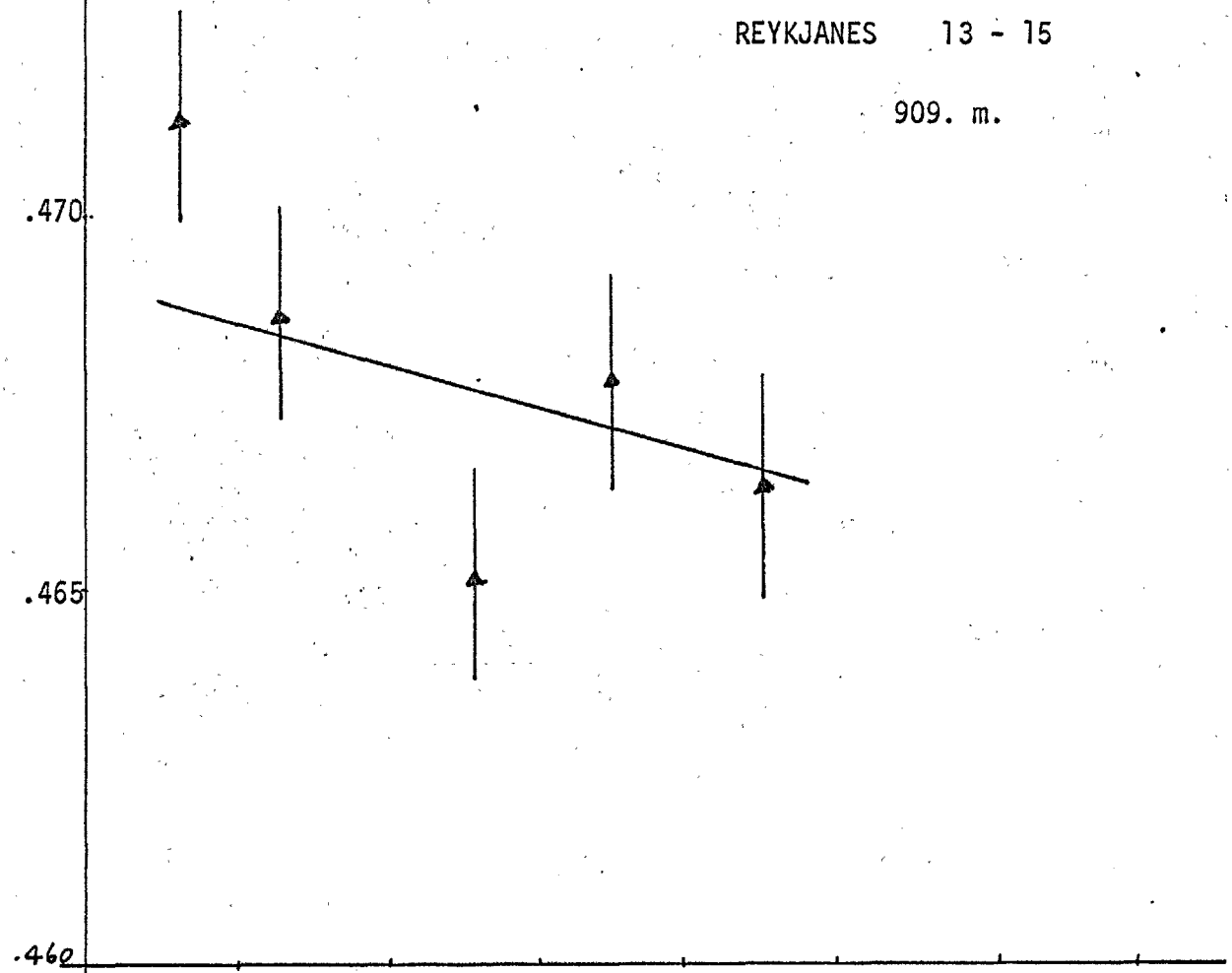
REYKJANES 13 - 14

756. m.



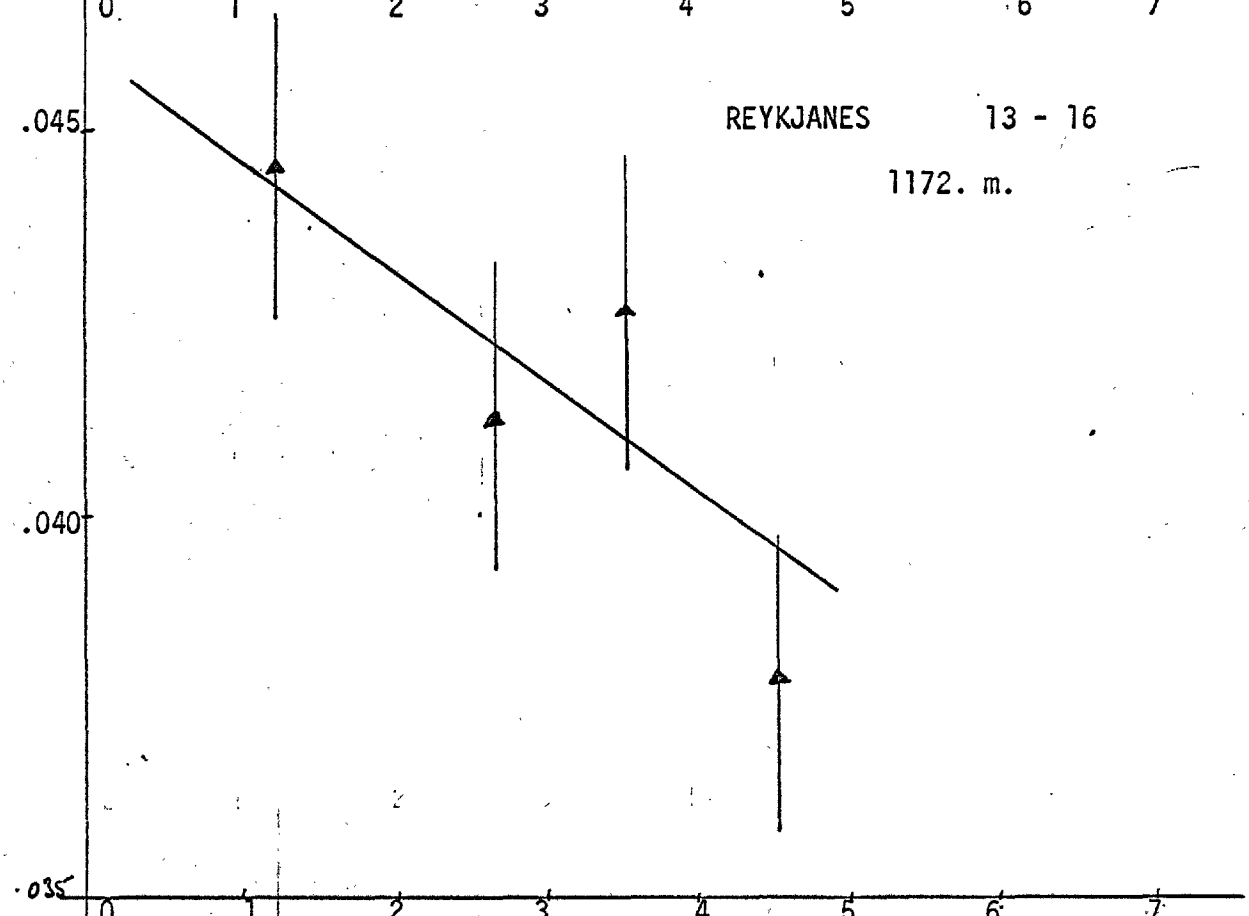
REYKJANES 13 - 15

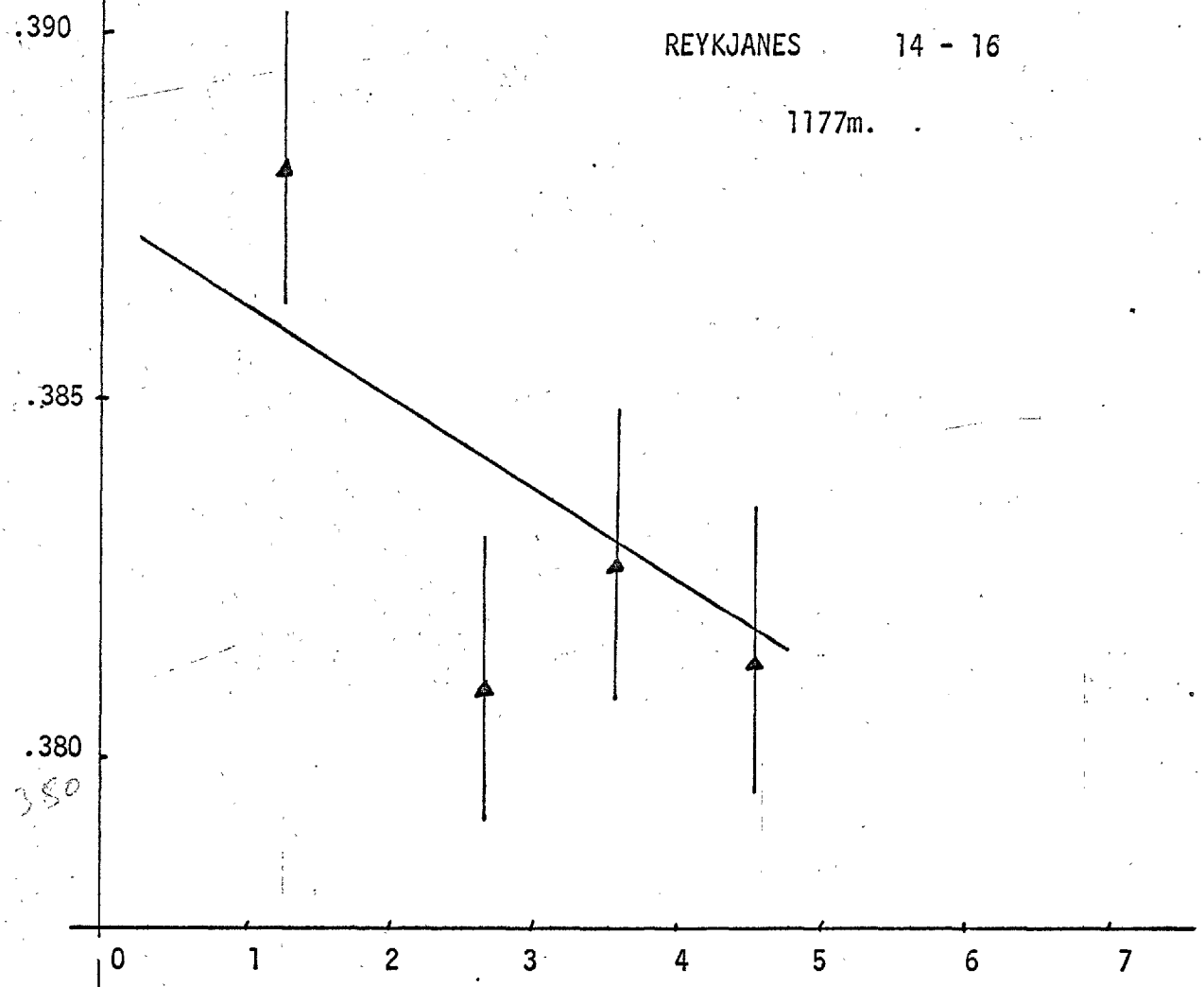
909. m.

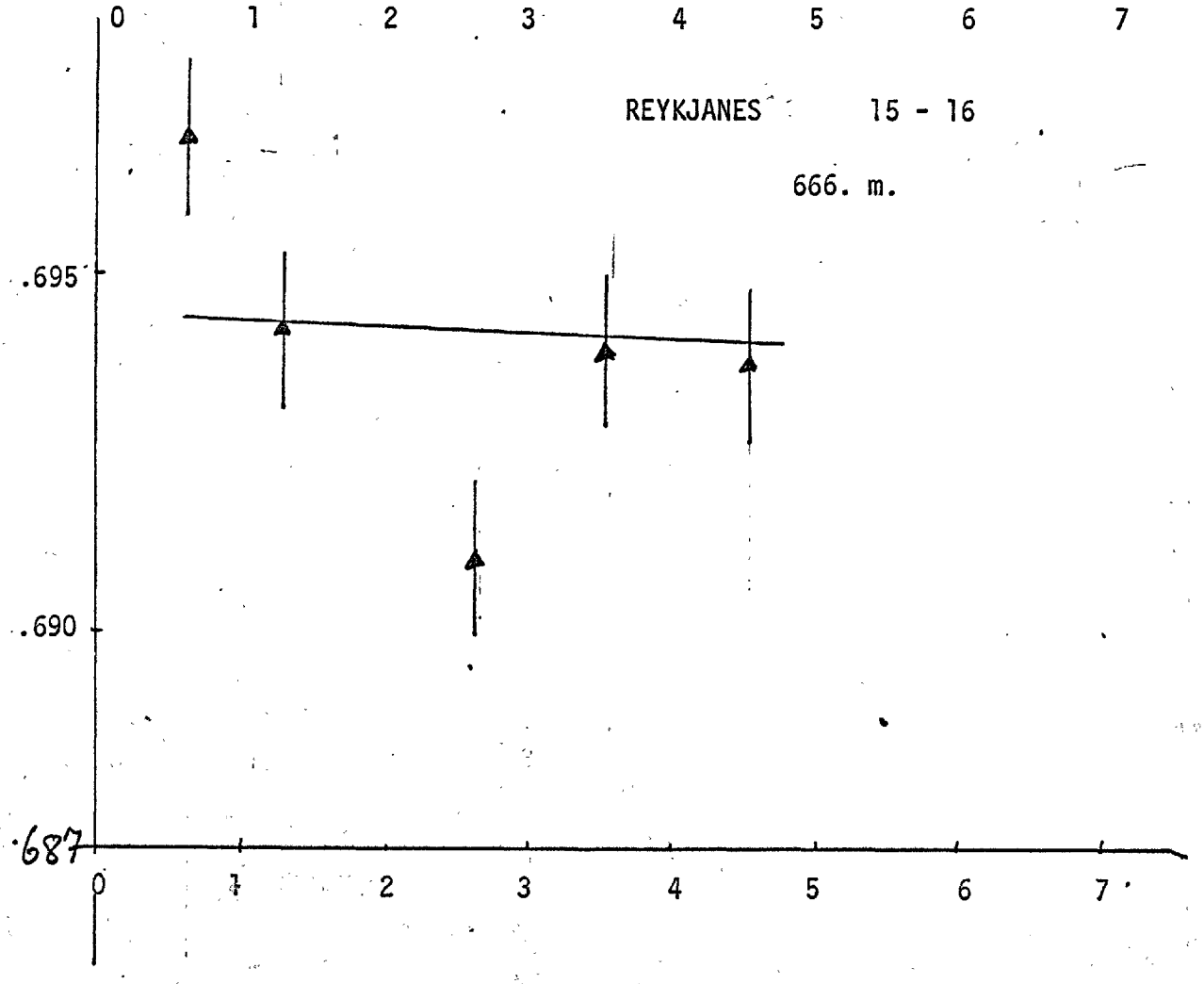


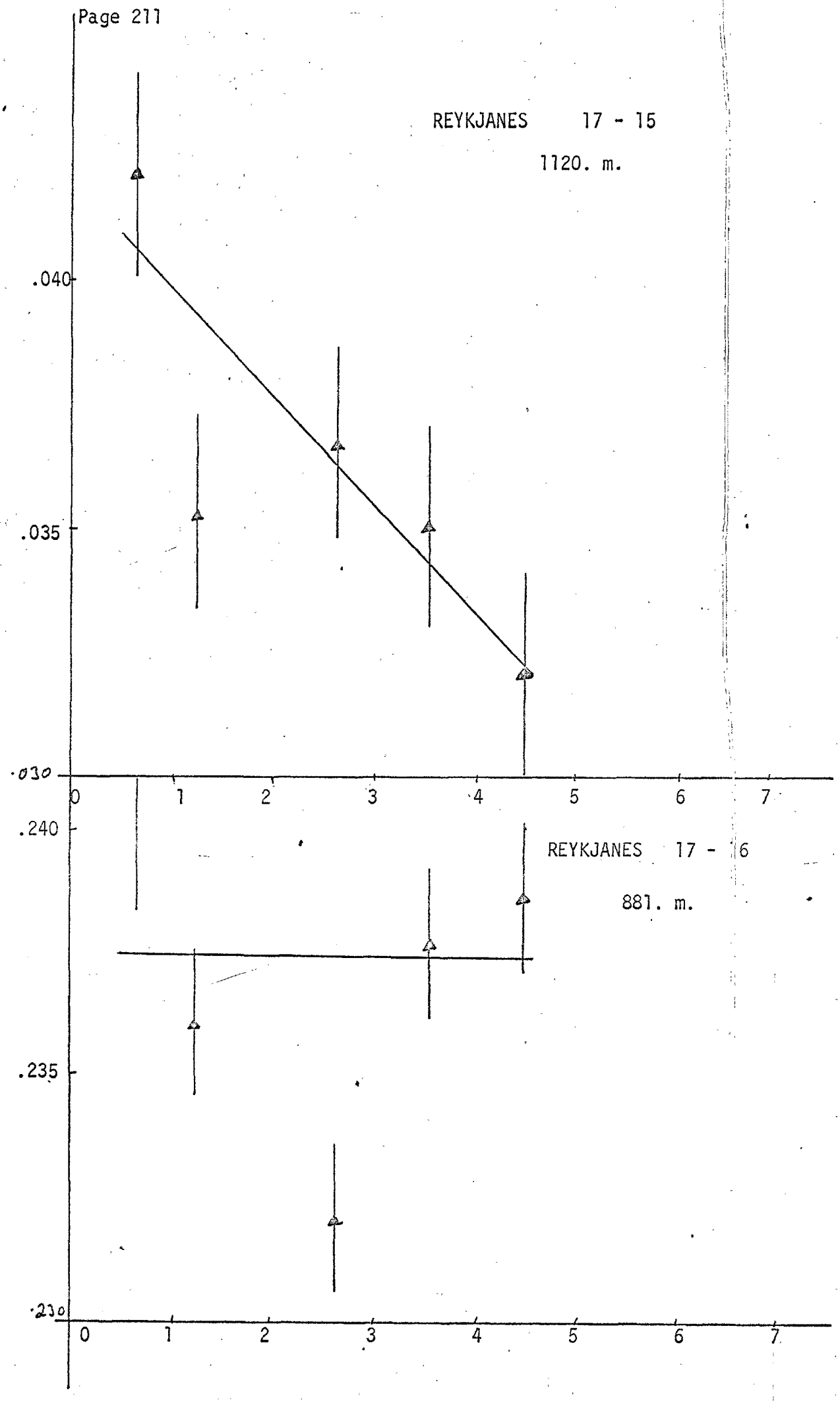
REYKJANES 13 - 16

1172. m.



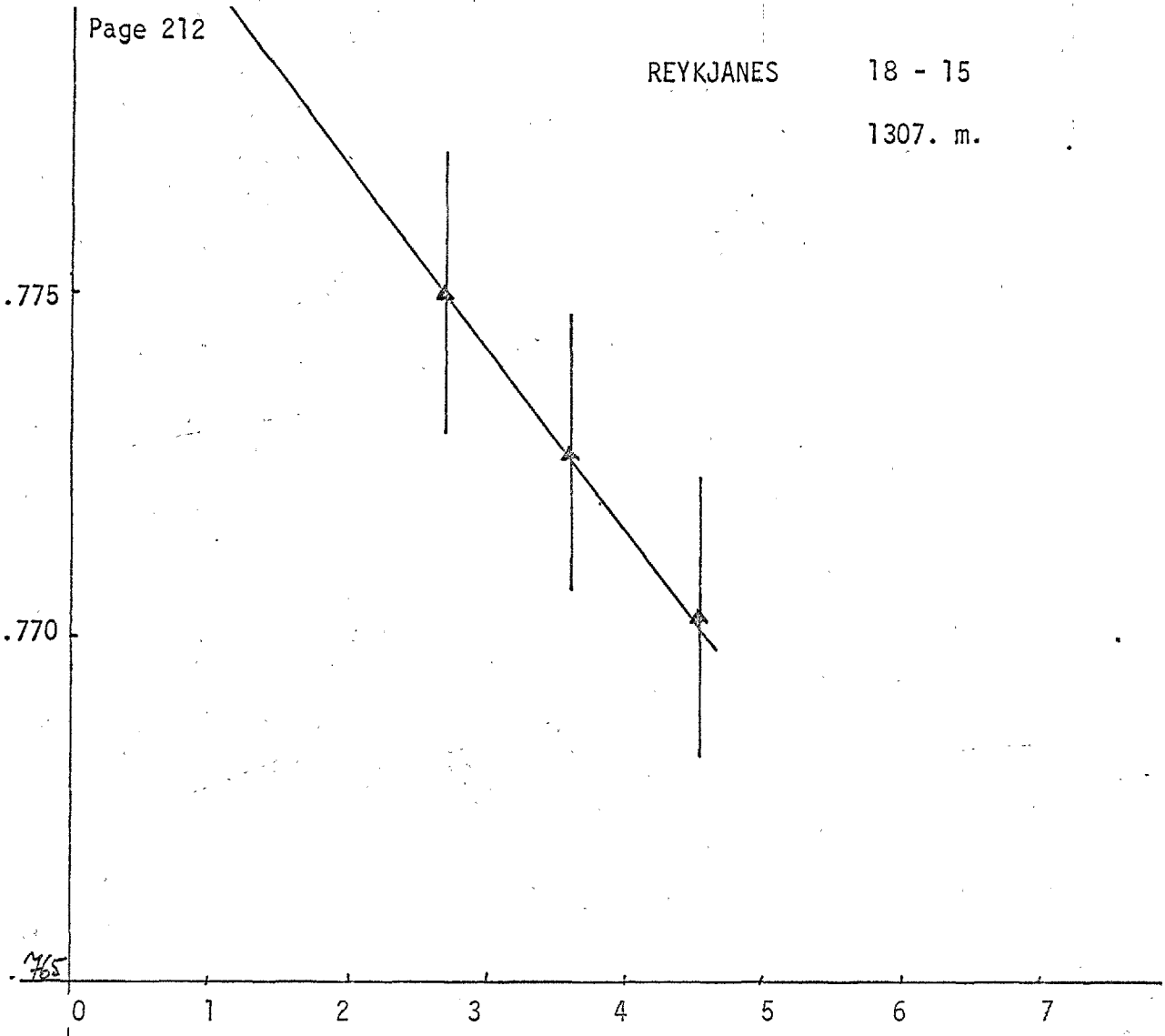

REYKJANES 14 - 16
1177m.
.390
.385
.380
350
0
1
2
3
4
5
6
7


REYKJANES 15 - 16
666. m.
.695
.690
.687
0
1
2
3
4
5
6
7


REYKJANES 17 - 15
1120. m.
.040
.035
.030
0
1
2
3
4
5
6
7
.240
REYKJANES 17 - 16
881. m.
.235
.230
0
1
2
3
4
5
6
7

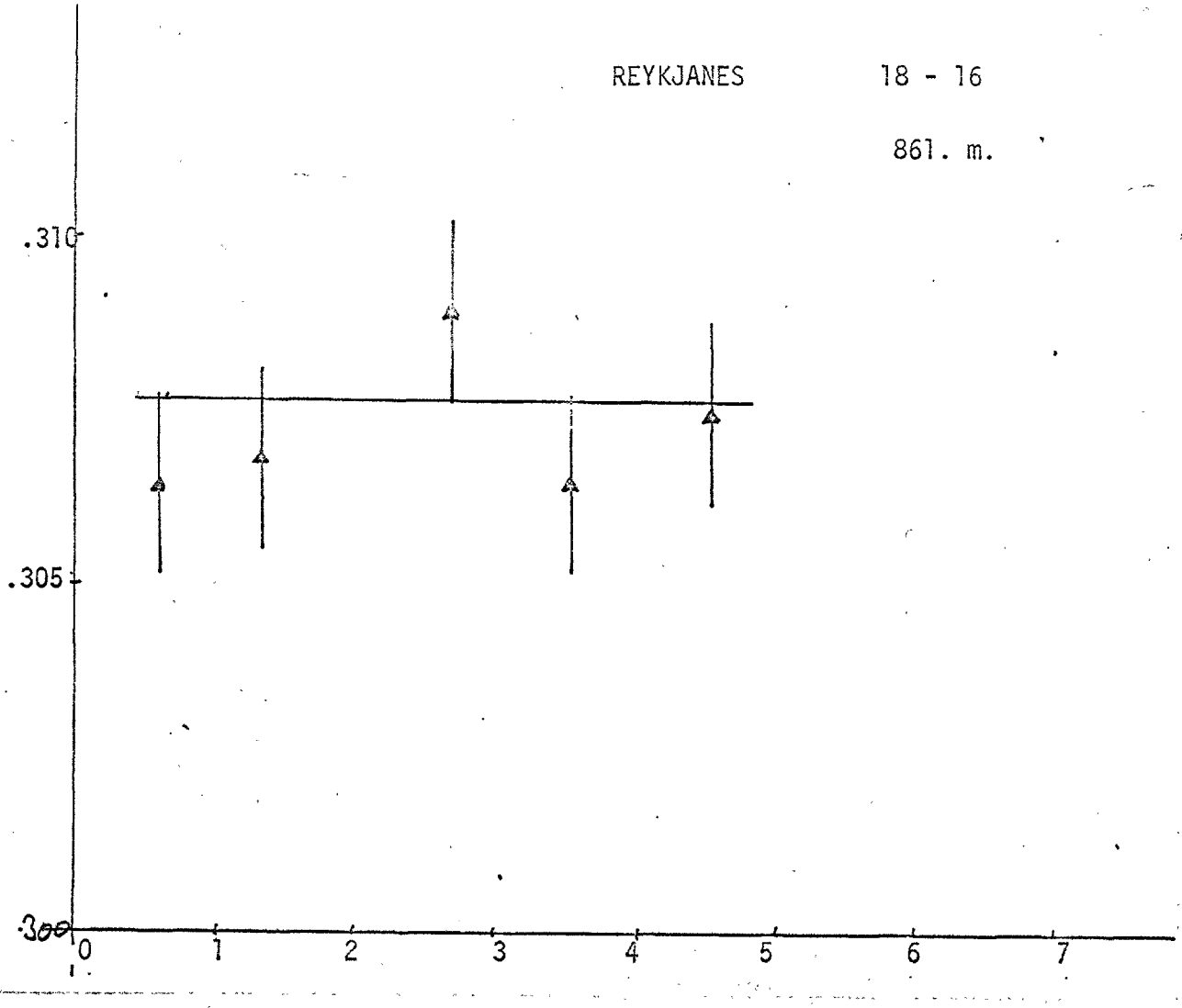
REYKJANES 18 - 15

1307. m.



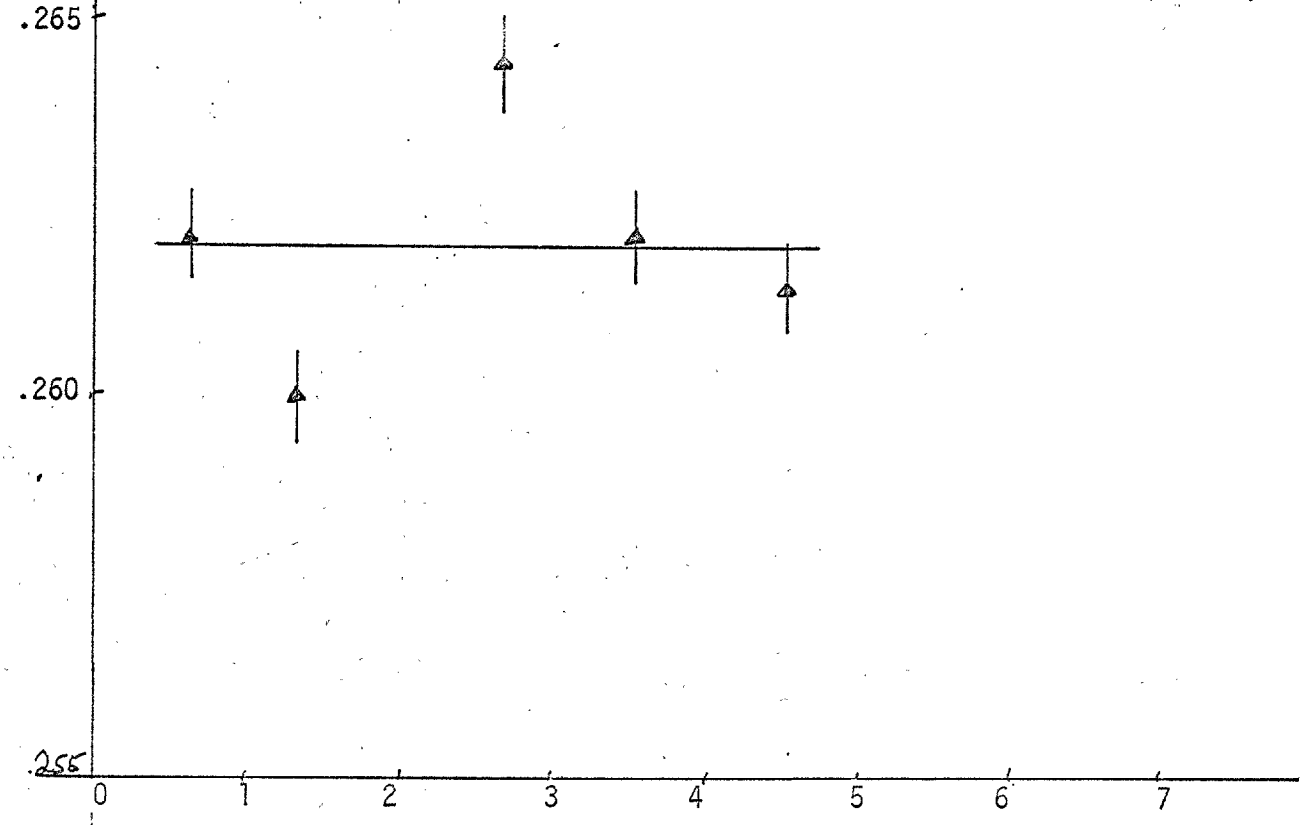
REYKJANES 18 - 16

861. m.



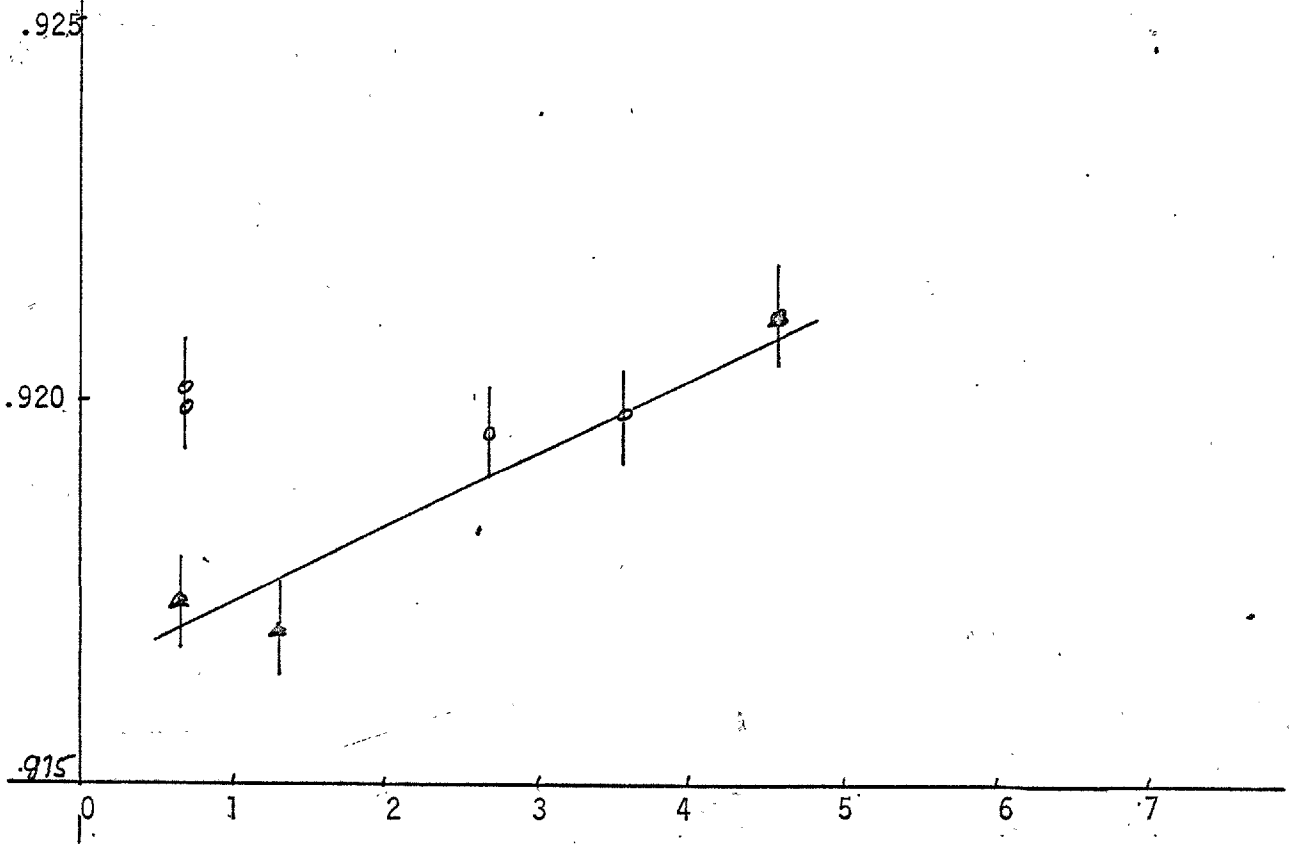
REYKJANES 17 - 18

385. m.



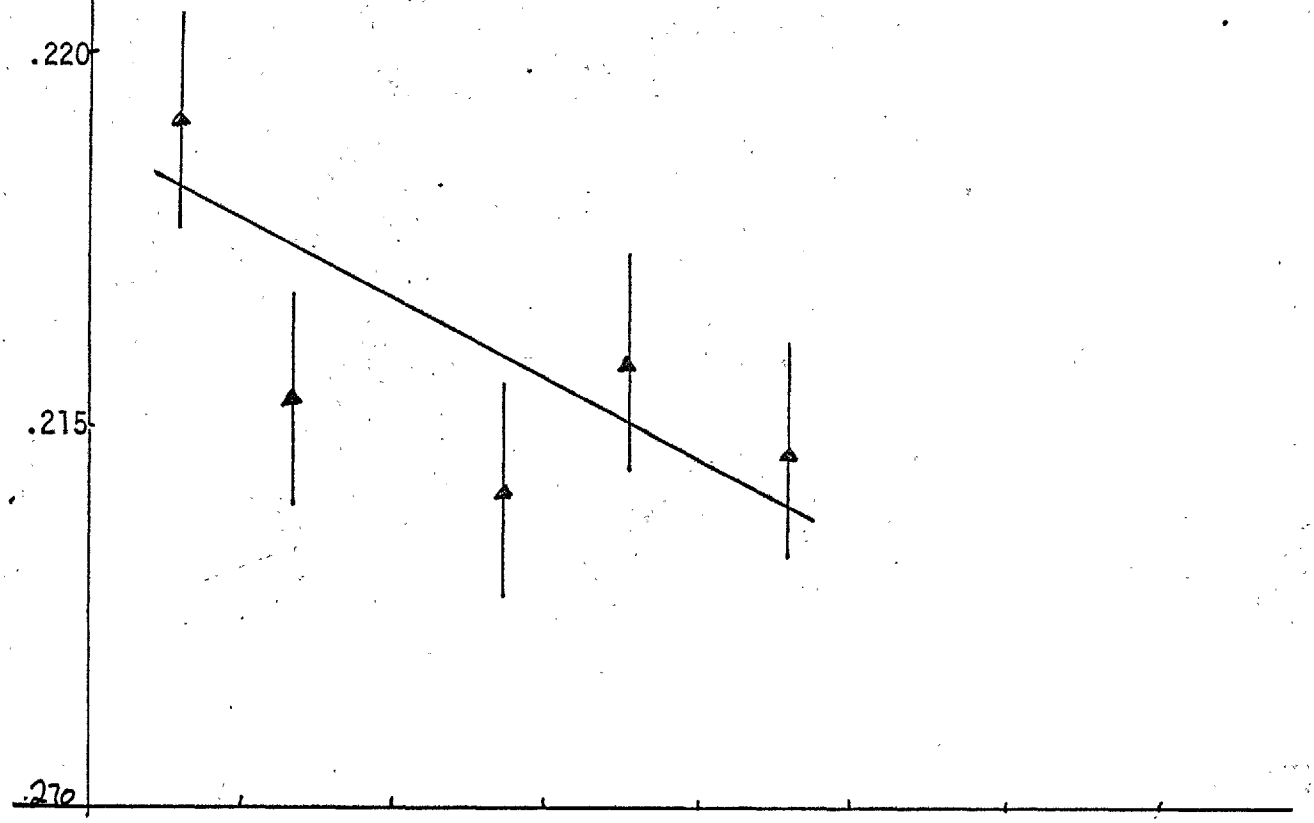
REYKJANES 18 - 19

438. m.



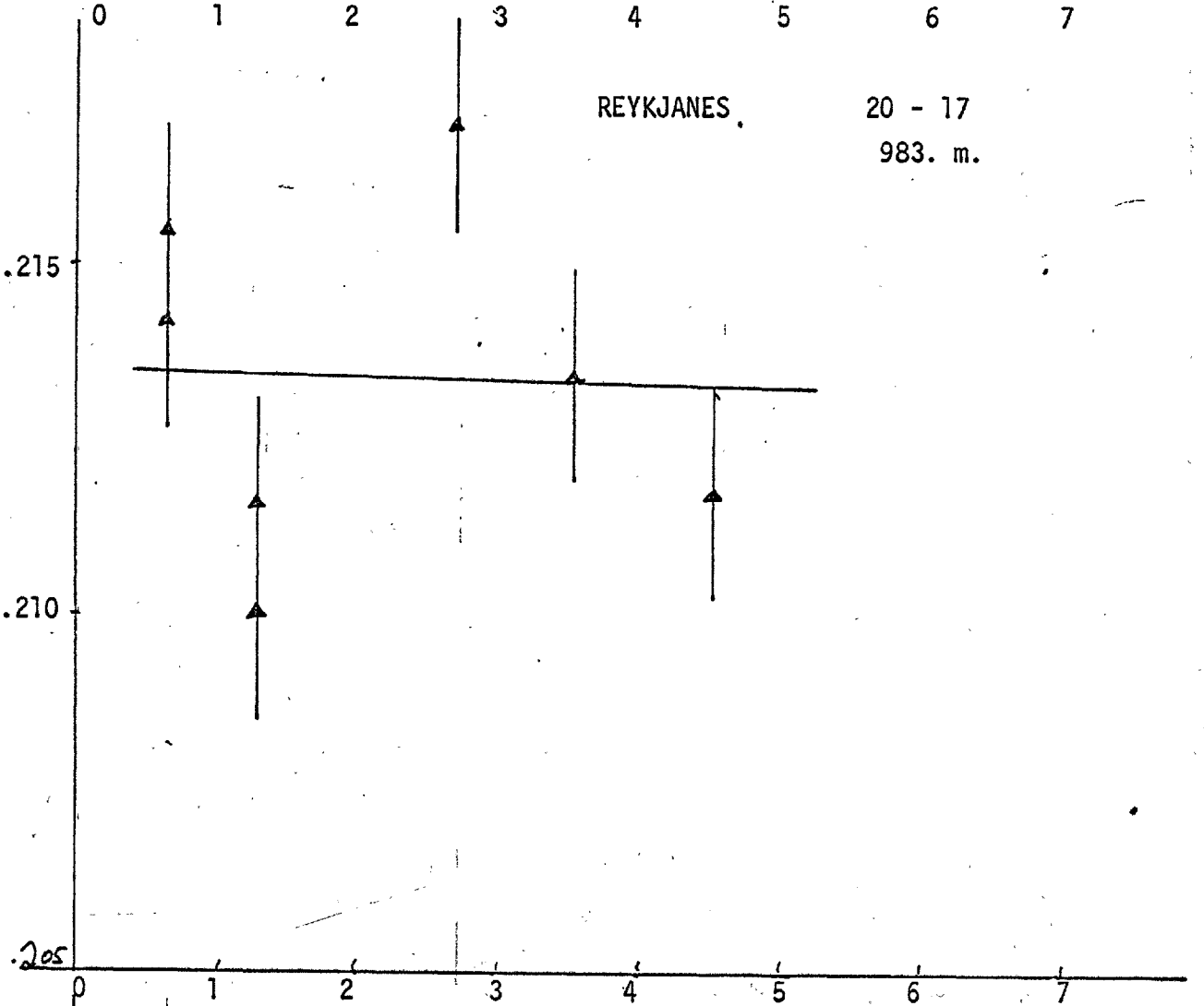
REYKJANES 19 - 16

911. m.



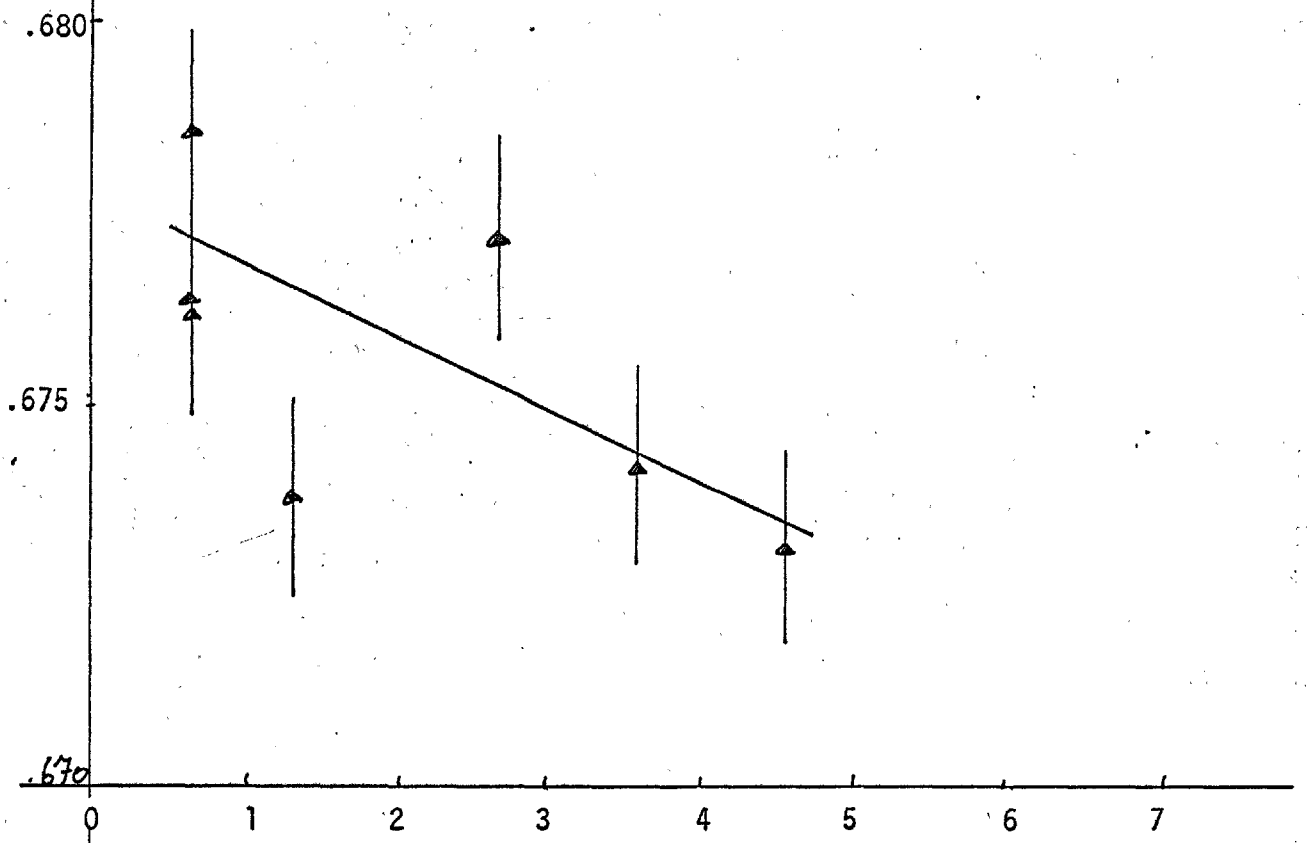
REYKJANES 20 - 17

983. m.



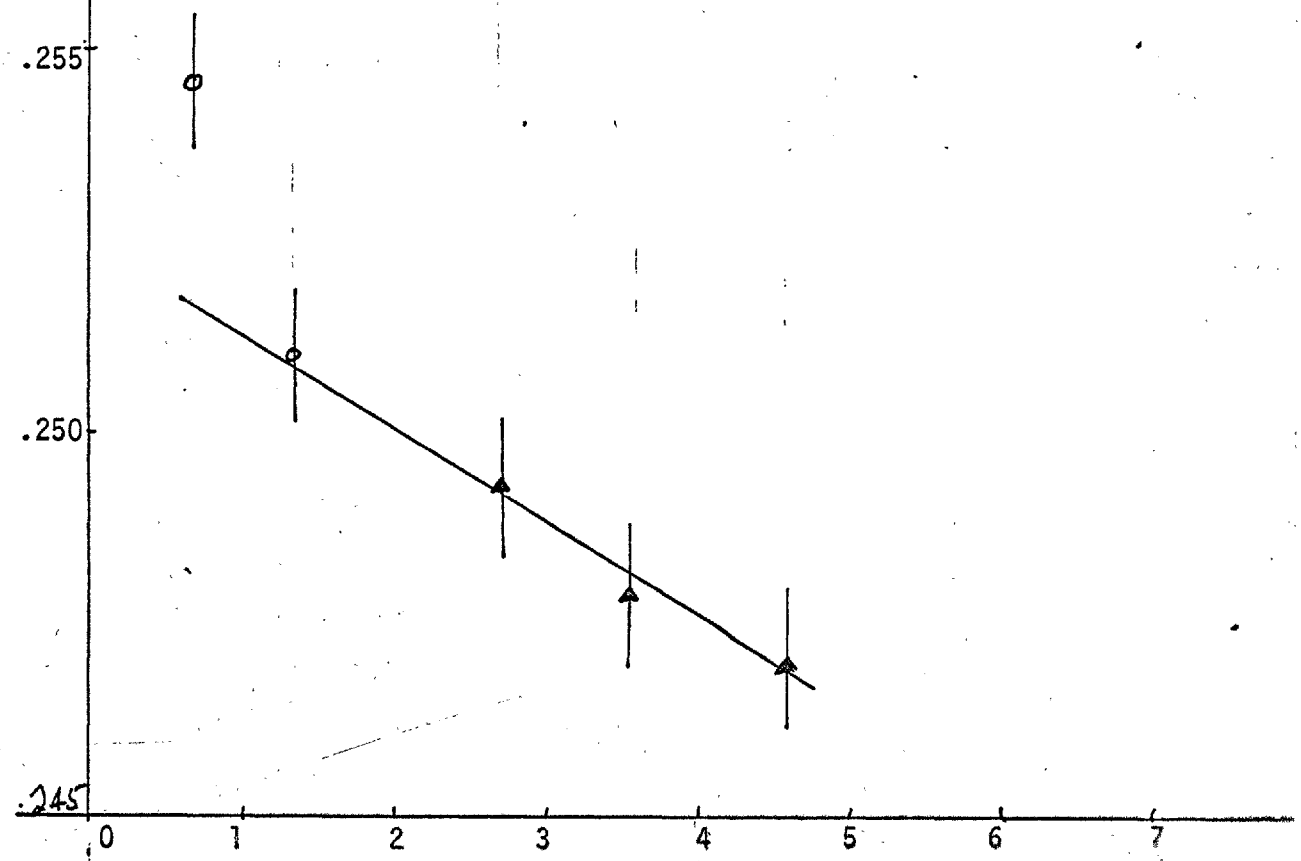
REYKJANES 20 - 18

868. m.



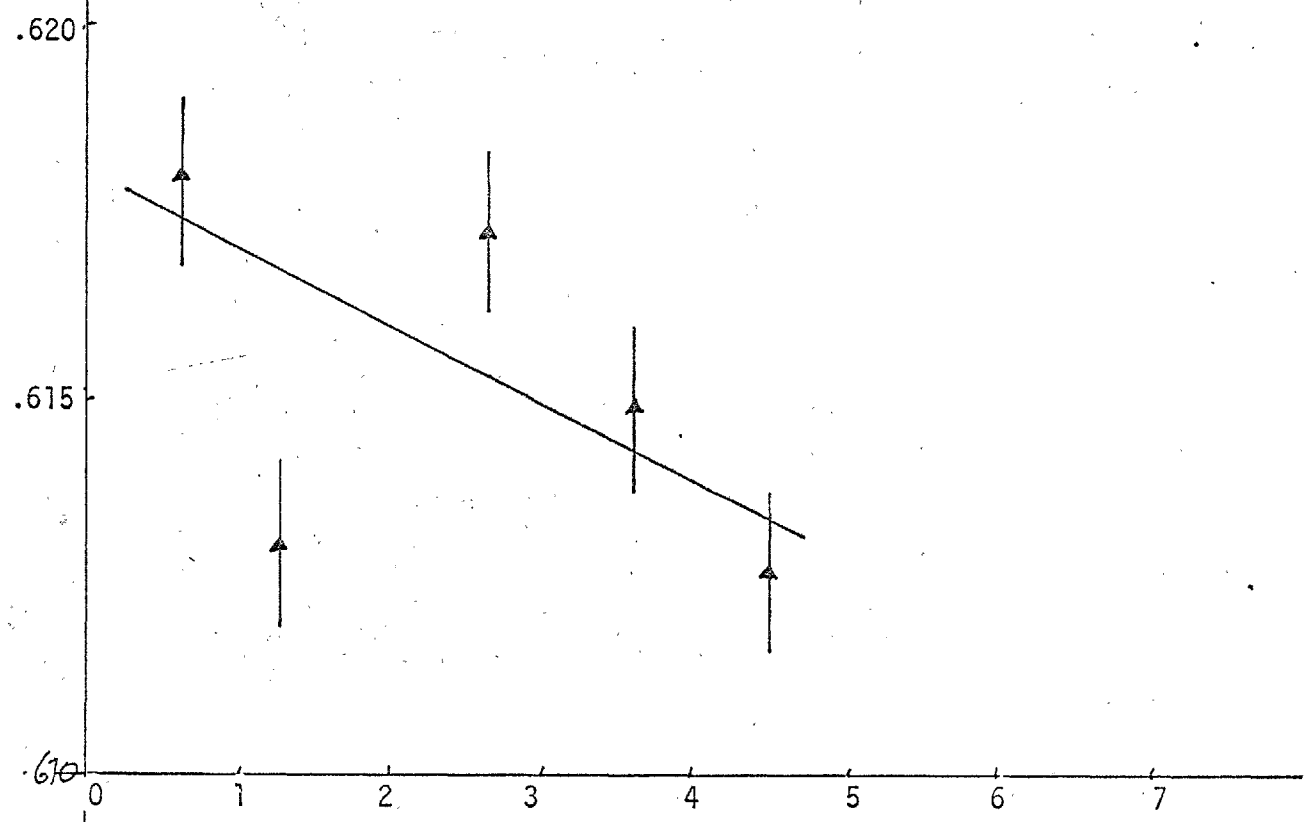
REYKJANES 20 - 25

618. m.



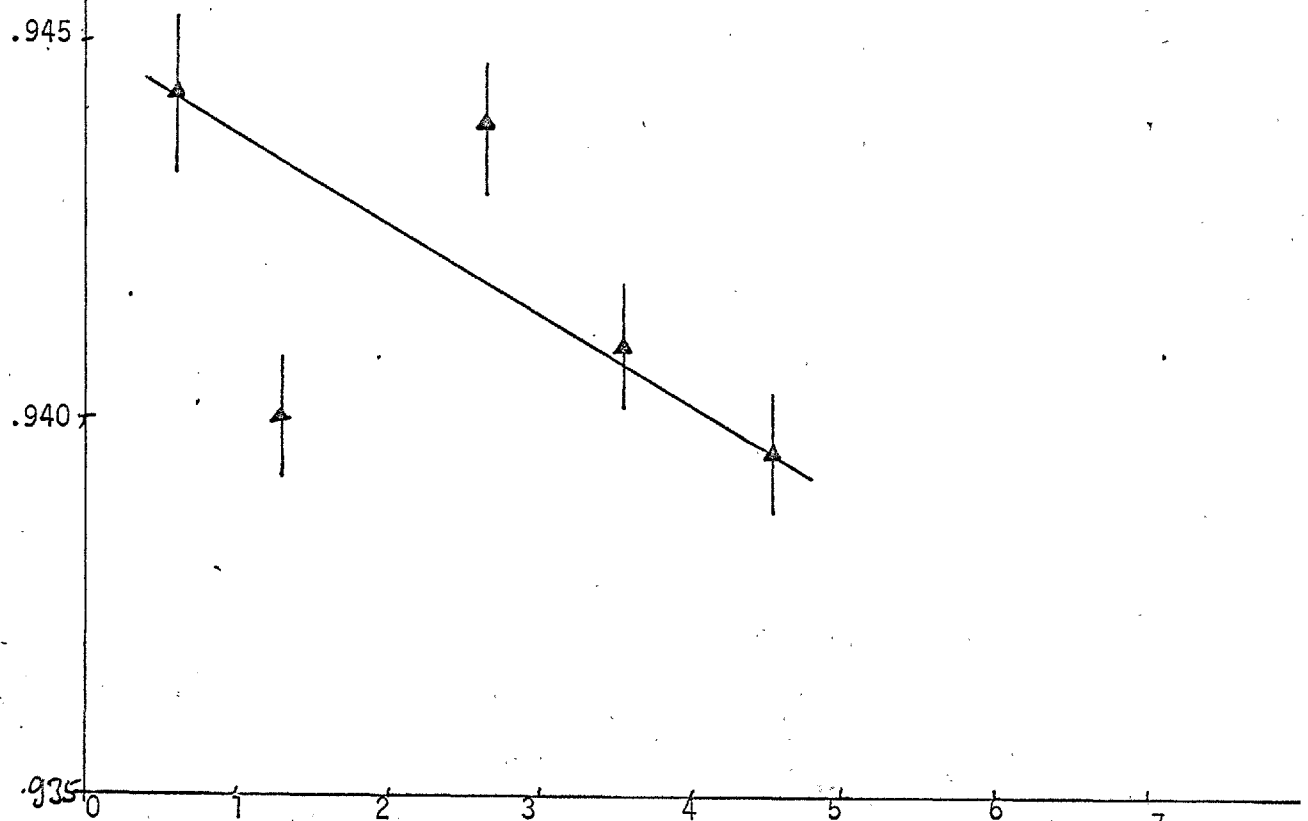
REYKJANES 21 - 18

739. m.



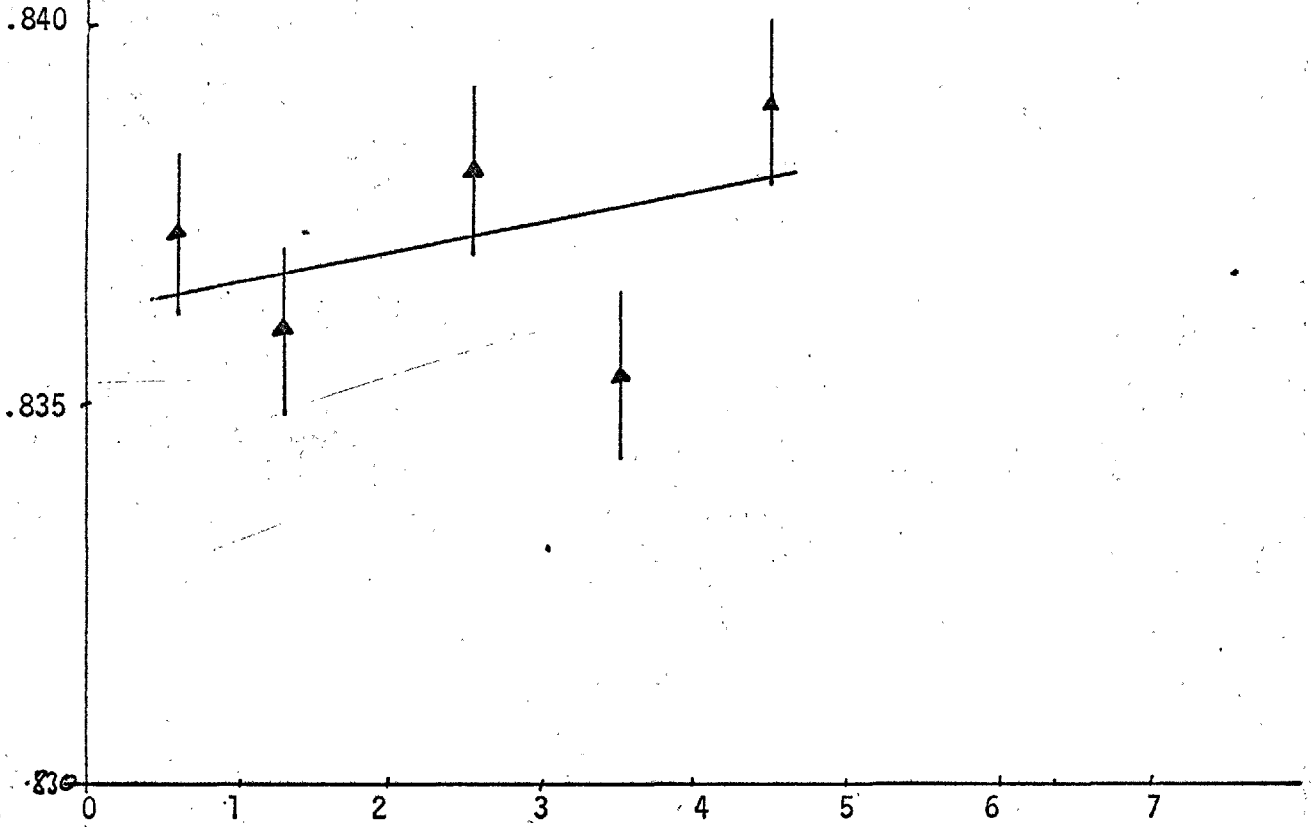
REYKJANES 21 - 19

558. m.



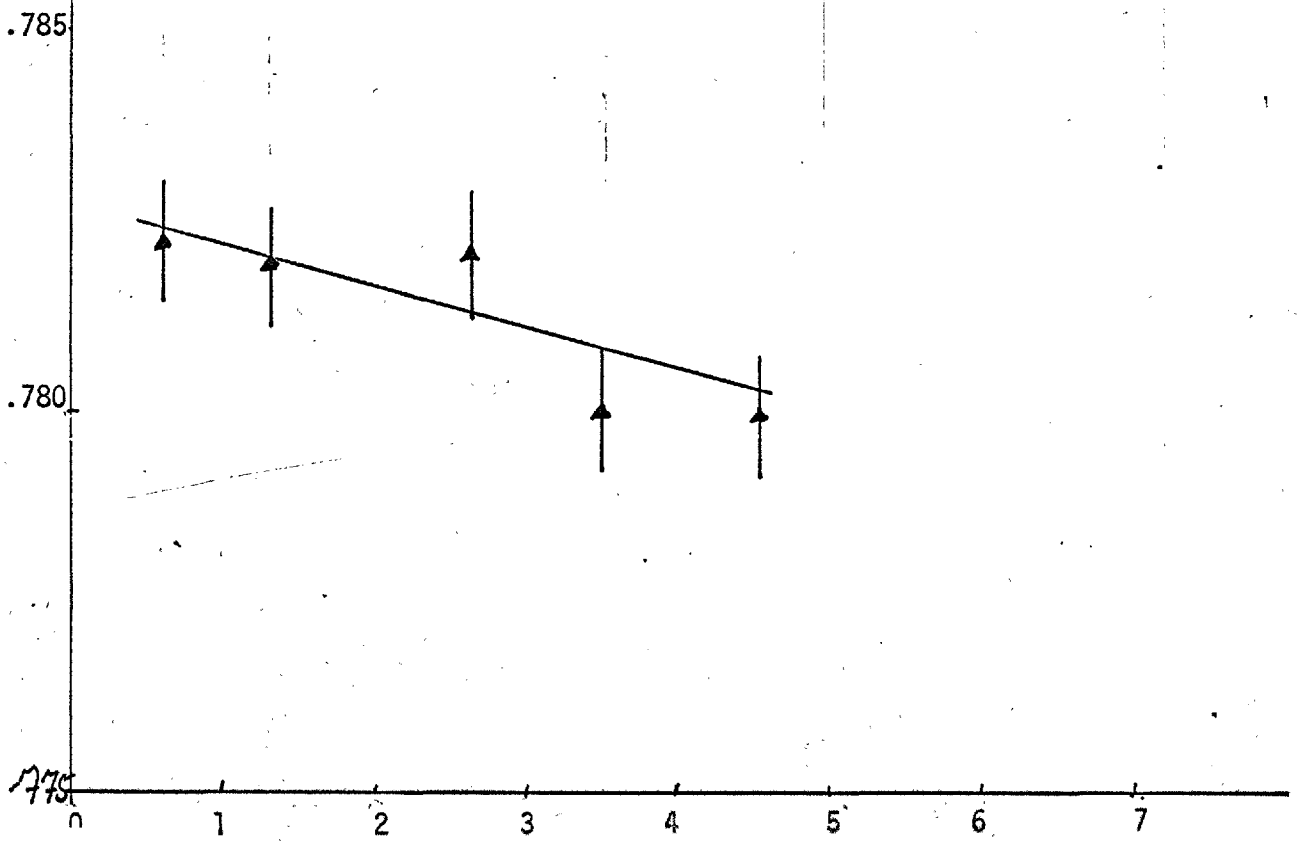
REYKJANES 21 - 20

731. m.



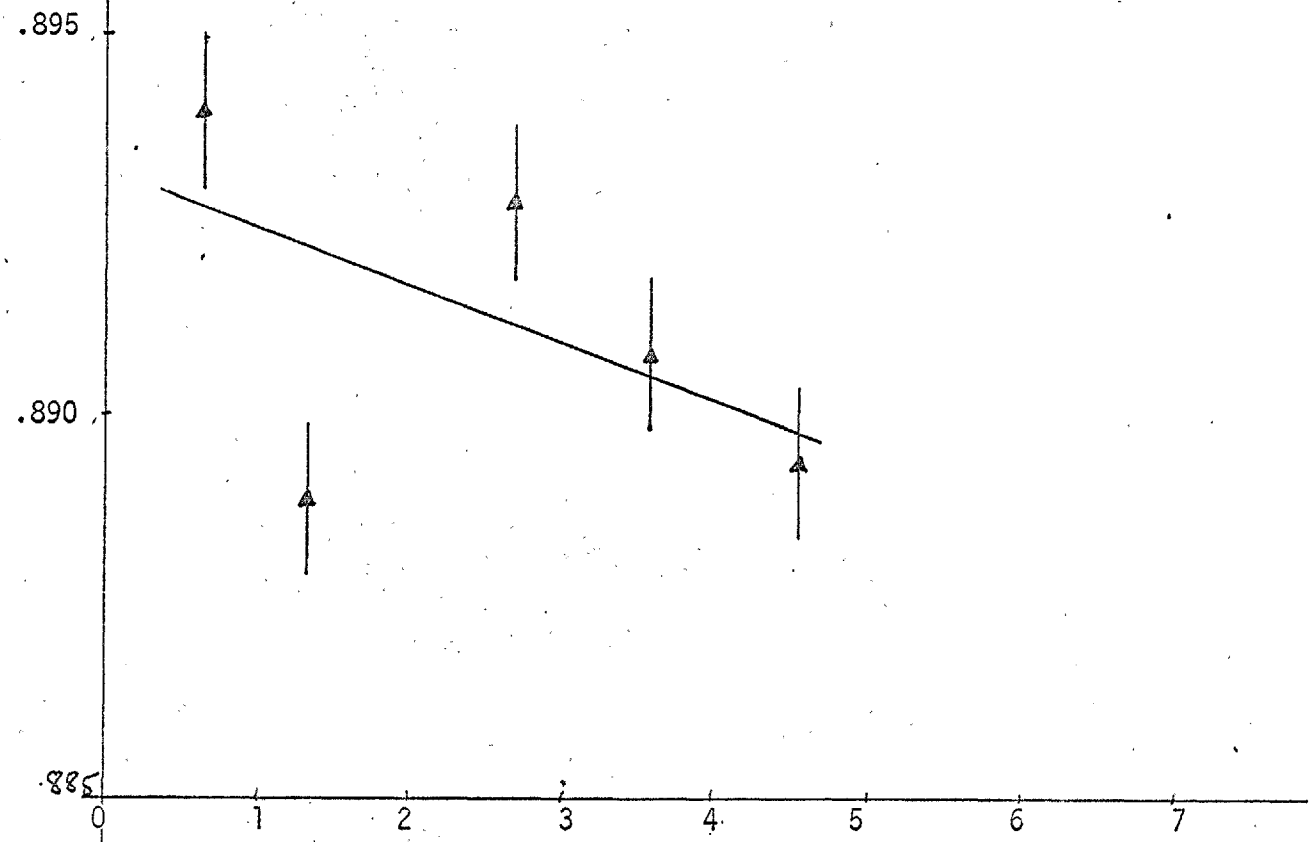
REYKJANES 21 - 22

553. m.



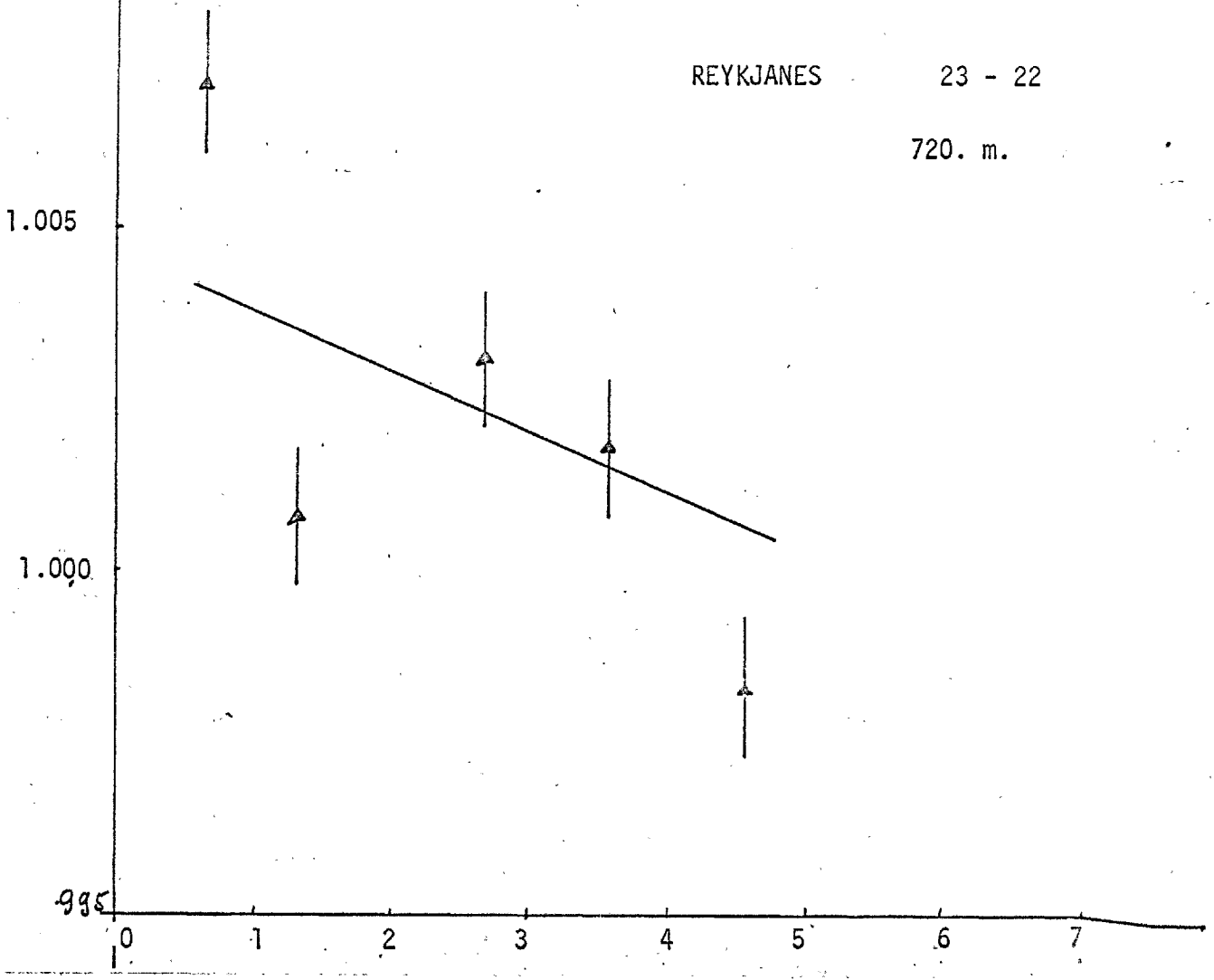
REYKJANES 21 - 25

679. m..



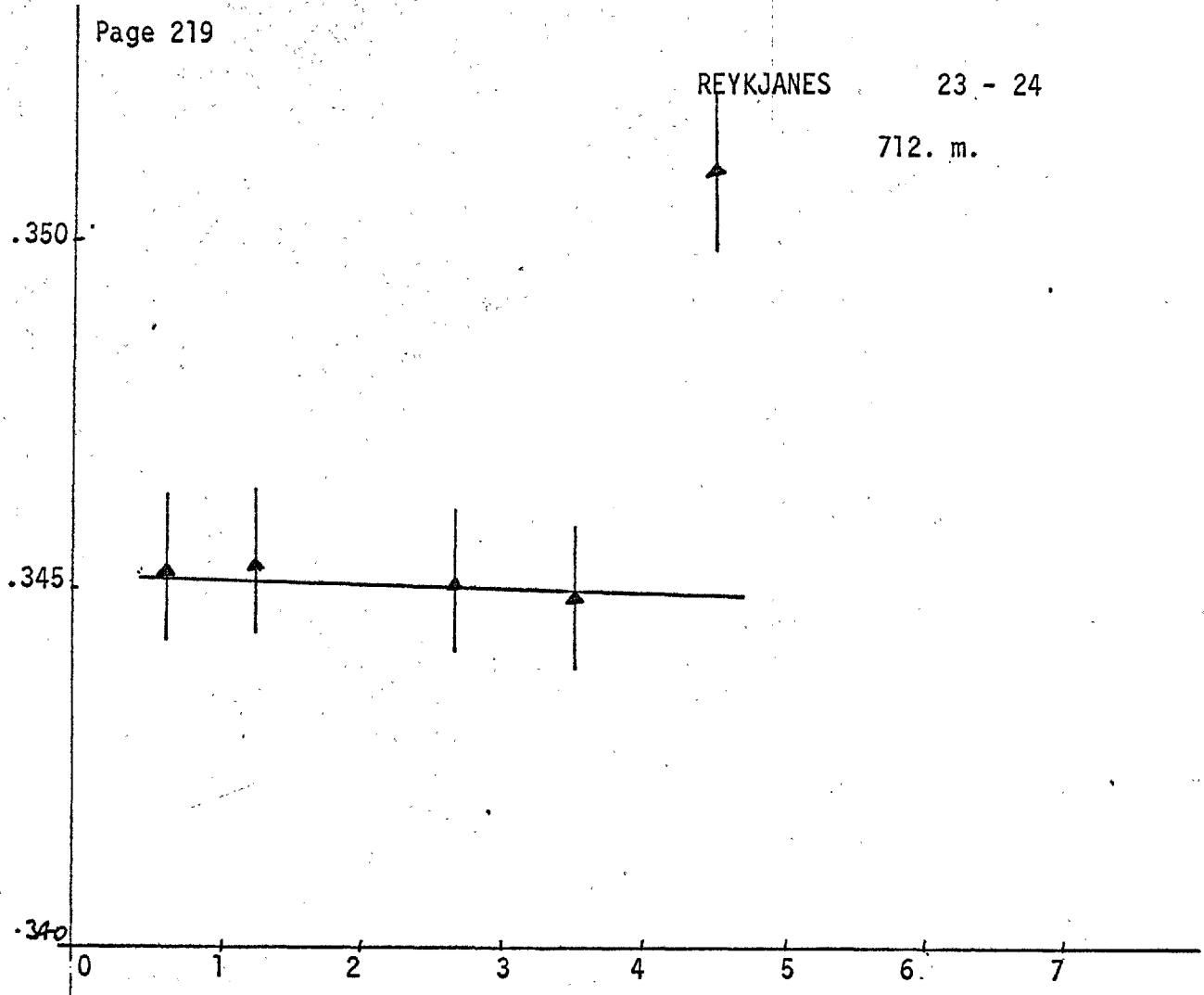
REYKJANES 23 - 22

720. m.



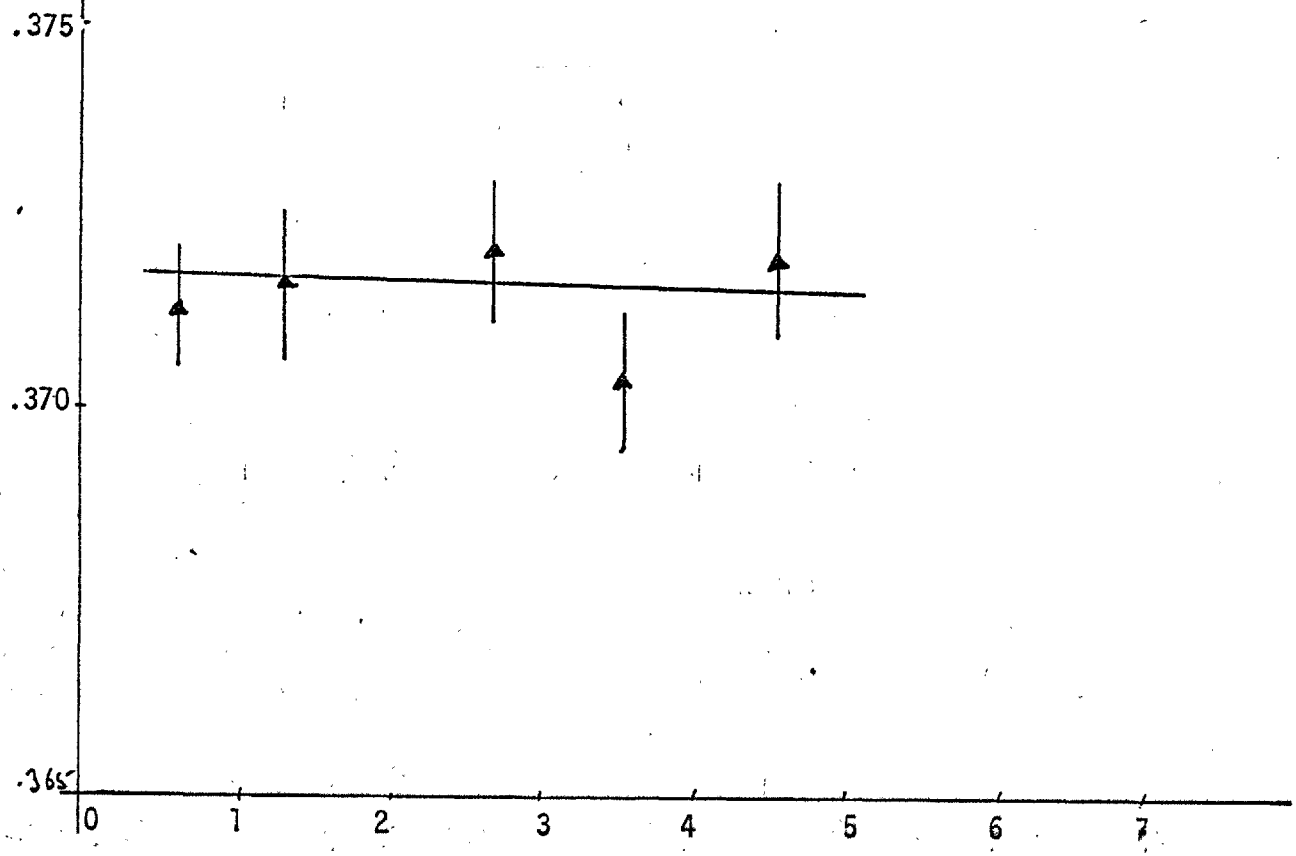
REYKJANES 23 - 24

712. m.



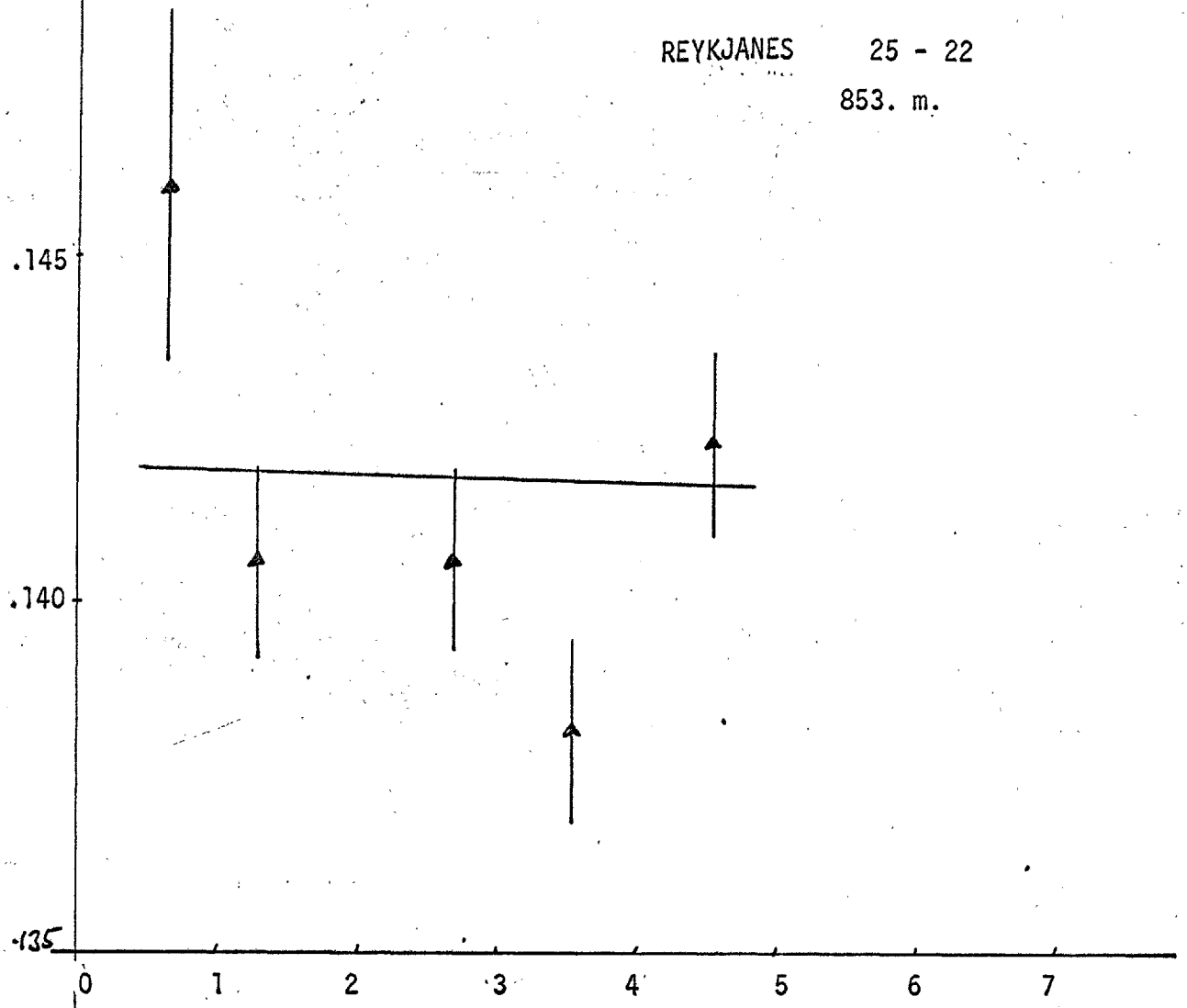
REYKJANES 23 - 26

547. m.



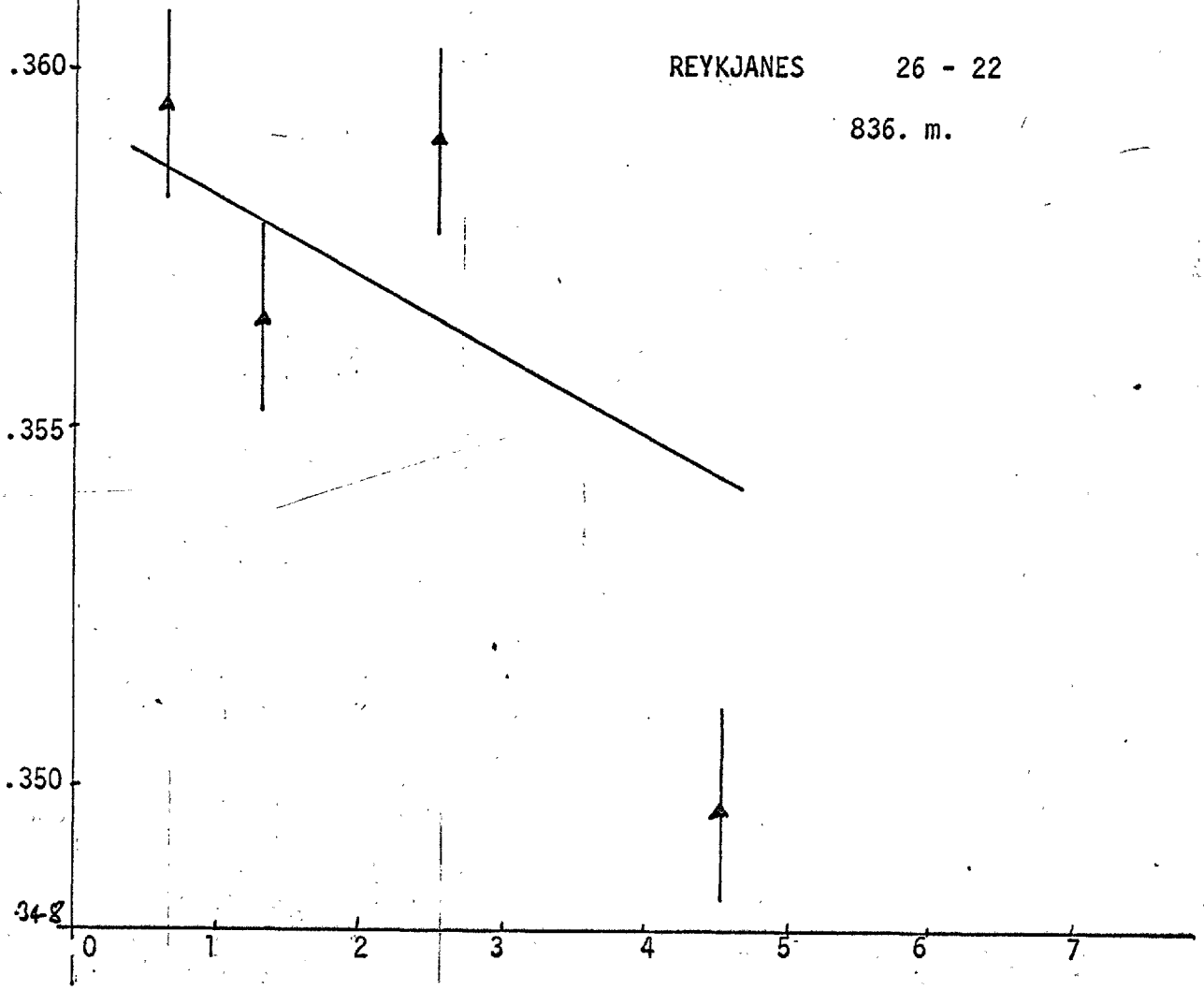
REYKJANES 25 - 22

853. m.



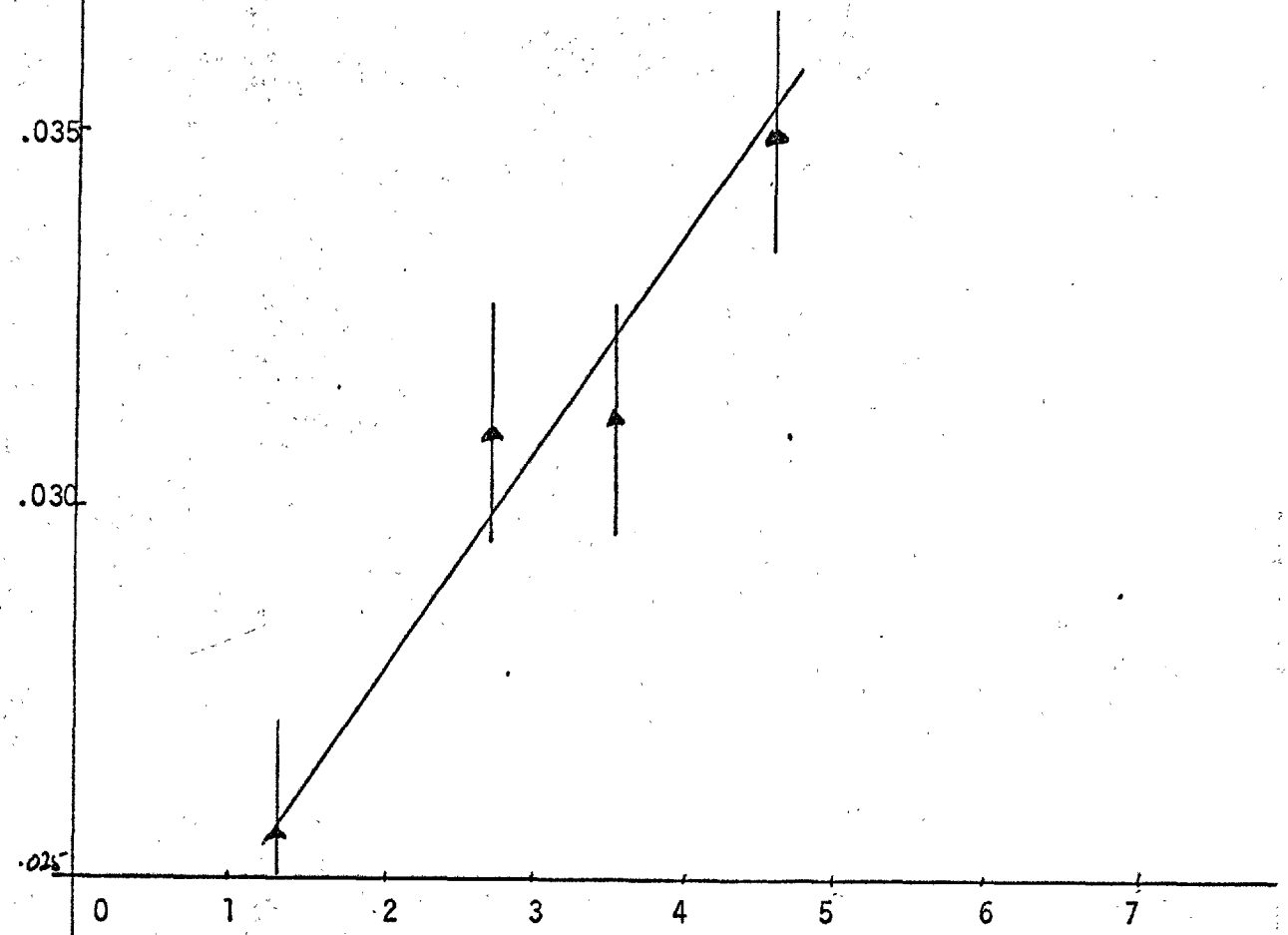
REYKJANES 26 - 22

836. m.



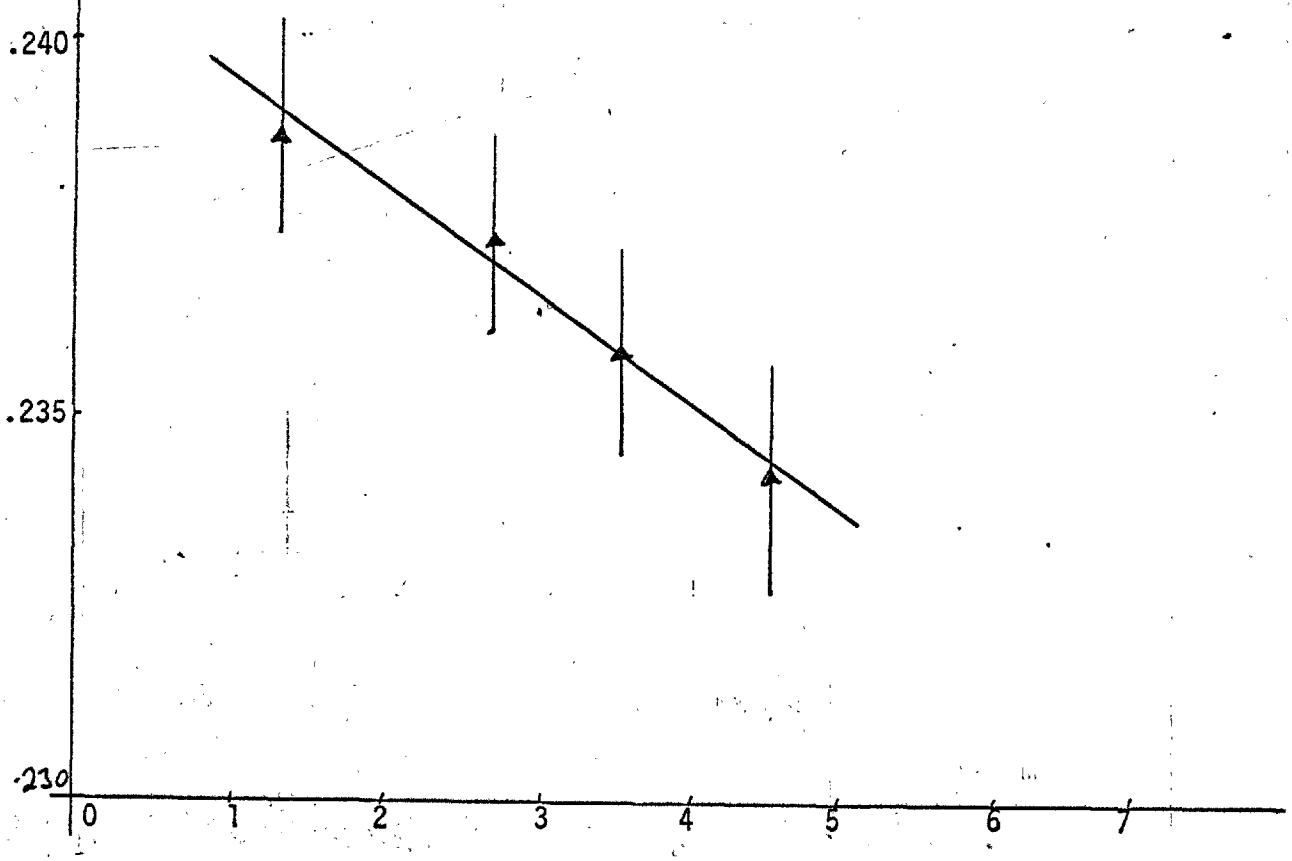
REYKJANES . 26 - 24

1134. m.



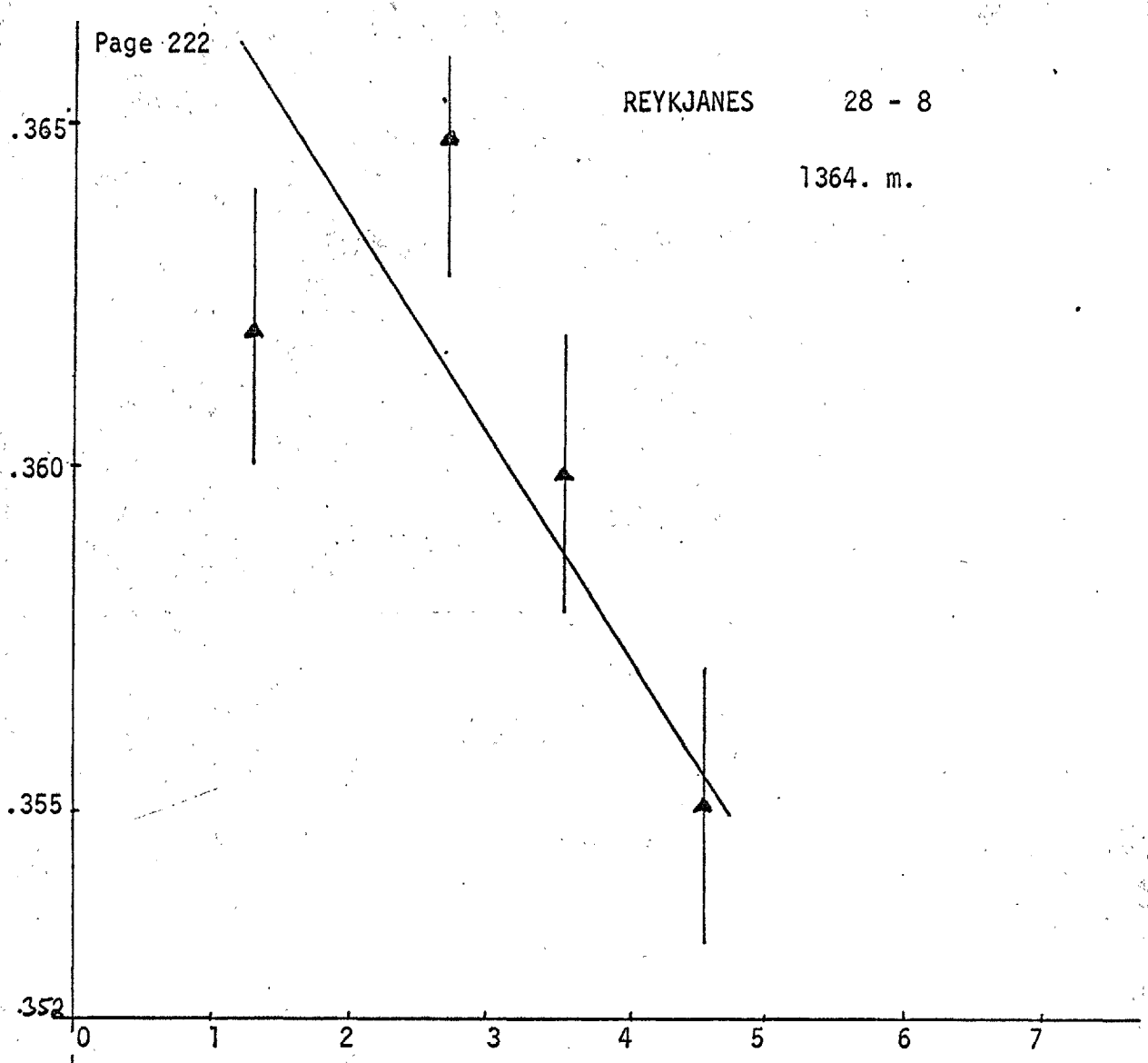
REYKJANES 25 - 26

894. m.



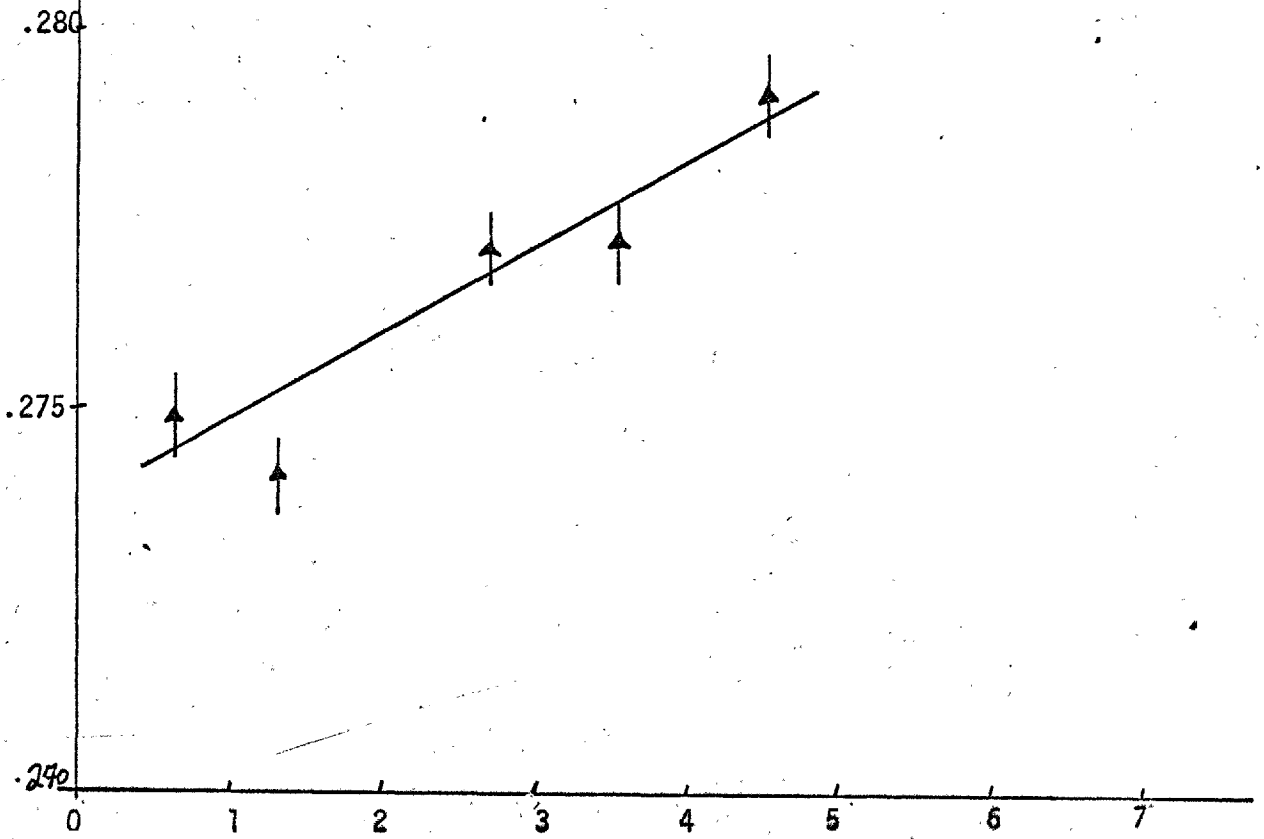
REYKJANES 28 - 8

1364. m.



REYKJANES 28 - 27

305. m.



REFERENCES CITED

Allen, C.R., M. Wyss, J.N. Brune, A. Grantz, and R.E. Wallace, 1972; Displacements on the Imperial, Superstition Hills, and San Andreas Faults Triggered by the Borrego Mountain Earthquake. U.S.G.S. Prof. Paper 787, p. 87, Washington.

Barrell and Sears, 1939; Phil. Trans. Royal Soc. London, Series A.

Bernauer, F., 1943; Junge Tektonik auf Island und ihre Ursachen, in Spalten auf Island, ed. O. Niemczyk, p. 14, Wittwer, Stuttgart.

Berninghausen, W., 1964; Catalogue of Historical Icelandic Volcanoes. Seism. Soc. America, Bull., v. 54, p. 443.

Björnsson, S., Stefán Arnórsson, and Jens Tómasson, 1972; An Economic Evaluation of the Reykjanes Thermal Brine Area, Iceland. A.A.P.G. Bull. v. 56, p. 2380.

Bolton, R.S., 1973; The Management of a Geothermal Field, in Geothermal Energy ed. C.H.H. Armstead, pp. 186, UNESCO, Paris, 1973.

Böthvarsson, G., and G.P.L. Walker, 1964; Crustal Drift in Iceland. Geophys. J. v. 8, p. 285.

Brander, J.L., and G. Wadge, 1973; Distance Measurements Across The Heimaey Eruptive Fissure. Nature, v. 244.

Calvert, R.W., The Measurement of Crustal Drift in Iceland by Horizontal Distance Measurements. Ph.D. Thesis, University of London.

Chernov, (tr. A.R. Silverman), 1967; Wave Propagation in a Random Medium. Dover, New York.

Chinnery, M.A., 1961; The Deformation of the Ground around Surface Faults. Seism. Soc. America, Bull., v. 51, p. 355.

Cloos, E., 1932; Feather Joints as Indicators of the Direction of Movements on Faults, Thrusts, Joints, and Magmatic Contacts. Proc. Nat. Acad. Sci. U.S., v. 18, p. 387.

Decker, R., Páll Einarsson, and P.A. Mohr, 1971; Rifting in Iceland: New Geodetic Data. Science, v. 173, p. 530.

Dietz, 1961; Continent and Ocean Basin Evolution by Sea Floor Spreading. Nature, v. 190, p. 854.

Elder, J., 1965; Physical Processes in Geothermal Areas, in Monograph on Terrestrial Heat Flow, ed. W.H.K. Lee, A.G.U., 1965.

Frank,F.C., 1966; Deduction of Earth Strains from Survey Data. Seism. Soc. Am., Bull., v. 56, p.35.

Froome, K.D., and R.H. Bradsell, 1961; J. Sci. Inst., v. 38, p. 458.

Froome, K.D., and Bradsell, R.H., 1966; A New Method for the Measurement of Distances up to 5000 feet by means of a Modulated Light Beam. J. Sci. Instr., v. 43, p.129.

Froome, K.D., 1971; Mekometer III; E.D.M. with Sub-Millimetre Resolution. Survey Review, v. 21, p.98.

Gass, I.G., 1972; Proposals Concerning the Variation of Volcanic Products and Processes Within the Oceanic Environment. Phil. Trans. Royal Soc. London, Series A, v. 271, p. 131.

Gibson, I.L., and J.D.A. Piper, 1972; Structure of the IcelandicBasalt Plateau and the Process of Drift. Phil. Trans. Royal Soc. London, Series A, v.271, p. 141.

Hayford, J.F., and A.L. Baldwin, 1908; Geodetic Measurements of Earth Movements in the California Earthquake of April 18th, 1906.Report of the State Earthquake Commission, 1, p.114, Carnegie Institut-ion of Washington, D.C.

Heirtzler, J.R., X. Le Pichon, and J.G. Baron, 1966; Magnetic Anomalies over the Reykjanes Ridge. Deep Sea Res., v. 13, p. 427.

Hodara, H., 1968; Effects of a Turbulent Atmosphere on the Phase and Frequency of Optical Waves. Proc. of I.E.E.E., v. 56.

Hoffman, R.B., 1968; Geodimeter Fault Movement Investigations in California. Cali. Dept. Water Res. Bull., v.6, p. 116.

Jakobsson, S.P., 1966; The Structure of the Islands of the Vestmannaeyjar Archipelago. Surtsey Res. Progress Report, v.4, p.18

Jakobsson, S.P., 1972; Petrology of the Basalts from the Vestmannaeyjar Archi-Pelago, Lithos, v. 5, p. 365.

Jakobsson, S.P., 1973; Petrochemistry of the Heimaey, Iceland, Basalts. Nature, v. 243, p.213.

Jónsson, Jón, 1967; The Rift Zone and the Reykjanes Peninsula, in, Iceland and Mid-Ocean Ridges: ed. S. Björnsson, Visindafélag Islendinga v. 38, p. 142.

Kjartánsson, G., 1960; Jarthfraethikort áf Islandi, Sheet 3. Raunvisindastófnun Háskólans, Reykjavik.

Kjartánsson, G., 1964; Aldur Nokkura Hrauna á Suthurlandi. Náttúrufraethingurinn v. 35, p.75.

Klein, F., Páll Einarsson, and M. Wyss, 1973; Microearthquakes on the mid-Atlantic Plate Boundary on the Reykjanes Peninsula in Iceland. J. Geophys. Res., v. 78, p.5084.

Miller, R.W., Pope, A.J., H. Stettner, and J.L. David, 1970; Triangulation Measurements of Crustal Movements in the Vicinity of El Centro, California. ESSA Operational Data Report, Geodesy Division, Rockville, Maryland.

Moody, J.D., and M.J.Hill, 1956; Wrench Fault Tectonics. Geol. Soc. America Bull., v. 67, p.1207.

Nakamura, K., 1970; En Echelon Features of Icelandic Fissures. Acta Naturalia Islandica, v.2, p.15.

Piper, J.D.A., 1971; Ground Magnetic Studies of Crustal Growth in Iceland. Earth and Planetary Science Letters, v. 12, p. 199.

Piper, J.D.A., 1973; Volcanic History and Tectonics of the North Langjökull Region of Iceland. Canadian Journal of Earth Sciences. v. 10, p. 164.

Pitman, W.C., and M. Talwani, 1968; Sea Floor Spreading in the North Atlantic. Geol. Soc. America Bull., v. 83, p.619.

Reid, H.F., 1910; The Mechanics of the Earthquake, in, The California Earthquake of April 18th, 1906, Report of the State Earthquake Commission 2; Carnegie Institute of Washington, D.C.

Saemundsson, K., 1967; An Outline of the Structure of South West Iceland, in, Iceland and MId-Ocean Ridges; ed. S. Björnsson,Vidindafélag Islendinga, v. 38, p.151.

Saemundsson, K., 1973; Evolution of the Axial Rifting Zone in Northern Iceland and the Tjörnes Fracture Zone. Orkustofnun Jarthhitadei

Savage, J.C., and R.O. Burford, 1970; Accumulation of Tectonic Strain in California. Seism. Soc. America Bull., v. 60, p.1877.

Savage, J.C., and R.O. Burford, 1973; Geodetic Determination of the Relative Plate Movement in Central California. J. Geophys. Res. v. 78, p.832.

Savage, J.C., D. Goodreau, and W.H. Prescott, 1973; Possible Fault Creep on th Brawley Fault, Imperial Valley, California. National Center for Earthquake Research Report.

Saxo Grammaticus (tr. Oliver Elton), 1894; The First NIne Books of the Danish History of S.G. David Nutt, London.

Scholtz, C.H., and T.J. Fitch, 1969; Strain Accumulation along the San Andreas Fault. J. Geophys. Res. , v. 74, p. 6639.

Scholtz, C.H., M. Wyss, and T.J. Fitch, 1969; Seismic and Aseismic Slip on the San Andreas Fault. J. Geophys. Res., v.74, p. 2049.

Sigurdsson, H, 1971; Structural Origin and Plate Tectonics of the Snaefellsnes Volcanic Zone in Western Iceland. Earth and Planetary Science Letters, v. 10, p.129.

Sigurgeirsson, Th., 1969; Aeromagnetic Map of Iceland, Sheet 3, South-West. Raunvisindastofnun Háskólans, Reykjavik.

Stefánsson, R., 1966; Methods of Focal Mechanism Studies with Application to Two Atlantic Earthquakes. Tectonophysics, v.3, p. 209.

Sykes, L.R., 1967; The Mechanism of Earthquakes and the Nature of Faulting on Mid-Ocean Ridges. J. Geophys. Res., v. 72, p. 2131.

Symposium on The World Rift System, 1965; ed. T.N. Irvine, Geol. Surv. of Canada, Ottawa.

Talwani, M., CC. Widisch, and M.G. Langseth, Jr., 1971; Reykjanes Ridge Crest: A Detailed Geophysical Survey. J. Geophys. Res.,v.76,p4

Thórarinsson, S., 1967; Surtsey, The New Island in the North Atlantic. Almennabókafélagith, Reykjavik.

Thórarinsson, S., S. Steinthórsson, Th. Einarsson, H. Kristmansdóttir, and N. Oskarsson, 1973; The Eruption on Heimaey, Iceland. Nature, v. 241, p.372.

Tocher, D., 1960; Creep Rate and Related Measurements at Vineyard, California. Seism. Soc, America Bull., v. 50, p. 396.

Tómasson, Haukur, 1967; Jarthfraethirannsókn virkjunarstatharins vith Búrfell. Tímarit Verkfraethingafélags Islands, v. 51, p. 52.

Tryggvason, E., 1967; Fault Displacements in Recent Icelandic Earthquakes (abstract). Trans. Am. Geophys. Union, v. 48, p.204.

Tryggvason, E., 1968; Measurement of Surface Deformation in Iceland by Precisior Levelling. J. Geophys. Res., v.73, p. 7039.

Tryggvason, E., 1970; Special Review of Crustal Movements and Sea Floor Spreading, in Morgunblthith (Reykjavik daily newspaper), Sept. 15th, 1970.

Vogt, P.R., N.A. Ostenso, and G.L. Johnston, 1970; Magnetic and Bathymetric Data Bearing on Sea Floor Spreading North of Iceland. J. Geophys. Res., v.75, p.903.

Walker, G.P.L., 1965; Evidence of Crustal Drift from Icelandic Geology. Phil. Trans. Royal Soc. London, Series A, v. 258, p.199.

Ward. P.L., G. Pálmason, and C. Drake, 1969; Microearthquake Survey and the Mid-Atlantic Ridge in Iceland. J. Geophys. Res.,v. 74, p.665.

Ward, P.L., and S. Björnsson, 1971; Microearthquakes, Swarms, and the Geothermal Areas of Iceland. J. Geophys. Res., v. 76, p.3953.

Ward, P.L., 1971; New Interpretation of the Geology of Iceland. Geol. Soc. America Bull., v. 82, p.2991.

Wegener, A., (tr. J.G.A. Skerl), 1924; The Origin of Continents and Oceans. 4th Edition, Methuen, London.

Whitten, C.A., 1955; Measurement of Earth Movements in California. Calif. Div. Mines Bull., v. 171, p.75.

Whitten, C.A., 1960; Horizontal Movement in the Earth's Crust. J. Geophys. Res. v. 65, p.2839.

Whitten, C.A., and C.N. Claire, 1960; Analysis of Geodetic Measurements along the San Andreas Fault. Seism. Soc. America Bull., v.50,p.404.

Wilson, J.T., 1965; A New Class of Faults and their Relation to Sea Floor Spreading. Nature v. 105.

Wilson, J.T., 1973; Mantle Plumes and Plate Motions. Tectonophysics, v.19,p.149.